



Development of Methods toward the Synthesis of Novel Bioactive Natural Product-like Scaffolds

Dissertation

For the achievement of the academic degree of

Doctor in Natural Sciences

(Dr. rer. nat.)

Submitted to

The Faculty of Chemistry and Chemical Biology

Technical University Dortmund

Caitlin Davies, M.Sc.

From Corby, England

Dortmund 2022

The work presented in this thesis was performed during the time period from October 2018 to July 2022 under the supervision of Prof. Dr. Dr. h.c. Herbert Waldmann at the Faculty of Chemistry and Chemical Biology at the Technical University Dortmund and Max Planck Institute of Molecular Physiology, Dortmund.

Dean: Prof. Dr. S. M. Kast

1st Examiner: Prof. Dr. Dr. h.c. H. Waldmann

2nd Examiner: Dr. A. Brunschweiler

Results presented in this dissertation contributed to the following publications:

C. Davies*, L. Doetsch*, E. Hennes, M.G. Ciulla, K. Yoshida, R. Gasper, R. Scheel, C. Strohmann, S. Sievers, K. Kumar, S. Ziegler, H. Waldmann, “Identification of Apoxidole Pseudo-Natural Products as Novel IDO1 Inhibitors”, *Angew. Chem. Int. Ed.* **2022**, *manuscript submitted*

S. Shaaban*, C. Davies*, C. Merten, J. Flegel, F. Otte, C. Strohmann, H. Waldmann, “Rh^{III}-Catalyzed C-H Activation of Aryl Hydroxamates for the Synthesis of Isoindolinones”, *Chem. Eur. J.* **2020**, *26*, 10729.

Acknowledgements

First and foremost, to my supervisor Prof. Dr. Dr. h.c. Herbert Waldmann who was generous enough to let me pursue my doctorate in his department. Thank you for listening, understanding and for allowing me to have flexibility and independence. You were always there when needed and your guidance, wisdom and unlimited knowledge have been inspiring and appreciated.

Additionally, I am grateful to Dr. Andreas Brunschweiger for taking the responsibility as my second examiner.

Huge thanks (and about 10 bottles of whisky) are owed to Dr. Saad Shaaban. From the start, you were always there if I had questions or needed advice. The knowledge and tips I have learnt from you, have been a big help. Your constant support and occasional torture session during my PhD, definitely played an important role in increasing my confidence and ability. It may not have been obvious in all of our discussions but I am truly grateful for your patience and friendship.

Special thanks go to some fabulous PhDs! These three women in science are destined for greatness. Firstly, my lab partner-in-crime, Sarah (soon to be Dr.) Zinken. Going through the quest for a PhD at the same time has been a lot of fun. You also significantly helped me get to grips with the initial stages of living in Germany. As a lab partner, you are one of the best. We have shared a lot of frustrations, stress and confusion but most importantly we stuck together and shared a lot of laughter. Secondly, I am deeply grateful to my desk buddy and project partner, Lara Dötsch, who performed all the biological experiments on the pseudo-NP project. You patiently answered stupid questions, even if it was my third time of asking. Sharing the drama and excitement of results with you is one of the reasons why I wanted to pursue a career in science. My only regret is not being able to keep our plants alive (except for Gisela) when you were away, sorry! Finally, to Aylin Binici, thank you for being there whenever I needed. Whether it was science, injuries or life, your constant “You can do it!” attitude and occasional dark chocolate induced motivation, were key to getting through the PhD. Furthermore, the amount of time you spent attempting to get me to reply in German instead of English has been heroic.

Special thanks go to Dr. Gregor Cremosnik and Dr. Michael Grigalunas. Two gems and valuable mentors. Both of you provided great company, advice and knowledge. I am grateful to have been able to work with you and to benefit from fruitful discussions that I am sure will help me navigate the science world. Thanks also go to Dr. Jana Flegel for her biological contributions in the C-H activation project. You always made time to help me whenever I needed. I hope I returned the favour.

Of course, I would like to thank all of Abt.4 for providing a great working environment. I still do not know how I was lucky enough to be part of a department with such superb expertise. Particular thanks to Jens Warmers for keeping the instruments running and for his quality BBQ skills!

Additional thanks to COMAS for biological screening of the compounds and to the HRMS team for compound analysis and Felix Otte and Rebecca Scheel for solving crystal structures.

I also want to mention the badminton group, Dr. Oliver Hofnagel, Dr. Daniel Prumbaum, Patrick Günther, Dr. Barathy Vinayagam, Carolin Koerner and Dr. Wout Oosterheert, who always kept me laughing but you also offered help and support if I needed it (even if it came with a big side of sarcasm). I am so glad to have met you all. To Oliver, to keep it short, I do not think any acknowledgement will cover how much you have done for me in my time in Dortmund. You have educated me in all things German (whether it was wanted or not). Yet, I am most grateful for your friendship and for helping me get through some of the really tough times and the medical dramas.

Additionally, a special mention to some colleagues and friends who have all contributed in some way to making my time here memorable. Dr. Rachel O’Dea, Chris Meis, Kai Gallant, Pascal Hommes, Jimin Hwang, Jen-Yao Chang, Dr. Annina Burhop, Dr. Georg Niggemeyer, Marina Gattiglio and Dr. Elisabeth Hennes, thank you all!

Finally, to my family and friends back home on “The Island”, your constant support is always appreciated. Let’s see what the next adventure brings!

Table of Contents

Abstract	1
Kurzzusammenfassung	3
General Introduction	5
Small Molecules to Probe Biology	5
Identification of Bioactive Small Molecules	6
Reverse Chemical Genetics: Target-based Screening	7
Forward Chemical Genetics: Phenotypic Screening	7
Morphological Profiling: Cell Painting Analysis.	8
CHAPTER I: Rhodium (III)-Catalyzed C-H Functionalisation of <i>N</i>-OBoc	
Benzamides to Access Isoindolinones	10
<i>1.1 Introduction</i>	10
1.1.1 C-H Functionalisation	10
1.1.2 Transition Metal-Catalysed C-H Functionalisation	11
1.1.2.1 Directed C-H bond functionalisation	11
1.1.2.2 RhCp* in <i>ortho</i> -directed C-H bond Functionalisation	13
1.1.2.2.1 Internal Oxidant Directing Groups	15
1.1.2.2.2 <i>N</i> -alkoxy Benzamides as Versatile Directing Groups	16
1.1.3 Isoindolinones	20
1.1.3.1 Synthetic Strategies toward 3-Isoindolinones.....	21
1.1.3.2 Isoindolinones <i>via</i> RhCp* catalysed C-H Functionalisation	22
<i>1.2 Project Aim</i>	25
<i>1.3 Results and Discussion</i>	26
1.3.1 Background and Initial Results	26
1.3.1.1 Solving the Puzzle: Exploring the Effect of <i>Ortho</i> -Substituted Styrenes..	27
1.3.2 Reaction Optimisation.....	29
1.3.3 Scope of Substrates	32

1.3.3.1 Reaction Limitations	34
1.3.4 Access to Natural Product-like Isoindolobenzazepines	34
1.3.4.1 Reaction Optimisation for the One-Pot-Two-Step Synthesis of Isoindolobenzazepines	35
1.3.4.2 Scope of Substrates	36
1.3.5 Mechanistic Investigation	38
1.3.5.1 Deuterium Labelling	38
1.3.5.2 Computational Experiments.....	39
1.3.5.3 Proposed Mechanism	41
1.3.6 Biological Evaluation	42
1.3.6.1 Background: Hedgehog (Hh) Dependent Osteoblast Differentiation	42
1.3.6.2 Inhibition of Hh Dependent Osteoblast Differentiation.....	44
1.4 Summary	46

CHAPTER II: Synthesis of Apoxidole Pseudo-Natural Products Reveals Novel

IDO1 Inhibitor	47
2.1 <i>Introduction</i>	47
2.1.1 Natural Products: Inspiration but not a Solution.....	47
2.1.1.1 Diversity Oriented Synthesis (DOS)	47
2.1.1.2 Complexity to Diversity (CtD)	50
2.1.1.3 Biology Oriented Synthesis (BIOS).....	51
2.1.1.4 Fragment-Based Drug Discovery (FBDD)	53
2.1.1.5 Pseudo-Natural Products.....	55
2.2 <i>Project Aim</i>	61
2.3 <i>Results and Discussion</i>	62
2.3.1 Background: Design of a Novel Pseudo-NP Class	62
2.3.1.1 Synthetic Strategy: Phosphine-Catalysed [4+2] Annulation	63
2.3.2 Method Development.....	64
2.3.2.1 Racemic Reaction Screen of <i>N</i> -Substituted Indoles	65
2.3.2.2 Chiral Phosphine Catalyst Screening.....	66

2.3.2.3 Solvent Screen	68
2.3.3 Substrate Scope and Limitations.....	69
2.3.4 Mechanistic Hypothesis.....	72
2.3.5 Access to an NP-like Bridged-Bicyclic Compound Class.....	74
2.3.6 Biological Evaluation.....	79
2.3.6.1 IDO1-dependent Kynurenine Modulation	80
2.3.6.1.1 IDO1 Inhibitors	81
2.3.6.2 Modulation of Kynurenine Production SAR	83
2.3.6.2.1 Activity of the Bridged-Bicyclic NP-like Compounds...86	
2.3.6.3 Target Identification: Inhibition of apo-IDO1	86
2.4 Summary	92
CHAPTER III: Experimental Methods	94
3.1 General Information.....	94
3.2 Chemical Synthesis for Chapter I.....	96
3.2.1 General Procedure for the reaction of <i>N</i> -OPiv-benzamides with styrenes ..96	
3.2.2 General Procedure for the synthesis of <i>N</i> -OBoc-benzamides	98
3.2.3 General Procedure for the synthesis of styrenes	98
3.2.4 General Procedure for the synthesis of 3-Isoindolinones	101
3.2.5 General Procedure for the synthesis of Isoindolobenzazepines	110
3.3 X-Ray Structure Analyses.....	121
3.4 DFT Calculations.....	125
3.5 Biological Data	137
3.6 Chemical Synthesis for Chapter II	138
3.6.1 General Procedure for the synthesis of α -Ketoester	138
3.6.2 General Procedure for the synthesis of Ketimines	139
3.6.3 General Procedure for the synthesis of Aldimines	142
3.6.4 General Procedure for the synthesis of Allenoates	144
3.6.5 General Procedure for the synthesis of Apoxidole Pseudo-NPs	147

3.6.5.1 Additional compounds for use in Bridged Bicyclic Synthesis	164
3.6.6 General Procedure for the synthesis of Bridged-Bicyclic Compounds	166
3.7 X-Ray Structure Analyses	175
4. References.....	178
5. Abbreviations	188
6. Appendix.....	191
6.1 Curriculum Vitae (<i>Lebenslauf</i>)	191
6.2 Eidesstattliche Versicherung (<i>Affidavit</i>)	193



Abstract

The complexity and inherent biological relevance of natural products (NPs) are key characteristics that have made them a constant source of inspiration in the development of novel bioactive compounds. However, NPs alone cannot solve the lack of diverse chemical scaffolds extending into unexplored chemical and biological space. As a result, this has led to innovative reaction methodology and design strategies both of which are used in order to design and synthesise new NP-like scaffolds that may simultaneously deliver new biological insight, with therapeutic potential. In this thesis, access to four different NP-like scaffolds, by means of unique reaction methodology or the pseudo-NP design principle will be discussed (Figure 1A).

Two of the reported scaffolds contain an isoindolinone core privileged scaffold which were obtained *via* a novel Rh(III)-catalysed C-H functionalisation reaction. The previously unexplored coupling of *N*-Boc benzamides with *ortho*-substituted styrenes affords NP-like isoindolinones under mild reaction conditions and tolerates a broad range of functionalities. Experimental and computational investigations provide strong evidence to support that the high regioselectivity observed for these substrates results from the combination of the *ortho*-substituent present on the styrene and the OBoc group of the benzamide. Furthermore, this scaffold was used as a valuable building block to generate a second class of NP-like compounds, isoindolobenzazepine derivatives, *via* an additional S_N2 reaction. Biological evaluation of selected compounds from both compound libraries revealed inhibitory activity in the Hedgehog (Hh)-dependent osteoblast differentiation of multipotent murine mesenchymal progenitor stem cells into osteoblasts.

The pseudo-NP approach is a design strategy involving the *de-novo* combination of natural product fragments in novel arrangements with the specific dual aim of targeting novel chemical and biologically relevant space. In the second chapter, the design and synthesis of a new class of pseudo-NPs combining indole- and tetrahydropyridine (THP)-fragments in an unprecedented arrangement is described (Figure 1B). The monopodal connectivity between the fragments has not yet been observed in nature, hence, facilitated by a phosphine-catalysed asymmetric [4+2] annulation reaction, efficiently yielded the new pseudo-NP scaffold. When submitted to biological screening in various cell-based assays, the pseudo-NPs were found to be potent in reducing cellular kynurenine (Kyn) levels. Further investigation identified the mode-of-action to be the selective

targeting and stabilisation of apo-indoleamine 2,3-dioxygenase 1 (apo-IDO1), a therapeutic target enzyme involved in immuno-suppression, linked to numerous disorders including cancer. Additionally, this pseudo-NP class was used to obtain the final NP-like class, in the form of bridged-bicyclic compounds. The synthesis of this pseudo-NP class therefore helps to validate the design principle with regard to unexplored fragment arrangements possibly providing a route to compound classes endowed with unexpected or new bioactivity.

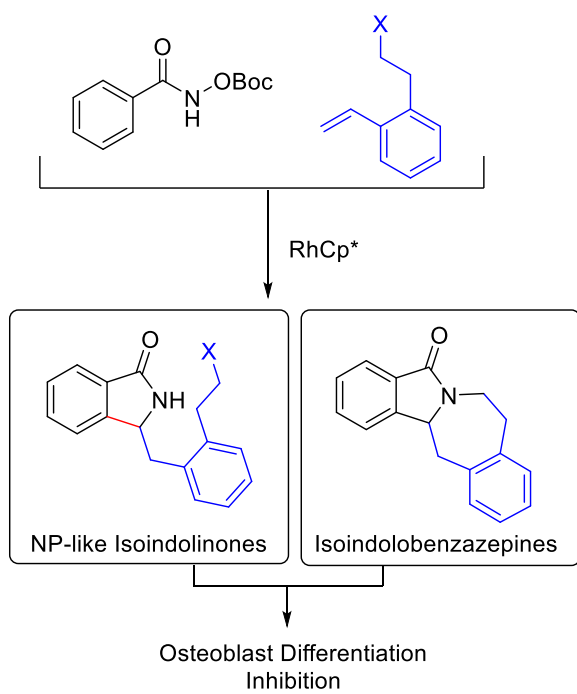
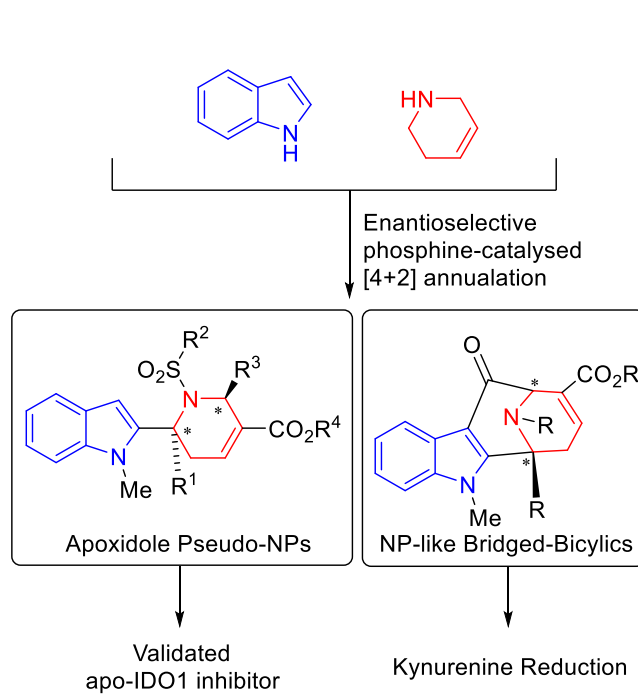
A) Reaction Methodology: C-H functionalisation**B) Design Strategy: Pseudo-NP approach**

Figure 1: Overview of two strategies accessing four diverse NP-like scaffolds with newly discovered bioactivity. A) Rh-catalysed C-H functionalisation and B) Use of the Pseudo-NP principle.

Overall, novel synthetic methodology and the pseudo-NP concept can provide the opportunity to discover unique structural scaffolds that may explore new areas of biologically relevant chemical space.

Kurzzusammenfassung

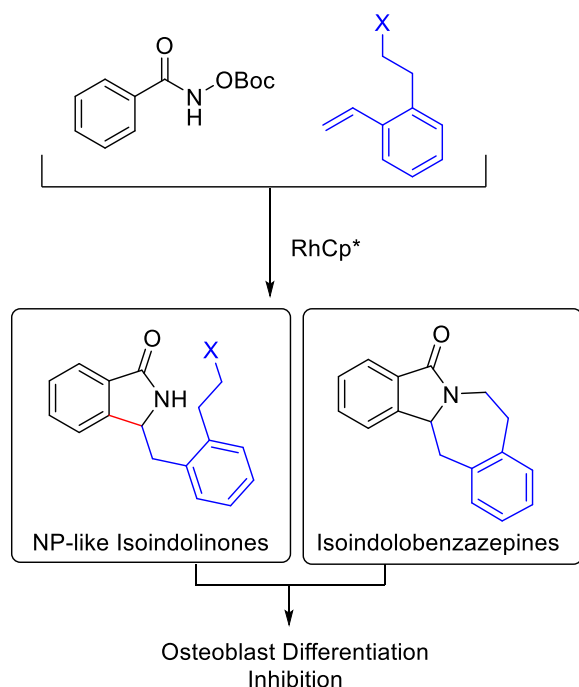
Die Komplexität und die inhärente biologische Relevanz von Naturstoffen (*Natural Products*, NPs) sind Schlüsseleigenschaften, die sie zu einer wichtigen Inspirationsquelle für die Entwicklung neuer bioaktiver Verbindungen gemacht haben. Allerdings können NPs allein den Mangel an vielfältigen molekularen Gerüststrukturen, die sich in unerforschte chemische und biologische Bereiche erstrecken, nicht beheben. Dies hat zur Entwicklung innovativer Reaktionsmethodiken und Designstrategien geführt, die eingesetzt werden können, um neue NP-ähnliche Verbindungsklassen zu entwerfen und zu synthetisieren. Die biologische Untersuchung dieser neuartigen Verbindungen kann zu neuen biologischen Erkenntnissen mit therapeutischem Potenzial führen. In dieser Arbeit wird der Zugang zu vier verschiedenen NP-ähnlichen Verbindungsklassen durch eine innovative Synthesemethode oder das Pseudo-NP-Designprinzip erörtert (Abbildung 1A).

Zwei der vorgestellten Grundstrukturen enthalten eine privilegierte Isoindolinon-Kernstruktur, die durch eine neuartige Rh(III)-katalysierte C-H-Funktionalisierungsreaktion erhalten wurde. Die bisher unerforschte Kopplung von N-Boc-Benzamiden mit *ortho*-substituierten Styrolen führt unter milden Reaktionsbedingungen zu NP-ähnlichen Isoindolinonen und toleriert ein breites Spektrum von Funktionalitäten. Experimentelle und computer-gestützte Untersuchungen belegen, dass die für diese Substrate beobachtete hohe Regioselektivität aus der Kombination des *ortho*-Substituenten am Styrol und der OBoc-Gruppe des Benzamids resultiert. Darüber hinaus wurde diese Struktur als Baustein verwendet, um eine zweite Klasse von NP-ähnlichen Verbindungen, die Isoindolobenzazepin-Derivate, über eine zusätzliche S_N2-Reaktion zu erzeugen. Die biologische Untersuchung ausgewählter Verbindungen aus beiden Substanzbibliotheken ergab eine inhibierende Wirkung auf die Hedgehog (Hh)-abhängige Osteoblasten-Differenzierung multipotenter, mesenchymaler Vorläufer-Stammzellen der Maus in Osteoblasten.

Der Pseudo-NP-Ansatz ist eine Designstrategie, bei der Naturstofffragmente in neuartigen Anordnungen *de-novo* kombiniert werden, mit dem Ziel, neue chemische und biologisch relevante Bereiche zu erschließen. Im zweiten Kapitel wird das Design und die Synthese einer neuen Klasse von Pseudo-NPs beschrieben, die Indol- und Tetrahydropyridin (THP)-Fragmente in einer bisher unbekanntem molekularen Anordnung miteinander verbinden (Abbildung 1B). Die monopodale Konnektivität zwischen den Fragmenten konnte bisher in der Natur nicht beobachtet werden, so dass die neue Pseudo-NP-Klasse durch eine phosphinkatalysierte asymmetrische [4+2]-

Annulierungsreaktion effizient hergestellt werden konnte. Beim biologischen Screening in verschiedenen zellbasierten Assays zeigte sich eine Senkung des zellulären Kynureninspiegels (Kyn) durch die beschriebenen Pseudo-NPs. Weitere Untersuchungen ergaben, dass der Wirkmechanismus in der selektiven Bindung und Stabilisierung der Apo-Indoleamin-2,3-Dioxygenase 1 (apo-IDO1) besteht, eines therapeutischen Targets, das an der Immunsuppression beteiligt ist und mit zahlreichen Erkrankungen, einschließlich Krebs, in Verbindung steht. Außerdem wurde diese Pseudo-NP-Klasse verwendet, um die zuletzt beschriebene NP-ähnliche Verbindungsklasse in Form von verbrückten, bizyklischen Verbindungen zu erhalten. Die Synthese dieser Pseudo-NP-Klasse trägt zur Validierung des Designprinzips im Hinblick auf unerforschte Fragment Anordnungen bei und bietet möglicherweise Zugang zu Verbindungsklassen mit unerwarteter oder neuer Bioaktivität.

A) Reaction Methodology: C-H functionalisation



B) Design Strategy: Pseudo-NP approach

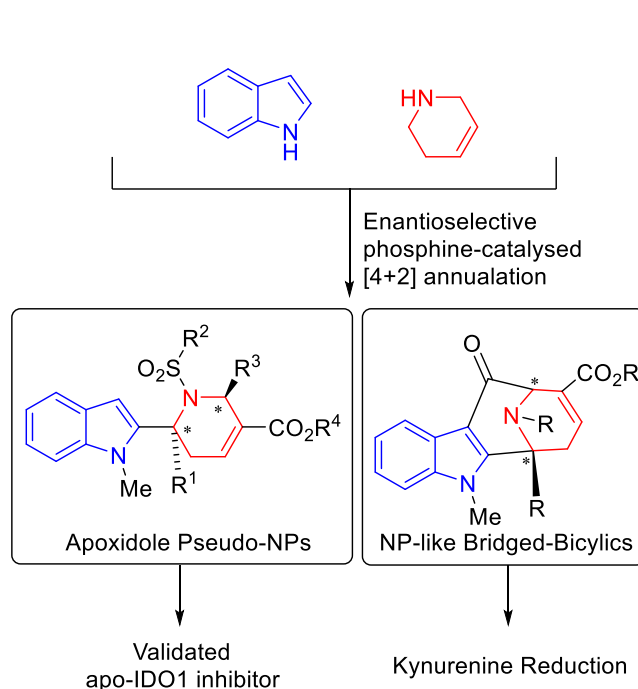


Abbildung 1: Überblick über zwei Strategien zur Entwicklung von vier verschiedenen NP-ähnlichen Verbindungsklassen mit neu entdeckter Bioaktivität. A) Rh-katalysierte C-H-Funktionalisierung und B) Anwendung des Pseudo-NP-Prinzips.

Insgesamt können neuartige Synthesemethoden und das Pseudo-NP-Konzept die Möglichkeit bieten, einzigartige molekulare Strukturen zu entdecken, um neue Bereiche des biologisch relevanten chemischen Raums zu erschließen.

General Introduction

Small Molecules to Probe Biology

Small molecules include natural products, metabolites and synthetic compounds (<1000 Da).^[1,2] Often these compounds bind to and modulate biological targets, such as enzymes, receptors and DNA. Small molecules continue to play a prominent role as therapeutic agents but also in answering important biological questions. More specifically, through dissecting and elucidating molecular mechanisms, enhancing our understanding of complex biological systems.^[3]

The classical approach to understand biological processes requires genetic manipulations. However, deleting or activating genes is a labour-intensive process and may be limited in its *in vivo* application.^[4] Often, it can completely remove a protein from a system, which can be detrimental but also removes the chance to study it.^[3,5] Whereas, small molecules may modulate one specific function of a multifunctional protein. The beauty of small molecules is that they offer a more flexible approach than working on a gene level. They can be easily modified and can act quickly and reversibly in a dose-dependent manner across multiple cell lines/species.^[4] Unfortunately, whilst any gene can be manipulated, only a fraction of known targets have known small molecule ligands.^[5,6] Yet, the advantages of small molecules cannot be ignored, and the desire to deliver novel compounds that can probe biology is extremely high.

Estimates of potentially synthesisable stable organic molecules is $\sim 10^{63}$ (<500 Da), showing that, with regard to chemical space, chemists have barely scratched the surface.^[7] In 2008, an analysis of the CAS registry (> 150 million compounds) by Lipkus *et al.* highlighted that $\sim 50\%$ all known compounds are based on just 0.25% of the known molecular scaffolds, whilst the most popular 5% of scaffolds were present in over 75% of compounds.^[8] Motivated by these statistics, advances in chemical reaction methodology and synthetic design strategies have led to innovative approaches to access novel scaffolds, including those with the potential for bioactivity.^[9] A decade later, the data was reassessed, revealing the number of new scaffolds had almost doubled between 2008 and 2018 (Figure 2).^[10]

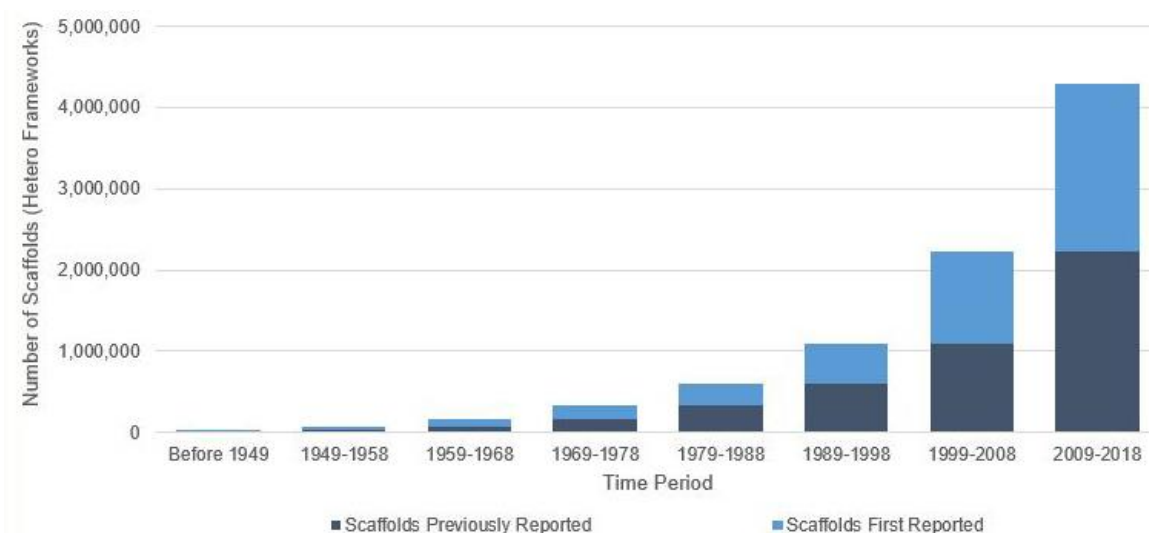


Figure 2: Volume of new and established Chemical Scaffolds in published literature pre-1949 to 2018.^[11]

This demonstrated that inventive strategies were indeed venturing into unexplored regions of chemical space. Nevertheless, the challenge remains. For the future, synthetic boundaries should continue to be pushed and chemists should have an awareness of the potential gold mine of scaffolds that are yet to be synthesised.^[12] It is of high importance in order to enable access to biologically relevant space and consequently, bioactive compounds.^[13]

Identification of Bioactive Small Molecules

The field of chemical genetics is a research paradigm that utilises small molecules that perturb biological systems in order to characterise cellular pathways or specific protein function.^[4] In order to increase the chance of finding active compounds (“hits”), large compound libraries are required.^[14,15] As parallel and combinatorial chemical synthesis generates a vast number of novel compounds in a short space of time, the development of high-throughput screening (HTS) techniques has greatly benefited chemical genetics.^[4,16] In academia, thousands of compounds can be screened and assayed per day, but the pharmaceutical industry are capable of screening millions. Usually this leads to multiple hits but the challenge is to discard false-positives while maintaining promising active leads.^[17,18]

Chemical genetics can be divided into two approaches, the forward and reverse, but both are composed of three parts: natural product or small-molecule libraries, phenotypic screening and target identification.^[5,19]

Reverse Chemical Genetics: Target-Based Screening

Reverse chemical genetics is referred to as being “from target to phenotype”.^[5] In this case, there is an established protein (or gene) target of interest, and the aim is to identify a compound that causes a phenotypic change. The protein will be screened with a vast pool of chemical compounds to identify functional ligands that induce a phenotypic change. A specific ligand will then be optimised and is used on cells or an organism to study and characterise the triggered phenotypic response. The main drawback with this method stems from the use of purified protein. Testing a compound with just one target *in vitro*, cannot give a clear picture as the how selective or specific the ligand will be *in vivo*. As a result, many compounds will fail in the later stages as they may have adverse effects that were not possible to observe earlier.^[19]

Furthermore, target-based screening remains difficult as not all possible targets are known or accessible. In fact, a report by Swinney and Anthony revealed that between 1999 and 2008, out of 50 new and approved drug compounds, 34% were target-based (reverse chemical genetics) whereas 56% were phenotype-based (forward chemical genetics).^[20]

Forward Chemical Genetics: Phenotypic Screening

Contrastingly, forward chemical genetics, which is defined as the “phenotype to target”, has continued to be the more accessible and applicable approach in discovering novel bioactivity.^[4] It begins with a library of natural products or small molecules which are submitted to a phenotypic screen. If a compound induces a phenotypic change of interest, it is subsequently used to identify the responsible molecular target (Figure 3).^[3]

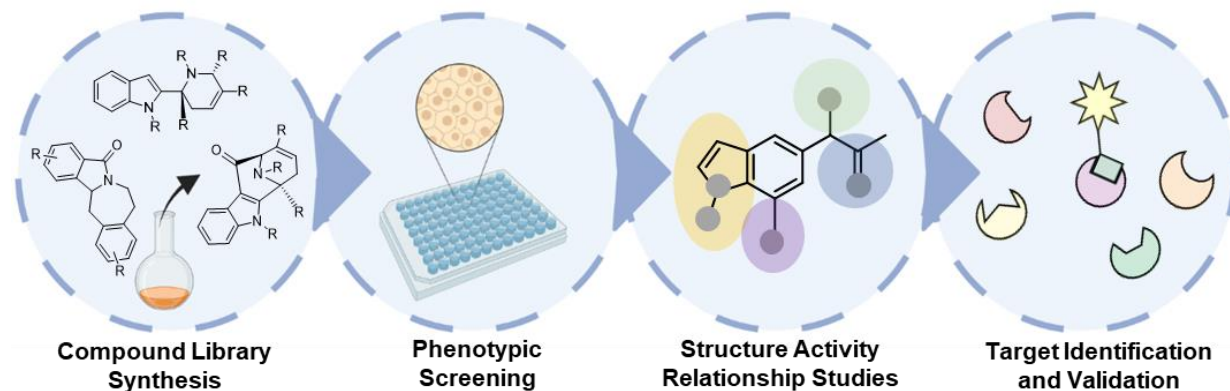


Figure 3: Schematic representation of forward chemical genetics.^[21]

Once a suitable compound has been identified, before it is taken further, it undergoes optimisation through “structure-activity-relationship” (SAR) studies. This requires synthetic modifications to improve the potency, selectivity (if relevant) and in parallel, physicochemical properties. This compound will then be used in target identification which may lead to an understanding of the compound’s mode of action and its involvement in the regulation of the molecular mechanisms that ultimately result in the phenotype of interest.^[3]

Phenotypic screening not only allows the opportunity to identify novel bioactive compounds, but a clear advantage over the reverse approach, it also discovers new targets and thereby identification of previously unknown molecular networks. This is predominantly due to the unbiased (with respect to a specific molecular target) nature of the technique because proteins are kept in their native environment and not incubated with a single protein target (see reverse chemical genetics). Something which often limits drug development is off-target effects but phenotypic screening can often escape this early on in compound development with HTS triage.^[17,22]

What both forward (and reverse) chemical genetics rely on are the compounds libraries. Herein, one returns to the necessary exploration of chemical space. Traditional combinatorial libraries yield disappointing hit return ratio, and it is now widely accepted that this poor rate of return is due to a lack of structural diversity or biological relevance.^[3] Pharmaceutical compound collections, despite their impressive size, lack diverse chemical structures in their compound collections which can slow the discovery of new drugs. Once again, the need to design and synthesise novel and structurally diverse compounds is clear. The ultimate goal being able to find a small molecule partner for every gene product.

Morphological Profiling: Cell Painting Analysis

It is worth noting that another form of phenotypic screening has become popular in recent years, is the Cell Painting Assay.^[23,24] This broadly-applicable, high-throughput method, combines microscopy and computational analysis to detect changes in cellular morphology. By staining specific cellular compartments (nuclei, endoplasmic reticulum, nucleoli, RNA, actin, Golgi apparatus and mitochondria) with six different dyes simultaneously, an unbiased approach to investigate cellular perturbations upon compound treatment is accomplished. Automated

fluorescent imaging and analysis leads to the extraction of several hundred morphological parameters that represent a phenotypic profile in the form of a “fingerprint”. If the compound has induced any significant change in the morphology, it is quantified and given an induction value, relative to DMSO. In addition, by comparing a fingerprint profile to a set of references, it may be possible to determine the biological target or mode-of-action of the compound.^[25,26]

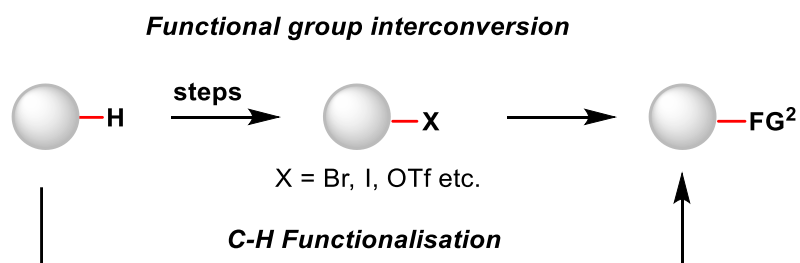
Chapter I: Rhodium (III)-Catalysed C-H Functionalisation of *N*-OBoc Benzamides to access NP-like Isoindolinones

1.1 Introduction

In the search for biologically active small molecules, a limiting factor was often the availability of synthetic methods that are able to access the necessary complexity, e.g. compared to natural products (NPs). However, with an increasing demand for more efficient and economical means to synthesise complex natural product-like scaffolds in the hope of delivering novel bioactivity, landmark chemical reaction methods have emerged,^[27,28] including C-H functionalisation.^[29,30]

1.1.1 C-H Functionalisation

Nature frequently performs carbon-hydrogen (C-H) bond functionalisation, taking inert C-H bonds and using them as latent functional groups to form new carbon-carbon (C-C) or carbon-heteroatom (C-X) connections.^[31] Yet despite the abundant presence of C-H bonds, in synthetic organic chemistry it remains a challenge to perform the same feat with such ease.^[32] An isolated, non-acidic C-H bond carries with it a high bond dissociation energy (≥ 90 – 110 kcal mol⁻¹),^[33] making it notoriously difficult to functionalise. However, the ability to selectively activate and functionalise C-H bonds is highly sought after as it provides novel reaction sites and more efficient synthetic routes. Typically, bond forming reactions rely on the manipulation of reactive groups which usually requires multi-step syntheses to prepare pre-functionalised starting materials.^[33] Whereas C-H functionalisation provides an alternative scenario; directly transforming the C-H bond to the desired functionality (Scheme 1), hence improving atom economy and reducing hazardous waste.^[34]



Scheme 1: Direct C-H functionalisation, a more efficient route compared to traditional approaches.

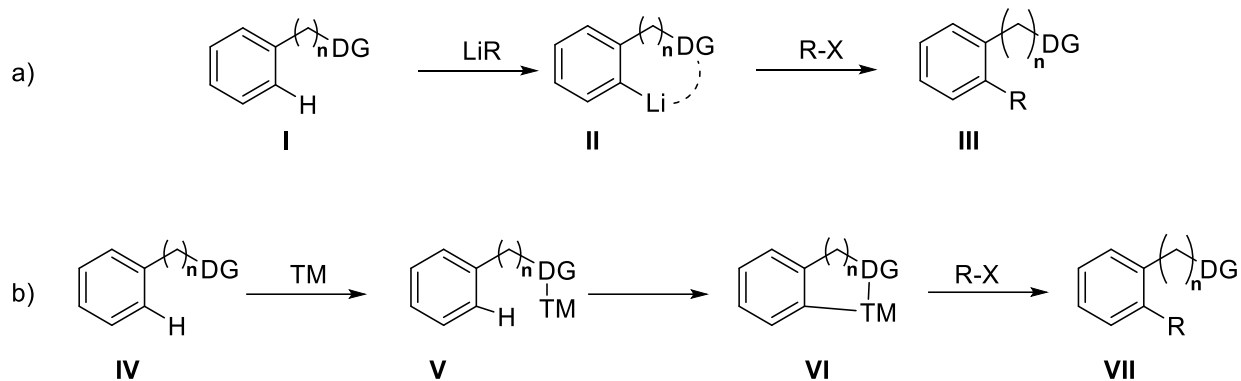
With the emergence of C-H functionalisation methodologies, it has simplified access to organic building blocks and more recently enabled late-stage functionalisation (LSF) of complex structures, particularly useful in the pharmaceutical industry.^[35]

1.1.2 Transition Metal-Catalysed C-H Functionalisation

The use of a transition metals (TMs) to facilitate C-H functionalisation is one of the most widely used approaches.^[36–38] The TM can “activate” the C-H bond by lowering the energy barrier for bond cleavage. It does so by coordinating to a C-H σ -bond and donating electron density into the σ^* orbital, weakening the C-H bond and allowing a metal carbon bond to be formed.^[39] In the last 30 years the field of transition metal-catalysed C-H functionalisation has gained tremendous attention. It has delivered novel transformations but has also been used to construct privileged scaffolds, often used as building blocks for the discovery of complex natural product-like compounds.^[37,40] As mentioned, the abundance of the C-H bond is part of the appeal that drives C-H functionalisation research, offering multiple sites for unique reactions. However, due to the complexity of organic substrates having the tools to selectively activate a specific C-H bond, maintaining chemo- and regioselectivity is one of the main challenges. In heterocyclic compounds, such as furans, indoles, and pyridines, the reactivity of a C-H bond can be controlled by the presence of the heteroatom.^[39] Whereas, less explored is the selective functionalisation of a non-biased sp^2 - or sp^3 -C-H bond.^[41] This is notoriously difficult and can cause unprecedented reactions.

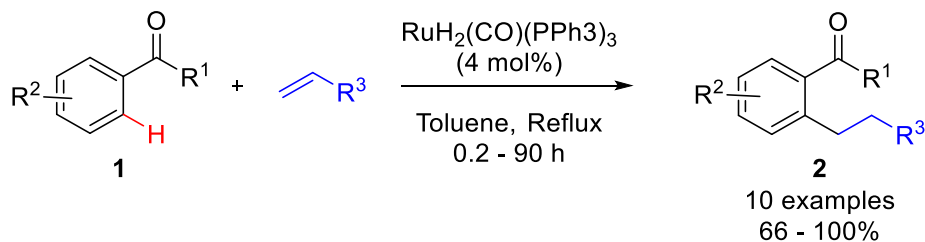
1.1.2.1 Directed C-H bond Functionalisation

An established strategy to obtain high regioselectivity is to employ a directing group (DG) in combination with a TM-complex.^[42,43] This approach avoids the need for stoichiometric quantities of strong lithium bases, a hindrance in terms of functional group tolerance, often used in the directed *ortho*-metalation (Scheme 2a).^[44] DG-assisted C-H functionalisation has matured into a powerful tool in organic synthesis, providing original disconnections in retrosynthetic analysis and improving the overall efficiency of the desired transformation.^[29] In particular, *ortho*-directed C-H functionalisation of aromatic rings (Scheme 2b), which is frequently used to obtain complex scaffolds.^[42,45]



Scheme 2: Comparison between *ortho*-metalation (A) and TM-catalysed *ortho*-directed C-H functionalisation (B).

Acting like an internal ligand, the DG coordinates to the TM catalyst **V** directing it in close proximity to the desired C-H bond, whilst leaving the rest “unreactive”. Subsequent insertion of the TM into the C-H bond and simultaneous proton loss, typically affords a 5- or 6-membered metalocycle **VI** which allows the reaction coupling partner to insert and form the new C-C/C-X bond **VII**. This initiates the eventual regeneration of the TM catalyst and yields the desired product. Various functionalities have been used as DGs for site-selective C-H activation, ranging from nitrogen containing heterocycles to amides carbonyl derivatives.^[42] One of the earliest examples of this strategy was the pioneering work of Murai in 1993.^[46] An *ortho*-selective, alkylation facilitated by a ruthenium catalyst using various aromatic ketones **1** and alkenes was successfully achieved (Scheme 3).



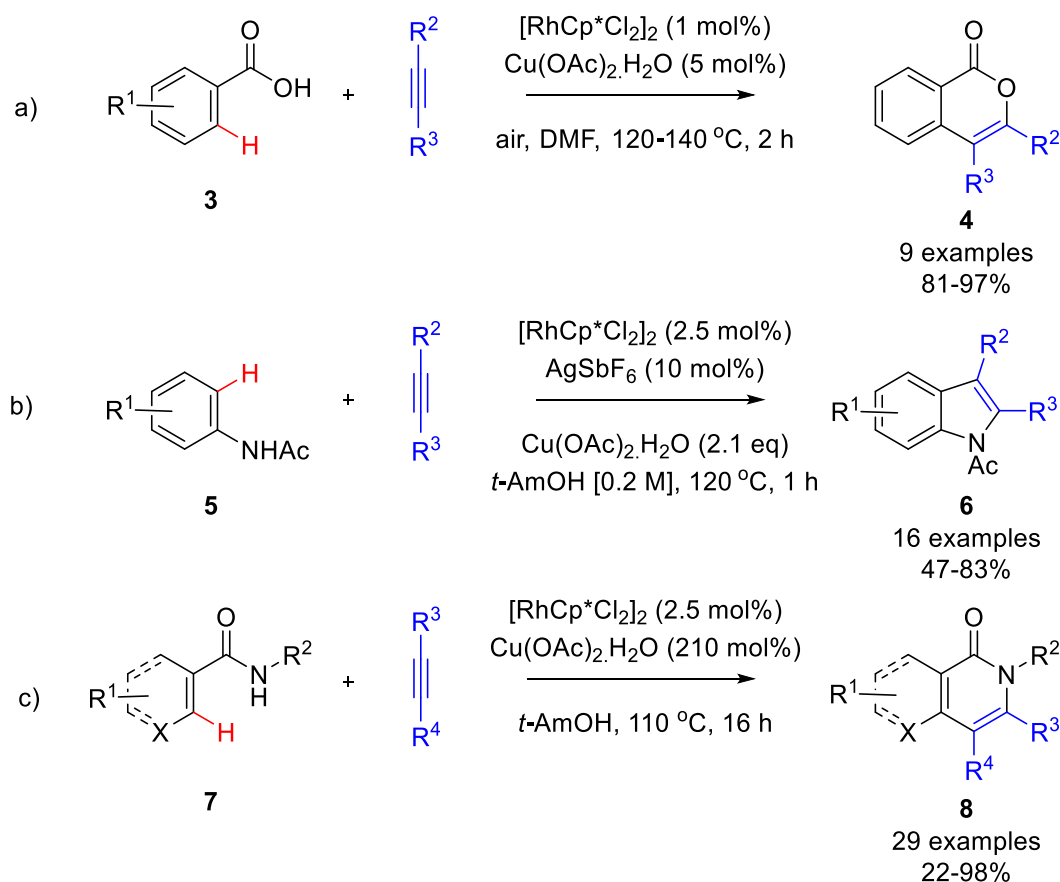
Scheme 3: First example of TM-catalysed *ortho* C-H functionalisation of aryl ketones.

Since then, directed C-H functionalisation reactions have grown in complexity and applicability generally working well with transition metals from groups 8-10, such as ruthenium (Ru), rhodium (Rh) and palladium (Pd).^[47] In particular, rhodium-catalysed C-H functionalisation has received

more attention over the years as it offers tuneable reactivity and a broad functional group tolerance, allowing access to many structurally complex and functionally diverse molecular motifs.^[48,49]

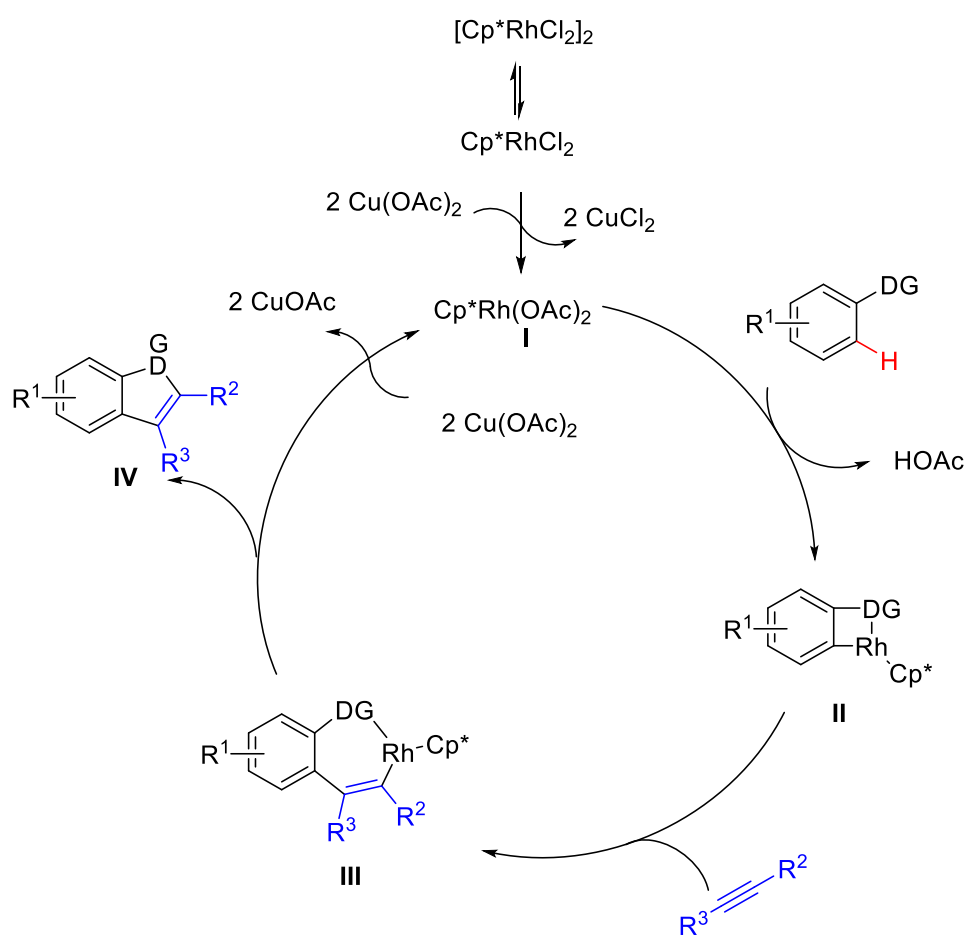
1.1.2.2 RhCp* in *ortho*-directed C-H bond Functionalisation

The transition metal complex, pentamethylcyclopentadienyl rhodium dichloride dimer, [RhCp*Cl₂]₂ has proven to be an influential pre-catalyst in C-H functionalisation, commonly being used in *ortho*-directed reactions with various coupling partners.^[42] Early work from Miura *et al.* (Scheme 4a) delivered isocoumarins **4** using benzoic acids to direct the C-H insertion in the presence of alkynes.^[50] Fagnou *et al.* used this approach demonstrating a regioselective synthesis of highly functionalised indoles (Scheme 4b) employing acetamides **5**.^[51] In 2010, using *N*-aryl benzamide **7** with internal alkynes, Rovis *et al.* gained access to a variety of isoquinolones **8** including those originating from heterocyclic carboxamides (Scheme 4c).^[52]



Scheme 4: Early examples of the RhCp*-catalysed *ortho*-C-H Functionalisation transformations with alkynes and different DGs

Yet, it should be noted that these early examples all include the use of a copper co-catalyst, which has a dual role in the mechanism (Scheme 5), resulting in the need for high temperatures. Initially the RhCp* dimer undergoes ligand exchange with copper acetate to form the active catalytic species **I** (Scheme 5). Guided by the directing group this species can insert into the C-H bond to form rhodacycle **II**, with concomitant acetic acid formation. The available coordination site of the rhodium allows coordination and subsequent insertion of the alkyne to access rhodacycle **III**, which forms the desired heterocycle upon reductive elimination of a Rh(I) species. The final stage of the cycle is the regeneration of the catalytic Rh(III) species *via* oxidation facilitated by copper acetate.

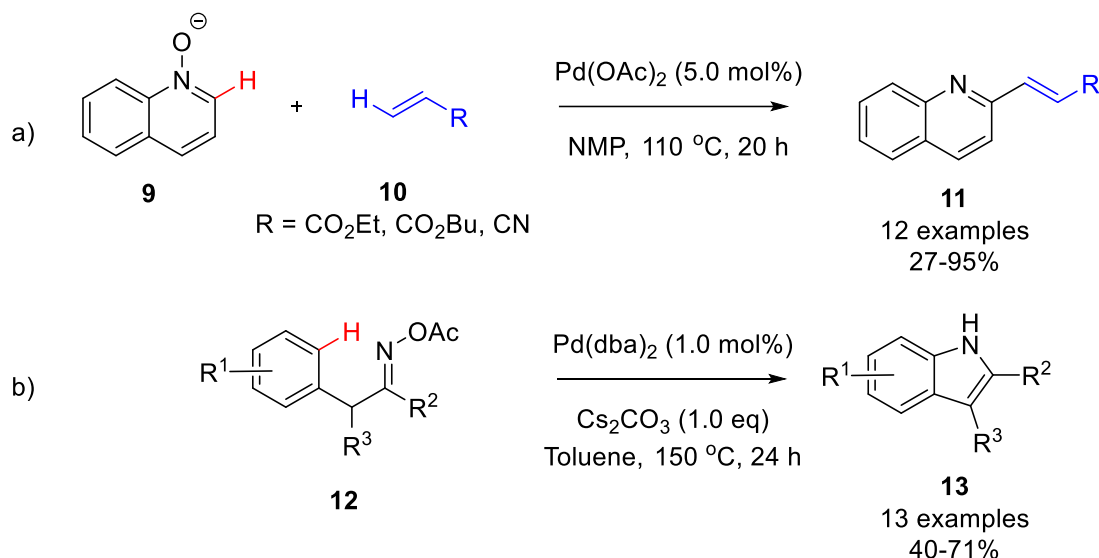


Scheme 5: General mechanistic cycle for Rh-catalysed *ortho*-directed C-H activation assisted by the use of copper acetate.

1.1.2.2.1 Internal Oxidant Directing Groups

In order to allow for reactions to proceed under milder conditions, which would also allow for a broader substrate scope, and reduce metal waste, significant development in C-H functionalisation has led to the use of internal oxidants.^[47,53] This internal oxidant acts as both a DG and oxidant, making the need for a co-catalyst redundant and in theory lowering reaction temperatures as a consequence of the intramolecular nature of the re-oxidation.^[54]

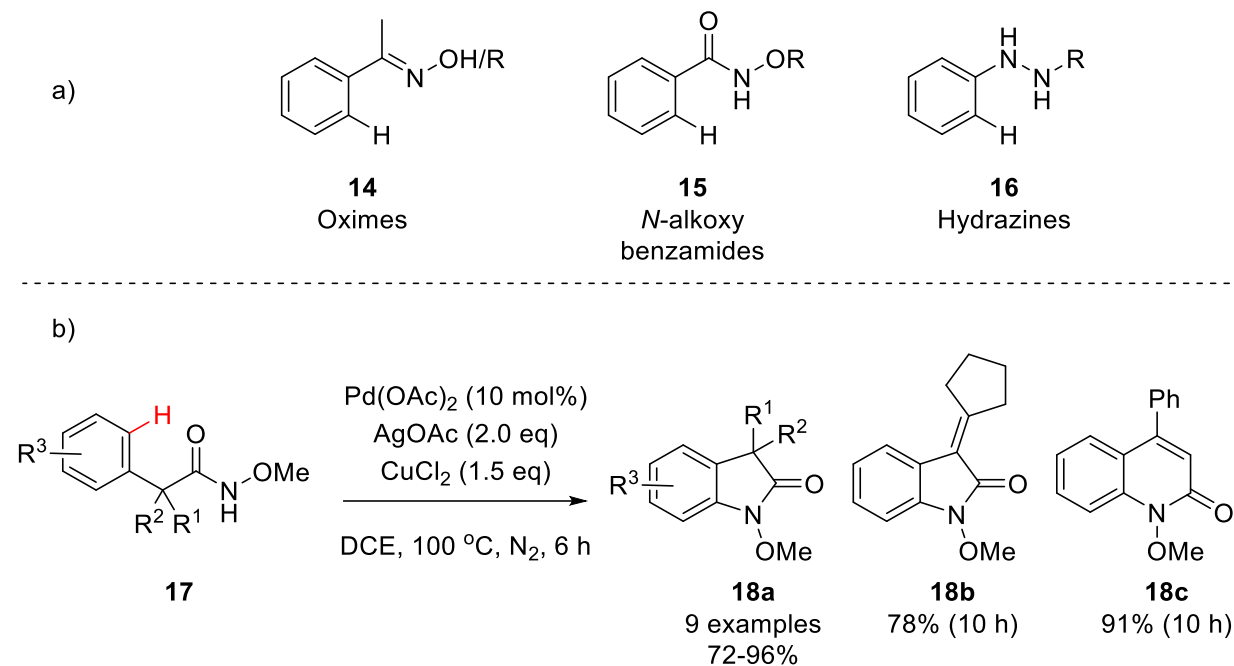
Early contributions to this concept were explored in palladium catalysed C-H transformations. For example, Cui and Wu performed a Pd-catalysed alkenylation of quinoline *N*-oxides **9** with electron poor alkenes **10**, where the *N*-oxide is the DG and internal oxidant (Scheme 6a).^[55] Hartwig *et al.* used with an oxime ester **12**, in a direct intramolecular amination reaction to make 2,3-substituted indoles **13** (Scheme 6b).^[56] However, in both cases, high temperatures were still required.



Scheme 6: Early examples of the Pd-catalysed C-H functionalisation strategies with internal oxidants

Nevertheless, a variety of oxidative DGs have been synthesised and employed successfully which has been particularly revolutionary for RhCp* catalysed C-H activation.^[42] The design is predominantly based on the weak covalent *N*-*O* bond (Scheme 7a), such as oximes **14** and *N*-alkoxy benzamides (can be referred to as hydroxamate) **15**. Also *N*-*N* bond directing groups, such as hydrazines **16**, have proved effective. In fact, the first successful report to exploit this directing group strategy was achieved by Yu *et al.* in 2008, employing *N*-OMe benzamides **21** (Scheme

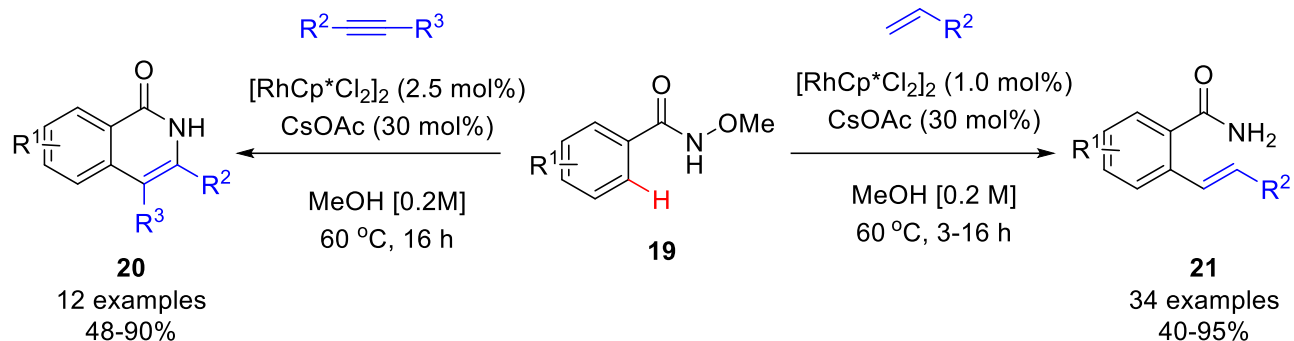
7b).^[57] This Pd(II)-catalysed intramolecular amination of sp^2 and sp^3 C-H provided access to a wide range of lactams **18a-c**.



Scheme 7: a) Selected oxidative DG. b) First successful report utilising palladium catalysed C-H activation of *N*-methoxy benzamides (OMe-aryl hydroxamate) by Yu *et al.* to obtain lactams.

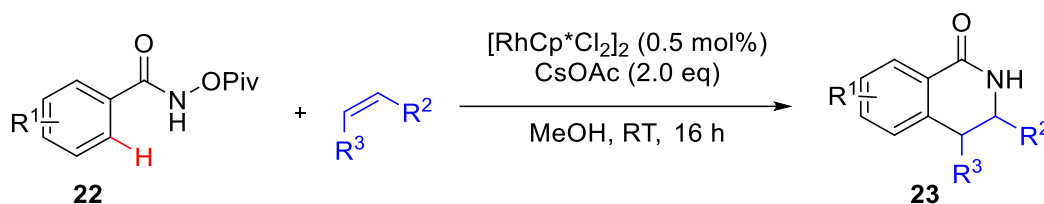
1.1.2.2.2 *N*-alkoxy Benzamides as Versatile Directing Groups

Owing to its simplicity and finely tuned coordination strength, the *N*-alkoxy benzamides have found wide application as directing groups in Rh-catalysed C-H activation. In 2010, Fagnou *et al.* reported the Rh(III)-catalysed annulation of *N*-OMe benzamides **19**, with internal alkynes to yield isoquinolones **20** (Scheme 8, left).^[58] The milder conditions, with temperatures reduced to 60 °C, allowed for high functional group tolerance without compromising reactivity or yields (48-90%).



Scheme 8: The use of *N*-OMe benzamides providing annulation (left) or olefination (right) products depending on the reaction partner.

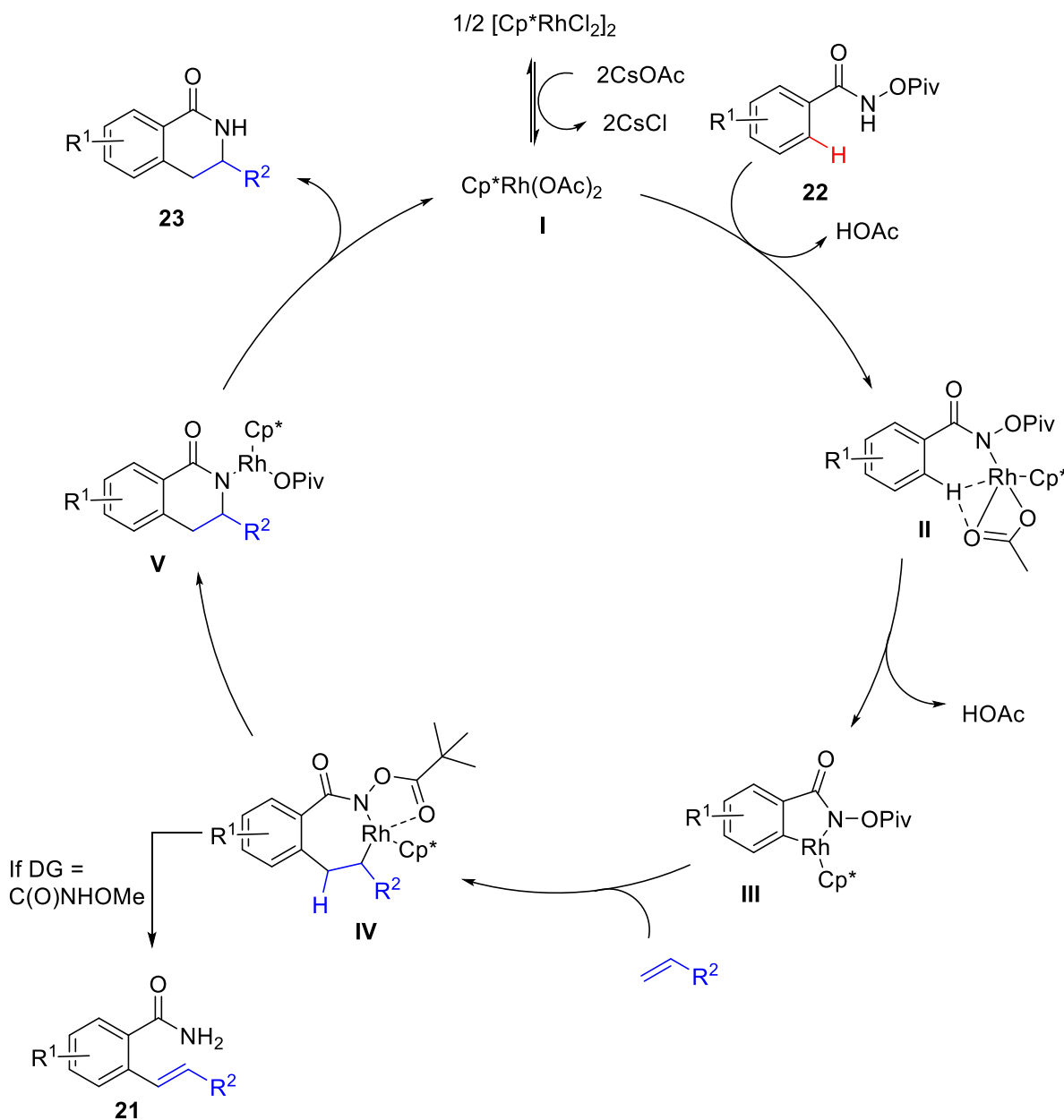
Interestingly, soon after, Glorius *et al.* presented a different outcome for the reaction when coupling alkenes with *N*-OMe benzamides; a regio- and stereoselective C-H olefination (Scheme 8, right). Moreover, when they employed *N*-pivalate (*N*-OPiv) benzamides, **22**, the reaction yielded dihydroisoquinolones (DHQs) **23**, as the sole product (Scheme 9).^[59] Concurrently, Fagnou *et al.* hypothesised that the same reaction favours the DHQ formation as the *N*-OPiv increases the stability of intermediates and behaves as a better leaving group. They found the pivaloyl group gave increased yields with reduced catalyst loading at room temperature.^[60]



Scheme 9: Synthesis of DHQs *via* Rh-catalysed annulation of *N*-OPiv benzamides **22** with alkenes

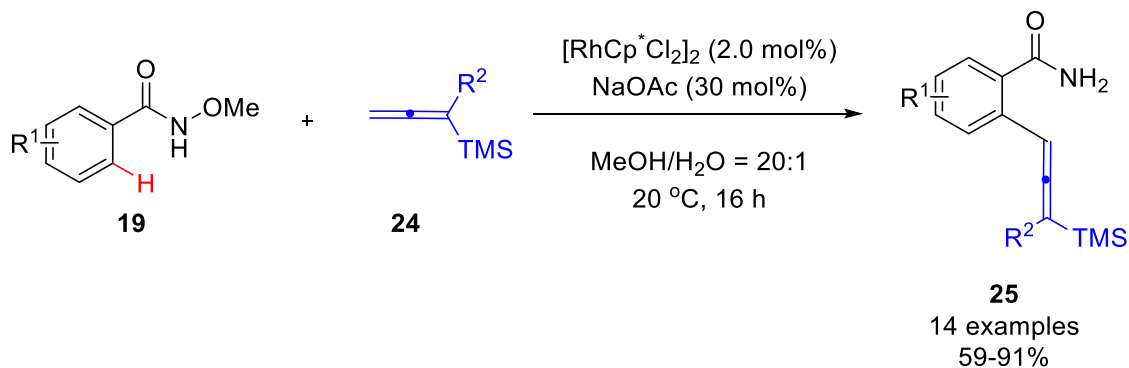
Both groups investigated and proposed reaction mechanisms that would explain the different product outcome with each directing group. Beginning with the formation of the active catalyst **I** by ligand exchange with the CsOAc (Scheme 10), this species then coordinates with the *N*-OPiv-benzamide **22** with a concomitant loss of acetic acid. Next, a concerted-metalation-deprotonation (CMD)^[32,61], whereby the C-H bond is cleaved with the aid of base, affords the 5-membered rhodacycle **III**. At this point the alkene associates and subsequently inserts in to the Rh-C bond to give the 7-membered rhodacycle **IV**. This intermediate is crucial in determining the product of the reaction. When the *O*-pivaloyl group is used, it is proposed that it stabilises the rhodium, by

coordination saturation, to allow for reductive elimination to give **V** which is quickly protonated to yield the 3,4-DHQ **23**. Whereas the *N*-OMe benzamide favours the β -hydride elimination pathway to give the olefin **21**.^[59]



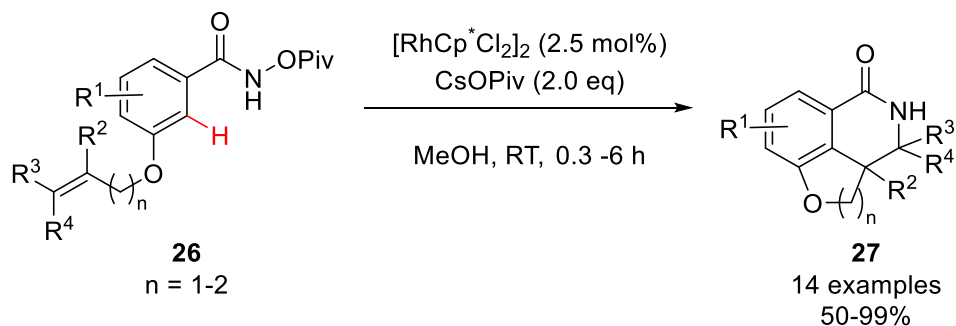
Scheme 10: Proposed catalytic cycle for the Rh(III)-catalysed reaction of *N*-OPiv benzamides with alkenes

This seminal work using *N*-alkoxy benzamides has proved extremely compatible with Rh-catalysed C-H functionalisation and its application has continued with novel coupling partners. For example, Ma *et al.* reported the Rh(III)-catalysed C-H bond allenylation coupling *N*-OMe benzamides with allenylsilanes **24** (Scheme 11).^[62] Under relatively mild conditions, the reaction afforded poly-substituted allenylsilanes **25** in excellent yields



Scheme 11: Rh(III)-Catalysed Heck-allenylation of *N*-OMe benzamides with silyl allenylsilanes **24**.

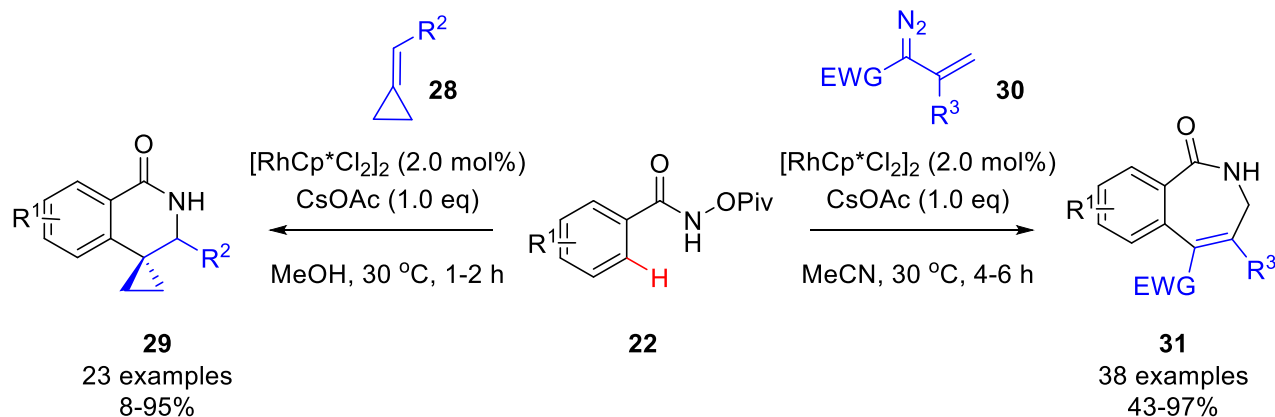
In 2013, Rovis *et al.* reported an intramolecular annulation with alkenes.^[63] The use of tethered olefins on *N*-OPiv benzamides **26** to access amidoarylation was demonstrated (Scheme 12). A wide variety of tethered alkenes were used to give five- and six-membered, biologically interesting 3-fused ring lactams **27** in good to excellent yields.



Scheme 12: Rh(III)-catalysed intramolecular amidoarylation to access fused-lactams **27**.

As the directing group can be incorporated into the final heterocyclic compound, other interesting NP-like scaffolds have been accessed with relative ease.^[49] Cui and co-workers were able to synthesise valuable spiro-DHQs **29** with complete regiocontrol using methylenecyclopropanes **28** (Scheme 13, left).^[64] The same group achieved a [4+3] cycloaddition-type C-H functionalisation

using vinylcarbenoids **30** to access azepinones **31**, a scaffold often found in natural products (Scheme 13, right).^[65] In both cases, a wide scope of substrate tolerating variable functional groups was demonstrated.



Scheme 13: Access to valuable lactams *via* Rh(III)-catalysed C-H functionalisation with *N*-OPiv benzamides.

1.1.3 Isoindolinones

Isoindolinones (1,3-dihydro-2H-isoindole-1-one), are considered a valuable privileged scaffold class, demonstrating diverse biological activity^[66] with therapeutic potential including antiviral,^[67] anti-inflammatory,^[68] and anti-cancer.^[69] It is often a key feature in many naturally occurring compounds like anti-fungal Pestachloride A **32**, and Taliscanine **33** which has shown anti-malarial properties as well as having links activity against Parkinsons disease.^[70,71] However it is also a popular core structure in many synthetic bioactive compounds, like sedative, Pazinaclone **34** (Figure 4).^[72]

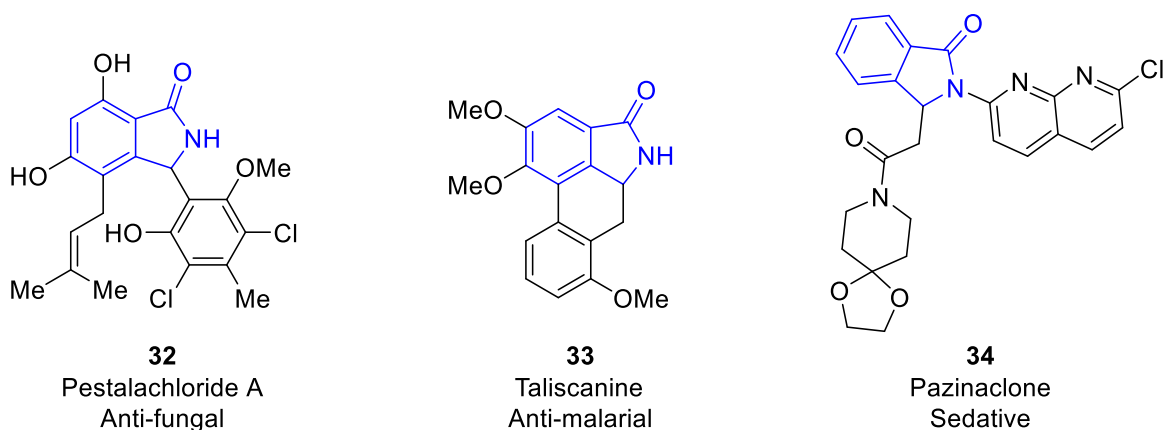
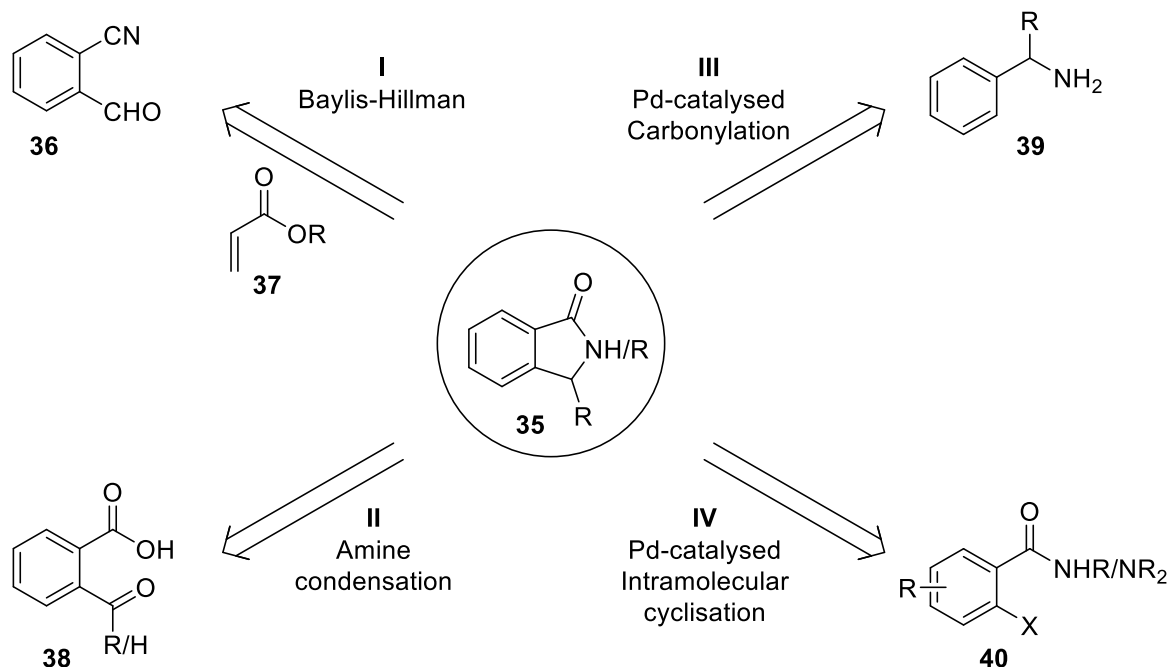


Figure 4: Selected examples of biologically active compounds possessing the isoindolinone scaffold.

1.1.3.1 Synthetic Strategies toward 3-Isoindolinones

The retrosynthetic analysis of the isoindolinone pharmacophore (Scheme 14, **35**) generally follows either the use of phthalimides^[73] or construction of the lactam ring. The former is not often used due to numerous steps required, including protection and deprotection of the nitrogen. The alternative, is the build the lactam, which can be achieved using various functionalised arenes (Scheme 14, path **I-IV**).^[74,75]



Scheme 14: Selected generic routes to access 3-substituted isoindolinones from simple starting materials.

For instance, 2-formylbenzonitriles **36** (path **I**) can undergo a Baylis-Hillman reaction with activated alkenes like **37** to form isoindolinones.^[76] Although a recent alternative, demonstrated by Li *et al.*, employed diaryliodonium in the presence of copper to activate the nitrile leading to a cascade cyclisation yielding 2,3-diarylisoinidolinones.^[77] Highly functionalised 3-isoindolinones are also formed using carboxybenzaldehydes **38**. Often this can be achieved through amide formation and cyclisation but more likely, imine formation *via* condensation would be employed to initiate multi-component reaction (MCR) cascades for lactamisation (path **II**). The Mannich reaction uses an amine and ketone, whereas an Ugi reaction uses amine with isocyanides.^[78]

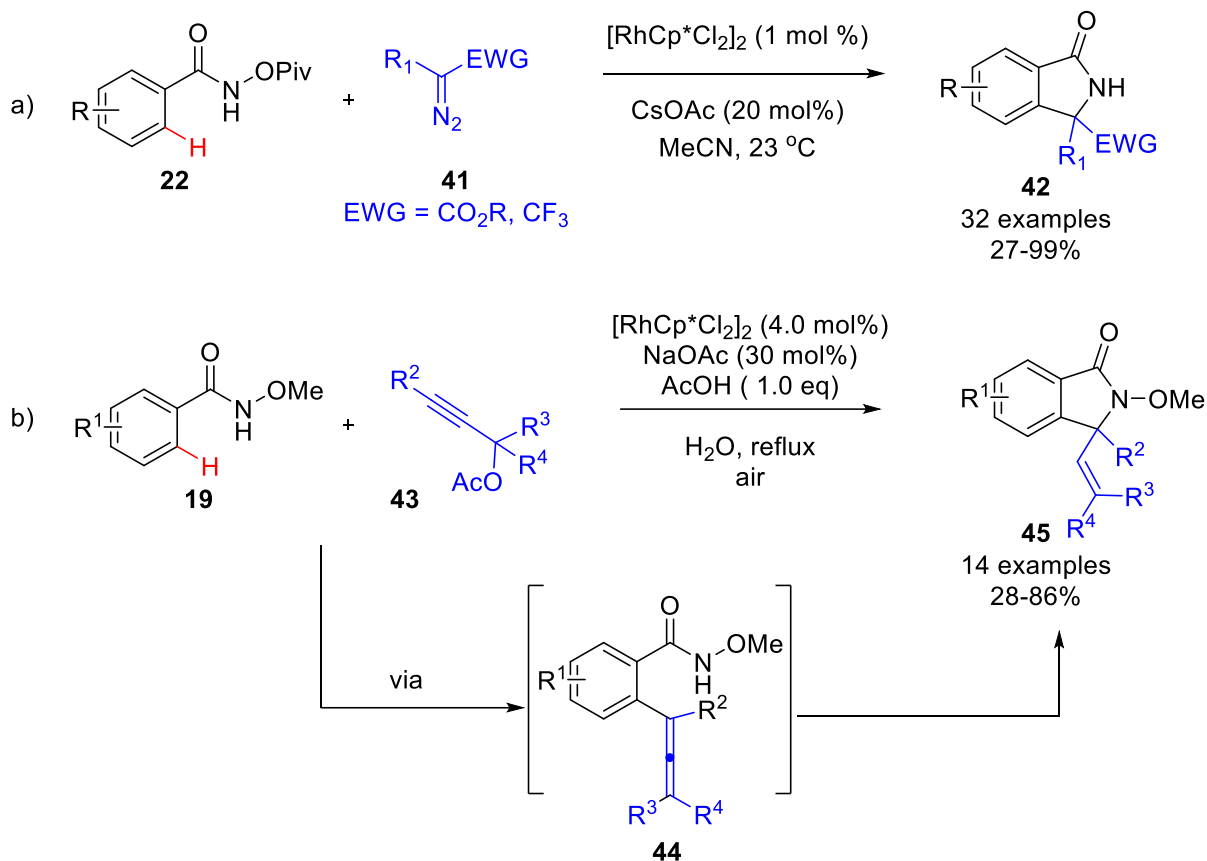
Transition metal-catalysed carbonylation methods have proven successful in synthesising isoindolinones with various starting materials. Recently, Wu *et al.* used a Pd-catalysed C-H

carbonylation of benzylamines **39** to obtain isoindolinone scaffolds (path **III**) in good yields under gas-free conditions with a CO surrogate.^[79] An alternative is to begin with cheap *ortho*-halobenzoylchlorides or even carboxylic acids that can be converted to amides **40** to allow for a Pd-mediated lactamisation with varying coupling partners (path **IV**).^[80] However, TM-catalysed C-H functionalisation, which avoids the need for halogenated starting materials, reduces number of steps and can be performed with various TMs has become an increasingly popular strategy to build heterocyclic structures including isoindoliones.^[74] Yet, reactions can come with certain structural caveats in order for reactions to succeed.

1.1.3.2 Isoindolinones *via* RhCp* catalysed C-H Functionalisation

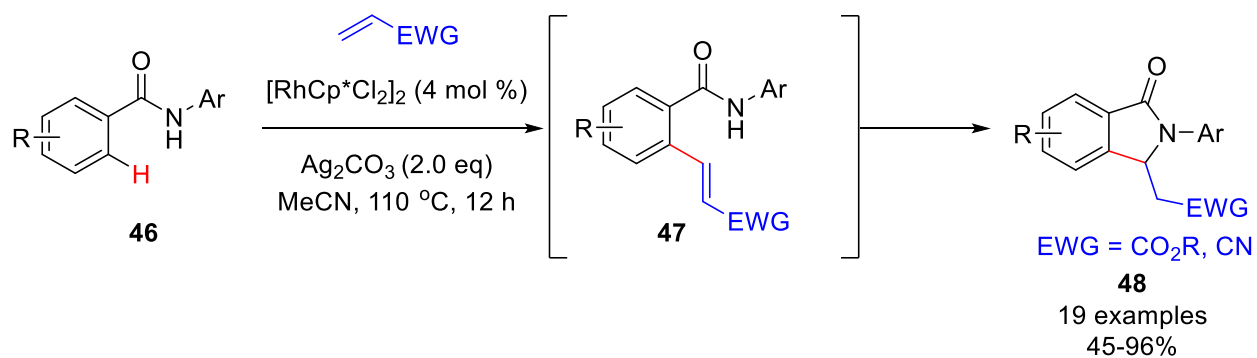
Synthetic methodologies using Rh-catalysis have been reported. An early example by Rovis *et al.* in 2013, was the coupling of diazo compounds **41** with *N*-OPiv benzamides **22** in a Rh-catalysed formal [4+1] cycloaddition (Scheme 15a).^[81] A limitation of this transformation is the need for an electron-withdrawing group in order to stabilize the carbene intermediate when nitrogen is released. Nevertheless, the method afforded a wide scope of isoindolinones **42** with good to excellent yields.

Another C1 annulation partner (propargyl acetates **43**) was employed by Ma *et al.* in an approach to access isoindolinones **45** with high yields.^[82] Interestingly, H₂O proved to be the optimal solvent, however, harsher conditions were required (Scheme 15b). The key intermediate in this transformation is the allene intermediate **44** which is formed following elimination of OAc. This allene can be coordinated to by rhodium to facilitate cyclisation.



Scheme 15: Strategies to access isoindolinones from *N*-OMe benzamides with RhCp* using diazo compounds and propargylic acetates as C1 annulation partners.

Isoindolinones could also be obtained using electron-deficient alkenes in a similar strategy. In this case, Li *et al.* described an oxidative C-H olefination using aryl carboxamides **46** to form the Heck-type intermediate **47** which was subsequently followed by a Michael-type addition yielding the desired isoindolinones **48** (Scheme 16).^[83] Again, elevated temperatures were required resulting in limited applicability.

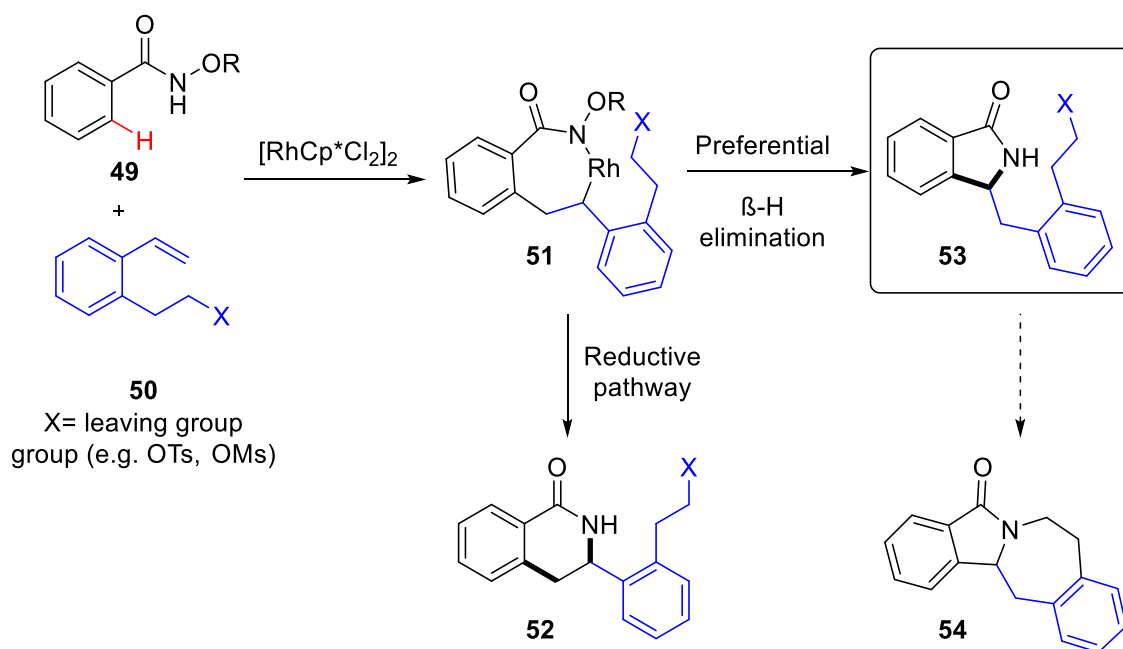


Scheme 16: RhCp^{*}-catalysed oxidative olefination/Michael addition to access isoindolinones with *e*-poor alkenes.

Despite advances in this field, direct formation of five-membered isoindolinones from *N*-alkoxy benzamides with a broader scope of alkenes under milder conditions would be valuable, particularly when exploring novel scaffold types.

1.2 Project Aim

With an understanding of the use of *N*-alkoxy benzamides in Rh(III)-catalysed C-H functionalisation, and typical routes to isoindolinones, a new synthetic route to this valuable scaffold was envisioned, with the hope of developing it in such a way to also access unexplored NP-like compounds. A principle aim of the project was to develop a Rh(III)-catalysed C-H functionalisation protocol, coupling *N*-alkoxy-protected benzamides like **49** with a designed *ortho*-substituted styrene. More specifically, a tethered *ortho*-substituent on the styrene bearing a leaving group **50** would lead to the 7-membered ring rhodacycle **51**. However, instead of the reductive pathway to DHQs **52**, the aim was to screen conditions in order to force its preferred pathway toward elimination. This could not only manipulate the reaction pathway toward novel isoindolinones **53** but also facilitate access to a second class of natural product-like (isoindolobenzazepines **54**) via an S_N2 reaction (Scheme 17).



Scheme 17: Design hypothesis to access isoindolinones **53** and isoindolobenzazepines **54** using *N*-protected benzamides with *ortho*-substituted styrenes.

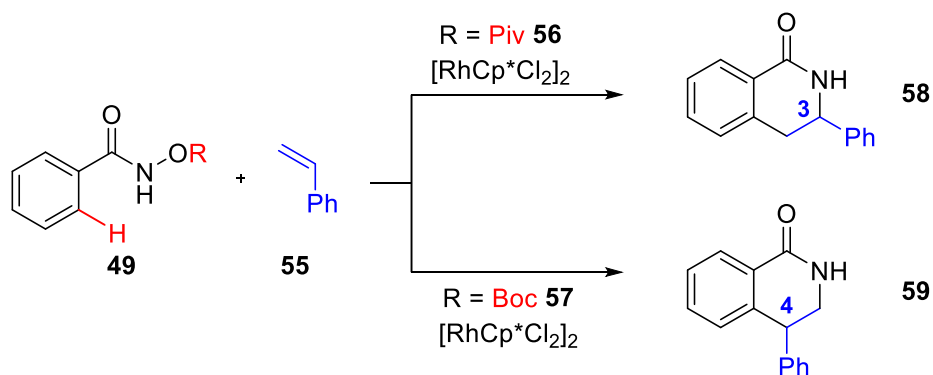
According to the current literature, there is so far no systematic study for the synthesis of these scaffolds. Therefore, establishing a reliable method would enable access to two unique and biologically relevant compound libraries and as such, these compounds should be screened in biological assays to determine if they would be a source for novel bioactivity.

1.3 Results and Discussion

This work was carried out in collaboration with Dr. Saad Shaaban. The results were reported in: *Chem. Eur. J.* **2020**, *26*, 10729.^[84]

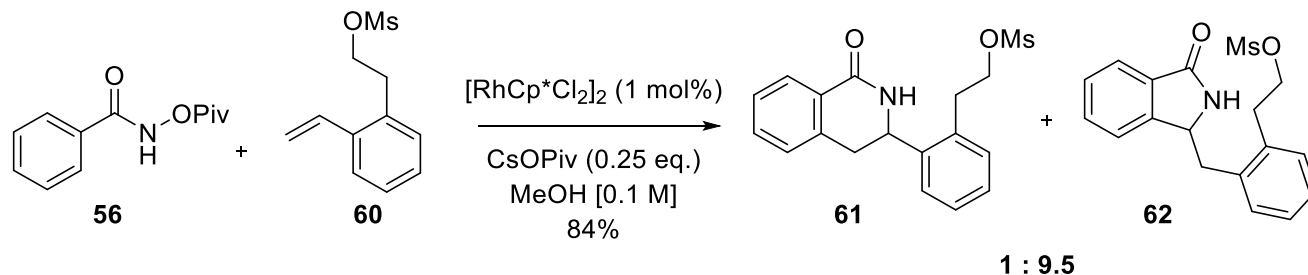
1.3.1 Background and Initial Results

The chemistry of coupling *N*-OPiv benzamides **22** with alkenes is known to produce 3-substituted DHQs and, in the case of styrene **55**, the 3-substituted derivative thereof **58**.^[59,60] In 2018 Perekalin *et al.* reported that the use of the *N*-OBoc benzamide **57** led to the formation of regioisomer, DHQ **59** as the sole product (Scheme 18).^[85] The reasoned switch in regioselectivity was attributed to steric hindrance.



Scheme 18: Effect of the alkoxy substituent on the region-control of the RhCp* C-H functionalisation with styrene.

However, there is, so far, no report employing *ortho*-substituted styrenes, a key component of the reaction hypothesis. Initial investigations began with the reaction of *N*-OPiv benzamide, **56**, with designed styrene **60**, under standard reaction conditions (Scheme 19). Surprisingly, the reaction resulted in a mixture of regioisomers (1: 9.5), in which the major product was the isoindolinone **62**

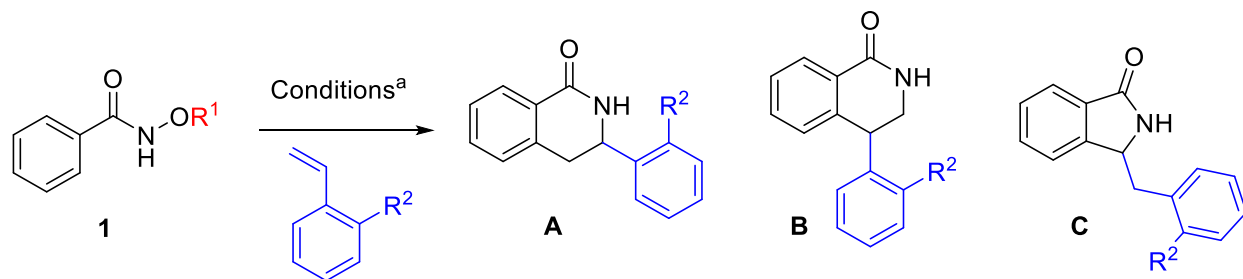


Scheme 19: Initial reaction of designed *ortho*-substituted styrene **60** with *N*-OPiv benzamide **56** to give isoindolinone **62** as the major product.

This result suggested a need to evaluate the effect of the *ortho*-substituent on the styrene and also the effect of the alkoxy group.

1.3.1.1 Solving the Puzzle: Exploring the Effect of *Ortho*-Substituted Styrenes

Investigation began with the screening of different *ortho*-substituted styrenes and compared the outcome when using *N*-OPiv- and *N*-OBoc-benzamides (Table 1). In accordance with the literature, the reaction of *N*-OPiv benzamide **56** with styrene provided DHQ-A^[60], whereas the reaction with *N*-OBoc gave a 1:10 mix of isomers A and C. With the addition of an *ortho*-substituent, a mixture of regioisomers (A and C) was observed with *N*-OPiv, but in all cases, C was the major product. However, when using *N*-OBoc **57**, regioisomer C was obtained as the only product in all cases. The structures of A and C with 2-bromostyrene were confirmed by X-Ray analysis (Figure 5). Importantly, regioisomer B was never obtained in any of the reaction conditions.

Table 1: Study of the effect of *ortho*-substituent of the styrene moiety on regioselectivity.

Styrene, R ²	H (55)	Me (63)	Br (64)	CH ₂ CH ₂ OMs (60)
R ¹ = Piv (56)	A	A : C 1 : 7.5	A : C 1 : 3.4	A : C 1 : 9.5
R ¹ = Boc (57)	A : C 1 : 10	C	C	C

[a] [RhCp*Cl₂]₂ (1.0 mol%), CsOPiv (25 mol%) in MeOH [0.1M] at RT for 14h. Yields were determined by ¹H-NMR using 1,3,5-trimethoxybenzene as internal standard. Ratios were determined from the crude ¹H-NMR.

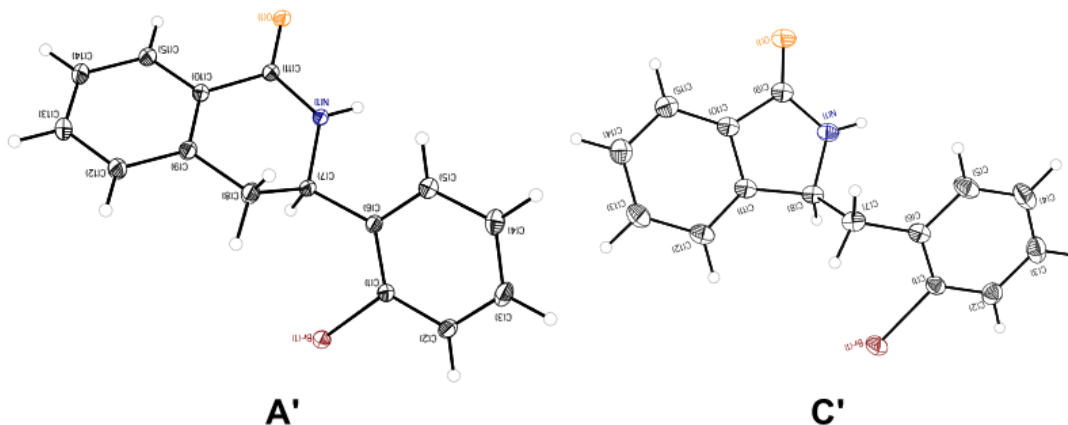


Figure 5: Crystal structures to confirm the structures of regioisomers A and C with from the reaction using 2-bromostyrene.

Moreover, compared to an alternative synthesis of DHQ-B **59** (with no *ortho*-substituent) reported by Ellman *et al.*, the key characteristic proton (adjacent to the nitrogen) chemical shift for DHQ-B is 4.32 ppm.^[86] This was in contrast to the reports of Perekalin of 4.81 ppm. It was therefore concluded that previous reports of Perekalin and also Cramer (enantioselective version)^[87] had erroneously assigned 4-DHQ and instead they had also been forming the 5-membered isoindolinone C.

1.3.2 Reaction Optimisation

From the outset, we explored the reaction conditions using *N*-OPiv benzamide **56** with 2.0 equivalents of the designed styrene **60**. Despite our initial result forming the isoindolinone **62** in excellent yield (Table 2, Entry 1) further optimisation was needed to reduce the formation of the 3-DHQ **61** in favour of a more selective reaction. Initial changes in solvent led to reduced yields and/or selectivity (Entries 2-5). Reducing the stoichiometry of the styrene led to an improvement in the total yield up to 93% (Entries 6 and 7), but offered no additional improvement to selectivity unless heated which compromised yield (Entry 8). The reaction was also performed with *N*-OBoc benzamide **57**. The resulting yields were comparatively lower than with *N*-OPiv but importantly the isoindolinone **62** was formed exclusively. There was also no significant difference in yield when using reduced equivalents of the styrene or increasing the temperature (Entries 9-11). Further optimisation of the base (Entries 13-18) revealed that a catalytic amount of potassium acetate KOAc in methanol (Entry 15) resulted in the formation of desired product **62** in 74% isolated yield.

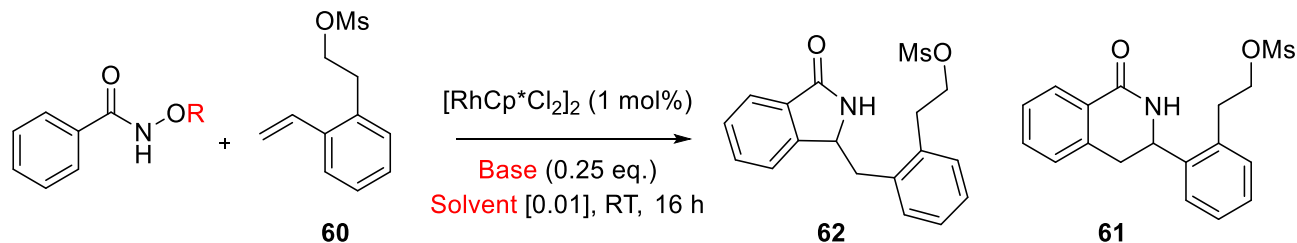


Table 2: General reaction optimisation of solvent, base, temperature and directing groups

Entry	R	Solvent	Base	Total yield (%) ^a	Ratio (62: 61)
1	Piv	MeOH	CsOPiv	84	8.3 : 1
2	Piv	DCM	CsOPiv	46	5.6 : 1
3	Piv	MeCN	CsOPiv	27	8.0 : 1
4	Piv	HFIP	CsOPiv	0	—
5	Piv	Toluene	CsOPiv	71	10.8 : 1
6	Piv	MeOH (1.2 styrene)	CsOPiv	86	8.6 : 1
7	Piv	MeOH (1.5 styrene)	CsOPiv	93	6.8 : 1
8	Piv	MeOH (40 °C)	CsOPiv	69	12.8 : 1
9	Boc	MeOH (2.0 styrene)	CsOPiv	70	>99:1
10	Boc	MeOH (1.5 styrene)	CsOPiv	70 (69) ^b	>99:1
11	Boc	MeOH (40 °C)	CsOPiv	71	>99:1
12	Boc	DCM	CsOPiv	43	>99:1
13	Boc	MeOH	KOPiv	60	>99:1
14	Boc	MeOH	CsOAc	77	>99:1
15	Boc	MeOH	KOAc	84 (74) ^b	>99:1
16	Boc	MeOH	K ₂ CO ₃	19	>99:1
17	Boc	Toluene	KOAc	24	>99:1
18	Boc	MeOH	-	0	-

[a] Determined by ¹H-NMR using 1,3,5-trimethoxybenzene as the internal standard (1.0 equiv.). [b] Isolated yield

With these optimised reaction conditions, the use of different protecting groups on the benzamide was also explored (Table 3). As mentioned previously, the Boc-protected amide led to the formation of isoindolinone **62** in a completely regioselective manner but interestingly, acetyl (Ac)- and Cbz-protected benzamides also produced **62** exclusively albeit in slightly lower yields (Entries

3 and 5). The benzoyl (Bz)-protected amide displayed lower regioselectivity (Entry 4) whilst the Me-protected benzamide showed no reactivity (Entry 6).

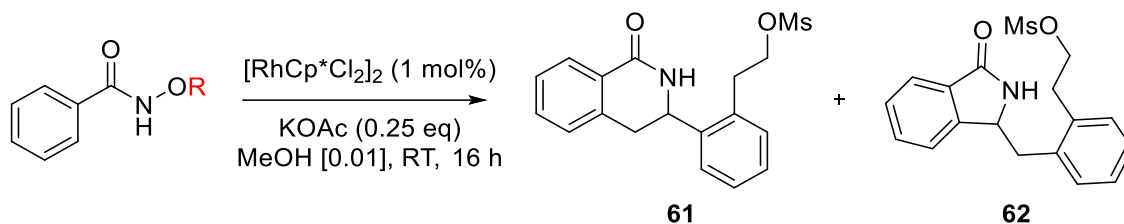


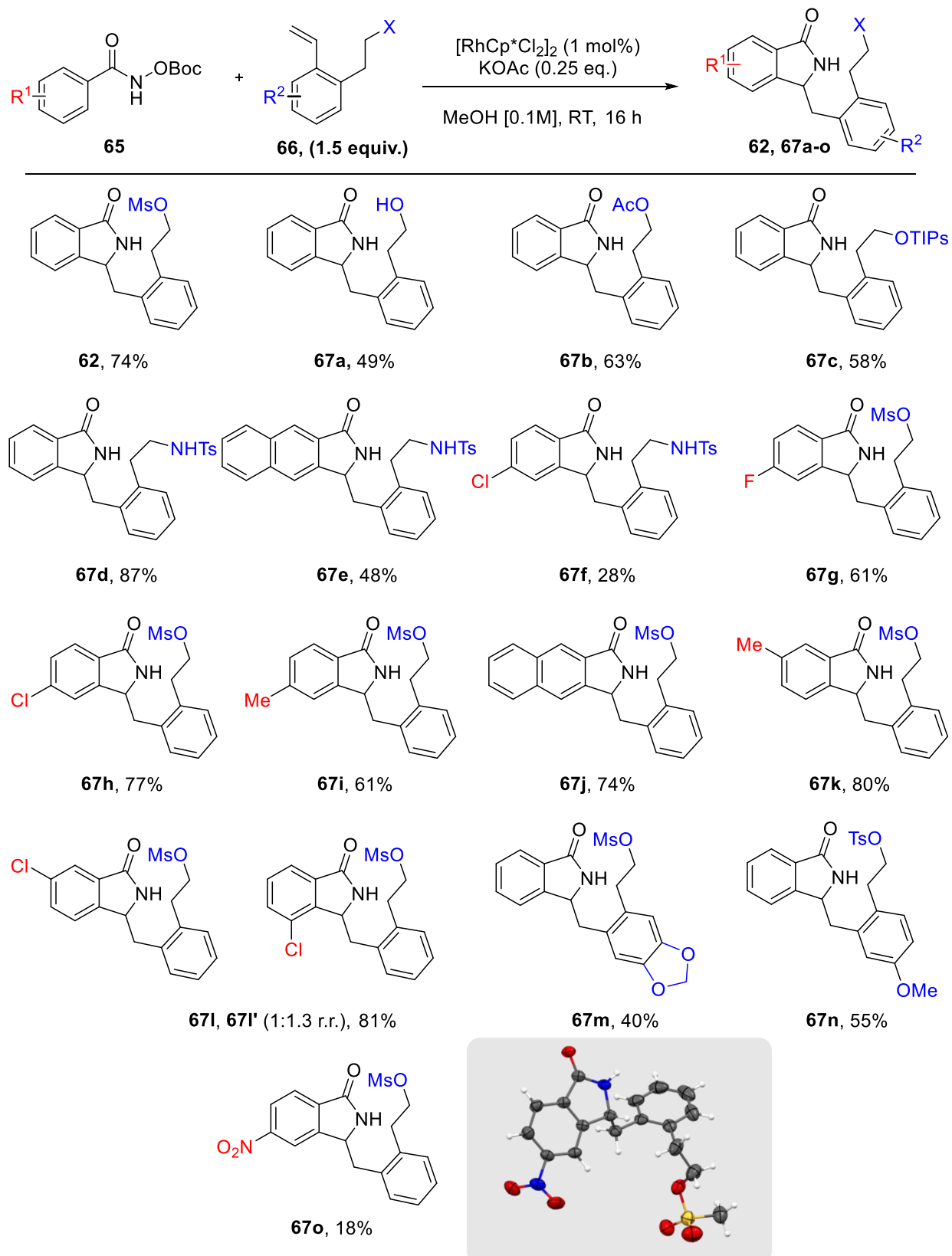
Table 3. Effect of the alkoxy benzamide protecting group.

Entry	R	Total yield % ^[a]	Ratio (A : C)
1	Piv	84	1 : 8.3
2	Boc	84	Only C
3	Ac	75	Only C
4	Bz	77	1 : 26
5	Cbz	71	Only C
6	Me	-	-

[a] Determined by H-NMR using 1,3,5-trimethoxybenzene as an internal standard (1.0 equiv.).

1.3.3 Scope of Substrates

With final optimised reaction conditions in hand, we proceeded to study the scope of this transformation (Scheme 20). Different alcohol protecting groups, on the *ortho*-substituted styrene, (OAc, OTIPs and NHTs) were well tolerated, giving the desired isoindolinone in yields ranging from 58% to 87% (**67b-d**). Interestingly, the reaction also proceeded well with the free alcohol (**67a**), indicating it does not interfere with the Rh catalyst during the reaction. Different functional groups (Cl, F, Me,) in varying positions on both the aryl benzamides and styrenes, were tolerated to yield the desired adducts in good yields (**67f-n**). Conversely, the nitro-substituted benzamide **67o** was isolated in low yield but was used to confirm the isoindolinone structure by means of X-Ray crystallography. Interestingly, also observed by Rovis *et al.*, was the influence of the benzamide *meta*-substituent on the regioselectivity of the C–H activation.^[81] In this case, the *meta*-methyl derivative yielded only a single regioisomer in high yield (**67k**), whereas its chloro-analogue gave a 1:1:3 mixture of regioisomers **67l** and **67l'**.



Scheme 20: Scope of Isoindolinones, with structure confirmation by X-Ray crystallography.

1.3.3.1 Reaction Limitations

During the course of exploring the substrate scope, some substrates probed were not successful (Figure 6). In particular, any *ortho*-substituent on the benzamide led to trace or no product formation. This configuration was tried with different electronic groups of varying sizes in order to determine an explanation, but all failed to provide the product. Disappointingly, carbonyl derivative **67u** and electron rich sulphur containing heterocycles **67v** and **67w** also provided only trace product.

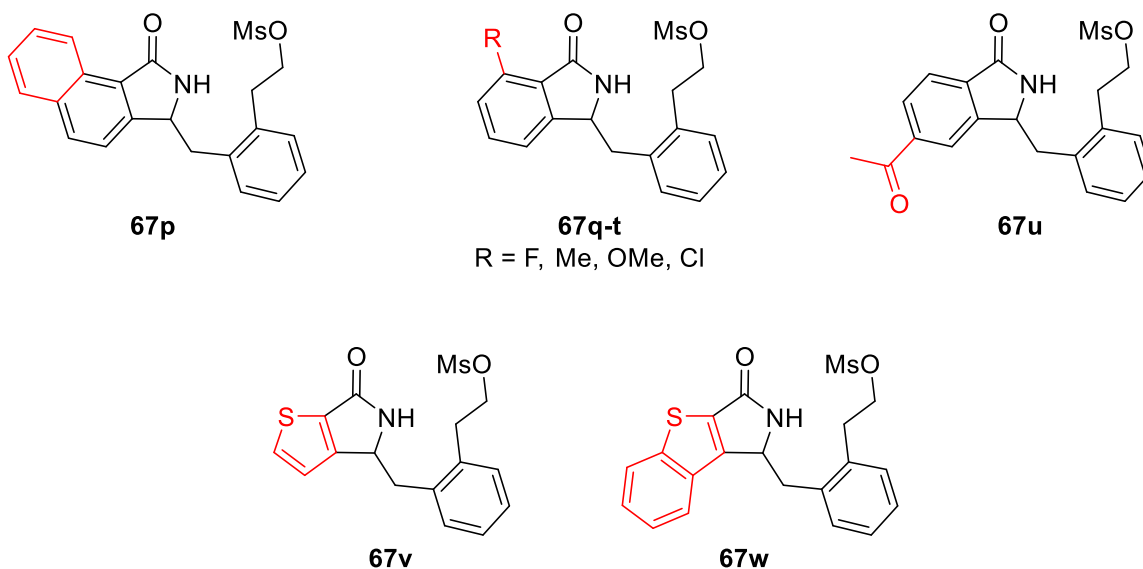


Figure 6: Unsuccessful substrates.

1.3.4 Access to Natural Product-like Isoindolobenzazepines

The isoindolinone scaffold, under basic conditions, could be used to induce a cyclisation and eliminate the in-built leaving group that originated from the pre-designed styrene. This would result in an isoindolobenzazepine scaffold **68** that is commonly found in the aporphoadane alkaloid family that includes compounds like lennoxamine **69** (Figure 7).^[88] However, members of this alkaloid family, to the best of our knowledge, have not previously shown significant pharmacological activity but their unique structural features render them attractive synthetic targets in the hunt for novel bioactive compounds.

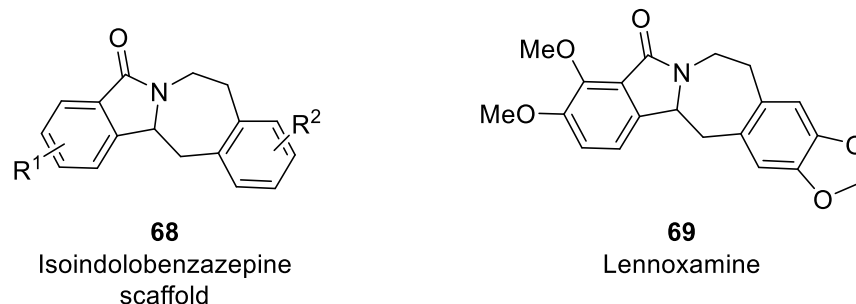
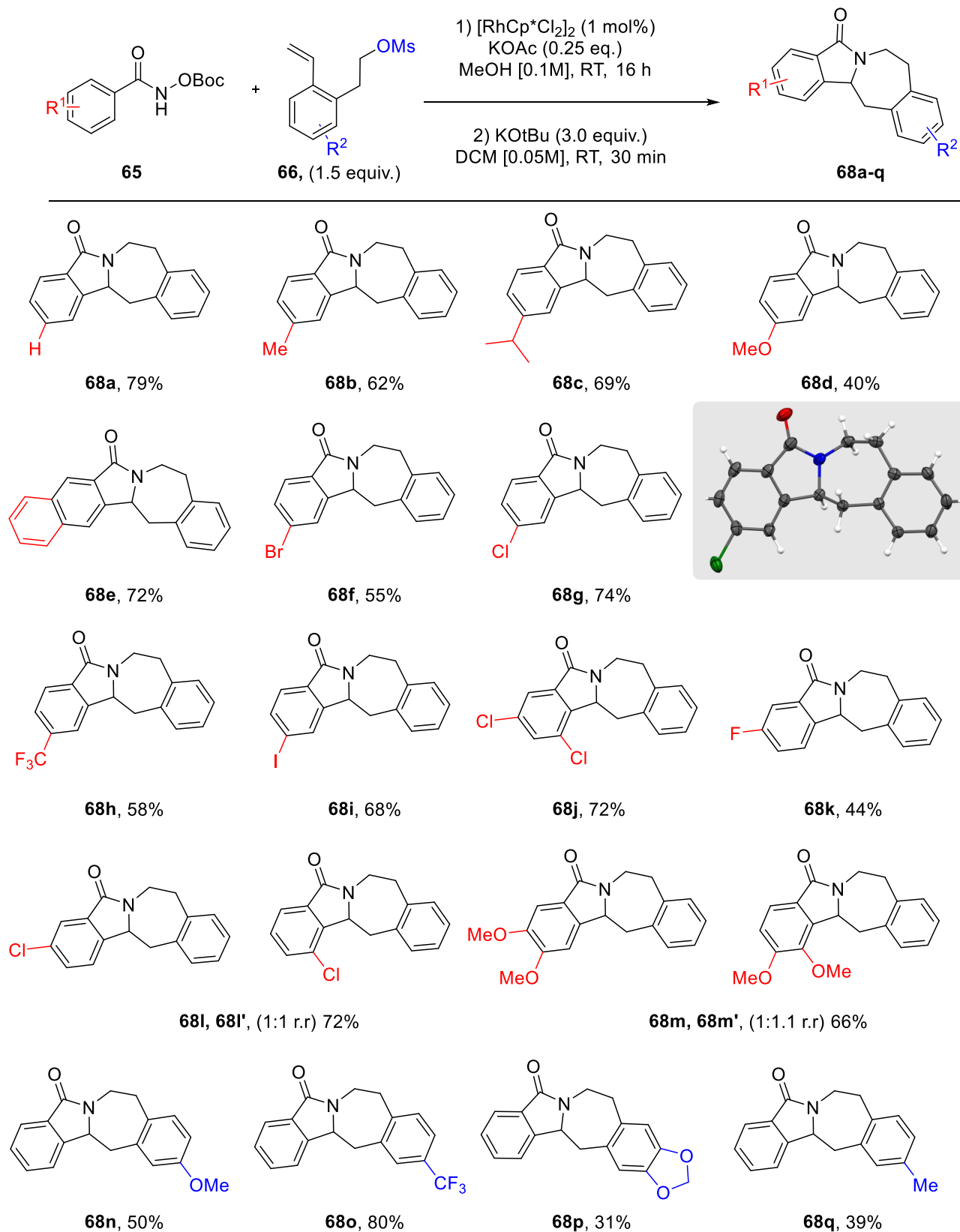


Figure 7: Illustration of the isoindolobenzazepine scaffold and a NP containing isolate from this family.

In this regard, the development of a one-pot-two-step reaction, where C-H functionalisation is subsequently followed by cyclisation, would be a simple and efficient way to afford isoindolobenzazepine derivatives.

1.3.4.1 Reaction Optimisation for the One-Pot-Two-Step Synthesis of Isoindolobenzazepines

Initial attempts to induce cyclisation used common bases (i.e. LDA, KOH, NaH), however this resulted in little or no conversion of starting material. It was found that potassium tert-butoxide in THF gave a reasonable yield of 50% in a short reaction time 10 minutes (Table 4, Entry 1). Other solvents were tested to find DCM gave a slightly better results and solubility (Entry 3) so was taken forward to explore other parameters. Reducing the stoichiometry of the base to 1.0 equivalent had a detrimental effect on the yield (Entry 5), whereas increasing the concentration to 0.1 M increased the yield to 60% (Entry 6) but no further significant increase was achieved at 0.25 M (Entry 7). Continual increase in the quantity of base (Entries 7-9) revealed 3.0 equivalents to be optimal at a concentration of 0.05 M for 30 minutes, with an isolated yield of 67% (Entry 8).



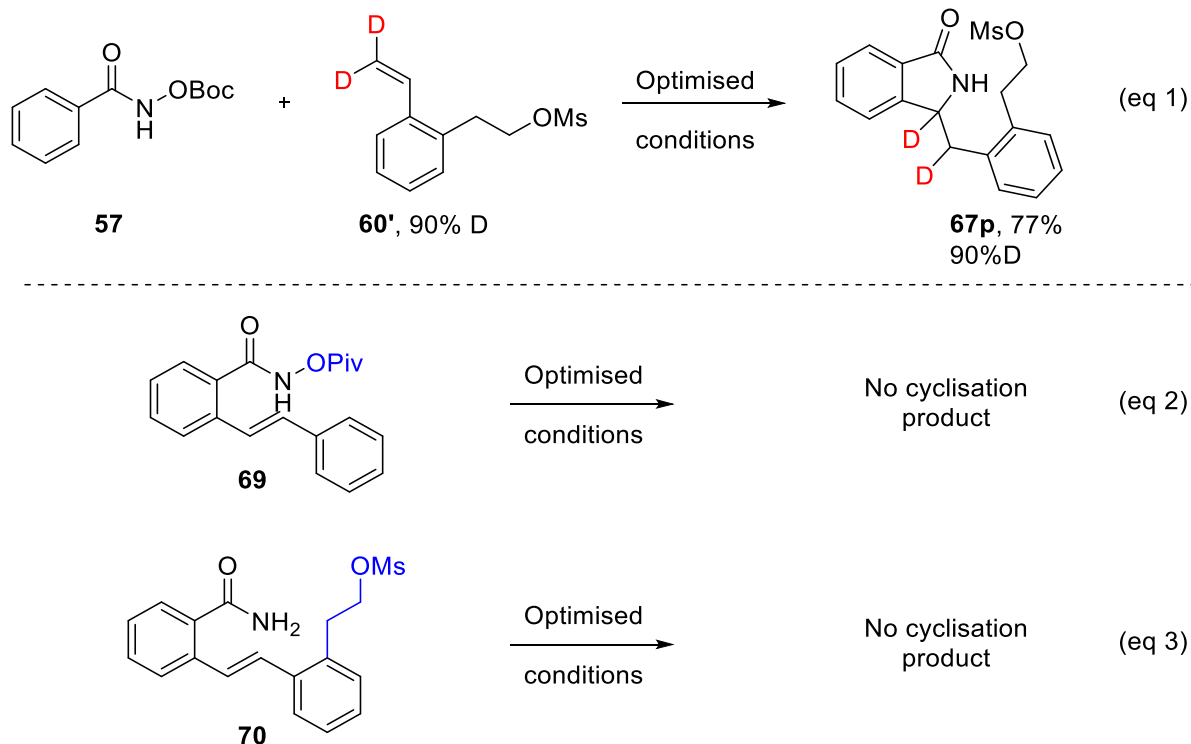
Scheme 21: Scope of isoindolobenzazepines with X-Ray structural confirmation.

1.3.5 Mechanistic Investigation

In order to propose a plausible mechanism for the regioselective formation of isoindolinones, we performed select experiments and DFT (Density Functional Theory) calculations of key intermediates.

1.3.5.1 Deuterium Labelling

The C-H functionalization reaction was performed under optimal conditions using deuterium labelled styrene **60'** (Scheme 22, eq 1). This afforded the desired, deuterium incorporated, isoindolinone product **67p**. Through $^1\text{H-NMR}$ analysis, it was determined that one deuterium atom had remained on the original carbon of the styrene starting material but the second deuterium atom had migrated. Additional experiments, involved submitting possible reaction intermediate starting material to the optimal conditions. Interestingly, the β -hydride elimination intermediate with simple styrene and designed styrene did not yield the cyclisation product (Scheme 22, eq 2 and 3). These findings supported the notion that the formation of the isoindolinone is not *via* a typical Michael-type addition, which agrees with the fact that RhCp^* does not catalyse a hydroamination reaction.^[89]

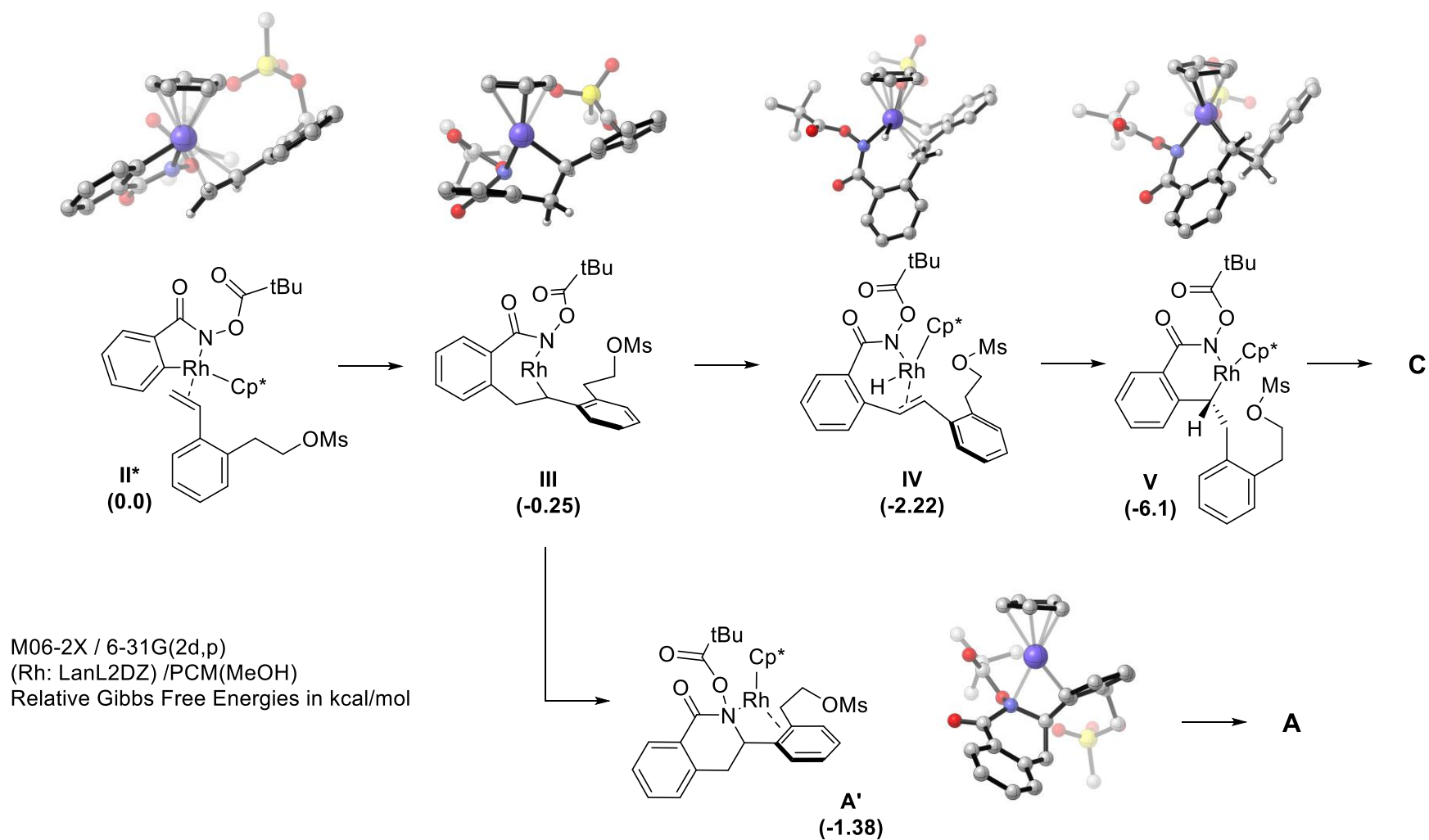


Scheme 22: Results of the deuterium labelled experiment and additional experiments to replicate intermediates.

1.3.5.2 Computational Experiments

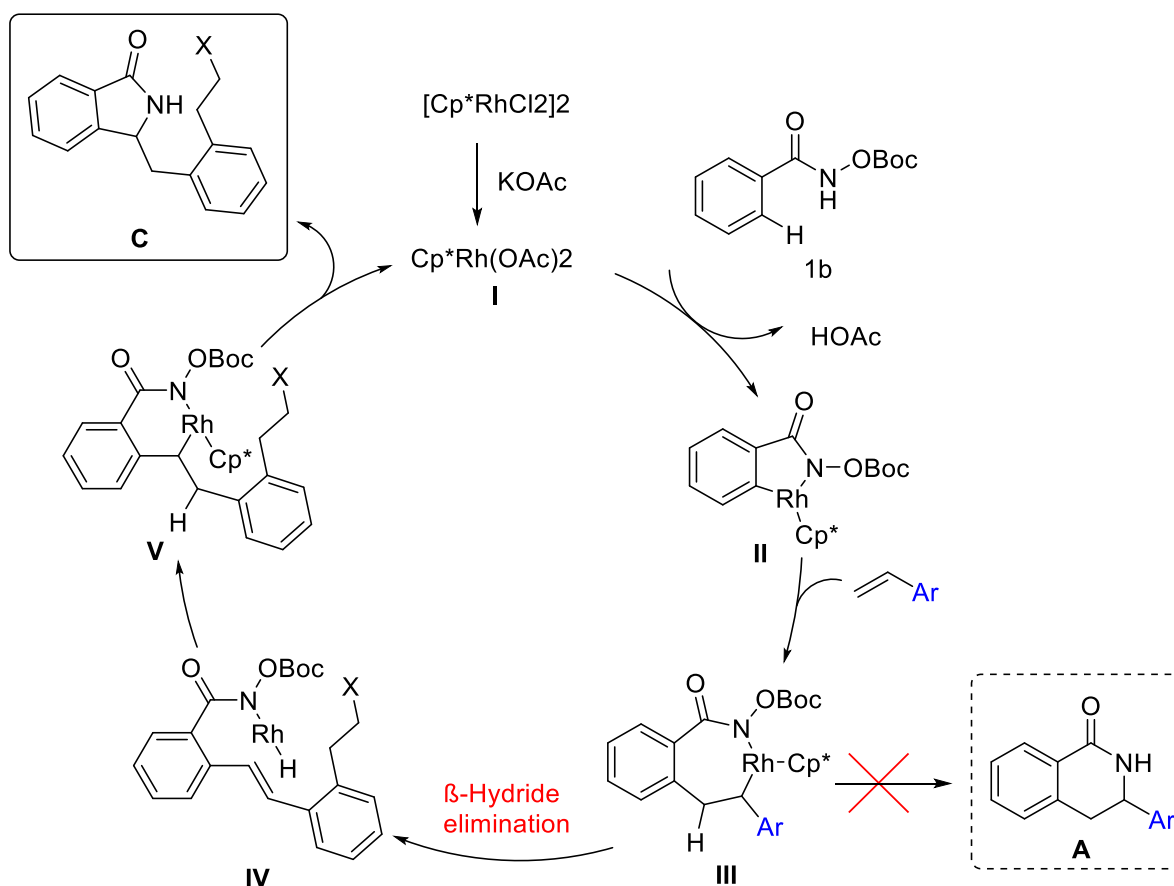
All simulations and calculation performed by Prof. Dr. Christian Merten.

Additional computational analysis of the reaction of *N*-OPiv benzamide **56** with designed styrene **60** were performed (Figure 8). The calculations begin with the pentarhodacycle **II*** converted to **III** via insertion of the styrene. Gratifyingly, the results indicated that the formation of key intermediate **V** from **III** is energetically favoured over the pathway leading to dihydroisoquinolone **A**. Notably, as the energy difference between **III** to **IV** and **III** to **A**' is not so large, it explains why minor amounts of DHQ-A can be formed. Overall, this analysis supported that β -hydride elimination is preferred with styrenes.

Figure 8: Computational analysis showing calculated energies for the proposed key intermediates with *N*-OPiv benzamide.

1.3.5.3 Proposed Mechanism

Based on the mechanistic investigation and previous reports^[59,90,91], the proposed mechanism (Scheme 23) for the reaction is initiated by ligand exchange to form the active catalyst **I**. Insertion of the rhodium species into the C-H bond affords pentarhodacycle intermediate **II** which is followed by insertion of the styrene to provide the seven-membered metallocycle **III**. This key intermediate may undergo reductive elimination to dihydroisoquinolone **A**^[90], however, the coordination of the tethered group to the Rh, favours the β -hydride elimination pathway leading to rhodium hydride species **IV**. Subsequent migratory insertion of the hydride into the olefin provides the six-membered ring rhodacycle **V**. Lastly, reductive elimination followed by *N-O* bond cleavage delivers the desired isoindolinone.



Scheme 23: Proposed mechanism for the RhCp*-catalysed formation of isoindolinones with *N*-OBoc benzamides with *ortho*-substituted styrenes.

1.3.6 Biological Evaluation

Given the novel nature of the two compound classes, the libraries of both isoindolinones and the cyclised isoindolobenzazepines were initially subjected to several cell-based assays. The Compound Management and Screening Center (COMAS) of the Max Planck Institute of Molecular Physiology are able to perform high-throughput screening of assays covering biological pathways associated with processes such as autophagy modulation, glucose uptake, reactive oxygen species (ROS) formation, kynurenine production and osteogenesis.

1.3.6.1 Hedgehog (Hh)-Dependent Osteoblast Differentiation

Misregulation of molecular signalling pathways that are responsible for cellular processes has been directly associated with a variety of diseases.^[92] The hedgehog (Hh) signalling pathway is critical for normal embryonic development but is also important in adults for stem cell homeostasis and regenerating adult tissues.^[93,94] Abnormal regulation of Hh signalling is involved in severe birth defects and various types of cancer, including basal cell carcinoma and medulloblastoma.^[93,95] Therefore, identifying novel small molecule inhibitors is of high interest.

Bone formation, otherwise known as osteogenesis, is a complex regeneration process that is regulated by many signalling pathways, including Hedgehog (Hh). During this process, osteoblasts, which differentiate from mesenchymal stem cells (MSCs), are responsible for bone development.^[96] This differentiation of cells requires Hh-signalling and as a result this process can be used, by means of a phenotypic assay, to identify possible pathway inhibitors.

In order to investigate the effect of small molecules on Hh signalling, a Hh-dependent osteoblast differentiation assay with C3H10T1/2 cells was employed for primary screening (Figure 9).^[95,97] The Hh pathway can be activated using the Smoothened (SMO) agonist purmorphamine **71**. The induced Hh signalling leads to the differentiation of MSCs into osteoblasts and, thereby to expression of the osteoblast-specific marker alkaline phosphatase (AP).^[98] The activity of this enzyme serves as a measure of Hh-dependent osteoblast differentiation whereupon treatment with CDP-Star, a chemiluminescent substrate for alkaline phosphatase, enables fast detection of biomolecules by producing visible light.

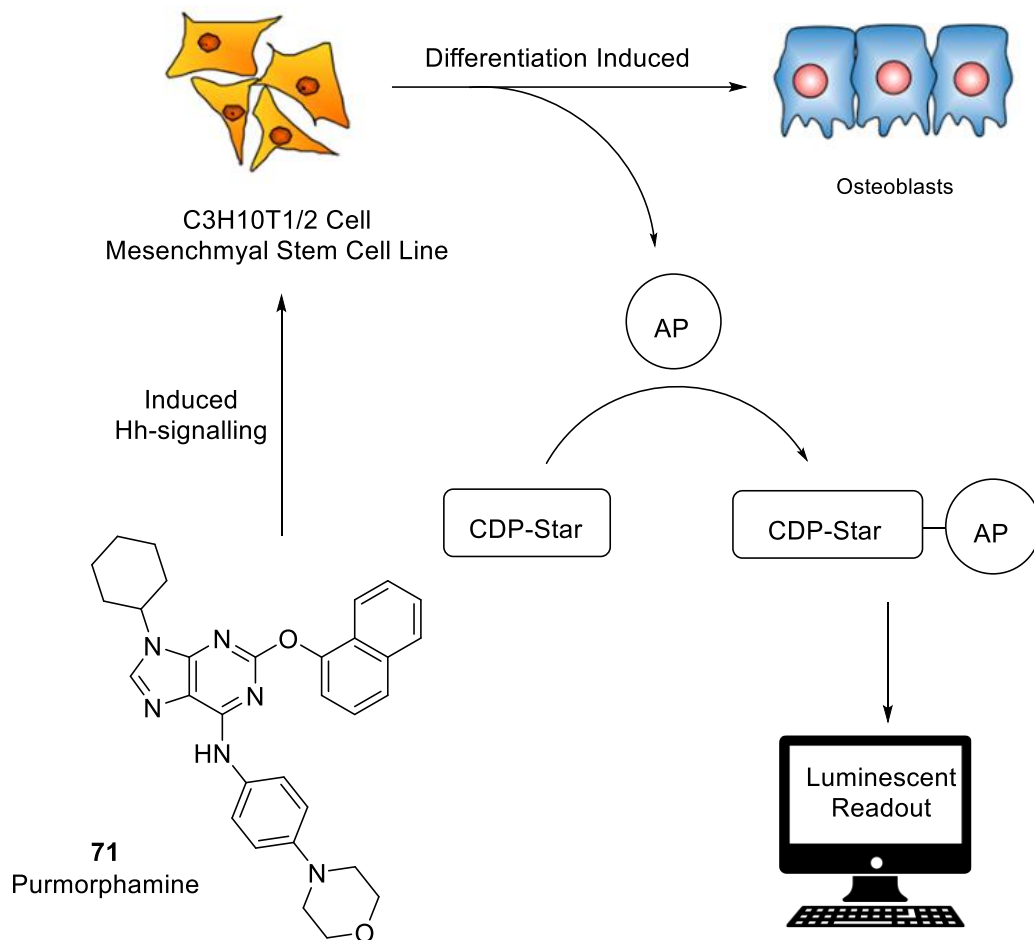


Figure 9: General assay principle for osteoblast differentiation

With compound treatment, inhibition would be shown *via* a reduced luminescent readout.

1.3.6.2 Novel Inhibitors of Hh-Dependent Osteoblast Differentiation

Additional biological investigation and assays were performed by Dr. Jana Flegel.

When subjected to the osteoblast differentiation assay the screen revealed several derivatives, both isoindolinones and isoindolobenzazepines, inhibited Hh-dependent differentiation of multipotent murine mesenchymal progenitor stem cells into osteoblasts. Interestingly, early results of both isoindolinones and isoindolobenzazepines revealed inhibitory effect. For the isoindolinones, there was a clear difference in the activity depending on the heteroatom on the alkene tether, even with the chloro-substitution at different positions (Figure 10, **67f** and **67i**). The NHTs provided a half-maximal inhibitory concentration (IC_{50}) of $2.1 \pm 1.1 \mu\text{M}$ whilst the mesylate group was more potent with an IC_{50} of $1.1 \pm 0.5 \mu\text{M}$. However, isoindolobenzazepine, **68r**, gave an IC_{50} of $0.6 \pm 0.2 \mu\text{M}$. When compared the acetal **67m**, it would seem the position of the chloro-substituent is key to activity. Of course, with this initial small screen, significantly more testing to establish a structure-activity relationship (SAR) would be needed particularly with the cyclised isoindolobenzazepines. Furthermore, in order to determine if they are Hh-signalling inhibitors more in-depth biological experiments should be performed.

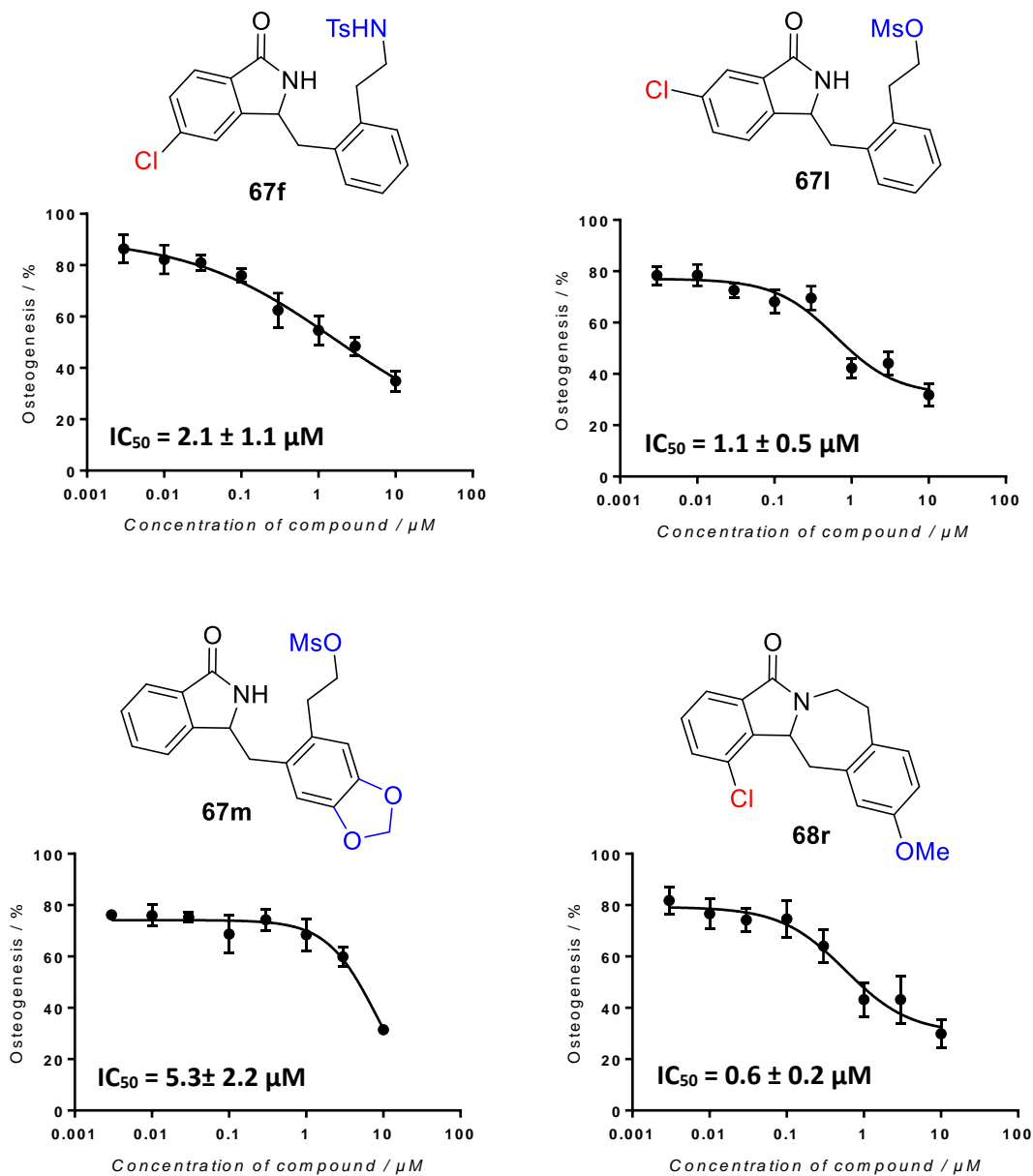


Figure 10: Influence of isoindolinones on Hh-dependent osteoblast differentiation of C3H10T1/2 cells. C3H10T1/2 cells were treated with 1.5 μM purmorphamine and different concentrations of the compounds or DMSO control. After 96 h the activity of alkaline phosphatase was detected by using a chemiluminescent substrate to determine activity. The DMSO purmorphamine control was set to 100 %. Data are mean values \pm SD and representative of two biological replicates, each performed in three technical replicates (Only two technical replicates for **68s**). IC_{50} values of the isoindolinones, obtained from the respective dose-response curve shown. To determine IC_{50} values, threefold dilutions starting from 10 μM were used.

1.4 Summary

The development of novel C-H functionalisation reactions has delivered useful transformation of scaffolds commonly found in bioactive compounds. In this case, a novel synthesis delivering unprecedented isoindolinone derivatives *via* a RhCp*-catalysed C-H functionalisation reaction of *N*-OBoc benzamides with specifically designed *ortho*-substituted styrenes was established. The method itself yielded a variety of examples in excellent yield under room temperature conditions. Unfortunately, the method was limited with regard to having an *ortho*-substituent on the benzamide starting material and some heterocycles were also not tolerated. Nevertheless, this method also provided an alternative route toward novel isoindolobenzazepine derivatives, the fundamental core structure of a family of indole alkaloid natural products with the same name.

Through mechanistic investigation, which included deuterium labelling and computational DFT calculations, there is strong evidence supporting a mechanistic hypothesis of β -hydride elimination followed by the formation of a six-membered ring rhodacycle to yield the isoindolinone. In addition, it is clear that the combination of the OBoc-protecting group and the coordinating *ortho*-substituent tether on the styrene proved to be responsible for favouring the exclusive formation of the five-membered ring.

Selected isoindolinones showed moderate inhibition of Hh-dependent osteoblast differentiation. However, the establishment of an SAR is necessary in order to increase activity. From here, further biological investigation would clarify if they actually are Hh-inhibitors. Nevertheless, both compound classes demonstrated novel bioactivity, not seen before with these scaffolds and the early results are promising.

Chapter II: Synthesis of Apoxidole Pseudo-Natural Products Reveals Novel IDO1 Inhibitor

2.1 Introduction

In addition to developing new synthetic methodology to access biologically interesting NP-like structures, design strategies to yield biologically relevant small molecule collections have also been developed. Several methods have been specifically designed to combat the lack of diverse chemical scaffolds.^[99] In doing so, they have become powerful tools, affording complex NP-like structures that efficiently navigate into previously unexplored chemical space whilst yielding bioactive compounds.

2.1.1 Natural Products: Inspiration but not a Solution

The incredible range of structural and stereochemical complexity of natural products (NPs) has provided starting points in the hunt for compound classes that modulate biological systems. In fact, a recent report by Cragg and Newman found that 32% of all approved drugs from 1981 to 2019 are NPs or NP-derived.^[100] In part, this is no surprise, as NPs have been refined by evolution to ensure optimal interaction with biological targets. Therefore, NPs can be treated as a source of pre-validated substructures for drug design.^[101] Nevertheless, NPs can be difficult to isolate and/or synthesise in sufficient quantities due to low biosynthetic or chemical yields. Furthermore, NPs cover only a fraction of NP-like chemical space.^[102] As such, NPs have limitations but can serve as inspiration to guide the exploration of biologically relevant chemical space

2.1.1.1 Diversity Oriented Synthesis (DOS)

First coined in the seminal work of Schreiber *et al*, diversity-oriented synthesis (DOS) aims to produce compound collections with high structural and functional diversity that resemble NPs, but in a rapid and efficient manner.^[103,104] Through the use of simple building blocks, in no more than five synthetic steps,^[104] unique compound libraries with the molecular complexity of NPs are obtained. The most challenging but crucial concept is the generation of high levels of skeletal diversity within the library. In order to achieve this, DOS requires “forward synthetic analysis,”

where the products of each step act as a branching point for future substrates (Figure 11).^[105] Due to the deliberate divergent synthetic routes, the compounds generated easily occupy various areas of unexplored chemical space but the resulting interesting small molecules are not necessarily biologically relevant.

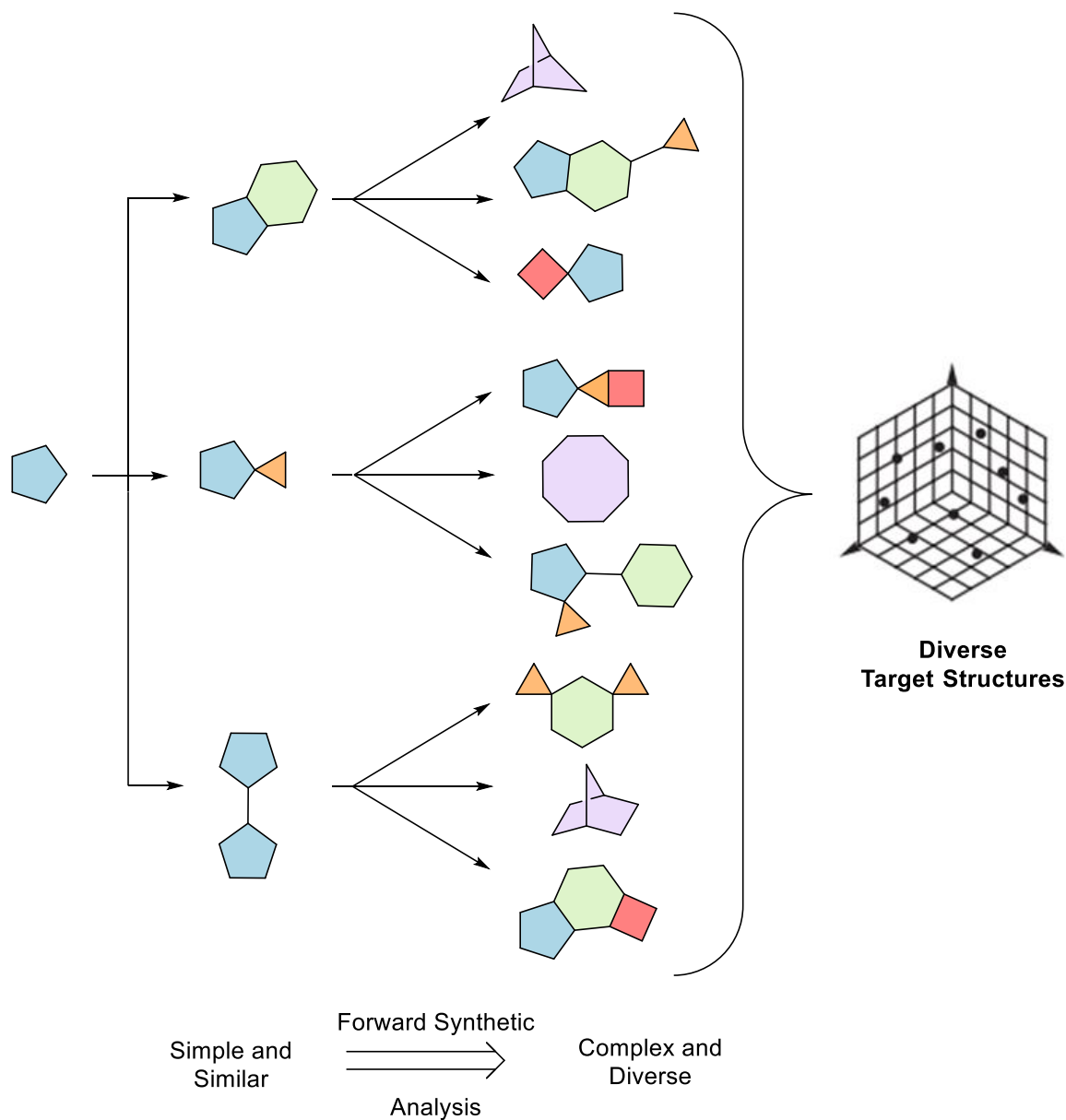
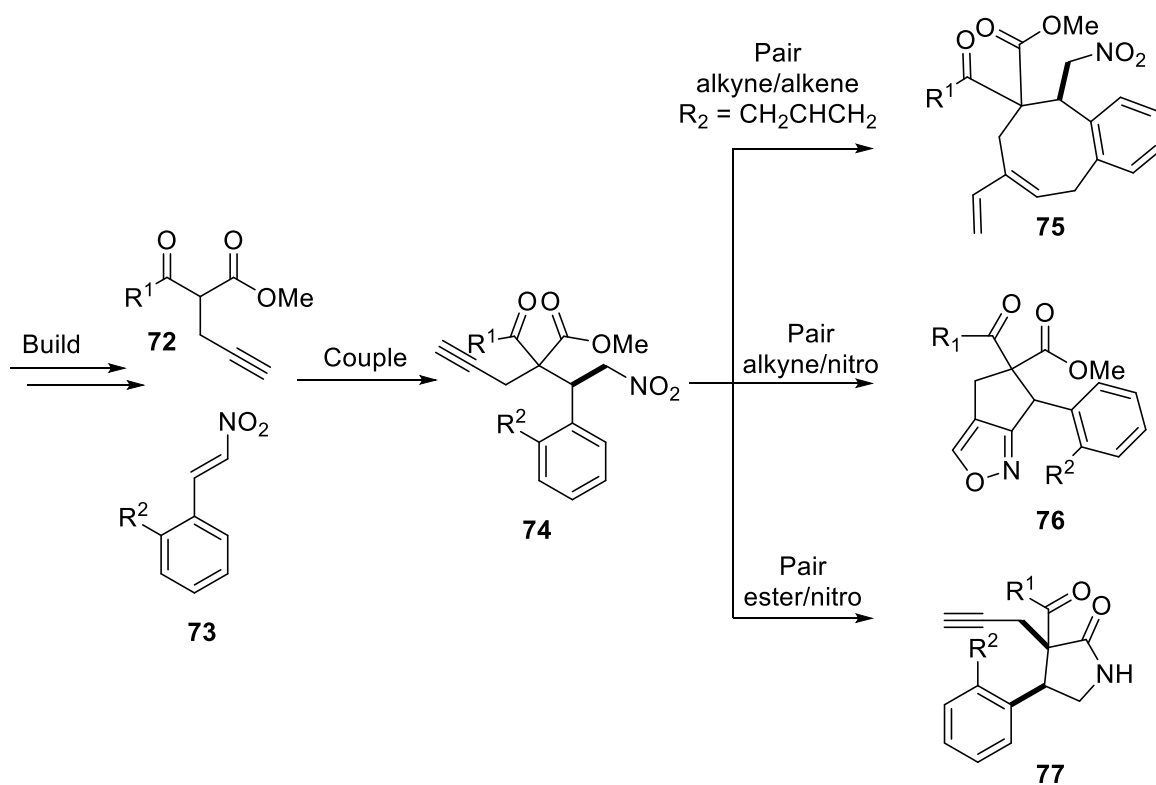


Figure 11: General principle of Diversity-Oriented-Synthesis (DOS).^[106]

Generating the diversity in DOS has been refined over time, now generally following the “build/couple/pair” strategy.^[107] This involves “building” the required (chiral) starting elements, which are then subsequently “coupled” in an intermolecular fashion to yield a densely functionalised molecule. The final “pairing”, is intramolecular, with different functional group specific reactions generating different final NP-like small molecules.

An interesting example was reported by Comer *et al.* (Scheme 24) who built alkylated 1,3-dicarbonyls **72** and substituted β -nitrostyrenes **73** and coupled them together in an enantioselective Michael addition reaction using a cinchona alkaloid-derived organocatalyst.^[108] The resulting compound **74** could then be undergo different pairings of the functional groups with different reaction condition to generate skeletal diversity **75-77**.



Scheme 24: Example of the build-couple-pair strategy using simple starting materials to generate diverse complex structures.^[106]

2.1.1.2 Complexity to Diversity (CtD)

This elegant approach, instead of using simple building blocks to build toward an NP-like compound, employs NPs as the starting point. Pioneered by Hergenrother *et al.*, this method is commonly referred to as the “Complexity-to-Diversity” method.^[109] The complexity commonly associated with stereochemistry, functionality, and other appendages are already present in the initial NP. The focus lies in altering the structure through ring distortion (Figure 12, **I**) such as ring expansion **II**, ring cleavage **III**, ring rearrangements **IV** and ring fusions **V** (Figure 12, above). This allows rapid access to challenging NP-like structures that have markedly different molecular topology to the parent NP but maintains biological relevance. Such transformations can be considered to be an extension of biosynthetic pathways, where enzymes manipulate the structure change.

Some examples of natural products that have been successfully distorted into novel chemotypes through the use of the CtD approach include gibberellic acid,^[109] adrenosterone,^[110] sinomenine,^[111] and limonin.^[112] Notably, the strategy has produced compounds with unique biological activity that differ from the parent NP. For example, pleuromutilin **78** was explored. Analogues of the ring contraction product of pleuromutilin **78a** (Figure 12, below) led to the identification of a potent inhibitor of thioredoxin and rapid inducer of ferroptotic cell death.^[113]

The dependency of this concept is on natural product starting materials that cause limitation in terms of the number of available and compatible NPs. The complexity of natural products also means that there may be reaction sensitive groups that limit the transformations, this can lead tedious screening of compatible conditions, additional steps or low yielding reactions.

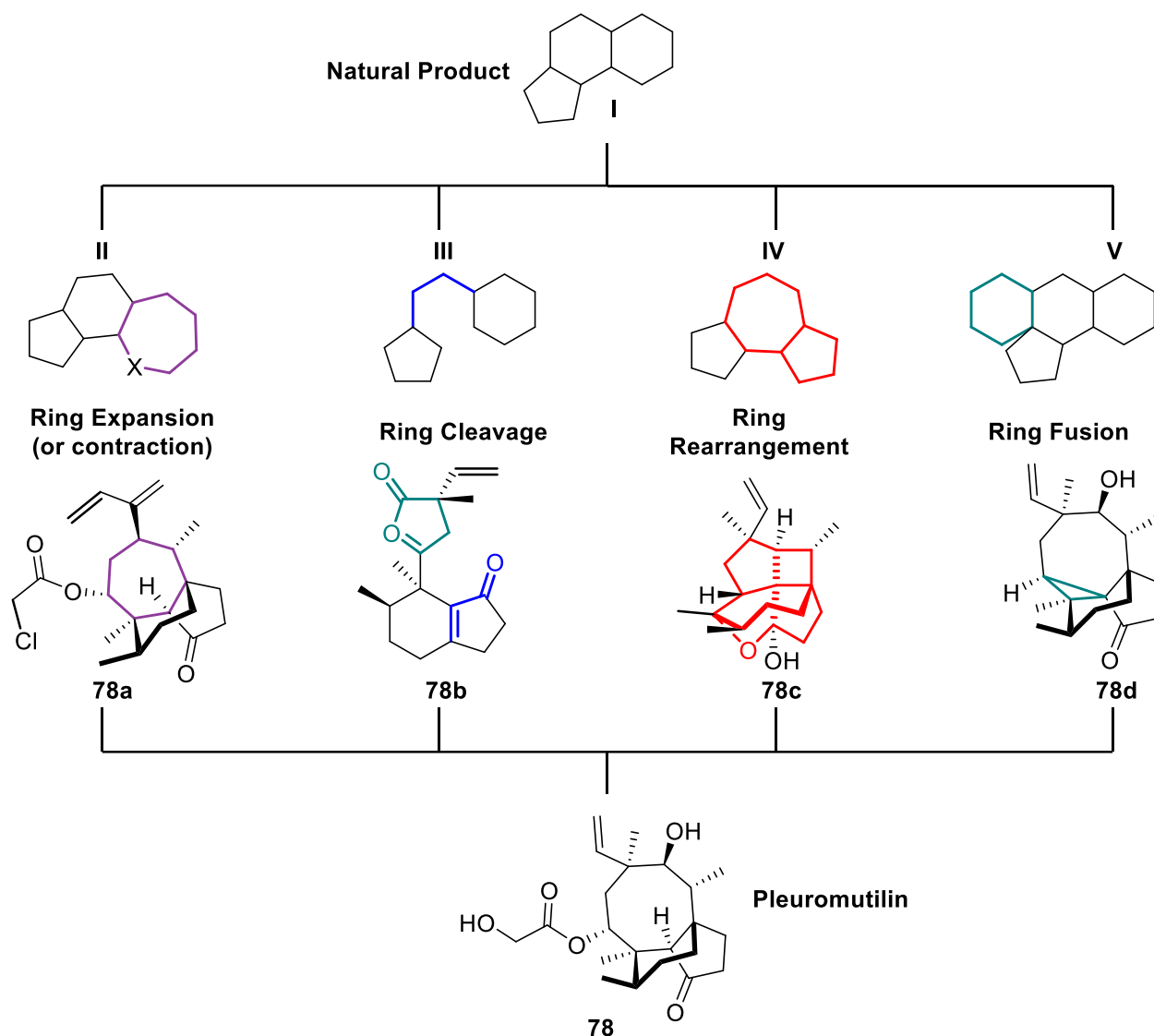
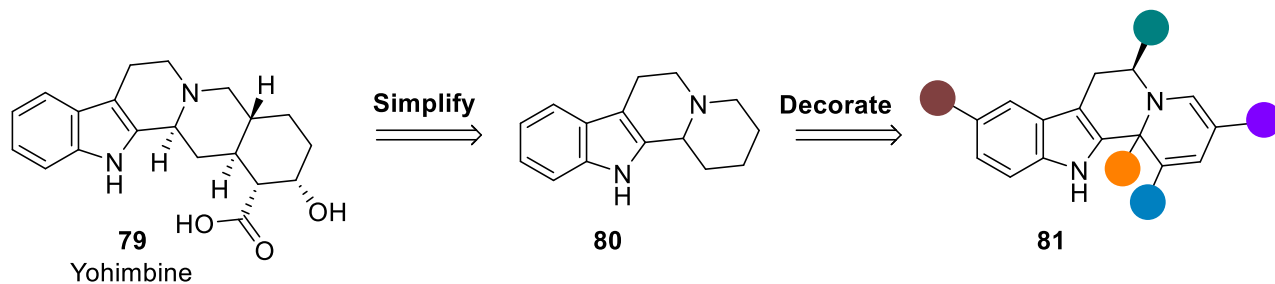


Figure 12: The four key strategies employed by the CtD approach with general structural examples (above) and demonstrated with NP, pleuromutilin (below).

2.1.1.3 Biology Oriented Synthesis (BIOS)

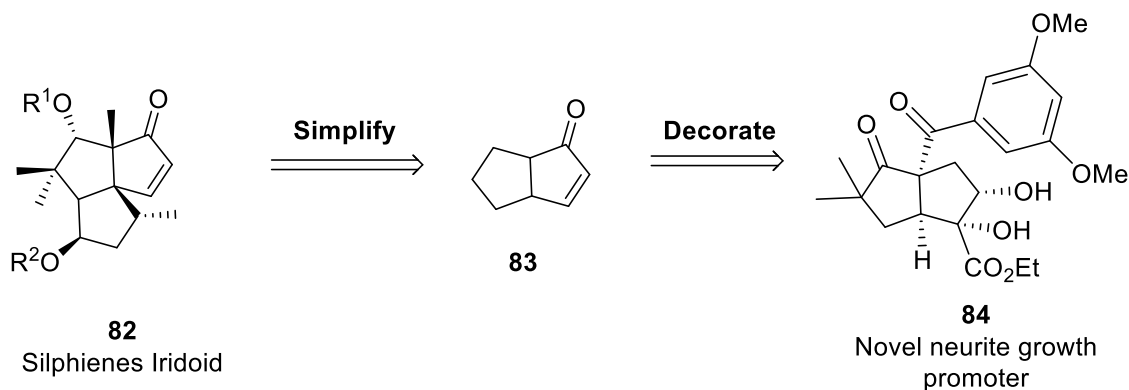
In contrast to DOS, where the focus is predominantly on exploring chemical space, the aim of BIOS is to generate structures that occupy biologically relevant chemical space from the outset.^[114,115] It is well known that NPs occupy chemical space that is biologically relevant. NPs are designed to interact with various biological entities, indicating that their molecular structure contains privileged information that enables them to do so. Like CtD, BIOS also begins with NPs,

but the design simplifies the NP to a basic core structure. In theory, the resulting “privileged scaffold” retains some form of bioactivity from the NP but it can now be modified and decorated leading to novel compounds with enhanced or even different bioactivity (Scheme 25).



Scheme 25: Simplification of a NP Yohimbine to leave a core scaffold for modification (BIOS).

For BIOS to transition from theory to reality, significant cheminformatic analysis of NPs using the Dictionary of Natural Products (DNP) database was performed.^[116,117] The end result was a structural classification of natural products (SCONP); a tree-branch representation of underlying structural frameworks (inc. oxygen- and nitrogen-heterocycles and carbo-cycles) examining the chemical space in which NPs populate.^[117] This gradual simplification from NP to small building blocks is an important hierarchical tool that can be used as templates in building pre-validated compound libraries. The BIOS concept has been successfully demonstrated through the simplification of silphienes **82**, to obtain an iridoid scaffold which are found in NPs reported to exhibit neuroprotective or neurite-growth-promoting properties. A [3+2] cycloaddition of functionalised fused-pentenones **83** with allenes generated a novel iridoid library that led to these compounds being identified as neurite growth promoters (Scheme 26).^[118]



Scheme 26: BIOS concept applied to the discovery of **84** from a simplified iridoid scaffold **83**.

However, the logic behind BIOS can be its own hindrance. When considering that NPs are responsible for a mere fraction of all chemical space, BIOS tends to generate structurally focused libraries that lack the chemical diversity of strategies like DOS. It is clear BIOS targets bioactivity, but with the core scaffolds present in the original guiding NPs, there is a limit to how much further the resulting products will extend into chemical and biological space. From a biological viewpoint, this risks retaining the same biological activity as the guiding NP.^[117]

2.1.1.4 Fragment-Based Drug Discovery (FBDD)

Initially designed to combat high attrition rates in drug discovery, FBDD has become increasingly important in the race to find novel bioactive compounds.^[119] In contrast to HTS campaigns, where large libraries (1-2 million compounds) of complex structures are screened, FBDD uses smaller libraries (1-2 thousand compounds) of simpler molecules.^[120,121] This strategy actually explores chemical space more efficiently. The theoretical premise behind FBDD is that there is a higher probability of a match between a ligand and a binding-site if there are fewer interactions to satisfy, and higher complexity risks unfavourable interactions.^[122]

Conceptually, FBDD starts by screening libraries of low-molecular weight compounds ($150 < MW < 300$), so-called “fragments”, against a target of interest.^[123,124] If a fragment binds it is normally a weak interaction with low potency (mM to μ M). However, this initial “hit” can be used to gain a structural understanding of its 3D-binding environment using biophysical methods such as X-Ray crystallography, NMR and thermal shift assays (binding only).^[125] The starting fragment can then be elongated and optimised to evolve into a more drug-like compound with higher affinity (Figure 13).

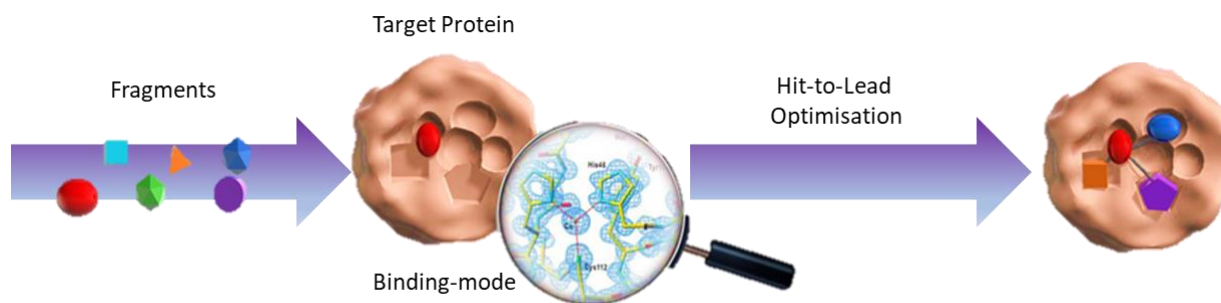


Figure 13: Conceptualised view of FBDD.^[126]

Despite the initial potency of screening “hits” being lower than that of HTS, FBDD offers more efficient monitoring of ligand efficiency and physicochemical properties during optimisation.^[120] There are not necessarily strict rules with regard to what qualifies as a fragment but there have been proposed guidelines. Most notably the “rule of three” (Ro3), suggesting (i) $MW \leq 300$ Da; (ii) hydrogen bond donors and acceptors ≤ 3 ; and (iii) $\text{Log}P \leq 3$.^[124,127] Additional physicochemical properties for a fragment have included three or less rotatable bonds and a polar surface area less than 60 \AA^2 ,^[120] but adhering to such guidelines too strongly may be a hindrance, not a help. In fact, NP fragments will often disregard these rules, in the same way that NPs do not fit the Rule of 5.

Most compound libraries used in FBDD are based on privileged substructures of known drugs and drug candidates. A favoured feature in such compounds is sp^2 centres, which often affords flat structures.^[116] Therefore, limitations in FBDD originate from two main areas. Firstly, fragments target chemical space already explored by final drug compounds and secondly, fragment libraries lack 3D shape and sp^3 character. With a realisation that 3D shape and sp^3 richness may be better starting points for drugs, efforts are being made to include these features in FBDD libraries.

Approaches by Over *et al.* and later Lizos *et al.* to meet this demand embarked on deconstruction of NPs into fragments.^[116,128] NPs are enriched in stereogenic centres and are inherently, recognised by protein binding sites. This means they are able to explore areas of chemical space that are not explored by synthetic compounds. Particularly useful was the cheminformatic method developed by Over *et al.* that sequentially deconstructed over 180,000 natural product structures (similar to the SCONP algorithm), adhering to the Ro3, to obtain a library of 2000 NP-derived fragments.^[116] Importantly, they are highly diverse and rich in sp^3 stereocentres. In terms of application, they discovered bicyclic cytosine/sparteine fragment derivatives as inhibitors of p38a MAP kinase binding to the allosteric site of the enzyme.^[116]

Overall, FBDD screening would benefit from incorporating such NP-based fragments. This was emphasised, when a study by Hert *et al.* found that 83% of the core ring scaffolds present in NPs are absent from the available molecules and screening libraries.^[129]

2.1.1.5 Pseudo-Natural Products

With the knowledge that neither synthetic compounds nor natural products can cover all chemical and biological space alone, the pseudo-NP approach strives to deliver hybrid compounds that explore both.^[130–132] In order to achieve this, NP fragments are synthetically (re)combined in arrangements not found in nature to afford distinct compound classes. These pseudo-NPs resemble NPs in structure and complexity but extend beyond them with regard to chemical space (Figure 14). Furthermore, as each fragment encodes biological relevance, recombining different fragments may provide a favourable platform to deliver unprecedented bioactivity. Importantly, synthetic (re)combinations should be of fragments that are biosynthetically unrelated, or combined in an orientation not previously seen in NPs.^[133–135] This two-pronged strategic approach provides libraries of diverse pseudo-NPs as an elegant solution that may avoid overlapping with previously explored chemical and biological space.

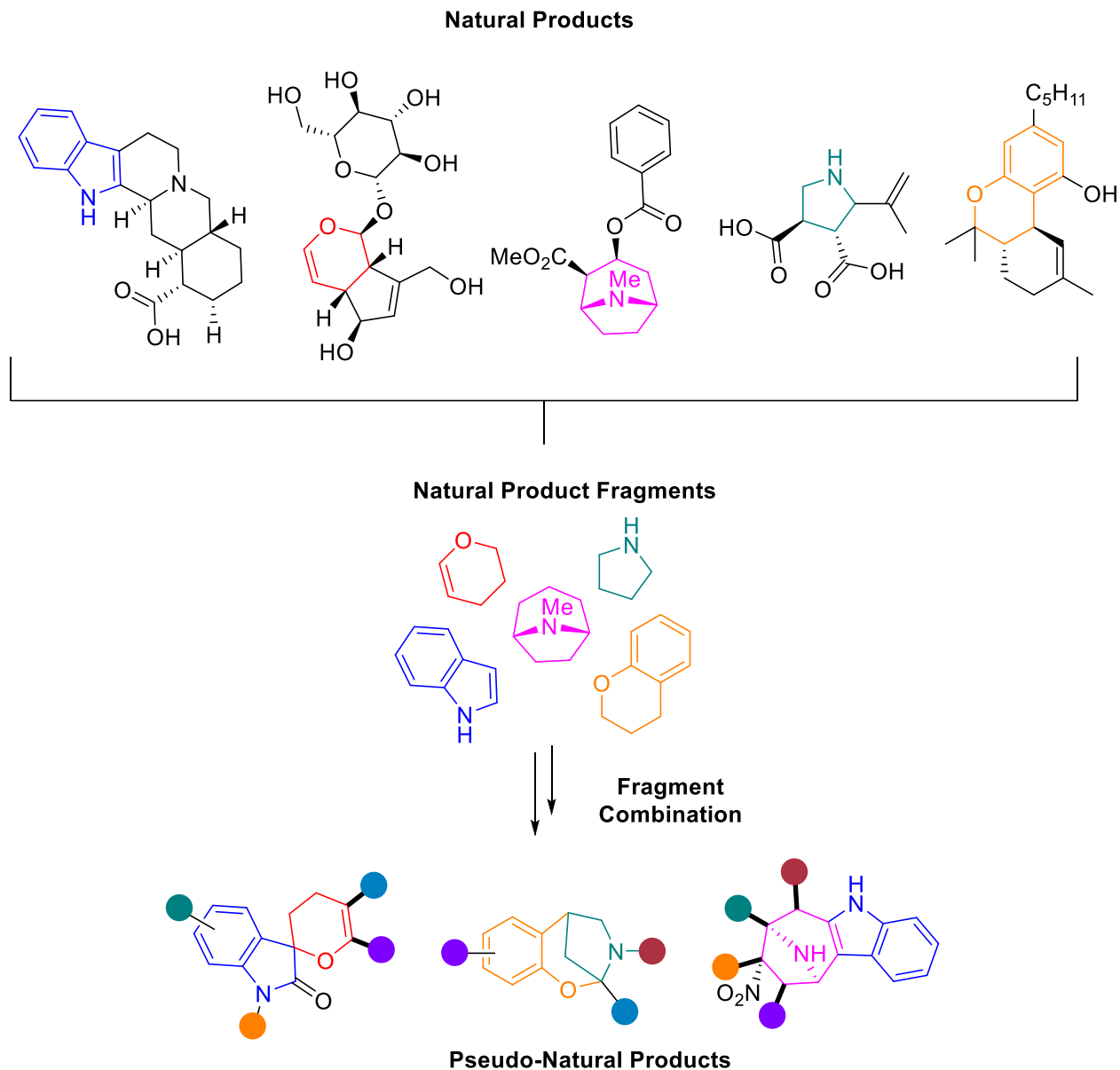


Figure 14: Theoretical examples of the pseudo-NP method by deconstruction of NPs to NP fragments followed by *de novo* recombination.^[132]

To access pseudo-NP libraries, one must decide how a fragment will be installed. For example, considering whether to use fragments as starting materials that have functional handles to enable the introduction of other fragments. Alternatively, fragments could be constructed before or during the synthesis using complexity generating or intramolecular reactions. The flexibility of the pseudo-NP concept has allowed the development of numerous pseudo-NPs that have also,

gratifyingly, revealed novel bioactivities.^[131,136–140] The first reported example are the bridge-fused chromopyrones, where biosynthetically unrelated chromane and tetrahydropyrimidinone (THPM) fragments were united (Figure 15a).^[139] This was enabled *via* construction of the THPM in a Biginelli reaction, followed by an intramolecular cyclisation. Biological investigations of the resultant library revealed that the chromopyrones are selective inhibitors of the glucose transporters GLUT-1 and -3, and inhibit cancer cell growth. Additionally, it was discovered that neither fragment, individually, showed the same inhibitory activity; therefore the combination of chromane and THPM is essential for the biological activity. In the case of the indotropanes (Figure 15b), a combination of two commonly occurring alkaloid fragments, an enantioselective copper-catalysed [3+2] was used.^[140] The indole fragment was modified to have an azomethine ylide that could couple to a nitroalkene to allow access to a pseudo-NP class with multiple stereocentres. Phenotypic screening showed that one member of this chemotype in particular, strongly induced changes in mouse L fibroblast morphology. Further biological investigation, led to this compound being named Myokinasib due to its inhibitory effect on myosin light chain kinase 1 (MLCK1).

Unlike FBDD, the NP-like fragments in the pseudo-NP approach strays further from the guiding Ro3,^[127] which leads to more sp³-rich fragment options. As a result, NP fragments can include fully synthetic fragments or even NPs that are fragment-sized, which in turn provides additional platform for complexity and topology. This was demonstrated in the synthesis of the indofulvin pseudo-NP class where the NP Griseofulvin was linked with a 4*H*-pyranoindole fragment.^[136] By means of an iso-oxa-Pictet-Spengler reaction, 2-hydroxyethyl-indoles and griseofulvin ketones were combined to produce a spiro-connected collection of indofulvin pseudo-NPs (Figure 15c). Once again, the pseudo-NP strategy proved how powerful it is, as this structural class led to novel autophagy inhibition targeting mitochondrial respiration, with the most potent compound having an IC₅₀ of = 0.82 μM. Similarly to the chromopyrones, neither griseofulvin nor the 4*H*-pyranoindole fragment had previously shown autophagy activity.

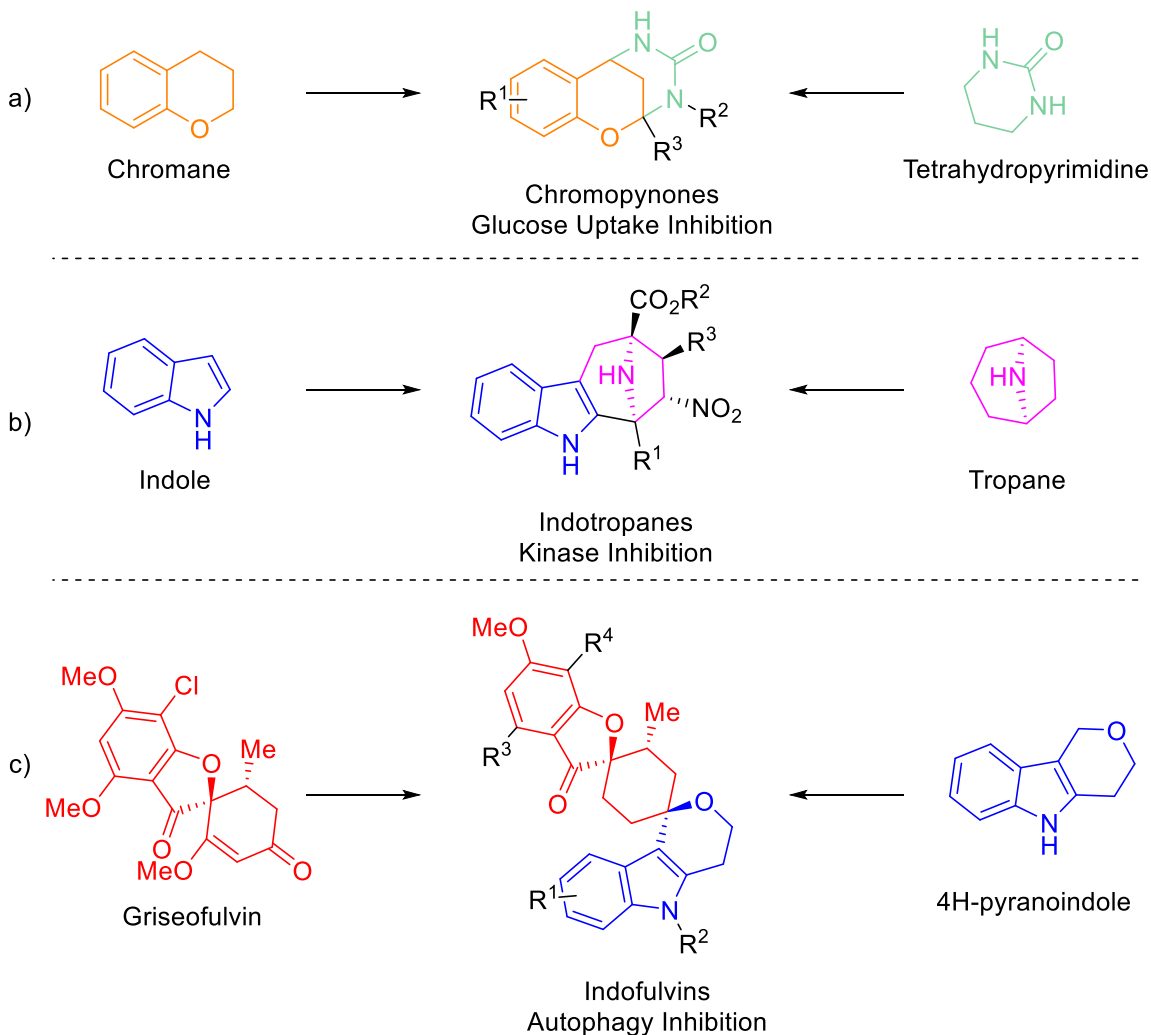


Figure 15: Pseudo-NP that demonstrated novel bioactivity: a) Chromopyrones, b) Indotropanes and c) Indofulvins.

As well as using different fragment combinations, diverse pseudo-NPs can arise from varying fragment connection as well as regioisomeric arrangements.^[132,135] This off-sets the limitation of avoiding fragment combinations already found in nature because such combinations can be connected or arranged in another manner to generate a different chemotype. These additional parameters further extend the range of chemical and biological space in which pseudo-NPs can occupy.

The most common connectivity patterns can be categorised into two groups: those with common/shared atoms and those without (Figure 16).^[132,141] The number of common atoms between fragments can vary depending on the connection type. Connection of two fragments through only one atom will result in spirocycles, as seen with indofulvins (Figure 15c).^[136] NPs are often involved in complex fused ring systems, so one of the more frequently observed connectivity styles is edge-fusion, in which there are two common atoms. Two fragments may share three or more common atoms, forming a bridged bicyclic scaffold. The desirable factor in this connection type is the three-dimensionality, often sought after due to the nature of biological target binding sites.

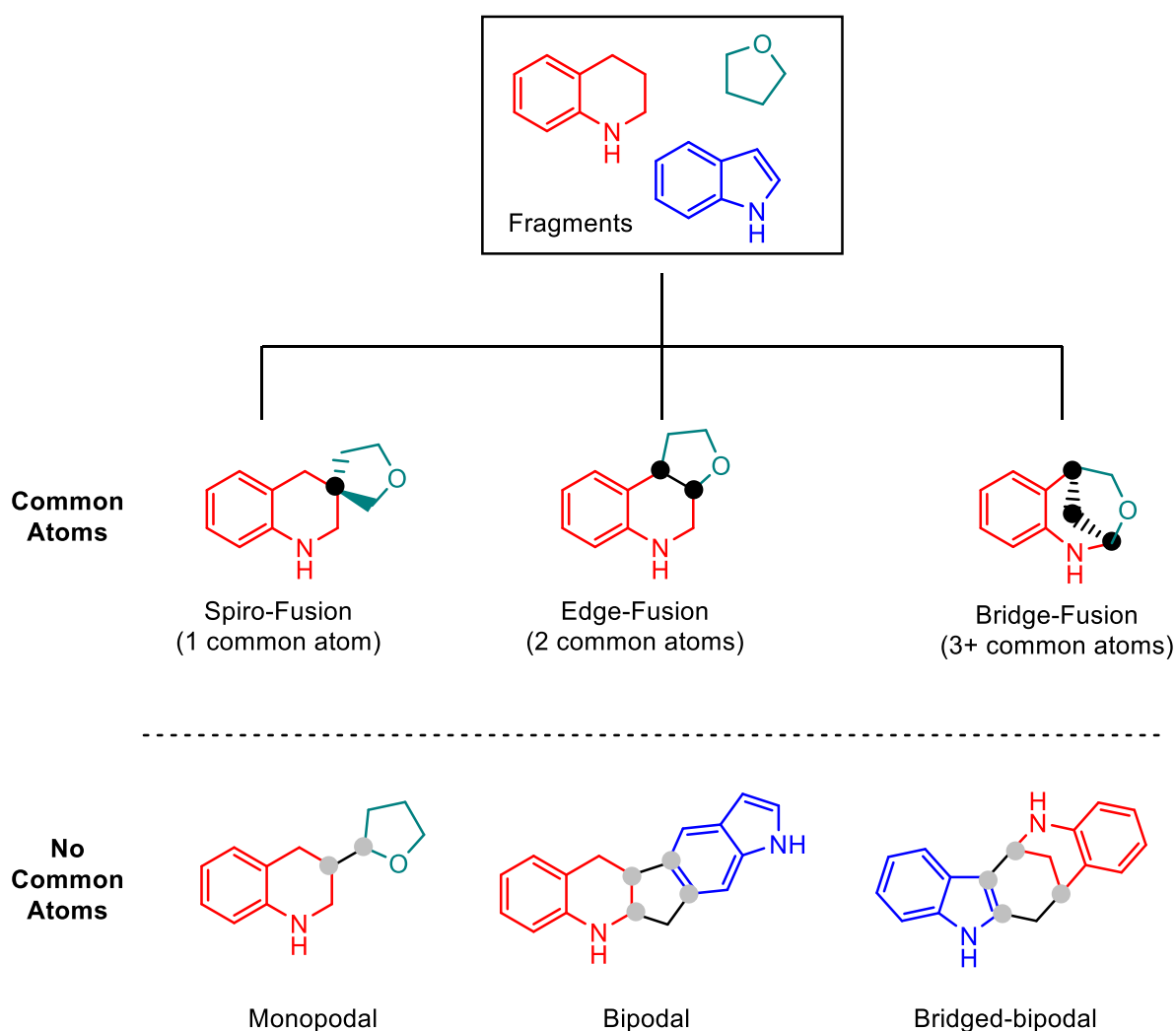


Figure 16: Connectivity patterns for two fragments often observed in NPs.^[132] Individual fragments indicated in blue, red or green. Black dots denote connectivity points, grey dots indicate connection points of intermediary rings.

Adjoining fragments may not share any common atoms, but may have one or two linking atoms as intervening connection points. The most basic connection without shared atoms is monopodal but also when generating pseudo-NPs, an additional ring (or third fragment) may form leading to more complex fusion patterns, such as bipodal, tripodal, bridged bipodal, and bridged tripodal.^[141]

It is generally preferred to incorporate chirality to the pseudo-NPs as this is more representative of natural product complexity. Therefore, patterns that generate stereogenic centres and more structurally complex scaffolds are prioritised. However, this will highly depend on the available functional handles of the fragments or the reaction used to combine/build fragments.

Overall, the pseudo-NP approach is a pioneering method with clear design principles to obtain novel NP-like but also drug-like structures. It can also be seen as an advance on some of the other methods used to generate NP-like compound libraries. For example, in DOS,^[103] small building blocks (fragments) are combined to generate diversity but predominantly focuses on exploring chemical space. The pseudo-NP approach advances this process by using biologically revalidated fragments as building blocks to attack chemical and biological space in parallel. Both the CtD^[109] and BIOS^[114] methods are both limited in their exploration of chemical space and consequently the observed biological activity of compound classes from them may not differ significantly from that of the original NP structure, thus limiting the range of biological space that can be interrogated. The pseudo-NP method is much more flexible in providing diversity and unprecedented biological activity.

2.2 Project Aim

The design principles of the pseudo-NP approach has produced various examples as proof-of-concept. The strategy itself is, to a certain degree, a unification of BIOS and FBDD that efficiently explores chemical and biological space. Several examples have boasted novel chemical methodology to ascertain the pseudo-NP, which in turn delivered novel bioactivity. In order to build on such success continual expansion of the pseudo-NP concept remains of high importance. In particular, in contrast to the majority of pseudo-NPs, where the emphasis is on the combination of biosynthetically unrelated fragments; differing connectivity or arrangements of previously related fragments has been less explored.

Therefore, the aim of this project is to identify suitable NP fragments that are already found together in NPs and design a feasible chemical method to connect them in a biologically unprecedented manner. This would not only provide a novel pseudo-NP class but would give interesting data on how different arrangements may lead to novel bioactivity, particularly if different to the activity of NPs that have the two fragments. Generation of such pseudo-NPs would require a search of chemical databases in order to determine the connectivity patterns which certain fragments have adopted together in NPs. The synthesis design would have to facilitate the unique connectivity but also be efficient in generating NP-like complexity. Furthermore, the synthesis will be tested and optimised in order to generate a diverse library of pseudo-NPs.

The resulting pseudo-NP collection will be evaluated in a high-throughput manner, by the in-house COMAS facility, in phenotypic screening assays to monitor biological effects. Any significant change can be treated as a potential lead for novel bioactivity and can be investigated from the structure-activity-relationship (SAR) of the library. The most active compound would then need to be investigated further in mode-of-action and target identification studies.

Analysis of this new pseudo-NP class should be highly valuable as another category of pseudo-NPs, not only as a way to extend into unknown biological space, but also in how to use NPs as inspiration for delivering compound that could be used in drug discovery or as tool compounds.

2.3 Results and Discussion

This work was carried out in collaboration with Lara Dötsch.

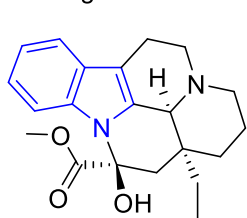
2.3.1 Background: Design of a Novel Pseudo-NP Class

Considering the fundamental design principles of the pseudo-NP approach, we sought to combine indole and tetrahydropyridine (THP) fragments to produce a novel three-dimensional scaffold with amenable outlets for synthetic modification and decoration. This would be facilitated by a balance of sp^2 and sp^3 centres, also allowing for the introduction of chirality, a favourable property with regard to exploring chemical and biological space.

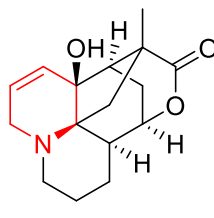
NPs that embody indole and THP fragments occur widely in nature, both individually and together (Figure 17a). Importantly, these fragments are endowed with bioactivity.^[142,143] For instance, the indole-containing NP Vincamine is a known vasodilator, used in the treatment of vascular dementia and THP-containing Annotine has displayed activity associated with anti-inflammatory properties.^[144,145]

In early reports, the pseudo-NP strategy has often generated compounds where the defining feature was the combination of biosynthetically unrelated fragments.^[139,140] In this particular case, the indole and THP fragments are already found in nature together, but the key emphasis will be their novel connection. An analysis of the DNP^[146] and Coconut^[147] databases indicated that indole and THP fragments are typically found together in complex fused ring systems where there is an intermediary ring between (bipodal-type connectivity) (Figure 17b). However, a direct monopodal connection (i.e. no intermediary rings) between indole– and THP-fragments in NPs was not found. Therefore, this unprecedented fragment recombination (Figure 17c) would result in the discovery of a novel chemotype and could lead to diverse biological activity.

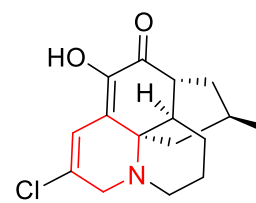
a) Isolated fragments



Vincamine

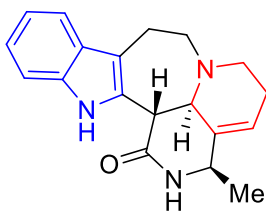


Annotine

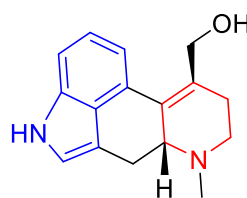


2-Chlorohuperzine E

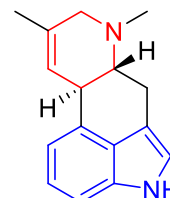
b) Both fragments



Arboflorine



Lysergol



Agroclavine

c) Pseudo-NP strategy

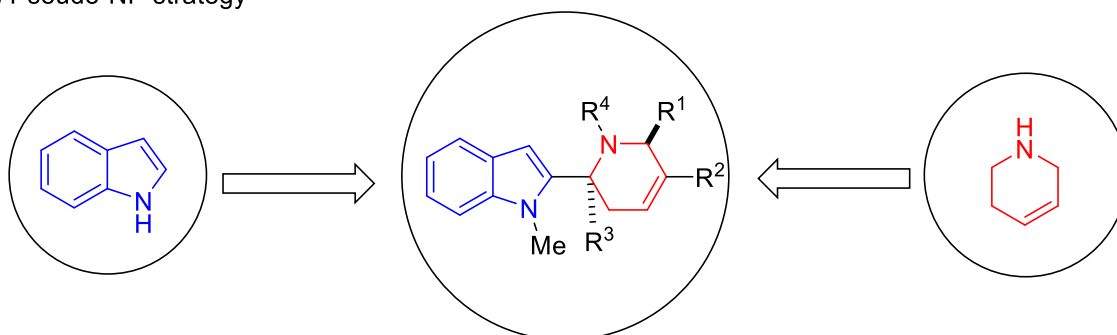
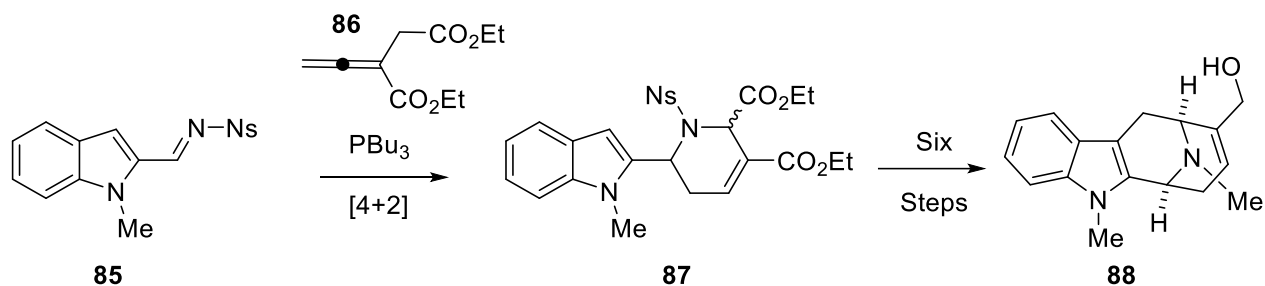


Figure 17: Design of the new pseudo-NP class: a) Fragments found individually in NPs, b) Fragments together in NPs, c) the novel combination of indole and THP.

2.3.1.1 Synthetic Strategy: Phosphine-Catalysed [4+2] Annulation

Nucleophilic phosphine catalysis has emerged as a powerful tool in organic synthesis.^[148,149] The last two decades have witnessed a significant increase in reports of the use of phosphine catalysed reactions, including the formation of six-membered heterocycles, via [4 + 2] cycloadditions.^[148] Our attention was drawn to the seminal work of Kwon *et al.* who used an organophosphine catalyst to facilitate a [4+2] annulation between *N*-tosylimines and allenates (1,4-dipole synthon precursors).^[150] The result was a series of highly substituted THPs in high yield and

regioselectivity. An extension of this methodology was its application in the formal synthesis of alstonerine and macroline indole alkaloids using allenates **86** with *N*-nosyl-indole-2-aldimines **85** (Scheme 27).^[151] Here, intermediate **87** was the foundation for the novel pseudo-NP class. Therefore, the two fragments would be connected *via* the C2 of the indole and the C6 of the THP, whereby the THP would be formed *in-situ*.



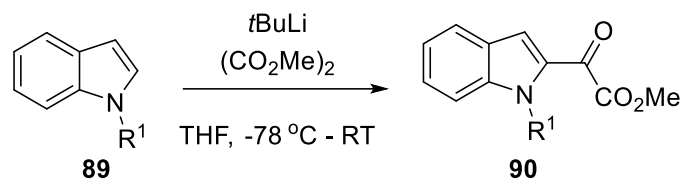
Scheme 27: Natural product synthesis using a phosphine catalyzed [4+2] annulation to generate a key pseudo-NP intermediate.

However, some of the methods shown in literature are limited to the use of aldimines.^[152,153] Therefore, in order to add another level of complexity to this chemistry, and the new pseudo-NP class, we sought to develop a more efficient and rapid protocol using ketimines. The advantage of this is two-fold. Firstly, it would distinguish itself from the original reaction, making it novel in its own right, and secondly, with the aim of developing an asymmetric version employing chiral phosphine catalysts, would enrich the stereogenic content of the resulting tertiary centre at C6 of the THP. Importantly, with the exception of the few examples in the report of Kwon *et al.*,^[151] this structural scaffold has not been investigated further from both a synthetic and biological perspective.

2.3.2 Method Development

Reaction optimisation was performed by Dr. Gessica Ciulla.

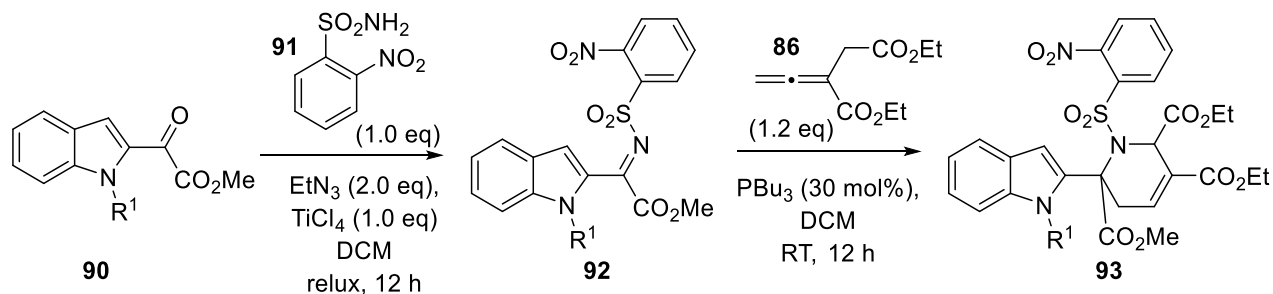
In order to enable the formation of the ketimine and consequently, a tertiary centre in the final product, the starting indole would need to be modified. The *N*-protected indole **90** was installed with a diketoester at the C2 position courtesy of lithiation *via* deprotonation of the indole **89** and subsequent nucleophilic addition-elimination with dimethyl glyoxalate (Scheme 28).



Scheme 28: Reaction procedure to synthesise the diketoester, later used to generate the ketimine.

2.3.2.1 Racemic Reaction Screen of *N*-Substituted Indoles

With the basic chemistry already established, the conditions of Kwon *et al.* were used in preliminary reaction screening with test allenolate **86**.^[151] Reassuringly, with the newly modified *N*-methyl indole substrate, the desired product was obtained in a yield of 63% (Table 5, Entry 1).

Table 5: Optimisation of the *N*-substituent of the indole diketoester.

Entry	R ¹	Ketimine	Isolated Yield [%]
1	Me	Isolated	63
2	Allyl	Isolated	51
3	PMB	Not observed	-
4	SO ₂ Ph	Not observed	-
5	H	90% SM recovered	-
6	Boc	No reaction	-
7	Bn	90% SM recovered	-
8	MOM	90% SM recovered	-

Reactions initially performed with ketimine formation *in-situ*.

A variety of other *N*-substituted indoles were also tested, with the allyl group affording the desired product in 51% yield. However, other substituents either resulted in only trace or no amount of ketimine **92** and as a result no product (Table 5, Entries 3-8). Interestingly, already in these orienting reactions, it was found that the desired product **93** was formed as a single

diastereoisomer. For further reaction optimisation, it was decided to proceed with the *N*-methyl indole.

2.3.2.2 Chiral Phosphine Catalyst Screening

An asymmetric analogue of the seminal work of Kwon was reported by Fu *et al.*, affording THPs with moderate to good diastereo- and high enantioselectivity using a binaphthyl-based C_2 -symmetric monophosphine catalyst.^[154] Therefore, it was hopeful the same result could be achieved with this reaction. By employing *N*-nosyl ketimine **92** with the model allenolate **86**, a subsequent screen of chiral phosphines was undertaken (Table 6).

A wide variety of chiral phosphines were screened, including aryl, alkyl and combination thereof. The main focus was on the use of chiral tertiary phosphines that had been previously used in cycloadditions of allenolates (Table 6, Entries 1-5).^[149] Within this series were C_2 -symmetric bisphosphines such as the (*S,S*)-Ph-BPE, Et-BPE, Me-BPE and *i*Pr-BPE. The aromatic (*S,S*)-Ph-BPE performed poorly with respect to both yield and enantiomeric excess (*ee*) (Entry 1). On the other hand, its alkyl variants, (*S,S*)-Et-BPE and Me-BPE (Entries 2-3) furnished excellent yields and improved enantioselectivity, particularly in the case of (*S,S*)-Et-BPE with 74% *ee*. The reaction also performed poorly with aromatic chiral phosphine (*S,S*)-SITCP and (*R,R*)-Me-DuPhos, which is commonly used as a ligand in metal-catalysed reactions (Entries 6-7). In addition, the binaphthyl-based C_2 -symmetric tert-butyl phosphine catalyst **C7** used by Fu *et al.* was also tested in this reaction to give an *ee* of 80% but unfortunately poor yield of only 20% (Entry 8).^[154] Interestingly, its aromatic variant **C8**, in a similar manner to bisphosphines, performed poorly in both yield and *ee* (Entry 9). Finally, two phosphine-containing α -amino acid catalysts, **C9** and **C10**, were screened as they have previously been found to be efficient catalysts for promoting enantioselective [3+2] cycloadditions.^[155] However, both showed no reaction in this case (Entries 10-11). Therefore, the best catalyst, which afforded [4+2] adduct with an *ee* of 74% and yield 96% was (*S,S*)-Et-BPE. Notably its opposite enantiomer provided a similar *ee* of 77% allowing easy access to both chiral enantiomers.

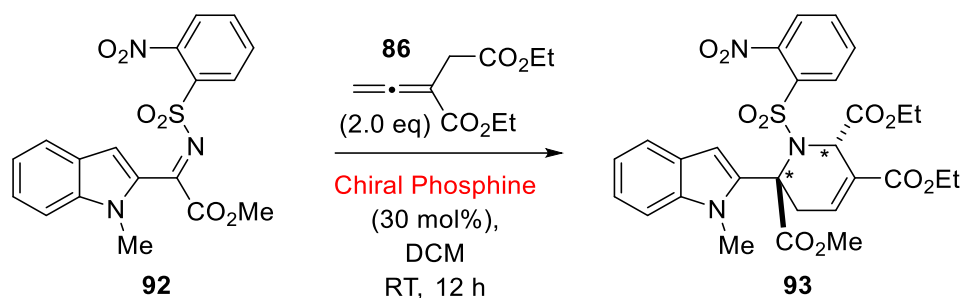
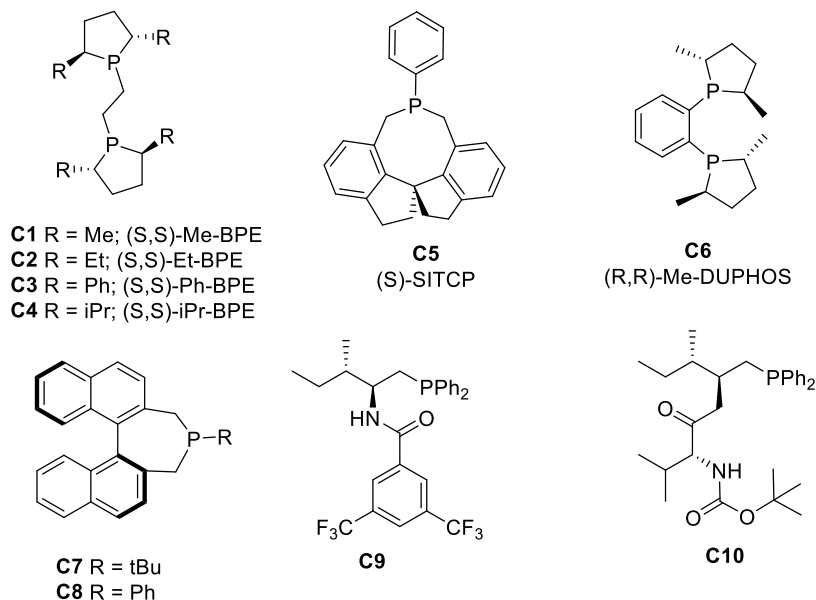


Table 6: Chiral phosphine catalyst (structures below) optimisation.

Entry	Catalyst (30 mol%)	Yield [%] ^b	ee [%]
1	(<i>S,S</i>)-Ph-BPE	20	11
2	(<i>S,S</i>)-Et-BPE	96	74
3	(<i>S,S</i>)-Me-BPE	81	54
4	(<i>R,R</i>)-Et-BPE	50	77
5	(<i>S,S</i>)-iPr-BPE	5	40
6	(<i>S</i>)-SITCP	42	40
7	(<i>R,R</i>)-Me-DUPHOS	26	18
8	C7^a	23	80
9	C8	10	5
10	C9	0	0
11	C10	0	0

[a] Catalyst synthesised using literature procedure. [b] Isolated yields



2.3.2.3 Solvent Screen

Different solvents were explored in order to improve the *ee* (Table 7). Initially toluene provided excellent improvement with 84% *ee*, however sacrificed the yield at 31% (Entry 1). In contrast to the success of DCM (Entry 2), DCE afforded no product (Entry 3). The use of THF gave an improved *ee* of 88%, whilst maintaining a good yield of 71% (Entry 4). Acetonitrile, ethyl acetate and dioxane produced good *ee* values but compromised yields (Entries 5-7). The solvents DMF and chloroform gave no reaction (Entries 8-9). When submitted to lower temperatures, DCM at 0 °C had a detrimental effect on the yield, and at -30 °C, the *ee* (Entries 10-11). The latter was likely due to the precipitation of the catalyst. For toluene and THF, both conditions at 0 °C (Entries 12-13) could not improve on the room temperature THF conditions.

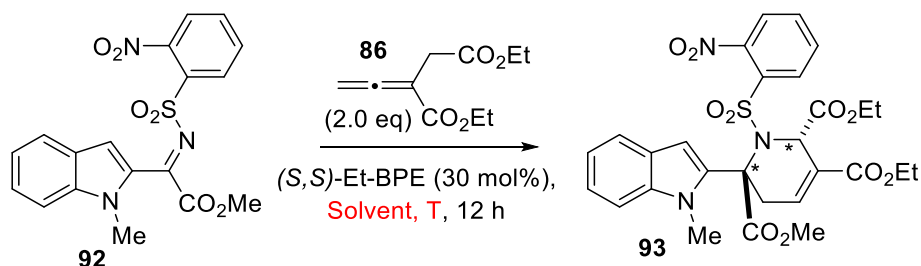


Table 7: Solvent and temperature optimisation

Entry	Solvent	Temperature	Yield [%] ^a	<i>ee</i> [%]
1	Toluene	RT	31	84
2	DCM	RT	96	74
3	DCE	RT	-	-
4	THF	RT	71	88
5	MeCN	RT	20	76
6	EtOAc	RT	53	82
7	Dioxane	RT	42	82
8	DMF	RT	-	-
9	Chloroform	RT	-	-
10	DCM	0 °C	18	79
11	DCM	-30 °C	7	40
12	Toluene	0 °C	80	79
13	THF	0 °C	54	77

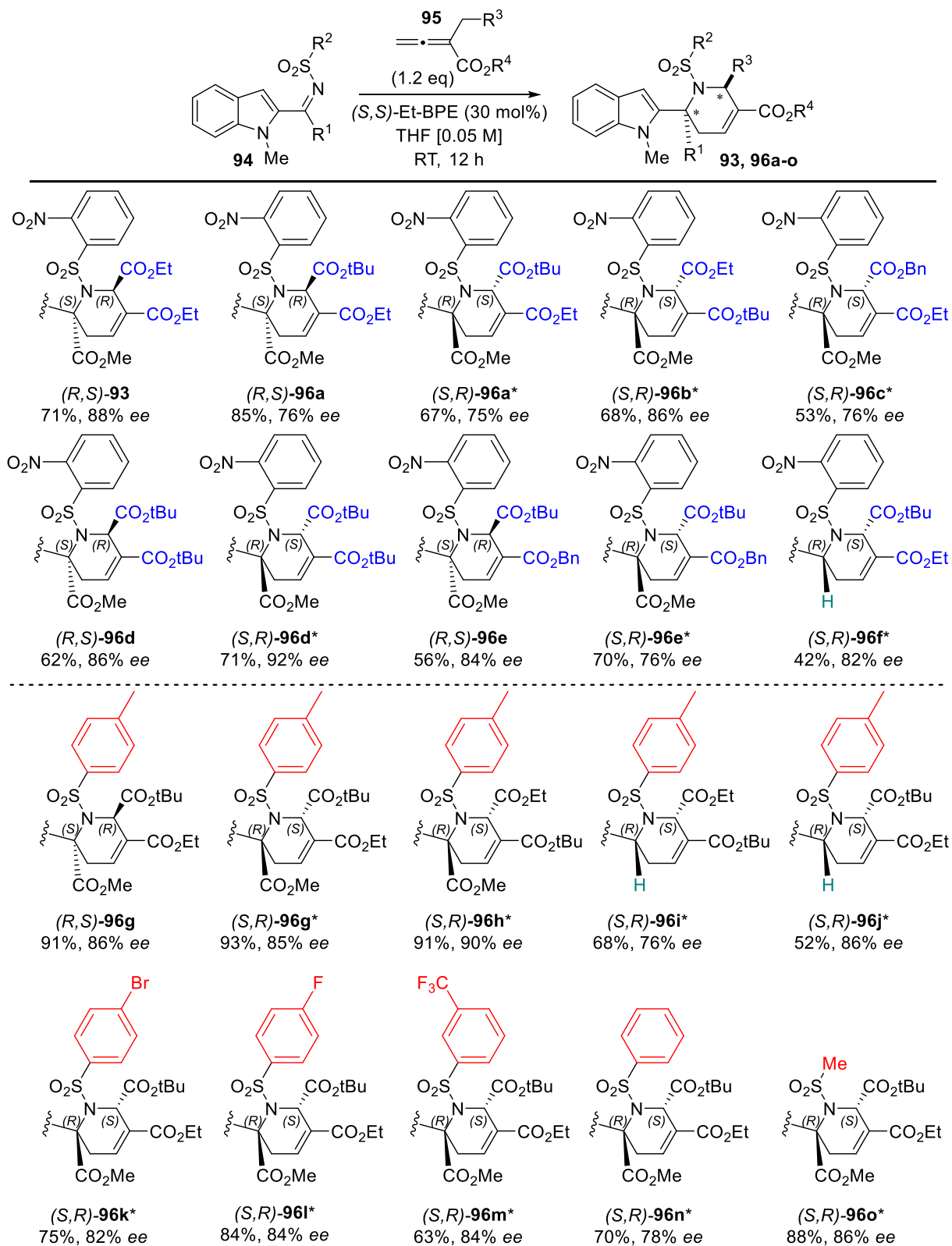
[a] Isolated yields

2.3.3 Substrate Scope and Limitations

With optimised conditions in hand, the reaction scope was explored (Scheme 29) to generate a broad collection of the pseudo-NP class. The initial focus was the exploration of the esters that originate from the starting allenolate **95**. Gratifyingly, deviations from the model allenolate **86**, bearing various ester substitutions, and combinations thereof, were well tolerated (**96a** - **96e**) with moderate to excellent yields and enantioselectivities. However, attempts to replace these esters at R³ with alkyl moieties, such as ethyl or complete removal (H), provided no reaction. In addition, charge stabilising groups, like phenyl (Ph), nitrile (CN) and aromatic ketones (COPh), only resulted in trace amounts of the desired adduct. Pleasingly, the reaction conditions also proceeded smoothly with the aldimine (R¹ = H) to generate (*S,R*)-**96f** diastereoselectively, in moderate *ee*, albeit with lower yield (42%). Attempts to replace the indole with other heterocycles or simple phenyl were not tolerated in this reaction, giving trace or no product formation.

Investigations then moved to switching the nosyl group with other sulphonamide moieties (**96g**-**96o**). The tosyl group in particular, afforded the desired pseudo-NP in high yields up to 93% and enantioselectivity up to 90% (**96g**-**96h**). The tosyl-aldimine was also well tolerated with good yields and enantioselectivity, (*S,R*)-**96i** and (*S,R*)-**96j**, but again the yields are comparatively lower than those originating from the ketimine. Other substitutions on the phenyl ring included *para*-bromo (*S,R*)-**96k**, *para*-fluoro (*S,R*)-**96l**, and *meta*-trifluoromethyl, (*S,R*)-**96m** performed well to afford the desired adducts in excellent yield and high enantioselectivities. The unsubstituted phenyl (*S,R*)-**96n** also performed to a high standard. Notably, an alkyl derivative in the form of a mesylate example (*S,R*)-**96o**, matched the results of the aromatic sulphonamides with a yield of 88% and 86% *ee*. When the reaction was tried with the *N*-*o*-nitrophenyl ketimine, there was no reaction, giving the impression that the sulphonamide moiety is favourable in formation of the desired adduct.

This initial scope of compounds holds promise for further expansion. Early exploration of the chemistry has neglected to include substituted indoles, therefore it would be interesting to see their compatibility. Additionally, with three esters able to be installed, it can be arranged for selective hydrolysis of the *tert*-butyl ester, for example in **96a** or **96b** to use the carboxylic acid for derivatisation.



Scheme 29: Pseudo-NP substrate scope exploring esters (blue) and sulphonamide moieties (red). *(*S,R*)-compounds obtained using (*R,R*)-Et-BPE.

The structure of the new pseudo-NP class and stereochemistry of the two stereocentres was confirmed by X-Ray analysis based on the major product of (*R,S*)-**96a** (Figure 18).

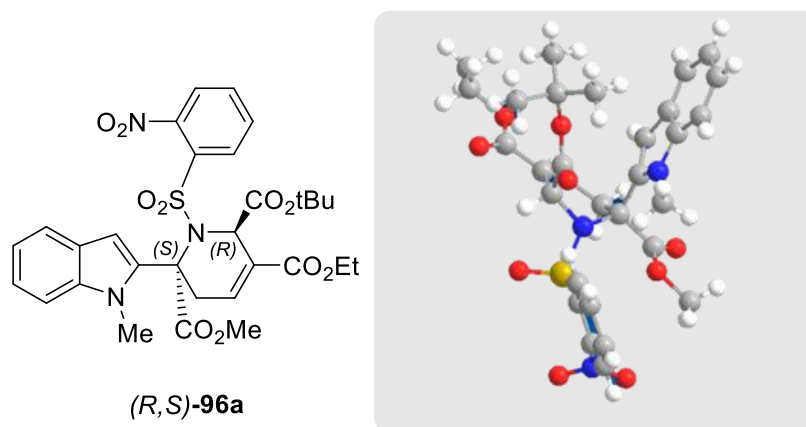
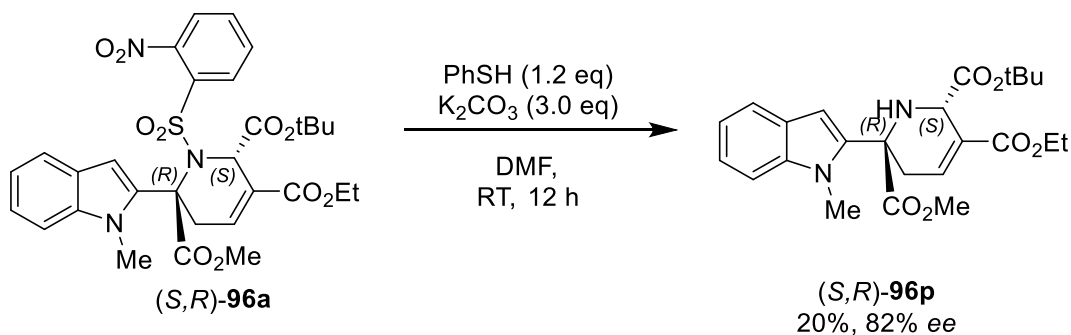


Figure 18: Crystal structure, confirming the configuration and stereochemistry of pseudo-NP (*R,S*)-**96a**

Furthermore, a valuable addition to the pseudo-NP collection was obtained through deprotection of the nosyl group using thiophenol with excess potassium carbonate (Scheme 30). This provided the free NH compound (*S,R*)-**96p**. Despite the low yield of 20%, the *ee* was retained (82%).

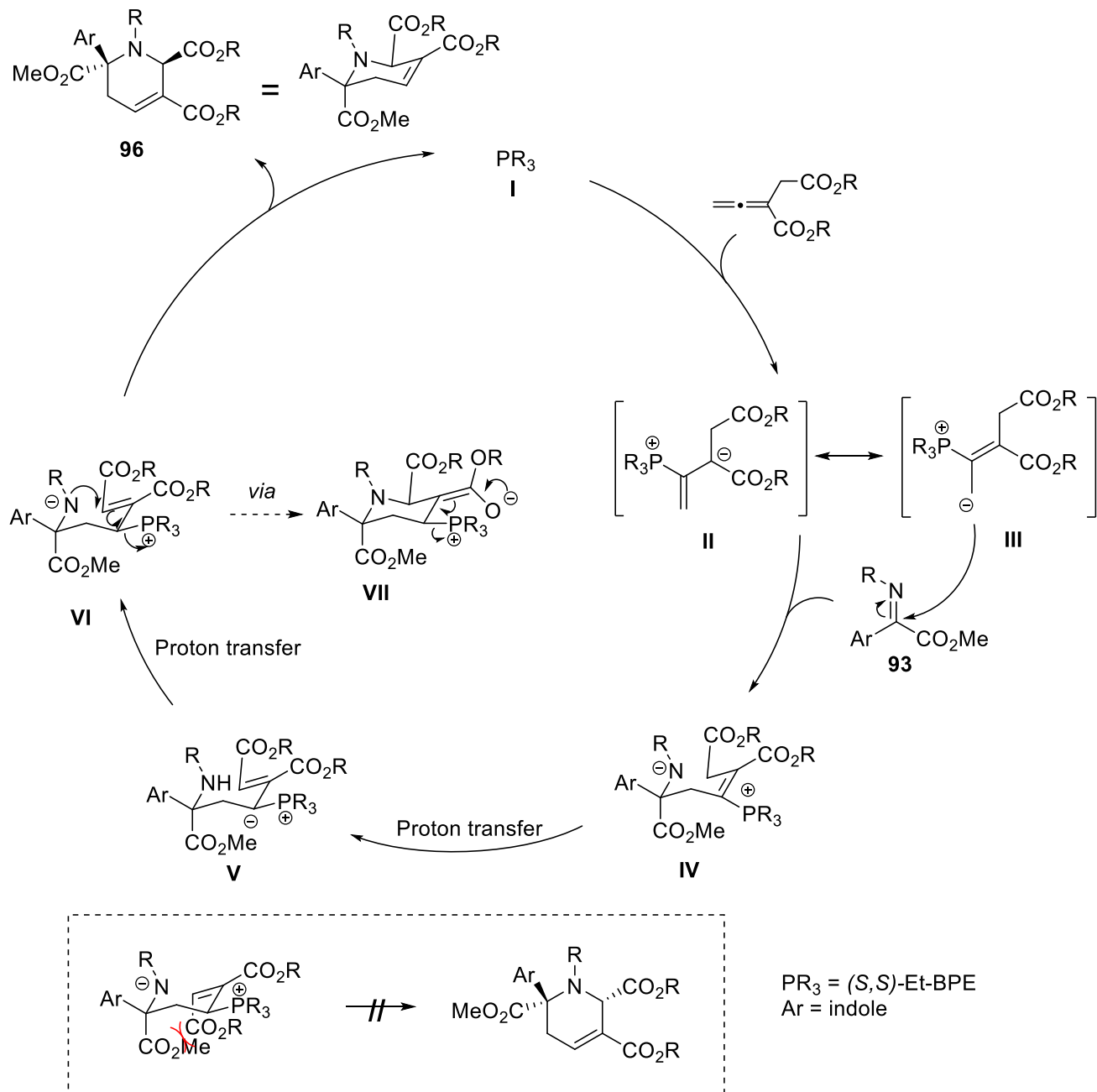


Scheme 30: Deprotection of the nosyl group to obtain the free NH pseudo-NP.

The low yield may in part be due to the formation of a dihydropyridine species that was isolable in minor amounts. Its formation may be facilitated by the excess thiophenol and base, resulting in the removal of the acidic proton of the chiral centre and subsequent rearrangement. Unfortunately, attempts to alkylate this scaffold resulted in no reaction. This would indicate that NH of the THP is sterically hindered by the adjacent ester groups, as well as the indole. Nevertheless, a broad scope of 21 compounds (excluding racemic variants) were synthesised.

2.3.4 Mechanistic Hypothesis

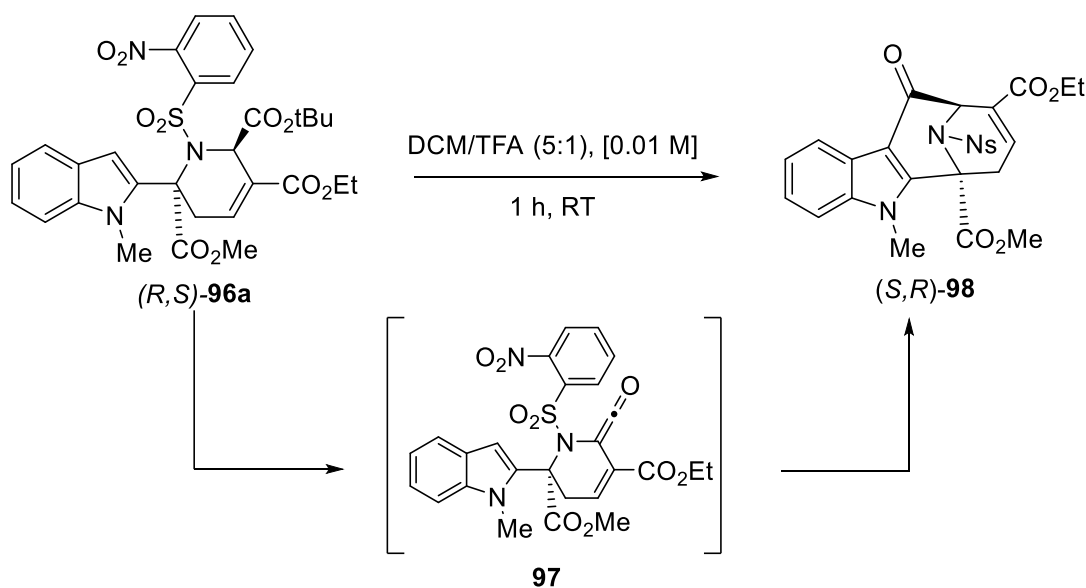
Using previous reports on other phosphine catalysed [4+2] annulations that use the aldimine and cyclic ketimine starting materials, a plausible mechanism for this transformation can be proposed.^[151,156] It should be noted, however, that this is the first example of a phosphine catalysed [4+2] annulation reporting the use of a ketimines with allenates (Scheme 31). The mechanism proceeds with a conjugate addition of the chiral phosphine catalyst **I** to the allenate to produce a zwitterionic intermediate **II**. This species exists in resonance with allylic carbanion **III**, which can perform a nucleophilic attack on the ketimine electrophile **93** to produce intermediate **IV**. Subsequently, this negatively charged nitrogen facilitates two consecutive proton-transfers. The resulting intermediate **V**, then undergoes the key 6-*endo* cyclisation to form the THP, with concomitant regeneration of the chiral phosphine catalyst ultimately yielding the desired pseudo-NP **96**. Significant computational analysis of this reaction-type with *N*-tosyl aldimine was performed by Han and Qiao.^[156] It suggests that the cyclisation-elimination process may ensue *via* an intramolecular Michael-type addition to the ester to form enolate **VII** that promptly reforms the carbonyl to expel the phosphine.



Scheme 31: Proposed mechanism for the phosphine-catalysed [4+2] annulation reaction.

2.3.5 Access to a NP-like Bridged-Bicyclic Compound Class

When exploring the modifications to the indole-THP pseudo-NP class, one of the initial strategies for diversifying the scaffold was hydrolysis of the tert-butyl ester of *(R,S)*-**96a**. This would allow the resulting carboxylic acid to be used in further transformations such as amide couplings. Upon treatment with acid, instead of the expected hydrolysis of tert-butyl ester, we discovered the formation of bridged-bicyclo compound *(S,R)*-**98** (Scheme 32).^[151]

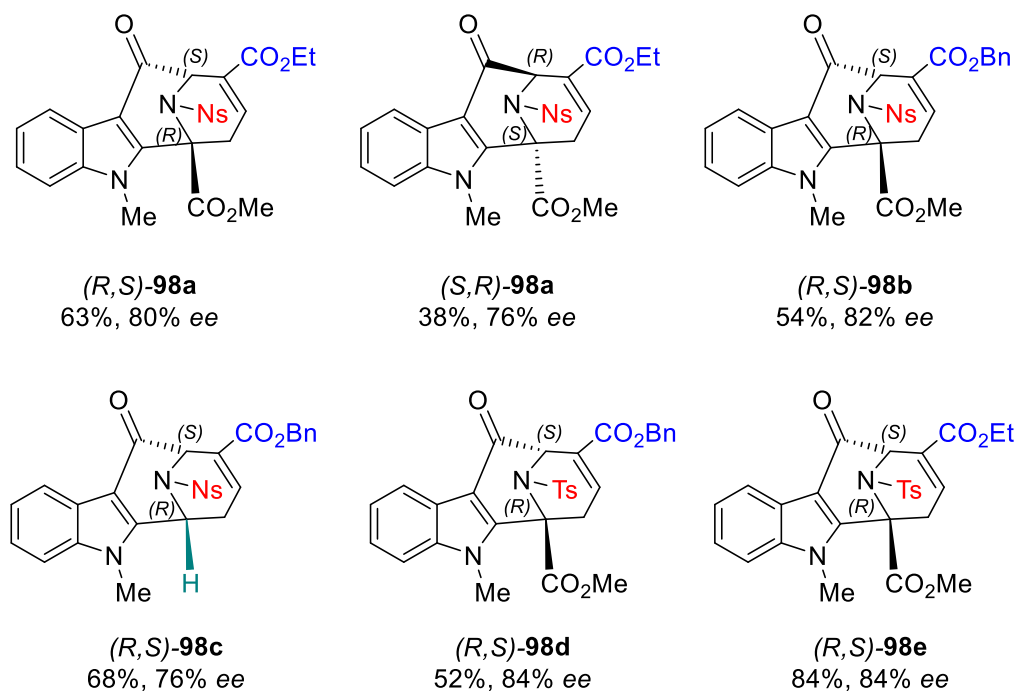
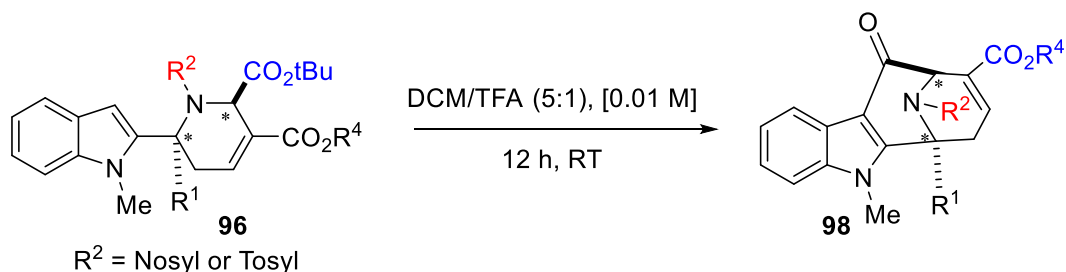


Scheme 32: Proposed route for formation of the bridged compounds *via* ketene formation.

This had previously been observed in the literature using conc. HCl for longer reaction times of 48 h,^[157] therefore it was surprising that even after 1 hour the major mass detected was that of the bridged compound. The cause of such a transformation may be due to the formation of ketene intermediate **97** (Scheme 32). More common ways of accessing ketenes is from acid chlorides, with expulsion of the chloride after deprotonation of the α -carbon under basic conditions or a Wolff-rearrangement. However, obtaining a ketene from a carboxylic acid is not unknown but it is often reported with harsh conditions combining high temperatures and strong excess acid.

It was still important to rule out the possibility of obtaining the carboxylic acid, therefore other conditions were explored for the selective hydrolysis (Table 8). This included finding alternatives

tert-butyl ester starting compounds to synthesise a small collection of bridged-bicyclo NP-like compounds (Scheme 33). Initially, nosyl protected compounds were submitted to acid hydrolysis to afford the desired bridged compounds in moderate yields (**98a-98c**). Pleasingly, the enantiomeric excess was carried through from the starting compounds. The tosyl-protected variants (**98d** and **98e**) were also able to undergo cyclisation to yield the bridged compounds.



Scheme 33: Initial scope of the bridged-bicyclo compounds originating from pseudo-NP analogues.

Due to the likely formation of a ketene and temporary loss of the stereocentre, it was important to obtain a crystal structure to determine whether the configuration had been retained or the stereocentre had inverted after the nucleophilic attack of the indole. The structure and stereochemistry were

confirmed by X-Ray analysis of the major isomer (*R,S*)-**98b**, displaying the retention of stereochemistry (Figure 19). This, in part, would be due to the stereochemistry of the indole, which in this case could only attack the ketene from below.

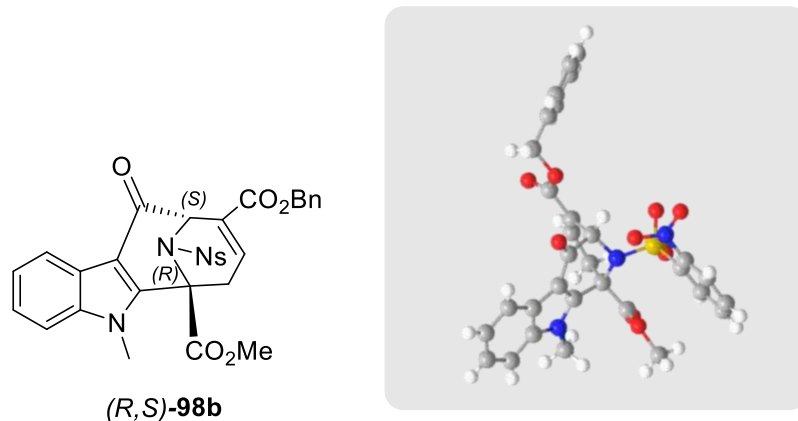
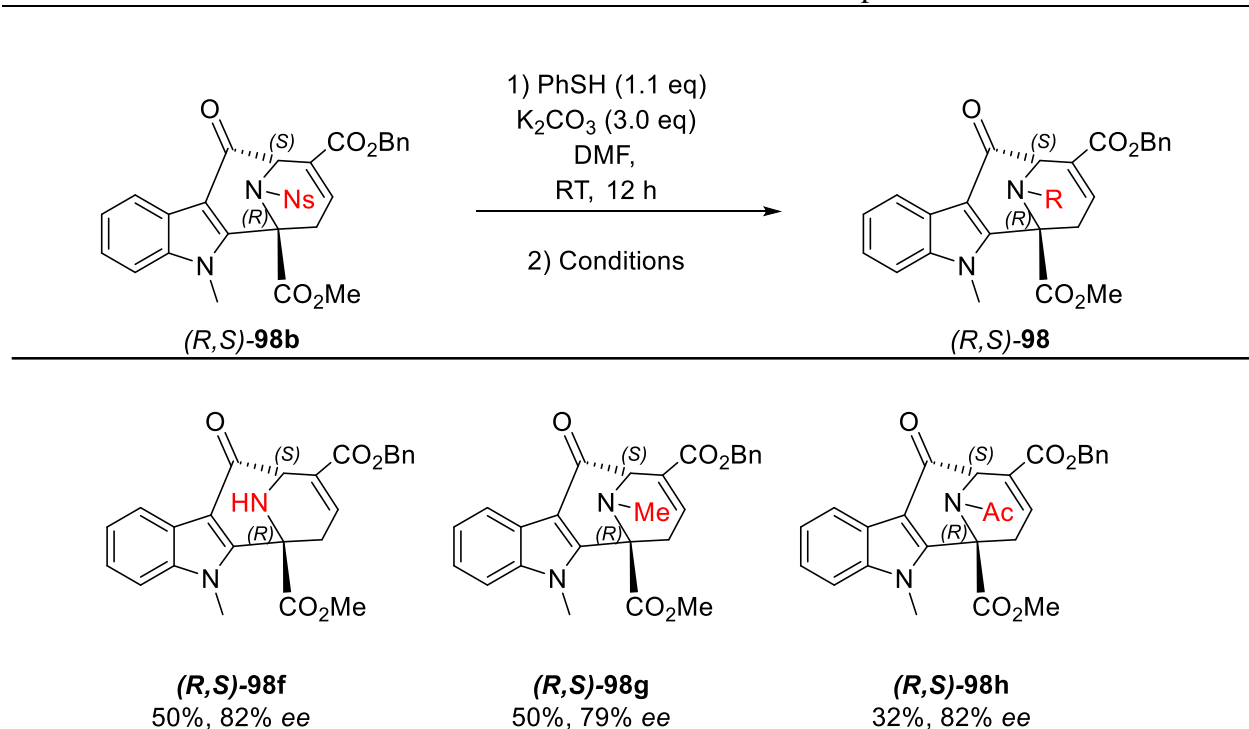


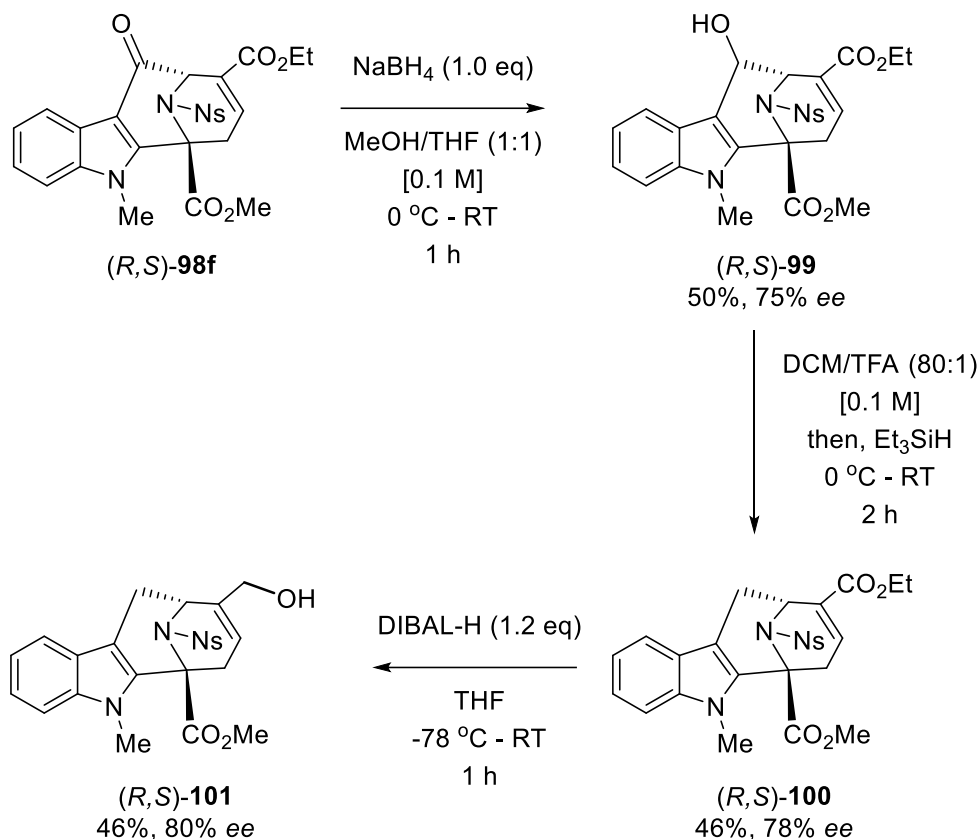
Figure 19: Crystal structure of the bridged-bicyclo compound (*R,S*)-**98b**.

This scaffold in itself has functional handles for modification, which were explored using (*R,S*)-**98b**. For example, deprotection of the nosyl group, using thiophenol with potassium carbonate afforded the free NH compound (*R,S*)-**98f** in moderate yield and high *ee*. Methylation of (*R,S*)-**98f** was accomplished in 50% yield and 79% *ee* using a combination of formic acid and formaldehyde under reflux in an Eschweiler–Clarke reaction to yield (*R,S*)-**98g**. Standard basic conditions for methylation, using methyl iodide for example, were avoided due to the presence of acidic protons at the γ -position to the α,β -unsaturated ester moiety which could lead to methylation on α -carbon adjacent to the carbonyl.^[151] Fortunately, acetylation was achievable, albeit in a low yield of 32% using Et₃N with acetic anhydride to give (*R,S*)-**98h**.



Scheme 34: Deprotection of the nosyl group allows for exploration of substituents on the nitrogen.

A second handle in which this series of bridged pseudo-NP class can be modified is through the ketone. It has been reported that with this scaffold-type that complete reduction of the ketone (Scheme 35) can be achieved with zinc iodide and sodium cyanoborohydride, however in this case, these conditions could only afford trace amounts of the desired compound. Instead, access to the fully reduced bridged compound was achieved *via* an isolated intermediary alcohol **(R,S)-99**, courtesy of treating compound **(S,R)-98f** with sodium borohydride. The secondary alcohol, which was obtained in 50% yield and 75 *ee*, was then removed under acidic conditions, employing Et₃SiH as a hydride source. The desired compound **(R,S)-100**, afforded in 46% yield was further treated with DIBAL-H to reduce the ethyl ester yielding primary alcohol **(R,S)-101**. The retained stereochemistry was confirmed using 2D ¹H-¹H NOESY NMR.



Scheme 35: Synthetic route to ketone reduction and ester reduction of the bridged-bicyclo compounds.

Opening this avenue of diversity is valuable in exploring chemical and biological space. According to the literature, there are NPs with similar scaffolds but expansion of this particular bridged-bicyclic compound class has not been explored or biologically investigated. Further synthetic alterations would be needed to build the library but this initial small collection already holds interest.

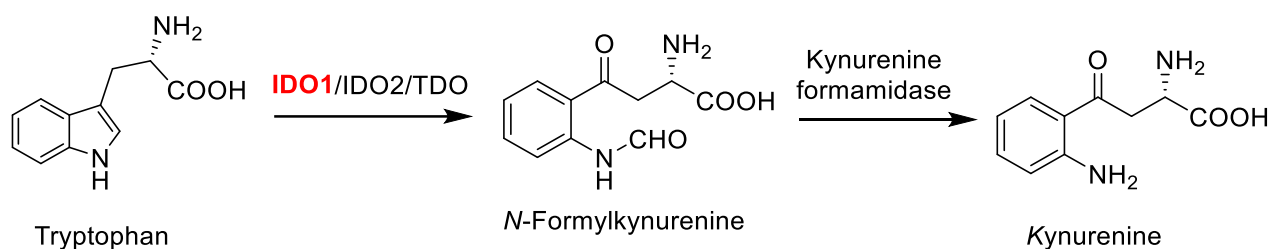
2.3.6 Biological Evaluation

As the goal of the pseudo-NP approach is to aim for novel bioactivity, given the unprecedented structures, compounds from the indole-THP pseudo-NP class were submitted for phenotypic screening by COMAS in parallel to the library synthesis (in part, this dictated compound synthesis). In addition, some bridged-bicyclic compounds were also submitted for screening. The different cell-based assays included Hedgehog (Hh) signalling, autophagy, reactive oxygen species

(ROS) induction and modulation of kynurenine levels. Screening of the pseudo-NP compound class revealed them to be an interesting chemotype in the modulation of kynurenine.

2.3.6.1 IDO1-dependent Kynurenine Modulation

Cancer cells often adapt their metabolism to promote growth and survival whilst remaining undetected by the immune system.^[159] A particular mechanism cancer has hijacked for immune escape is through the kynurenine pathway.^[160,161] This is the major route by which tryptophan (Trp), an essential amino-acid, is catabolised into kynurenine (Kyn, and other metabolites). The first and rate-limiting step of this pathway, that accesses *N*-formylkynurenine (Scheme 36), is facilitated by three heme-containing enzymes: indoleamine 2,3-dioxygenase 1 (IDO1), indoleamine 2,3-dioxygenase 2 (IDO2), and tryptophan 2,3-dioxygenase (TDO).^[162]



Scheme 36: Catabolic pathway for the conversion of tryptophan (Trp) into kynurenine (Kyn).^[160]

IDO1 is the most broadly expressed and most widely studied of the three enzymes. It is found in numerous tissue types including immune privileged organs such as the placenta, but is also present in numerous cancer types.^[163] Often this is displayed as an over-expression, likely aided from the induction of the *IDO1*-gene by cytokines like Interferon- γ (IFN- γ).^[164] Tumour progression therefore leads to an IDO1-mediated decrease in Trp levels and concomitant increase in Kyn in the tumour microenvironment (TME) (Figure 20). The result of this metabolic change is a suppressed immune response. The underlying cause is the inactivation of immune cells due to Trp deprivation, which also leads to a reduction in natural killer (NK) and T-cell proliferation.^[165] In addition, the increase in Kyn levels induces the differentiation of regulatory T-cells through its binding to aryl hydrocarbon receptors (AhR). The overall effect allows cancer to escape immune surveillance and supports tumour progression.^[165,166]

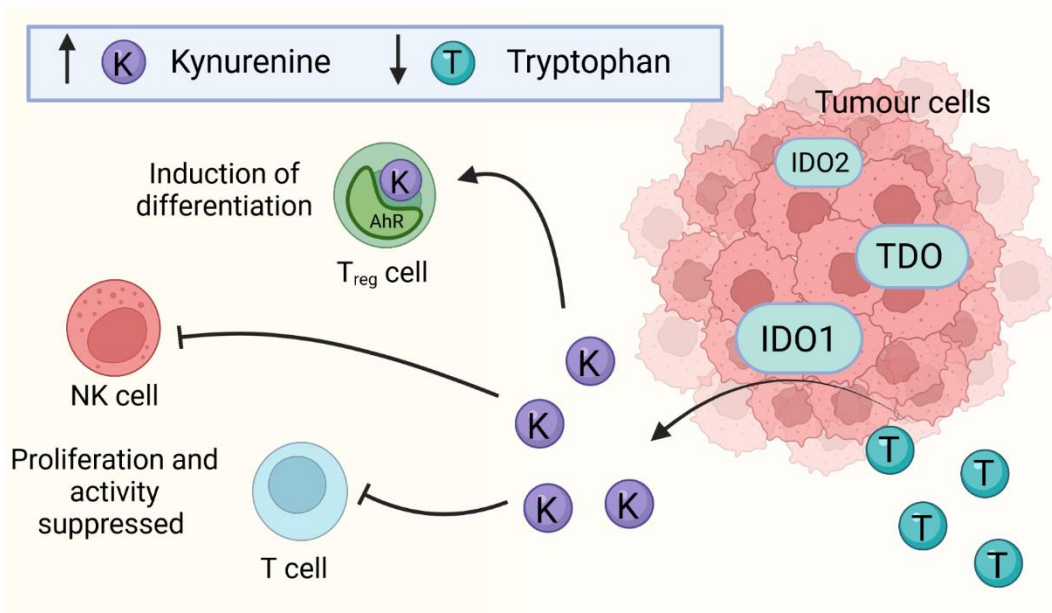


Figure 20: IDO1 expression in tumour cells leads to depletion of Trp (T) and the production of Trp metabolites, such as Kyn (K), resulting in immune cell inactivation and, through AhR activation, T Reg proliferation also suppressing T cell function.^[21,165]

Hence, small molecule inhibition of IDO1 has emerged as a strategy to restore or prevent a compromised immune response, simultaneously affording novel therapeutic agents against cancer.^[166–168] There is also interest in targeting IDO2 and TDO, however, in contrast to IDO1, both enzymes cannot be induced by cytokines in cancer cells and their natural expression level is much lower than that of IDO1.^[169,170] Therefore, screening small molecules for modulation of Kyn levels is a crucial start point in identifying potential novel chemotypes that interfere with IDO1.

2.3.6.1.1 IDO1 Inhibitors

Over the past decade, the hunt for IDO1 inhibitors has led to the discovery of various compound classes that successfully reduce Kyn levels through different mechanisms.^[171,172] However, there is still a lack of IDO1 inhibitors on the drug market as many have failed in clinical trials, but there are still a lot of studies ongoing. Notable examples include Epacadostat, BMS-986205 (Linrodostat), Navoximod and Indoximod (Figure 21).^[173] Epacadostat is a Trp-competitive inhibitor, 1000-fold selective over IDO2 and TDO. Linrodostat is the most potent, IDO1-selective compound with Kyn inhibition measuring an $IC_{50} = 1.7$ nM in HeLa cells. Navoximod has recently

completed phase I clinical trials, whereas methyl-tryptophan, Indoximod has recently been granted FDA approval in the US for treatment of type of melanoma. Interestingly, even though it is a Trp derivative, it does not directly inhibit IDO1.^[160,174]

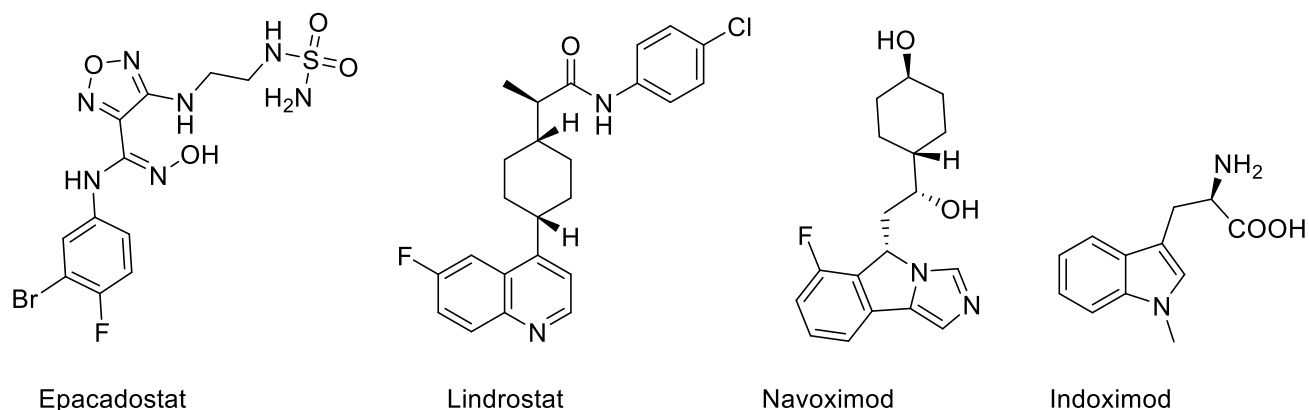


Figure 21: Selected examples of IDO1 inhibitors.

As mentioned, IDO1 is a heme-containing enzyme, and with such a structure come different mechanisms in which IDO1 can be inhibited. Röhrig *et al.* categorised these inhibitory means into four types of direct IDO1 inhibitors: I) tryptophan-competitive, binding to oxygen-bound holo-IDO1, II) oxygen-competitive, binding to free ferrous holo-IDO1, III) inhibitors binding to free ferric holo-IDO1 and IV) inhibitors binding to apo-IDO1.^[172,175] In contrast to inhibitor types I-III, type IV inhibitors do not coordinate to the heme in the IDO1 active site, but target IDO1 exclusively in its heme-free form. Redox cyclers, like quinones were also described as IDO1 inhibitors but rather in a cellular environment, able to generate antitumor cytotoxicity through the generation of reactive oxygen species (ROS).^[171] Despite multiple chemotypes and mechanisms of action, including those containing indole (e.g Indoximod), there is still a need to discover compounds that modulate kynurenine production.

2.3.6.2 Modulation of Kynurenine Production SAR

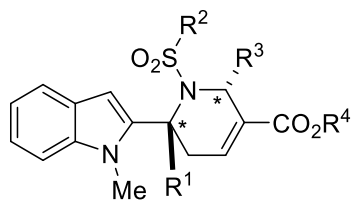
Kyn assay performed by Lara Dötsch

Several derivatives of the pseudo-NP class demonstrated particularly potent activity in selectively decreasing Kyn levels in HeLa cells upon stimulation with the cytokine IFN- γ (Table 9). Initially, the activities of enantioreiched compounds, **93** and **96a** were determined (Entries 1-3), which then dictated the synthetic modifications. The model compound (*R,S*)-**93**, used in reaction optimisation, showed no influence on Kyn levels (Entry 1). However, a change in the ester combination, (*R,S*)-**96a**, revealed moderate activity (Entry 2). Crucially, its enantiomer, (*S,R*)-**96a** was substantially more active with an $IC_{50} = 0.49 \pm 0.10 \mu M$ (Entry 3). Further exploration of the structure-activity-relationship based on this “hit” then favoured the formation of compounds with the (*S,R*) configuration. Gratifyingly, lack of a methyl ester, (*S,R*)-**96f**, derived from the aldimine starting substrate, was two-fold less active (Entry 4). This justified the installation of the tertiary centre but also enhances the value of this pseudo-NP class. Continuing to probe the ester combinations at R³ and R⁴ derived from the allenolate, (Entries 5-10) revealed no further improvement in activity, with the optimal pairing still the tertiary butyl- and ethyl ester, respectively. The (*S,R*) configuration remained the more active of the compounds in all cases.

Exchange of the nosyl group with other sulphonamide moieties at R² (Table 1, entries 11-19) generally provided sub-micromolar activity. Tosylated compound (*S,R*)-**96g** afforded double-digit nanomolar activity with $IC_{50} = 0.07 \pm 0.01 \mu M$ (Entry 12). Again, it was found that removal of the methyl ester was detrimental to activity (Entry 15). Other substituted phenyl rings with electron withdrawing groups (*p*-Br and *m*-CF₃) diminished activity (Entries 16 and 17), whereas phenyl (*S,R*)-**96n** and methyl (*S,R*)-**96o** moieties recorded comparable nanomolar potency (Entries 18 and 19). The importance of having a substituted nitrogen on the THP ring was confirmed when its removal led to inactivity (*S,R*)-**96p** (Entry 20).

As in most cases with enantiomeric mixtures, one enantiomer is more active than the other. In terms of biology this could mean one enantiomer behaves differently than the other. The most infamous example being the enantiomers of thalidomide.^[176] Therefore, a series of selected compounds, were purified in order to obtain single enantiomers to determine their activity (Entries 21-25).

Table 9: SAR for reduction of Kyn levels in HeLa cells. Data are mean values (n=3) ± SD.



Entry	Compound	R ¹	R ²	R ³	R ⁴	<i>ee</i> [%]	Configuration	IC ₅₀ [μM]
1	93 ^a	CO ₂ Me	<i>o</i> -NO ₂ -Ph	CO ₂ Et	Et	88	(<i>R,S</i>)	>10
2	96a ^a	CO ₂ Me	<i>o</i> -NO ₂ -Ph	CO ₂ tBu	Et	76	(<i>R,S</i>)	2.44 ± 0.56
3	96a	CO ₂ Me	<i>o</i> -NO ₂ -Ph	CO ₂ tBu	Et	75	(<i>S,R</i>)	0.49 ± 0.10
4	96f	H	<i>o</i> -NO ₂ -Ph	CO ₂ tBu	Et	82	(<i>S,R</i>)	1.04 ± 0.08
5	96b	CO ₂ Me	<i>o</i> -NO ₂ -Ph	CO ₂ Et	tBu	86	(<i>S,R</i>)	2.46 ± 0.29
6	96c	CO ₂ Me	<i>o</i> -NO ₂ -Ph	CO ₂ Bn	Et	76	(<i>S,R</i>)	7.52 ± 0.80
7	96d ^a	CO ₂ Me	<i>o</i> -NO ₂ -Ph	CO ₂ tBu	tBu	88	(<i>R,S</i>)	0.82 ± 0.70
8	96d	CO ₂ Me	<i>o</i> -NO ₂ -Ph	CO ₂ tBu	tBu	92	(<i>S,R</i>)	0.65 ± 0.08
9	96e ^a	CO ₂ Me	<i>o</i> -NO ₂ -Ph	CO ₂ tBu	Bn	84	(<i>R,S</i>)	2.88 ± 0.13
10	96e	CO ₂ Me	<i>o</i> -NO ₂ -Ph	CO ₂ tBu	Bn	76	(<i>S,R</i>)	1.39 ± 0.09
11	96g ^a	CO ₂ Me	<i>p</i> -Me-Ph	CO ₂ tBu	Et	86	(<i>R,S</i>)	0.28 ± 0.04
12	96g	CO ₂ Me	<i>p</i> -Me-Ph	CO ₂ tBu	Et	85	(<i>S,R</i>)	0.07 ± 0.01
13	96h	CO ₂ Me	<i>p</i> -Me-Ph	CO ₂ Et	tBu	90	(<i>S,R</i>)	0.76 ± 0.04
14	96i	H	<i>p</i> -Me-Ph	CO ₂ Et	tBu	76	(<i>S,R</i>)	1.63 ± 0.16
15	96j ^d	H	<i>p</i> -Me-Ph	CO ₂ tBu	Et	86	(<i>S,R</i>)	0.26 ± 0.05
16	96k	CO ₂ Me	<i>p</i> -Br-Ph	CO ₂ tBu	Et	82	(<i>S,R</i>)	0.43 ± 0.15
17	96m	CO ₂ Me	<i>m</i> -CF ₃ -Ph	CO ₂ tBu	Et	84	(<i>S,R</i>)	1.54 ± 0.41
18	96n	CO ₂ Me	Ph	CO ₂ tBu	Et	78	(<i>S,R</i>)	0.08 ± 0.01
19	96o	CO ₂ Me	Me	CO ₂ tBu	Et	86	(<i>S,R</i>)	0.08 ± 0.01
20	96p	CO ₂ Me	Free NH	CO ₂ tBu	Et	82	(<i>S,R</i>)	> 10
21	96a	CO ₂ Me	<i>o</i> -NO ₂ -Ph	CO ₂ tBu	Et	>99	(<i>S,R</i>)	0.49 ± 0.10
22	96g ^{ab}	CO ₂ Me	<i>p</i> -Me-Ph	CO ₂ tBu	Et	>99	(<i>R,S</i>)	3.41 ± 0.26
23	96g ^b	CO ₂ Me	<i>p</i> -Me-Ph	CO ₂ tBu	Et	>99	(<i>S,R</i>)	0.047 ± 0.002
24	96j ^b	H	<i>p</i> -Me-Ph	CO ₂ tBu	Et	>99	(<i>S,R</i>)	0.16 ± 0.05
25	96n ^c	CO ₂ Me	Ph	CO ₂ tBu	Et	>99	(<i>S,R</i>)	0.09 ± 0.01

[a] Acquired using (*S,S*)-Et-BPE. [b] purified on chiral preparative HPLC, IC column, DCM:EtOH (100:2)/*iso*-hexane, flow rate = 3 mL min⁻¹. [c] Purified using DCM:MeOH (100:5)/*iso*-hexane. [d] In Bx-PC3 cells.

Enantiomeric purification of the most potent compound (*S,R*)-**96g**, yielded minor enantiomer (*R,S*)-**96g** and the major product (*S,R*)-**96g** (Entries 22 and 23). This clearly demonstrated the significant influence the minor enantiomer had on activity, as single enantiomer, (*S,R*)-**96g**, had an IC_{50} value of 46.7 ± 2.4 nM, while (*R,S*)-**96g** was 72-fold less active in HeLa cells (Figure 22). The difference was also apparent when measured in another cancer cell line, BxPC-3.

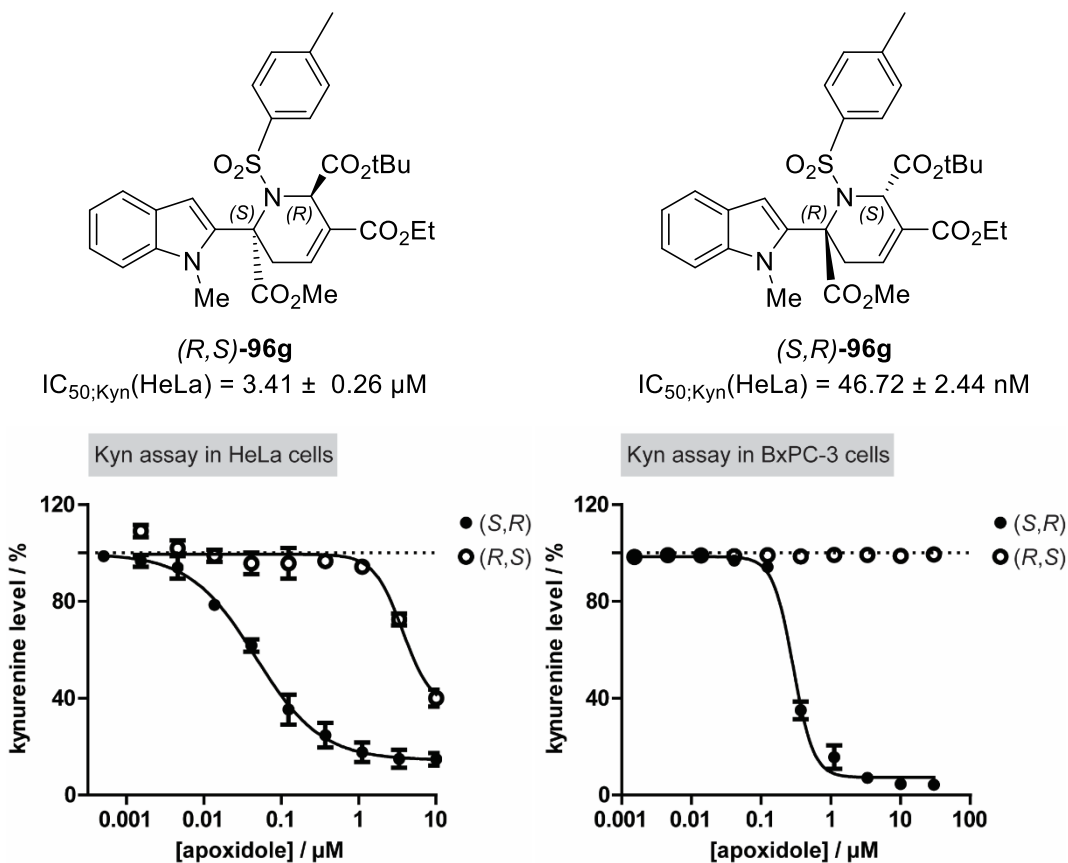


Figure 22: Structures and IC_{50} values of single enantiomers (*R,S*)-**96g** and (*S,R*)-**96g** (mean \pm SD, $n = 3$) in HeLa cells and in BxPC-3 cells upon treatment with IFN- γ , L-Trp and compounds for 48 h and detection of Kyn using *p*-DMAB (mean \pm SD, $n = 3$).

It was therefore decided that the enantiopure (*S,R*)-**96g** would be taken further in target identification studies to determine its mode of action in reducing Kyn levels.

2.3.6.2.1 Activity of the Bridged-Bicyclic NP-like Compounds

Alongside the pseudo-NP class, a few derivatives of the bridged-bicyclic compounds were also submitted for screening (Figure 23). In comparison to the pseudo-NPs, the bridged compounds were weakly active in reducing Kyn levels. However, the benzyl ester-containing compound (*R,S*)-**98b** revealed sub-micromolar activity with an $IC_{50} = 0.53 \pm 0.16 \mu\text{M}$ in an osteoblast differentiation assay.

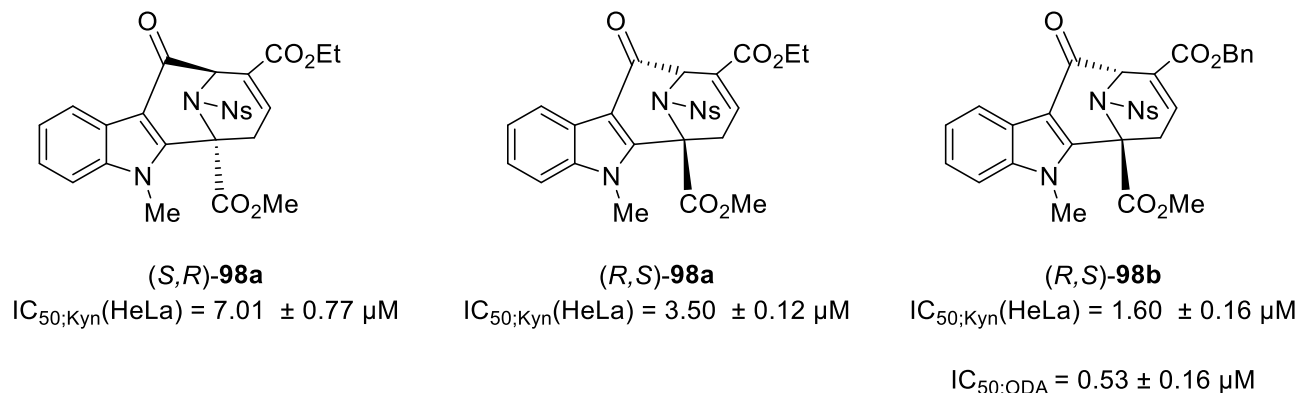


Figure 23: Results of initial phenotypic screening of the bridged-bicyclo compounds.

These early indications of biological activity has prompted significant library expansion and SAR studies. This is particularly important, as such a compound class has not been studied for bioactivity before.

2.3.6.3 Target Identification: Inhibition of apo-IDO1

All biological investigation and assays were performed by Lara Dötsch

Understanding where a small molecule binds and how it binds in order to regulate the function of the biological target is critical, especially from a therapeutic standpoint. As a result, a range of methods to identify and validate targets were employed.

In order to determine how (*S,R*)-**96g** was causing a reduction in cellular Kyn levels, initial experiments explored the possibility of interference in IDO1 expression. The impact on the *IDO1* promoter was analysed by means of a reporter gene assay (Figure 24A). However, the pseudo-NP (*S,R*)-**96g** showed no reduction of the expression of the reporter, indicating that *IDO1* gene

expression is not inhibited. Furthermore, (*S,R*)-**96a** did not alter IDO1 mRNA level and (*S,R*)-**96g** had no influence on the protein level of IDO1 (Figure 24B and 24C), again strongly suggesting that there is no interference of IDO1 expression.

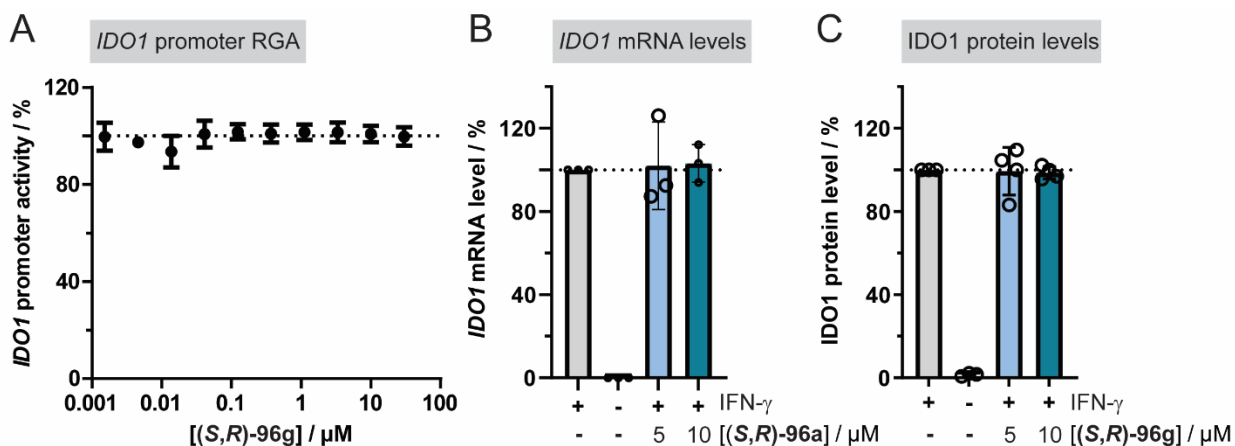


Figure 24: The pseudo-NP class reduces cellular kynurenine (Kyn) levels, but does not inhibit IDO1 expression. A) Reporter gene assay (RGA) in HEK293T cells expressing firefly luciferase (Fluc) under the control of the *IDO1* promoter and constitutive *Renilla* luciferase expression. Expression of Fluc was induced by IFN- γ with simultaneous treatment with (*S,R*)-**96g** for 48 h (mean \pm SD, n = 3). B) *IDO1* mRNA expression in HeLa cells upon treatment with IFN- γ and (*S,R*)-**96a** or DMSO for 24 h (mean \pm SD, n = 3) C) IDO1 protein levels in HeLa cells that were treated with IFN- γ and (*S,R*)-**96g** or DMSO for 24 h.

Altered tryptophan uptake into IDO1-expressing cells could also cause reduced Kyn levels. Transport of Trp into cells is typically facilitated by L-type amino acid transmembrane transporters (LATS)^[177] or tryptophanyl-tRNA synthetases (TrpRS). The latter are highly expressed upon treatment with IFN- γ ^[178] and can be inhibited by Trp analogue 1-methyl-L-tryptophan (1-MT).^[178,179] In order to gauge if (*S,R*)-**96g** was interfering with uptake mechanisms, BxPC-3 cells were treated with and without IFN- γ and starved of Trp for 72h (Figure 25). In the presence of IFN- γ , a higher L-Trp uptake was observed upon treatment with IFN- γ . However, this is likely due to induced expression of TrpRS and IDO1, so there is a higher demand for the Trp substrate. Importantly, when compared to known Trp uptake inhibitors, L-Leu (known to saturate amino acid transporters^[180]) and 1-methyl-Trp, it was determined^[180] that (*S,R*)-**96g** does not have influence on Trp transportation into the cell.

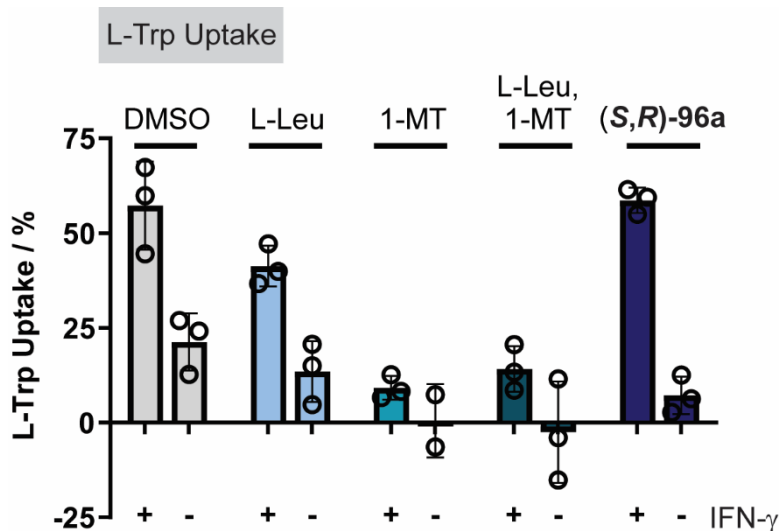


Figure 25: Influence of (*S,R*)-**96a** on L-Trp uptake. BxPC-3 cells were starved for L-Trp for 72h and treated with IFN- γ for 24h prior to addition of control inhibitors (5 mM L-Leu, 1 mM 1-MT) or 5 μ M (*S,R*)-**96a** for 30 min. Afterwards, 50 μ M L-Trp was added and L-Trp uptake was quantified with HPLC-MS/MS (mean \pm SD, $n = 3$). IFNGR: Interferon-gamma receptor. LAT: system L-amino acid transporter. L-Leu: L-leucine. 1-MT: 1-methyl-L-tryptophan. TrpRS: tryptophanyl-tRNA synthetase.

Attention was then turned to direct inhibition of IDO1 *in vitro*. Typically, to evaluate IDO1 inhibitors, this assay is performed at 25°C, however (*S,R*)-**96a** showed no activity. However, *in vitro*, holo-IDO1 (heme containing IDO1 form) is the dominant enzyme form present and to evaluate activity of apo-IDO1 (non-heme containing) inhibitors, a higher temperature is needed for heme dissociation.^[161,181] Therefore, after pre-incubation at 37°C, (*S,R*)-**96a** showed a dose-dependent decrease in IDO1 activity (Figure 26A). This requirement for heme displacement is the reason why apo-IDO1 inhibitors have less potent IC₅₀ values *in vitro* than in cells. Crucially, the observed inhibition was recognised as a common characteristic for small molecules that bind to the apo form of IDO1 (e.g. Linrodostat) thus preventing heme binding.^[161]

In order to prove that (*S,R*)-**96g** was binding to IDO1, the thermal denaturation of IDO1 was analysed using nano differential scanning fluorimetry (Figure 26B). Treatment of IDO1 with (*S,R*)-**96g** positively shifted the thermal denaturation temperature, T_m , from $45.7 \pm 0.2^\circ\text{C}$ to $53.5 \pm 0.2^\circ\text{C}$, a difference of $7.7 \pm 0.3^\circ\text{C}$, showing that (*S,R*)-**96g** directly binds to IDO1. In order to ascertain if binding of (*S,R*)-**96g** induced heme loss, UV/Vis spectroscopy was used to monitor the “Soret peak” (Figure 26C). The Soret peak shows the maximum absorbance of heme-containing enzymes

at 405 nm. A red-shift of the maximum indicates ligand coordination to the heme, whilst reduced signal intensity indicates heme loss.^[182] Single enantiomer (*S,R*)-**96g** dose-dependently reduced the Soret peak, proving that compound binding to IDO1 releases heme. In addition, increasing concentrations of free hemin reduced the potency of (*S,R*)-**96g** in the Kyn assay (Figure 26D) which in hand with the Soret plot suggest that (*S,R*)-**96g** competes with heme for apo-IDO1.

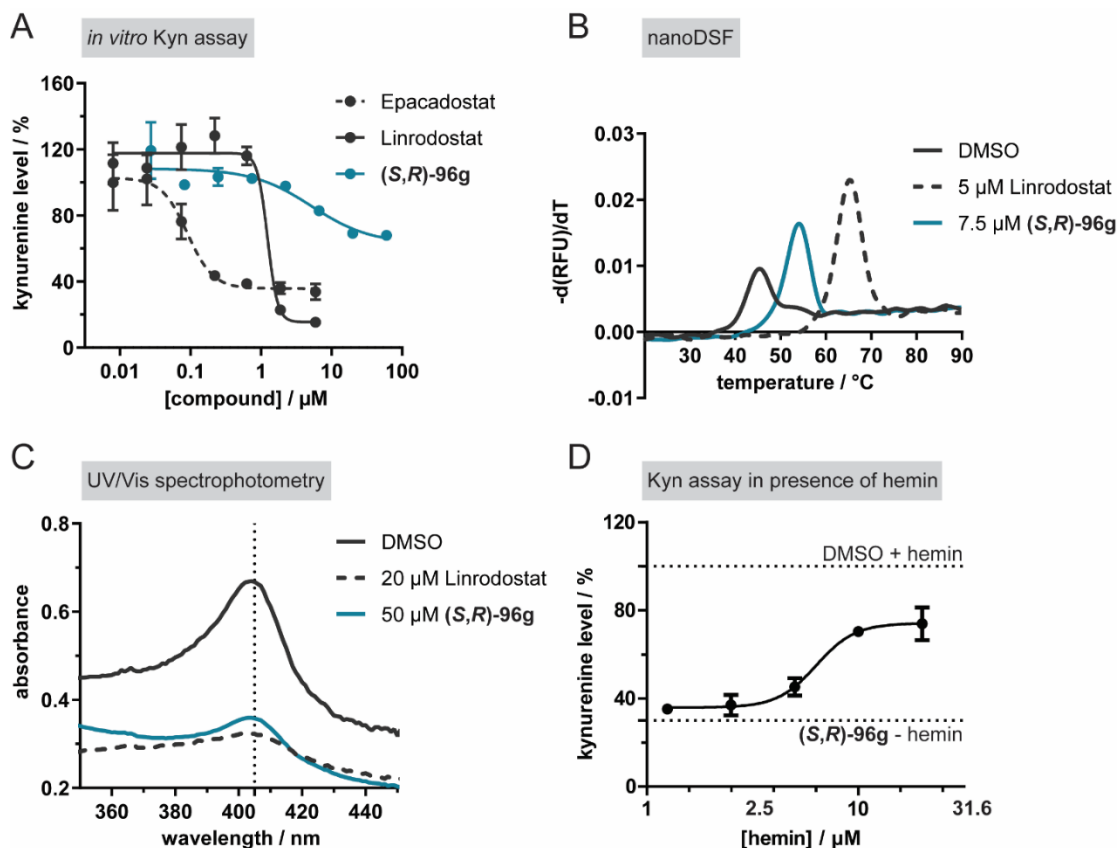


Figure 26: Pseudo-NP (*S,R*)-**96g** inhibits IDO1 by binding to apo-IDO1 and releasing heme. A) Purified IDO1 protein was treated with (*S,R*)-**96g**, Linrodostat or epacadostat for 40 min at 37°C prior to detection of Kyn levels using *p*-DMAB (mean ± SD, n = 2). B) Dose-dependent influence of (*S,R*)-**96g** on the melting temperature of IDO1. Purified IDO1 was treated with (*S,R*)-**96g** or DMSO for 60min at 37°C prior to detection of the intrinsic tryptophan/tyrosine fluorescence upon melting. Representative melting curves shown. C) UV/Vis spectra of IDO1. Purified IDO1 was treated with (*S,R*)-**96g**, Linrodostat (20 μM) or DMSO for 2h at 37°C prior to acquiring UV/Vis spectra. Representative spectra shown (n = 3). Dotted line indicates the Soret peak at 405 nm. D) Determination of Kyn levels in presence of hemin. BxPC-3 cells were treated with IFN- γ , L-Trp, hemin and 600 nM apoxidole-1 for 48 h prior to measuring Kyn levels with *p*-DMAB (mean ± SD, n = 3).

However, it was important to confirm that (*S,R*)-**96g** was targeting apo-IDO1 in cells. In order to validate this the thermal stability of IDO1 in a cellular thermal shift assay (CETSA) was measured.^[183] Initial treatment of SKOV-3 cells with (*S,R*)-**96g** did not show any shift in T_m after 15min. However, as mentioned, pre-incubation of IDO1 with compounds at 37°C is required to identify apo-IDO1 inhibitors *in vitro* as heme dissociation from holo-IDO1 is a slow and reversible process. Therefore, the short treatment time was not long enough to allow (*S,R*)-**96g** to displace heme and bind to apo-IDO. Instead, cells were pre-treated with the heme synthesis inhibitor succinylacetone 24 h prior to CETSA to ensure that apo-IDO1 was the major form upon compound exposure. Upon treatment with (*S,R*)-**96g**, a shift in T_m of $7.9 \pm 0.6^\circ\text{C}$ (Figure 27) was measured. Interestingly, comparing the protein melting behaviour of holo-IDO1 (without heme synthesis inhibitor) and apo-IDO1 (with heme synthesis inhibitor), there was a clear difference. For holo-IDO1, a T_m of $59.9 \pm 0.2^\circ\text{C}$ was recorded, whereas apo-IDO1 was $50.2 \pm 0.2^\circ\text{C}$. This finding indicates that holo-IDO1 has a higher thermal stability than apo-IDO1 but heme binding or the binding of (*S,R*)-**96g** to apo-IDO1 stabilises the protein (positive thermal shift).

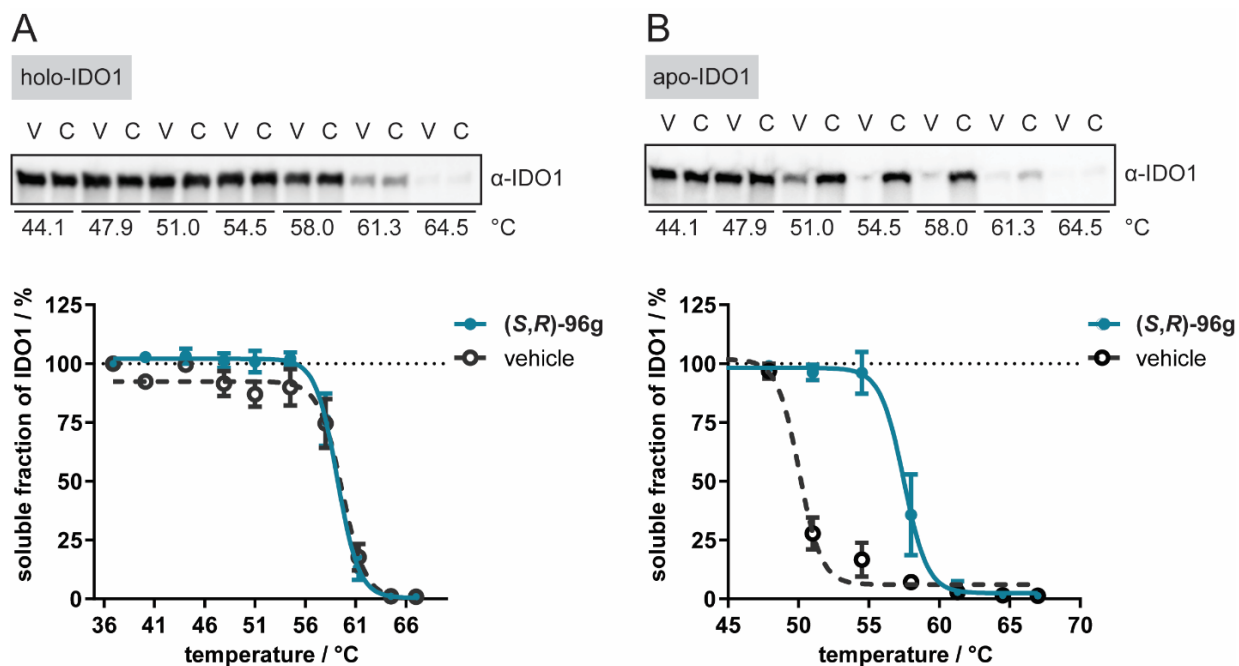


Figure 27: Cellular thermal shift assay (CETSA) for IDO1 in SKOV-3 cells with quantification of IDO1 band intensities (mean \pm SD, $n = 3$). A) Representative immunoblot ($n = 3$) and thermal profile of holo-IDO1 (in absence of SA). B) Representative immunoblot ($n = 3$) and thermal profile apo-IDO1 (in presence of SA) upon compound treatment. (apo-IDO1. Cells were treated with IFN- γ and 10 μM succinylacetone (heme synthesis inhibitor) for 24 h prior to addition of 30 μM (*S,R*)-**96g** or DMSO for 15min.

Finally, the selectivity of (*S,R*)-**96g** was explored. As well as IDO1 in its various forms, also expressed in cells are TDO and IDO2.^[184,185] These enzymes of IDO1 also catabolise Trp and have a heme-containing active site, so it is therefore important to confirm if pseudo-NP(*S,R*)-**95h** is binding to them. Both Epacadostat and Lindorostat are reported to have high selectivity for IDO1.^[32] In the case of Epacadostat a >1000-fold selectivity over TDO and IDO2^[173]. Gratifyingly, pseudo-NP (*S,R*)-**96g** did not inhibit TDO or IDO2, comparable to the known apo-IDO1 inhibitor Lindorostat (Figure 28). This strongly supports that the type IV inhibitor (*S,R*)-**96g** is selective to IDO1.

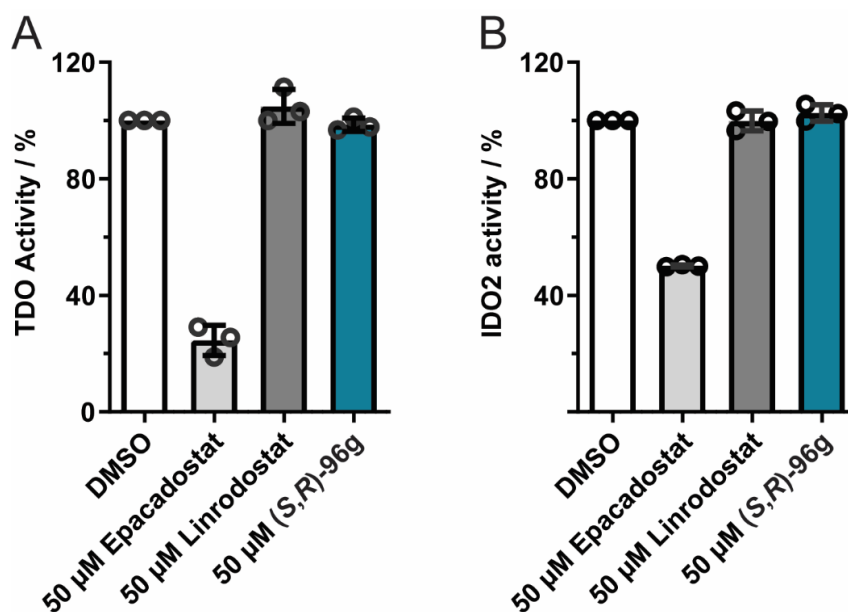


Figure 28: (*S,R*)-**96g** does not inhibit TDO and IDO2. A) Purified TDO protein was treated with epacadostat, Lindorostat or (*S,R*)-**96g** for 120 min at 37°C prior to detection of the reaction product (mean \pm SD, n = 3). B) Purified IDO2 protein was treated with epacadostat, Lindorostat or (*S,R*)-**96g** for 90 min at 30°C prior to addition of the IDO2 substrate. Samples were incubated for another 120 min at 30°C prior to detection of the reaction product (mean \pm SD, n = 3).

Confirmation of these results led to the pseudo-NP class being reassigned as “Apoxidoles” This name incorporates both the chemical and biological relevance of the compound class. It acknowledges the indole core structure of the pseudo-NP class whilst combining the mode-of-action of the most potent compound, apoxidole-1 (formerly (*S,R*)-**96g**) inhibiting apo-IDO1..

2.4 Summary

In summary, the pseudo-NP approach was applied successfully in the design and synthesis of a novel pseudo-NP class, apoxidoles, which combines indole and THP fragments *via* a monopodal connection. Despite being found together in nature, the fragment arrangement is unprecedented and was obtained using a complexity-generating and stereoselective, phosphine-catalysed [4+2] annulation reaction under ambient conditions. The reaction was limited with regard to allene substituents and was unable to tolerate heterocycles other than indole. However, the latter should be explored further, alongside other modifications to deliver further, diverse variants that would benefit the exploration of chemical space. Nevertheless, the reaction was employed to afford 24 examples with yields up to 93% and *ee* up to 92%.

In parallel to the investigation of the apoxidoles, a bridged-bicyclic NP-like compound class was also accessible, through an acid promoted ketene formation, at room temperature with notably short reaction times. Here, the indole and THP fragments were connected in a bridged-bipodal pattern. This scaffold, to the best of our knowledge, has not been previously undergone biological studies. Early biological results from cell-based screening assays indicated activity in both kynurenine modulation and osteoblast differentiation. Further chemical expansion of this class is ongoing.

On the other hand, biological evaluation of the apoxidoles pseudo-NP class in various cell-based assays revealed that they represent a new chemotype in the modulation (specifically reduction) of kynurenine levels in cancer cells. Deeper analysis revealed the mode of action using the most potent derivative, apoxidole (*S,R*)-**96g**, which selectively targets and stabilises apo-IDO1. This inhibition of apo-IDO1 classifies apoxidole (*S,R*)-**96g** as a type IV direct inhibitor.

These findings provide further validation that the pseudo-NP approach is not limited to the combination of biosynthetically unrelated fragments. In fact, NP fragments that already appear together in natural products can be combined in unexplored arrangements to enable the discovery of unique compound classes endowed with biological activity. The *de-novo* combination of NP fragments is an advance of other strategies such as BIOS, by avoiding being guided by the starting

scaffold or, in the case of BIOS and CtD, being limited in exploring chemical space. As a result the pseudo-NP approach is able to uncover novel chemical structures and biological activity.

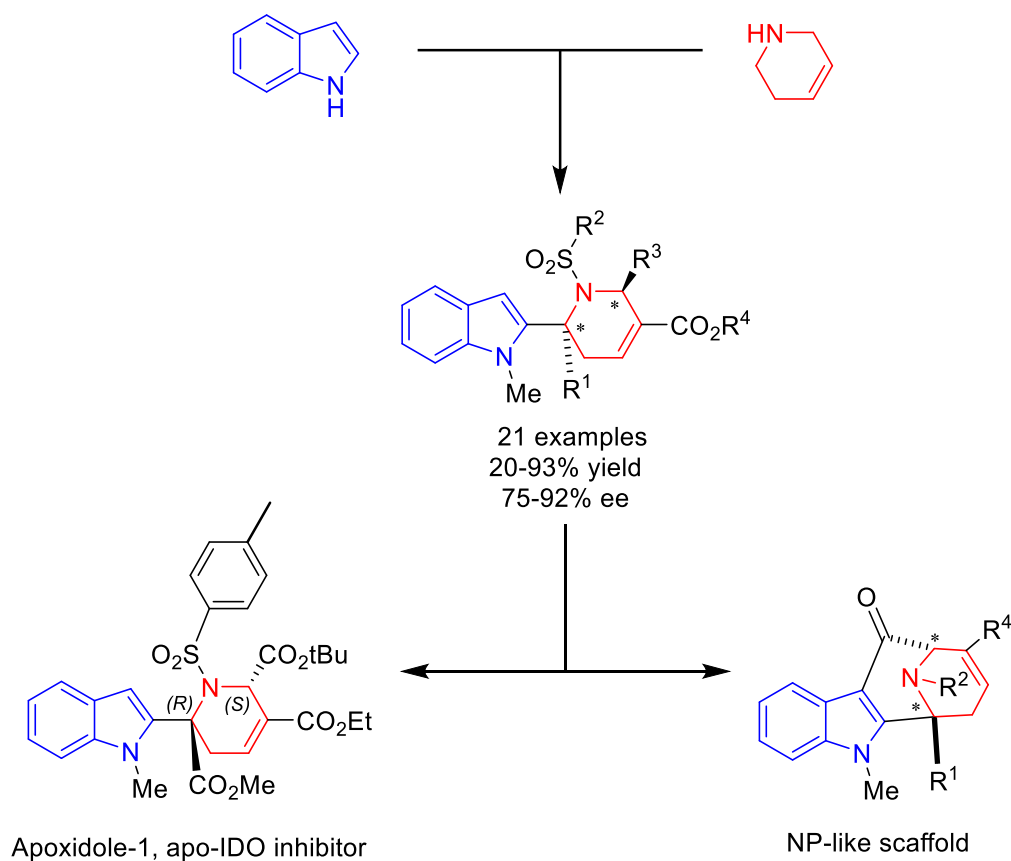


Figure 29: Summary of the design, synthesis and biological evaluation of the Apoxidole pseudo-NP class that also gave access to a bridged-bicyclo NP-like compound class.

Chapter III: Experimental Methods

3. Experimental

3.1 General Information

Unless otherwise stated, all commercially available compounds were used as provided without further purification. Solvents for chromatography were technical grade.

Analytical thin-layer chromatography (TLC) was performed on Merck silica gel aluminium plates with F-254 indicator. Compounds were visualized by irradiation with UV light or potassium permanganate staining (1.5 g KMnO_4 , 10 g K_2CO_3 , 1.25 mL 10% aqueous NaOH solution and 200 mL H_2O) with additional heating with a heat gun. Column chromatography was performed using silica gel Merck 60 (particle size 0.040-0.063 mm).

^1H -NMR, ^{13}C -NMR and ^{19}F -NMR were recorded on Bruker AV 400 Avance III HD (NanoBay), Agilent Technologies DD2, Bruker AV 500 Avance III HD (Prodigy), Bruker AV 600 Avance III HD (CryoProbe) or Bruker AV 700 Avance III HD (CryoProbe) spectrometers using CDCl_3 , CD_2Cl_2 or DMSO-d_6 as solvent. Data are reported in the following order: chemical shift (δ) values are reported in ppm with the solvent resonance as internal standard (CDCl_3 : $\delta = 7.26$ ppm for ^1H , $\delta = 77.16$ ppm for ^{13}C , CD_2Cl_2 : $\delta = 5.32$ ppm for ^1H , $\delta = 54.00$ ppm for ^{13}C , DMSO-d_6 : $\delta = 2.50$ ppm for ^1H , $\delta = 39.52$ ppm for ^{13}C). Multiplicities are indicated by s (broad singlet), s (singlet), d (doublet), t (triplet), q (quartet), m (multiplet); coupling constants (J) are given in Hertz (Hz). 2D NMR correlations, including $^1\text{H}/^1\text{H}$ COSY, $^1\text{H}/^1\text{HNOESY}$, $^1\text{H}/^{13}\text{C}$ HSQC, $^1\text{H}/^{13}\text{C}$ HMBC, were applied for the assignment of the signals

High resolution mass spectra (HR-MS) were recorded on an LTQ Orbitrap mass spectrometer coupled to an Accela HPLC-System (HPLC column: Hypersyl GOLD, 50 mm x 1 mm, particle size 1.9 μm , ionization method: electron spray ionization (ESI)).

The enantiomeric excesses were determined by HPLC analysis using a chiral stationary phase column (CHIRALCEL IC, CHIRALCEL IA; eluent: (DCM/EtOH = 100/2) / *iso*-hexane or

(DCM/MeOH = 100/5) / *iso*-hexane (4.6 mm x 250 mm, particle size 5 μm). The chiral HPLC methods were calibrated with the corresponding racemic mixtures.

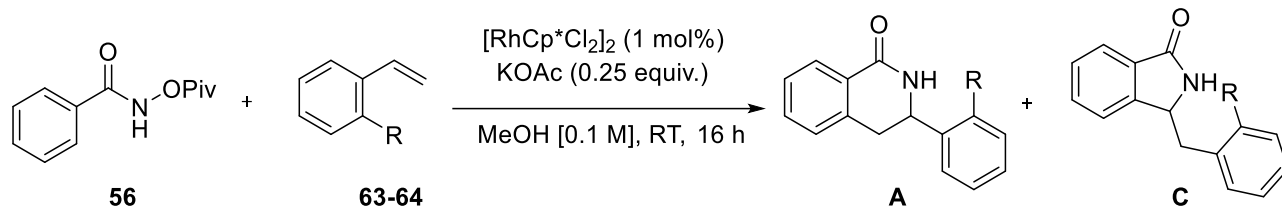
Fourier transform infrared spectroscopy (FT-IR) spectra were obtained with a Bruker Tensor 27 spectrometer (ATR, neat) and are reported in terms of frequency of absorption (cm^{-1}).

Acid chlorides were either commercially available or made from their corresponding carboxylic acid following the reported procedure.^[186] 2-Bromostyrenes were also commercially available or made from their corresponding 2-Bromobenzaldehyde following a modified version of the reported procedure.^[187]

Material and methods for biological experiments of Chapter II can be found in the thesis of Lara Dötsch.

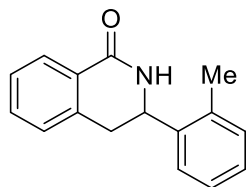
3.2 Chemical Synthesis for Chapter I

3.2.1 General Procedure for the reaction of *N*-OPiv benzamides and styrenes

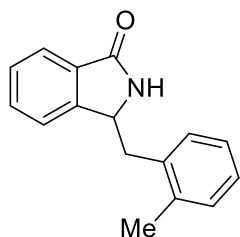


In a dram vial equipped with a stirring bar was added $[\text{RhCp}^*\text{Cl}_2]_2$ (1.0 mol%), KOAc (0.025 mmol, 0.25 eq.), *N*-OPiv benzamide (**56**) (0.1 mmol, 1.0 eq.) and dry MeOH [0.1 M]. The mixture was stirred for 30 seconds before the addition of the styrene (**2**), (0.15 mmol, 1.5 eq.). The reaction was left to stir at room temperature for 16 h. The solvent was then evaporated under reduced pressure and the crude mixture was purified by silica gel chromatography using Pent: EtOAc (3:1) as eluent to afford the **A** and **C**.

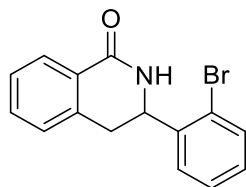
3-(2-methylphenyl)-3,4-dihydroisoquinolin-1(2*H*)-one (**A'**)



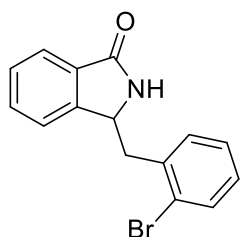
Off-white solid, 6% yield. $^1\text{H-NMR}$ (500 MHz - CDCl_3): δ 8.15 (dd, $J = 7.7, 1.4$ Hz, 1H), 7.59 – 7.43 (m, 2H), 7.40 (tt, $J = 7.6, 1.1$ Hz, 1H), 7.31 – 7.23 (m, 1H), 7.27 – 7.13 (m, 3H), 6.04 (s, 1H), 5.14 (ddd, $J = 11.4, 4.7, 1.1$ Hz, 1H), 3.23 – 3.12 (m, 1H), 3.12 – 3.03 (m, 1H), 2.39 (s, 3H); $^{13}\text{C-NMR}$ (125 MHz - CDCl_3): δ 166.76, 138.73, 137.73, 135.00, 132.64, 130.98, 128.25, 128.15, 128.12, 127.40, 126.92, 125.68, 52.25, 36.07, 19.19.

3-(2-methylbenzyl)isoindolin-1-one (C')

White solid, 37% yield. $^1\text{H-NMR}$ (500 MHz - CDCl_3): δ 7.81 (dt, $J = 7.5, 1.0$ Hz, 1H), 7.50 (td, $J = 7.5, 1.2$ Hz, 1H), 7.47 – 7.38 (m, 1H), 7.29 (dq, $J = 7.6, 0.9$ Hz, 1H), 7.15 (tt, $J = 3.7, 1.6$ Hz, 4H), 6.21 (s, 1H), 4.72 (dd, $J = 10.0, 4.8$ Hz, 1H), 3.23 (dd, $J = 13.7, 4.9$ Hz, 1H), 2.67 (dd, $J = 13.8, 10.0$ Hz, 1H), 2.30 (s, 3H); $^{13}\text{C-NMR}$ (125 MHz - CDCl_3): δ 170.22, 147.01, 136.38, 135.43, 131.94, 131.70, 130.93, 129.80, 128.49, 127.43, 126.54, 124.06, 122.64, 56.95, 38.78, 19.69.

3-(2-bromophenyl)-3,4-dihydroisoquinolin-1(2H)-one (A'')

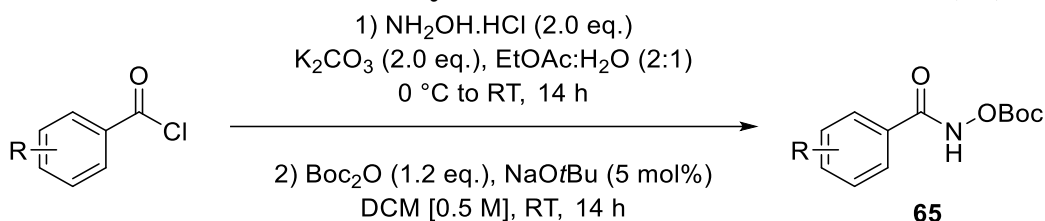
White solid, 16% yield. $^1\text{H-NMR}$ (500 MHz - CDCl_3): δ 8.06 (dd, $J = 7.8, 1.4$ Hz, 1H), 7.52 (dd, $J = 8.0, 1.2$ Hz, 1H), 7.45 – 7.35 (m, 2H), 7.32 (td, $J = 7.6, 1.2$ Hz, 1H), 7.25 (td, $J = 7.6, 1.3$ Hz, 1H), 7.18 – 7.07 (m, 2H), 6.16 (s, 1H), 5.29 – 5.21 (m, 1H), 3.29 (dd, $J = 15.8, 5.2$ Hz, 1H), 3.04 (dd, $J = 15.8, 9.3$ Hz, 1H); $^{13}\text{C-NMR}$ (125 MHz - CDCl_3): δ 166.99, 139.71, 136.95, 133.38, 132.87, 129.67, 128.18, 128.09, 127.98, 127.64, 127.48, 127.46, 122.64, 54.65, 34.90.

3-(2-bromobenzyl)isoindolin-1-one (C'')

White solid, 53% yield. $^1\text{H-NMR}$ (500 MHz - CDCl_3): δ 7.78 (d, $J = 7.6$ Hz, 1H), 7.55 (dd, $J = 7.9, 1.3$ Hz, 1H), 7.51 (td, $J = 7.5, 1.2$ Hz, 1H), 7.43 (t, $J = 7.4$ Hz, 1H), 7.34 (d, $J = 7.6$ Hz, 1H), 7.25 – 7.17 (m, 1H), 7.17 – 7.07 (m, 2H), 6.48 (s, 1H), 4.89 (dd, $J = 9.3, 4.7$ Hz, 1H), 3.43 (dd, J

= 13.6, 4.6 Hz, 1H), 2.75 (dd, $J = 13.6, 9.4$ Hz, 1H); $^{13}\text{C-NMR}$ (125 MHz - CDCl_3): δ 170.38, 146.75, 136.52, 133.35, 131.97, 131.72, 131.68, 129.15, 128.53, 127.90, 124.73, 124.00, 122.82, 56.14, 41.84.

3.2.2 General Procedure for the synthesis of *N*-OBoc-benzamides (**65**)

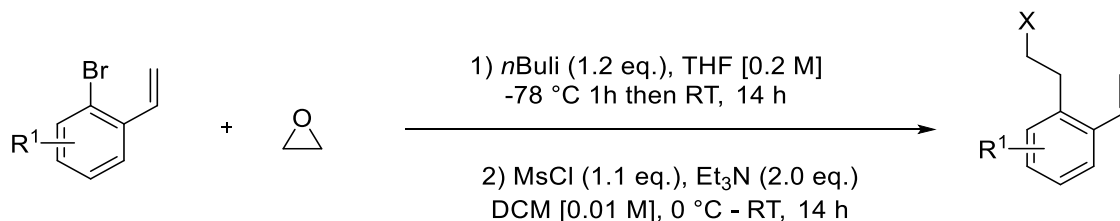


Following a modified procedure by Fagnou *et al.*^[60], a flask was charged with hydroxylamine hydrochloride (1.5 equiv.), potassium carbonate (2.0 equivalent) and solvent (EtOAc/water; 2:1). The reaction was cooled to $0\text{ }^\circ\text{C}$ with vigorous stirring before dropwise addition of acid chloride (1 equiv.) dissolved in EtOAc (2 ml). The reaction was stirred at RT for 14 h. The reaction mixture was diluted with water and extracted with EtOAc (2 x 20 ml). The combined organic layers were washed with brine (10 ml), dried over anhydrous sodium sulfate and concentrated *in vacuo*. The crude hydroxamic acid was used in the next step without further purification.

The hydroxamic acid (1.0 equiv.), NaOtBu (5 mol%) and di-*tert*-butyl dicarbonate (1.2 equiv.) were dissolved in DCM [0.5 M]. The mixture was stirred at RT for 14 h. The reaction mixture was quenched with saturated NaHCO_3 solution (10 ml) and extracted with DCM (2x 10 ml). The organic layer was dried over Na_2SO_4 , concentrated *in vacuo*, and then purified by silica gel chromatography (Pent/EtOAc, 5:1) to give the title products **1**.

All the benzamides are reported and their characterisation matches the literature.^[188,189]

3.2.3 General Procedure for the synthesis of styrenes



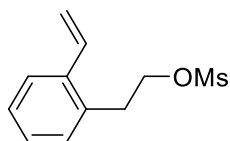
According to the reported procedure^[190], a 100 mL round bottom flask was charged with 2-bromostyrene (1.0 eq.) and THF [0.2M]. The solution was then cooled to $-78\text{ }^\circ\text{C}$ and $n\text{-BuLi}$ (1.2

eq., 1.6 M solution in hexanes) was added dropwise. The resulting mixture was then stirred at -78 °C for 1 h. Ethylene oxide (3.0 eq., 2.5 M solution in THF) was then added to the reaction mixture and stirred for an additional 0.5 h at -78 °C. The reaction was then warmed to RT and stirred for 14 h. A saturated solution of NH₄Cl (10 mL) was added, and the aqueous layer washed with Et₂O (3 x 25 mL). The combined organic layers were dried over Na₂SO₄, filtered and concentrated *in vacuo* to afford the corresponding alcohol which was used in the next step without further purification.

The resulting alcohol (1.0 equiv.) and triethylamine (1.1 equiv.) were dissolved in DCM [0.01M] and cooled to 0°C. Then MsCl (1.1 equiv.) was added dropwise and the reaction was stirred at RT for 12h. The solvent was removed under reduced pressure and the crude material was purified by silica gel chromatography (Pent/EtOAc, 4:1) to afford the title styrenes **2**.

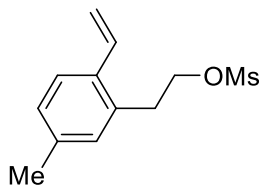
Some of the styrenes are reported and our characterization matches the literature.^[191,192]

2-vinylphenethyl methanesulfonate (**60**)



Colourless oil, 78% yield. **¹H-NMR (400 MHz – CDCl₃):** δ 7.56 – 7.46 (m, 1H), 7.29 – 7.25 (m, 1H), 7.25 – 7.22 (m, 1H), 7.21 – 7.18 (m, 1H), 6.97 (dd, *J* = 17.3, 11.0 Hz, 1H), 5.68 (dd, *J* = 17.3, 1.3 Hz, 1H), 5.37 (dd, *J* = 11.0, 1.3 Hz, 1H), 4.36 (t, *J* = 7.2 Hz, 2H), 3.15 (t, *J* = 7.2 Hz, 2H), 2.83 (s, 3H); **¹³C-NMR (101 MHz – CDCl₃):** δ 137.3, 134.0, 133.4, 130.5, 128.2, 127.7, 126.4, 117.0, 69.6, 37.4, 33.1; **HR-MS:** calc. for [M+H]⁺ C₁₁H₁₅O₃S: 227.07364, found: 227.07423

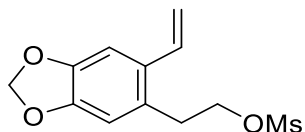
5-methyl-2-vinylphenethyl methanesulfonate (**66a**)



Colourless oil, 70% yield. **¹H-NMR (500 MHz - CD₂Cl₂):** δ 7.43 (d, *J* = 7.9 Hz, 1H), 7.11 – 7.04 (m, 1H), 7.03 (d, *J* = 1.7 Hz, 1H), 6.95 (dd, *J* = 17.3, 10.9 Hz, 1H), 5.65 (dd, *J* = 17.3, 1.3 Hz, 1H), 5.32 – 5.29 (m, 1H), 4.32 (t, *J* = 7.2 Hz, 2H), 3.10 (t, *J* = 7.2 Hz, 2H), 2.82 (s, 3H), 2.32 (s, 3H);

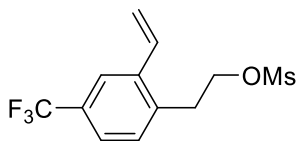
^{13}C -NMR (126 MHz - CD_2Cl_2): δ 138.52, 134.71, 134.22, 133.90, 131.57, 128.81, 126.42, 116.00, 70.54, 37.60, 33.38, 21.31; **HR-MS:** calc. for $[\text{M}+\text{H}]^+$ $\text{C}_{12}\text{H}_{17}\text{O}_3\text{S}$: 241.08929, found: 241.08939.

2-(6-vinylbenzo[d][1,3]dioxol-5-yl)ethyl methanesulfonate (66b)



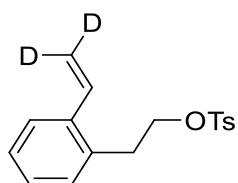
Colourless oil, 40% yield. **^1H -NMR (500 MHz - CD_2Cl_2):** δ 6.99 (s, 1H), 6.86 (dd, $J = 17.2, 10.9$ Hz, 1H), 6.66 (s, 1H), 5.95 (s, 2H), 5.55 (dd, $J = 17.2, 1.1$ Hz, 1H), 5.26 (dd, $J = 10.9, 1.1$ Hz, 1H), 4.30 (t, $J = 7.2$ Hz, 2H), 3.06 (t, $J = 7.2$ Hz, 2H), 2.89 (s, 3H); **^{13}C -NMR (126 MHz - CD_2Cl_2):** δ 147.6, 147.4, 133.4, 130.9, 127.3, 115.2, 110.2, 106.0, 101.3, 69.6, 37.5, 33.0; **HR-MS:** calc. for $[\text{M}+\text{H}]^+$ $\text{C}_{12}\text{H}_{15}\text{O}_5\text{S}$: 271.06347, found: 271.06357.

4-(trifluoromethyl)-2-vinylphenethyl methanesulfonate (66c)



Colourless oil, 52% yield. **^1H -NMR (400 MHz - CDCl_3):** δ 7.66 (s, 1H), 7.43 (d, $J = 7.9$ Hz, 1H), 7.03 (d, $J = 1.7$ Hz, 1H), 6.95 (dd, $J = 17.3, 10.9$ Hz, 1H), 5.65 (dd, $J = 17.3, 1.3$ Hz, 1H), 5.32 – 5.29 (m, 1H), 4.32 (t, $J = 7.2$ Hz, 2H), 3.10 (t, $J = 7.2$ Hz, 2H), 2.82 (s, 3H); **^{13}C -NMR (101 MHz - CDCl_3):** δ 137.96, 137.23, 132.85, 130.78, 129.90, 124.55, 124.52, 123.29, 123.26, 118.80, 68.54, 37.48, 32.93.; **^{19}F -NMR (470 MHz, CDCl_3):** $\delta = -62.68$.

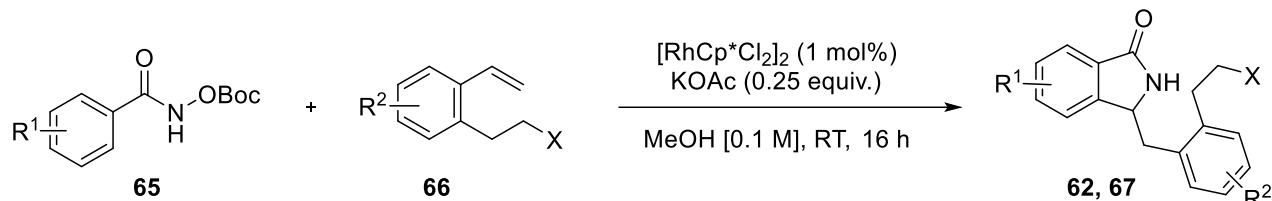
2-(vinyl-2,2-d₂)phenethyl-d₂ 4-methylbenzenesulfonate (60')



Colourless oil, 75% yield (90% D). **^1H -NMR (500 MHz - CDCl_3):** δ 7.66 – 7.59 (m, 2H), 7.34 (dd, $J = 7.6, 1.5$ Hz, 1H), 7.24 – 7.17 (m, 2H), 7.14 (td, $J = 7.5, 1.4$ Hz, 1H), 7.10 (td, $J = 7.4, 1.5$ Hz, 1H), 7.01 (dd, $J = 7.5, 1.4$ Hz, 1H), 6.76 – 6.70 (m, 1H), 4.12 – 4.01 (m, 2H), 2.97 (t, $J = 7.5$

Hz, 2H), 2.37 (s, 3H); $^{13}\text{C-NMR}$ (126 MHz - CDCl_3): δ 144.66, 144.62, 137.09, 133.72, 133.69, 133.61, 133.37, 133.17, 132.98, 130.27, 129.83, 129.82, 129.77, 127.97, 127.88, 127.84, 127.44, 127.17, 126.20, 126.19, 70.19, 69.78, 66.80, 32.80, 32.10, 21.63, 14.73.

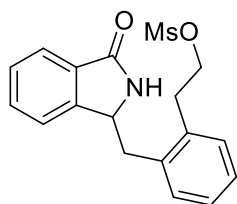
3.2.4 General Procedure for the synthesis of 3-Isoindolinones (67)



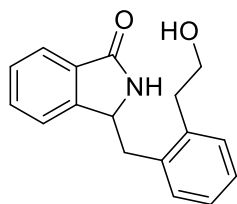
In a dram vial equipped with a stirring bar was added $[\text{RhCp}^*\text{Cl}_2]_2$ (1.0 mol%), KOAc (0.025 mmol, 0.25 eq.), *N*-(OBoc) benzamide substrate (**65**) (0.1 mmol, 1.0 eq.) and dry MeOH [0.1 M]. The mixture was stirred for 30 seconds before the addition of the alkene substrate (**66**), (0.15 mmol, 1.5 eq.). The reaction was left to stir at room temperature for 16 h. The solvent was then evaporated under reduced pressure and the crude mixture was purified by silica gel chromatography using DCM to DCM: DMA* (10:1) as eluent to afford the title 3-Isoindolinones **3**.

*DMA: is a mixture of DCM:MeOH: NH_3 (100:5:0.15).

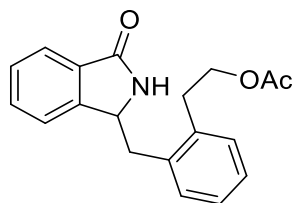
2-((3-oxoisoindolin-1-yl)methyl)phenethyl methanesulfonate (62)



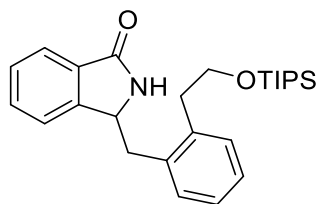
Colourless oil, 74% yield. $^1\text{H-NMR}$ (500 MHz - CDCl_3): δ 7.86 (d, $J = 7.3$, 1.0 Hz, 1H), 7.58 (td, $J = 7.5$, 1.2 Hz, 1H), 7.51 (t, 1H), 7.39 (d, $J = 7.6$, 0.9 Hz, 1H), 7.30 – 7.26 (m, 4H), 6.40 (br s, 1H, NH), 4.80 (dd, $J = 9.7$, 4.9 Hz, 1H), 4.43 – 4.29 (m, 2H), 3.36 (dd, $J = 14.0$, 4.9 Hz, 1H), 3.13 (t, 2H), 2.91 (s, 3H), 2.81 (dd, $J = 9.2$, 4.8 Hz, 1H); $^{13}\text{C-NMR}$ (125 MHz - CDCl_3): δ 170.36, 146.80, 135.87, 134.68, 132.18, 131.73, 130.66 (2C), 128.74, 128.00, 127.98, 124.16, 122.91, 69.71, 57.64, 38.18, 37.60, 32.75; **FT-IR**: $\tilde{\nu} = 3245$, 2514, 2159, 2030, 1976, 1690, 1468, 1346, 1168, 947 cm^{-1} ; **HR-MS**: calc. for $[\text{M}+\text{H}]^+$ $\text{C}_{18}\text{H}_{20}\text{O}_4\text{NS}$ 346.1107, found: 346.1108.

3-(2-(2-hydroxyethyl)benzyl)isoindolin-1-one (67a)

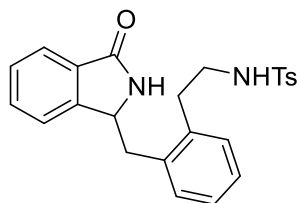
Red solid, 49% yield. **¹H-NMR (400 MHz - CDCl₃):** δ 7.80 (dt, *J* = 7.5, 1.0 Hz, 1H), 7.60 – 7.40 (m, 2H), 7.34 (d, *J* = 7.6 Hz, 1H), 7.26 – 7.13 (m, 4H), 7.11 (s, 1H), 4.77 (dd, *J* = 9.6, 4.7 Hz, 1H), 3.86 (tp, *J* = 7.7, 3.6 Hz, 2H), 3.27 (dd, *J* = 14.0, 4.7 Hz, 1H), 2.98 – 2.75 (m, 3H); **¹³C-NMR (100 MHz - CDCl₃):** δ 161.51, 147.07, 137.32, 135.97, 131.90, 130.52, 130.38, 130.15, 128.84, 128.46, 127.55, 127.43, 126.96, 123.98, 122.68, 63.17, 58.25, 38.16, 35.14; **FT-IR:** $\tilde{\nu}$ = 3059, 2348, 1680, 1542, 1492, 1449, 1153, 1094, 1062, 1011, 856 cm⁻¹; **LC-MS:** calc. for [M+H]⁺ C₁₇H₁₇O₂N 268.1, found: 268.1.

2-((3-oxoisoindolin-1-yl)methyl)phenethyl acetate (67b)

Red oil, 63% yield. **¹H-NMR (400 MHz - CDCl₃):** δ 7.79 (d, *J* = 7.3, 1.0 Hz, 1H), 7.48 (td, *J* = 7.5, 1.2 Hz, 1H), 7.42 (t, 1H), 7.30 (d, *J* = 7.7 Hz, 1H), 7.20 – 7.11 (m, 4H), 6.47 (br s, 1H, NH), 4.73 (dd, *J* = 9.5, 4.9 Hz, 1H), 4.17 – 4.11 (m, 2H), 3.32 (dd, *J* = 14.0, 4.9 Hz, 1H), 2.91 (t, 2H), 2.75 (dd, *J* = 9.2, 4.8 Hz, 1H), 1.93 (s, 3H); **¹³C-NMR (101 MHz - CDCl₃):** δ 171.08, 170.33, 146.88, 135.92, 135.70, 131.95, 131.73, 130.46, 130.40, 128.83, 128.51, 127.64, 127.44, 127.39, 124.01, 122.78, 119.50, 64.50, 57.62, 38.16, 31.94, 20.98; **FT-IR:** $\tilde{\nu}$ = 3045, 2486, 2159, 1976, 1690, 1468, 1289, 1163, 973 cm⁻¹; **LC-MS:** calc. for [M+H]⁺ C₁₉H₁₉O₃N 309.3, found: 309.3.

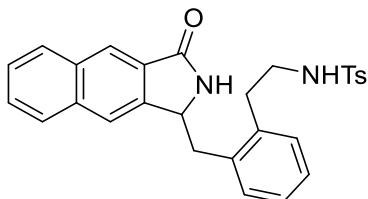
3-(2-(2-((triisopropylsilyl)oxy)ethyl)benzyl)isoindolin-1-one (67c)

Red oil, 58% yield. **¹H-NMR (500 MHz - CDCl₃):** δ 7.83 – 7.78 (m, 1H), 7.57 – 7.39 (m, 3H), 7.39 – 7.11 (m, 4H), 6.31 (s, 1H), 4.76 (dd, J = 10.1, 4.9 Hz, 1H), 3.81 (t, J = 7.0 Hz, 2H), 3.32 (dd, J = 13.8, 4.8 Hz, 1H), 2.86 (td, J = 6.9, 2.1 Hz, 2H), 2.71 (dd, J = 13.9, 10.1 Hz, 1H), 1.05 – 0.96 (m, 3H), 0.99 – 0.78 (m, 18H); **¹³C-NMR (125 MHz - CDCl₃):** δ 170.21, 147.00, 137.74, 135.64, 131.97, 131.57, 130.68, 130.02, 129.17, 128.85, 128.51, 127.47, 126.89, 124.06, 122.66, 64.50, 57.79, 38.41, 36.15, 17.93, 17.71, 13.67, 11.89.; **FT-IR:** $\tilde{\nu}$ = 3023, 2861, 1683, 1545, 1294, 1175, 1065, 1013, 849 cm⁻¹; **LC-MS:** calc. for [M+H]⁺ C₂₆H₃₇O₂NSi 432.2, found: 432.2.

4-methyl-N-(2-((3-oxoisoindolin-1-yl)methyl)phenethyl)benzenesulfonamide (67d)

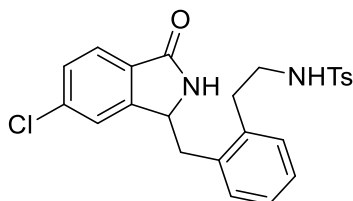
Red oil, 87% yield. **¹H-NMR (400 MHz - CDCl₃):** δ 7.74 (dd, J = 7.0, 1.3 Hz, 1H), 7.64 – 7.52 (m, 2H), 7.41 (dtd, J = 22.8, 7.4, 1.2 Hz, 3H), 7.21 (d, J = 7.4 Hz, 1H), 7.16 – 7.08 (m, 2H), 7.12 – 7.01 (m, 3H), 6.88 (s, 1H), 5.56 (t, J = 6.2 Hz, 1H), 4.62 (dd, J = 8.9, 5.6 Hz, 1H), 3.12 (dd, J = 13.8, 5.6 Hz, 1H), 3.09 – 2.96 (m, 2H), 2.91 – 2.75 (m, 2H), 2.71 (dd, J = 13.9, 8.9 Hz, 1H), 2.28 (s, 3H); **¹³C-NMR (101 MHz - CDCl₃):** δ 170.65, 146.91, 143.36, 137.04, 136.57, 135.48, 132.09, 131.90, 131.66, 130.61, 130.10, 129.71, 128.81, 128.44, 127.65, 127.42, 127.24, 127.00, 123.91, 122.95, 57.68, 53.47, 43.86, 38.01, 33.17, 21.49; **FT-IR:** $\tilde{\nu}$ = 3592, 3057, 1681, 1486, 1320, 1152, 1017, 866, 815 cm⁻¹; **LC-MS:** calc. for [M+H]⁺ C₂₄H₂₄O₃N₂S 421.1, found: 421.1.

4-methyl-N-(2-((3-oxo-2,3-dihydro-1H-benzo[f]isoindol-1-yl)methyl)phenethyl)benzenesulfonamide (67e)

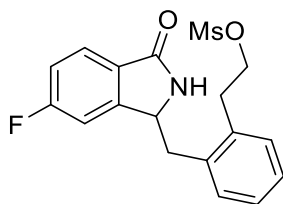


Red solid, 48% yield. **¹H-NMR (500 MHz - CDCl₃):** δ 8.33 (d, J = 4.8 Hz, 1H), 7.94 (d, J = 8.2 Hz, 1H), 7.81 (d, J = 8.2 Hz, 1H), 7.76 (s, 1H), 7.70 – 7.61 (m, 4H), 7.59 – 7.48 (m, 3H), 7.19 – 7.03 (m, 5H), 4.89 (d, J = 7.0 Hz, 1H), 3.21 (dd, J = 13.7, 5.8 Hz, 1H), 3.18 – 3.04 (m, 2H), 2.92 (dt, J = 55.9, 7.9 Hz, 3H), 2.27 (s, 3H.); **¹³C-NMR (125 MHz - CDCl₃):** δ 170.61, 143.35, 141.50, 136.97, 136.72, 135.27, 132.94, 130.83, 130.17, 129.70, 129.63, 128.96, 128.26, 128.09, 127.79, 127.22, 127.01, 126.61, 124.63, 122.15, 58.03, 43.95, 38.54, 33.18, 29.73, 21.47; **FT-IR:** $\tilde{\nu}$ = 3630, 3057, 2549, 2148, 1685, 1492, 1321, 1207, 1073, 1017, 956, 905, 814 cm⁻¹; **LC-MS:** calc. for [M+H]⁺ C₂₈H₂₆O₃N₂S 471.1, found: 471.1.

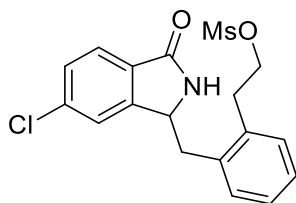
N-(2-((6-chloro-3-oxoisindolin-1-yl)methyl)phenethyl)-4-methylbenzenesulfonamide (67f)



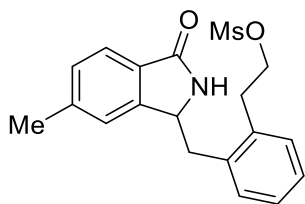
Yellow oil, 28% yield. **¹H-NMR (500 MHz - CDCl₃):** δ 7.74 (d, J = 8.1 Hz, 1H), 7.69 (d, J = 8.1 Hz, 2H), 7.46 (dd, J = 8.0, 1.7 Hz, 1H), 7.32 (d, J = 1.7 Hz, 1H), 7.25 – 7.19 (m, 4H), 7.16 (ddd, J = 15.4, 6.8, 2.1 Hz, 2H), 6.70 (s, 1H), 5.07 (s, 1H), 4.70 (dd, J = 9.4, 5.4 Hz, 1H), 3.21 (dd, J = 14.0, 5.4 Hz, 1H), 3.15 (dt, J = 9.8, 7.3 Hz, 2H), 2.88 (t, J = 7.4 Hz, 2H), 2.78 (dd, J = 14.0, 9.3 Hz, 1H), 2.38 (s, 3H); **¹³C-NMR (125 MHz - CDCl₃):** δ 168.34, 147.35, 142.51, 137.43, 135.94, 135.41, 134.01, 129.54, 129.17, 129.02, 128.73 (2C), 128.13, 126.92, 126.42, 125.97 (2C), 124.20, 122.40, 56.29, 42.79, 36.86, 32.19, 20.47; **FT-IR:** $\tilde{\nu}$ = 3182, 2514, 2360, 2159, 2030, 1977, 1692, 1327, 1155, 925 cm⁻¹; **HR-MS:** calc. for [M+H]⁺ C₂₄H₂₄O₃N₂SCl 455.1190, found: 455.1189.

2-((6-fluoro-3-oxoisindolin-1-yl)methyl)phenethyl methanesulfonate (67g)

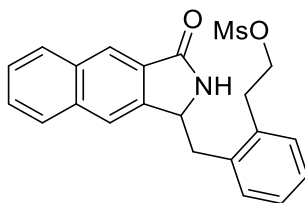
Colourless oil, 61% yield. **¹H-NMR (500 MHz - CDCl₃):** δ 7.83 (dd, *J* = 8.4, 5.0 Hz, 1H), 7.33 – 7.23 (m, 4H), 7.19 (td, *J* = 8.7, 2.2 Hz, 1H), 7.06 (dd, *J* = 8.2, 2.2 Hz, 1H), 6.39 (br s, 1H, NH), 4.77 (dd, *J* = 9.6, 5.0 Hz, 1H), 4.43 – 4.31 (m, 2H), 3.32 (dd, *J* = 14.0, 5.1 Hz, 1H), 3.13 (t, *J* = 7.8, 6.8 Hz, 2H), 2.93 (s, 3H), 2.87 – 2.77 (m, 1H); **¹³C-NMR (125 MHz - CDCl₃):** δ 169.29, 166.46, 164.46, 149.23, 135.45, 134.68, 130.70, 128.15, 128.07, 127.80, 126.24, 116.57, 110.43, 69.64, 57.26, 38.08, 37.66, 32.81; **¹⁹F-NMR (470 MHz, CDCl₃):** δ = -106.13 (q, *J* = 7.6); **HR-MS:** calc. for [M+H]⁺ C₁₈H₁₉O₄NFS 364.1013, found: 364.1013.

2-((6-chloro-3-oxoisindolin-1-yl)methyl)phenethyl methanesulfonate (67h)

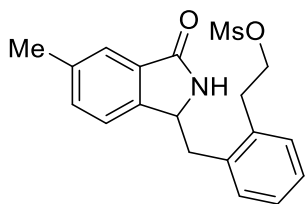
Yellow solid, 77% yield. **¹H-NMR (500 MHz - CDCl₃):** δ 7.78 (d, *J*=8.1 Hz, 1H), 7.48 (dd, *J*=8.1, 1.7 Hz, 1H), 7.39 (d, *J*=1.7 Hz, 1H), 7.34 – 7.27 (m, 4H), 6.27 (br s, 1H, NH), 4.78 (dd, *J*=9.9, 4.9 Hz, 1H), 4.43 – 4.35 (m, 2H), 3.34 (dd, *J*=14.0, 4.9 Hz, 1H), 3.14 (t, *J*=7.3 Hz, 2H), 2.94 (s, 3H), 2.84 – 2.78 (m, 1H); **¹³C-NMR (125 MHz - CDCl₃):** δ 169.04, 148.21, 138.50, 135.31, 134.59, 130.58, 130.52, 130.12, 129.26, 128.07, 127.97, 125.32, 123.34, 69.48, 57.13, 37.97, 37.56, 32.65; **FT-IR:** $\tilde{\nu}$ = 3199, 2507, 2360, 2159, 2029, 1977, 1708, 1376, 1162, 946 cm⁻¹; **HR-MS:** calc. for [M+H]⁺ C₁₈H₁₉O₄NSCl 382.0685, found: 382.0688.

2-((6-methyl-3-oxoisindolin-1-yl)methyl)phenethyl methanesulfonate (67i)

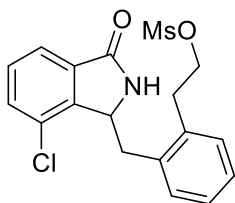
Colourless oil, 61% yield. **¹H-NMR (500 MHz - CDCl₃):** δ 7.73 (d, J=7.8 Hz, 1H), 7.33 – 7.30 (d, 1H), 7.28 (m, 4H), 7.21 (d, J=1.6 Hz, 1H), 6.25 (br s, 1H, NH), 4.74 (dd, J=10.0, 4.6 Hz, 1H), 4.37 (m, 2H), 3.35 (dd, J=14.0, 4.6 Hz, 1H), 3.13 (t, J=7.3 Hz, 2H), 2.91 (s, 3H), 2.75 (dd, J=14.0, 10.0 Hz, 1H), 2.47 (s, 3H); **¹³C-NMR (125 MHz - CDCl₃):** δ 170.47, 147.27, 142.97, 136.02, 134.68, 130.63, 130.59, 129.74, 129.11, 127.99, 127.94, 123.92, 123.35, 69.73, 57.48, 38.26, 37.57, 32.69, 22.13; **FT-IR:** $\tilde{\nu}$ = 3232, 2513, 2159, 2029, 1977, 1690, 1618, 1346, 1168, 947 cm⁻¹; **HR-MS:** calc. for [M+H]⁺ C₁₉H₂₂O₄NS 360.1264, found: 360.1264.

2-((3-oxo-2,3-dihydro-1H-benzo[f]isoindol-1-yl)methyl)phenethyl methanesulfonate (67j)

Yellow oil, 74% yield. **¹H-NMR (500 MHz - CDCl₃):** δ 8.40 (s, 1H), 8.03 (d, J = 8.1 Hz, 1H), 7.92 (d, J = 8.1 Hz, 1H), 7.82 (s, 1H), 7.62 (td, J = 8.2, 6.8, 1.4 Hz, 1H), 7.58 (td, J = 8.1, 6.8, 1.4 Hz, 1H), 7.31 (d, J = 2.5 Hz, 4H), 6.56 (br s, 1H, NH), 4.97 (dd, J = 9.7, 4.9 Hz, 1H), 4.47 – 4.30 (m, 2H), 3.46 (dd, J = 14.0, 4.9 Hz, 1H), 3.23 – 3.11 (m, 2H), 2.92 (dd, 1H), 2.91 (s, 3H); **¹³C-NMR (125 MHz - CDCl₃):** δ 170.13, 141.45, 135.67, 135.32, 134.64, 133.08, 130.63, 130.58, 129.67, 129.18, 128.26, 128.09, 127.96 (2C), 126.68, 124.64, 121.93, 69.62, 57.56, 38.78, 37.49, 32.67; **FT-IR:** $\tilde{\nu}$ = 3189, 2928, 2522, 2360, 2159, 2029, 1977, 1690, 1639, 1342, 1178 cm⁻¹; **HR-MS:** calc. for [M+H]⁺ C₂₂H₂₂O₄NS 396.1264, found: 396.1260.

2-((5-methyl-3-oxoisindolin-1-yl)methyl)phenethyl methanesulfonate (67k)

Colourless oil, 80% yield. **¹H-NMR (500 MHz - CDCl₃):** δ 7.64 (d, J = 1.7 Hz, 1H), 7.36 (dd, J = 7.7, 1.6 Hz, 1H), 7.29 – 7.26 (m, 1H), 7.26 – 7.23 (m, 3H), 7.21 (d, J = 7.7 Hz, 1H), 6.58 (br s, 1H, NH), 4.75 (dd, J = 9.5, 5.2 Hz, 1H), 4.34 (m, 2H), 3.28 (dd, J = 14.0, 5.2 Hz, 1H), 3.10 (t, J = 7.3 Hz, 2H), 2.89 (s, 3H), 2.81 (dd, J = 14.0, 9.4 Hz, 1H); **¹³C-NMR (125 MHz - CDCl₃):** δ 170.61, 144.14, 138.82, 135.93, 134.72, 133.16, 131.82, 130.65, 130.60, 127.94, 127.89, 124.32, 122.64, 69.71, 57.57, 38.24, 37.57, 32.72, 21.48; **FT-IR:** $\tilde{\nu}$ = 3189, 2522, 2362, 2159, 2029, 1977, 1690, 1343, 1168, 947 cm⁻¹; **HR-MS:** calc. for [M+H]⁺ C₁₉H₂₂O₄NS 360.1264, found: 360.1264.

2-((5-chloro-3-oxoisindolin-1-yl)methyl)phenethyl methanesulfonate (67l and 67l')

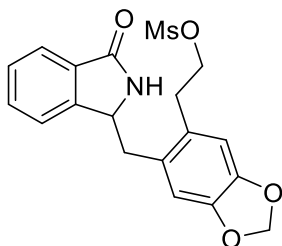
A mixture of regioisomers (1:1.3) were isolated as a colourless oil (81%).

Major isomer: **¹H-NMR (500 MHz - CDCl₃):** δ 7.75 (d, J = 7.5 Hz, 1H), 7.59 (d, J = 7.9 Hz, 1H), 7.48 (t, J = 7.7 Hz, 1H), 7.27 (m, 3H), 7.24 (m, 1H), 6.47 (br s, 1H, NH), 4.83 (dd, J = 10.4, 3.1 Hz, 1H), 4.43 (t, J = 7.1 Hz, 2H), 3.98 (dd, J = 14.2, 3.1 Hz, 1H), 3.22 (m, 2H), 2.92 (s, 3H), 2.56 (dd, J = 14.1, 10.3 Hz, 1H); **¹³C-NMR (125 MHz - CDCl₃):** δ 167.75, 142.53, 134.60, 133.80, 133.17, 132.48, 131.69, 129.52, 129.29, 128.42, 126.87, 126.82, 121.64, 68.63, 56.31, 36.37, 34.61, 31.36; **FT-IR:** $\tilde{\nu}$ = 3198, 2515, 2360, 2159, 2028, 1977, 1693, 1344, 1166, 947 cm⁻¹; **HR-MS:** calc. for [M+H]⁺ C₁₈H₁₈O₄NSCl 382.0685, found: 382.0688.

Minor isomer: **¹H-NMR (500 MHz - CDCl₃):** δ 7.80 (d, J = 1.9 Hz, 1H), 7.52 (dd, J = 8.1, 2.0 Hz, 1H), 7.27 (m, 3H), 7.24 (m, 2H), 6.63 (br s, 1H, NH), 4.78 (dd, J = 9.4, 5.3 Hz, 1H), 4.36 (m, 2H), 3.30 (dd, J = 14.0, 5.3 Hz, 1H), 3.11 (t, J = 7.3 Hz, 2H), 2.92 (s, 3H), 2.84 (dd, J = 14.4, 9.1 Hz, 1H); **¹³C-NMR (125 MHz - CDCl₃):** δ 167.81, 143.75, 134.36, 133.87, 133.56, 131.13, 129.59 (2C), 129.56, 126.96, 126.89 – 126.88 (m), 123.16, 123.15, 68.53, 56.27, 36.94, 36.50, 31.67; **FT-**

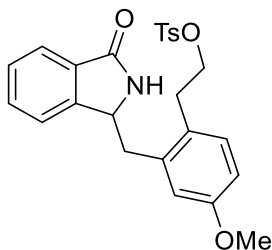
IR: $\tilde{\nu}$ = 3198, 2515, 2360, 2159, 2028, 1977, 1693, 1344, 1166, 947 cm^{-1} ; **HR-MS:** calc. for $[\text{M}+\text{H}]^+$ $\text{C}_{18}\text{H}_{19}\text{O}_4\text{NSCl}$ 382.0685, found: 382.0688.

2-(6-((3-oxoisindolin-1-yl)methyl)benzo[d][1,3]dioxol-5-yl)ethyl methanesulfonate (67m)



Colourless oil, 40% yield. **$^1\text{H-NMR}$ (500 MHz - CDCl_3):** δ 7.86 (d, J = 7.5, 1.2 Hz, 1H), 7.59 (t, J = 7.5, 1.2 Hz, 1H), 7.51 (t, J = 7.5 Hz, 1H), 7.41 (d, J = 7.6, 1.0 Hz, 1H), 6.73 (d, J = 2.0 Hz, 2H), 6.41 (br s, 1H, NH), 5.98 – 5.96 (m, 2H), 4.75 (dd, J = 9.7, 4.9 Hz, 1H), 4.35 – 4.23 (m, 2H), 3.25 (dd, J = 14.2, 5.0 Hz, 1H), 3.02 (t, J = 7.3 Hz, 2H), 2.96 (s, 3H), 2.71 (dd, J = 14.2, 9.7 Hz, 1H); **$^{13}\text{C-NMR}$ (125 MHz - CDCl_3):** δ 169.24, 146.21, 146.19, 145.55, 131.14, 130.46, 127.81, 127.64, 126.65, 123.08, 121.73, 109.19, 109.14, 100.35, 68.50, 56.82, 36.94, 36.55, 31.64; **FT-IR:** $\tilde{\nu}$ = 3182, 2516, 2159, 2030, 1977, 1694, 1502, 1485, 1367, 1276, 1166, 1039, 976 cm^{-1} ; **HR-MS:** calc. for $[\text{M}+\text{H}]^+$ $\text{C}_{19}\text{H}_{20}\text{O}_6\text{NS}$ 390.1007, found: 390.1005.

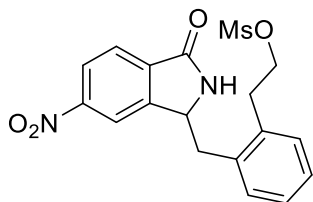
4-methoxy-2-((3-oxoisindolin-1-yl)methyl)phenethyl 4-methylbenzenesulfonate (67n)



Pink oil, 55% yield. **$^1\text{H-NMR}$ (600 MHz - CDCl_3):** δ 7.81 (d, J = 7.5, 1.2 Hz, 1H), 7.60 (d, J = 7.4 Hz, 2H), 7.52 (t, J = 7.5, 1.2 Hz, 1H), 7.42 (t, J = 7.5 Hz, 1H), 7.29 – 7.18 (m, 1H), 7.16 – 6.99 (m, 2H), 6.81 (d, J = 2.0 Hz, 2H), 6.73, (d, J = 7.5 Hz, 1H), 6.66 (br s, 1H, NH), 4.69 (dd, J = 9.7, 4.9 Hz, 1H), 4.07 – 4.05 (m, 2H), 3.72 (s, 3H), 3.58 (dd, J = 14.2, 5.0 Hz, 1H), 3.02 (t, J = 7.3 Hz, 1H), 2.89 – 2.68 (m, 2H), 2.32 (s, 3H); **$^{13}\text{C-NMR}$ (167 MHz - CDCl_3):** δ 170.52, 158.90, 146.68, 144.86, 136.67, 132.91, 132.41, 131.59, 131.04, 129.83, 128.85, 128.74, 127.76, 127.44, 126.49, 124.18, 122.84, 115.80, 113.20, 70.21, 58.12, 55.35, 38.07, 31.65, 31.45, 29.71, 21.63; **FT-IR:** $\tilde{\nu}$

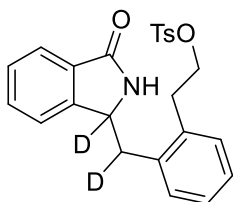
= 2923, 1684, 1609, 1466, 1291, 1188, 1096, 1010, 897, 814 cm^{-1} ; **LC-MS**: calc. for $[\text{M}+\text{H}]^+$ $\text{C}_{25}\text{H}_{25}\text{O}_5\text{NS}$ 452.3, found: 452.3.

2-((6-nitro-3-oxoisindolin-1-yl)methyl)phenethyl methanesulfonate (67o)



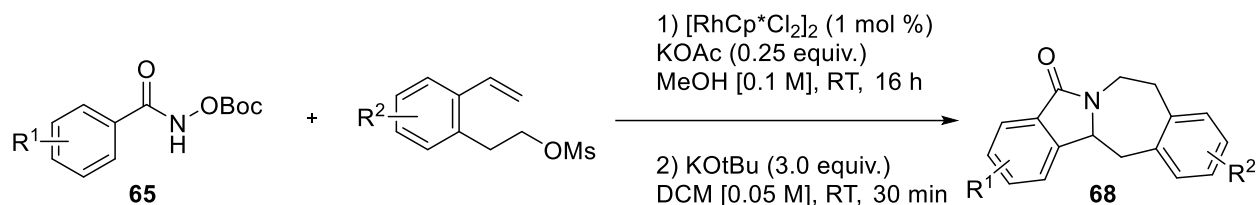
Yellow solid, 18% yield. **$^1\text{H-NMR}$ (500 MHz - CDCl_3)**: δ 8.39 (dd, $J = 8.2, 2.0$ Hz, 1H), 8.29 – 8.25 (m, 1H), 8.01 (d, $J = 8.3, 0.6$ Hz, 1H), 7.37 – 7.28 (m, 3H), 7.26 – 7.23 (m, 1H), 6.50 (br s, 1H, NH), 4.91 (dd, $J = 9.7, 5.0$ Hz, 1H), 4.45 – 4.37 (m, 2H), 3.43 (dd, $J = 14.0, 5.1$ Hz, 1H), 3.16 (t, $J = 7.3$ Hz, 2H), 2.97 (s, 3H), 2.89 – 2.85 (m, 1H); **$^{13}\text{C-NMR}$ (125 MHz - CDCl_3)**: δ 167.60, 150.44, 147.44, 137.06, 134.80, 134.61, 130.68, 130.59, 128.33, 128.10, 125.24, 124.32, 118.67, 69.44, 57.41, 37.83, 37.62, 32.73; **FT-IR**: $\tilde{\nu} = 3192, 2929, 2523, 2360, 2159, 2030, 1977, 1715, 1690, 1525, 1342, 1163, 976$ cm^{-1} ; **HR-MS**: calc. for $[\text{M}+\text{H}]^+$ $\text{C}_{18}\text{H}_{19}\text{O}_6\text{N}_2\text{S}$ 391.0959, found: 391.0958.

2-((3-oxoisindolin-1-yl-1- d_2)methyl- d_2)phenethyl- d_2 4-methylbenzenesulfonate (67p)



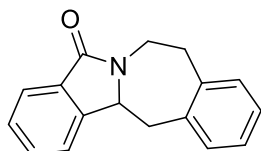
Colorless oil, 67% yield. **$^1\text{H-NMR}$ (600 MHz - CDCl_3)**: δ 7.76 (d, $J = 7.5, 1.2$ Hz, 1H), 7.59 (d, $J = 7.4$ Hz, 2H), 7.49 – 7.39 (m, 2H), 7.19 – 7.08 (m, 6H), 6.57 (br s, 1H, NH), 4.14 – 4.04 (m, 2H), 3.12 (s, 1H), 2.96 – 2.92 (m, 2H), 2.35 (dd, $J = 14.2, 5.0$ Hz, 1H), 2.32 (s, 3H); **$^{13}\text{C-NMR}$ (151 MHz - CDCl_3)**: δ 170.47, 146.67, 144.90, 144.66, 135.62, 134.64, 133.59, 133.16, 132.90, 132.82, 131.97, 131.70, 130.45, 130.38, 130.27, 129.86, 129.79, 128.78, 128.55, 127.97, 127.87, 127.82, 127.75, 127.73, 127.65, 127.44, 126.19, 123.97, 122.82, 119.31, 77.29, 69.99, 69.81, 66.84, 32.78, 32.28, 21.63, 14.73; **FT-IR**: $\tilde{\nu} = 3061, 1684, 1692, 1597, 1493, 1354, 1188, 1095, 1010, 960, 815$ cm^{-1} ; **LC-MS**: calc. for $[\text{M}+\text{H}]^+$ $\text{C}_{24}\text{H}_{21}\text{D}_2\text{O}_2\text{NS}$ 424.1, found: 424.1.

3.2.5 General Procedure for the synthesis of Isoindolobenzazepines (68)

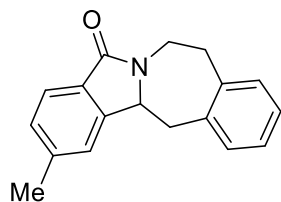


In a dram vial equipped with a stirring bar was added $[\text{RhCp}^*\text{Cl}_2]_2$ (1.0 mol%), KOAc (0.0025 mmol, 0.25 eq.), *N*-((*tert*-butoxycarbonyloxy)benzamide substrate (1) (0.1 mmol, 1.0 eq.) and dry MeOH [0.1 M]. The mixture was stirred for 30 seconds before the addition of the alkene substrate (2), (0.15 mmol, 1.5 eq.). The reaction was left to stir at room temperature for 16 h. The solvent was then evaporated under reduced pressure. Dry DCM [0.05 M] was added to the crude mixture followed by *t*BuOK (0.30 mmol, 3.0 eq.). The reaction mixture was stirred for 30 minutes at room temperature. The reaction was then quenched with H_2O and extracted with DCM (2 x 5 mL). The organic layer was washed with brine, dried over MgSO_4 , filtered, and the solvent was evaporated. The crude material was purified by silica gel chromatography (Pent/EtOAc, 4:1) to afford the title compounds 4.

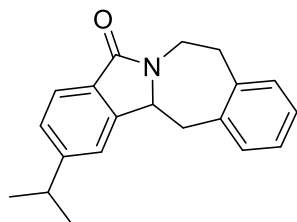
8,13-dihydro-6,13-methanodibenzo[*c,f*]azonin-5(7H)-one (68a)



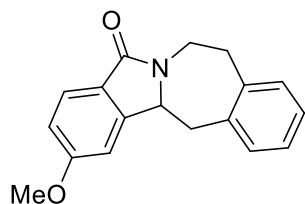
White solid, 79% yield. **$^1\text{H-NMR}$ (500 MHz - CDCl_3):** 7.82 (d, $J = \text{Hz}$, 1H), 7.55-7.48 (m, 2H), 7.43 (t, $J = \text{Hz}$, 1H), 7.62-7.22 (m, 1H), 7.19-7.13 (m, 3H), 4.80-4.72 (m, 1H), 4.38 (d, $J = \text{Hz}$, 1H), 3.22 (d, $J = \text{Hz}$, 1H), 3.00-2.81 (m, 4H); **$^{13}\text{C-NMR}$ (125 MHz - CDCl_3):** 167.1, 144.9, 141.4, 137.8, 131.9, 131.6, 129.9 (2C), 128.4, 127.4, 123.8, 122.2, 61.3, 42.3, 41.3, 36.2; **FT-IR:** $\tilde{\nu} = 2910, 2508, 2159, 2029, 1976, 1679, 1451 \text{ cm}^{-1}$; **HR-MS:** calc. for $[\text{M}+\text{H}]^+ \text{C}_{17}\text{H}_{16}\text{ON} = 250.1226$ found: 250.1227.

2-methyl-7,8,13,13a-tetrahydro-5H-benzo[4,5]azepino[2,1-a]isoindol-5-one (68b)

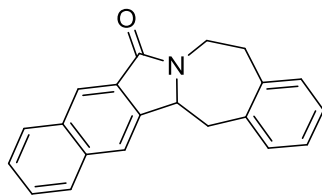
White solid, 62% yield. **¹H-NMR (500 MHz - CDCl₃):** 7.77 (d, *J* = 7.7 Hz, 1H), 7.36 (s, 1H), 7.32 – 7.28 (m, 2H), 7.26 – 7.19 (m, 3H), 4.86 – 4.74 (m, 1H), 4.42 – 4.35 (d, 1H), 3.27 (dd, *J* = 14.6, 1.7 Hz, 1H), 3.05 – 2.88 (m, 4H), 2.50 (s, 3H); **¹³C-NMR (125 MHz - CDCl₃):** 167.20, 145.28, 142.19, 141.50, 137.94, 129.88 (2C), 129.42, 127.43, 127.05, 123.59, 122.63, 60.99, 42.68, 41.17, 36.38, 21.98; **FT-IR:** $\tilde{\nu}$ = 2921, 2513, 2159, 2030, 1976, 1676, 1415 cm⁻¹; **HR-MS:** calc. for [M+H]⁺ C₁₈H₁₈ON = 264.1382 found: 264.1384.

2-isopropyl-7,8,13,13a-tetrahydro-5H-benzo[4,5]azepino[2,1-a]isoindol-5-one (68c)

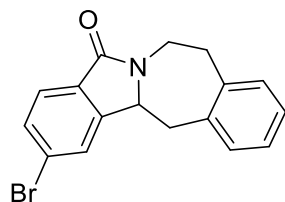
White solid, 69% yield. **¹H-NMR (500 MHz - CDCl₃):** 7.80 (d, *J* = 7.8 Hz, 1H), 7.39 (d, *J* = 1.4 Hz, 1H), 7.36 (dd, *J* = 7.8, 1.4 Hz, 1H), 7.34 – 7.31 (m, 1H), 7.26 – 7.21 (m, 3H), 4.81 (dd, *J* = 11.6, 5.5 Hz, 1H), 4.44 – 4.35 (m, 1H), 3.29 (dd, *J* = 14.6, 1.7 Hz, 1H), 3.04 – 2.98 (m, 3H), 2.96 – 2.88 (m, 2H), 1.33 (d, *J* = 6.9 Hz, 6H); **¹³C-NMR (125 MHz - CDCl₃):** 167.18, 153.26, 145.27, 141.53, 137.99, 129.90, 129.87, 129.82, 127.42, 127.04, 127.00, 123.70, 119.93, 61.13, 42.69, 41.18, 36.42, 34.69, 24.09 (2C); **FT-IR:** $\tilde{\nu}$ = 2962, 2514, 2159, 2029, 1977, 1671, 1417 cm⁻¹; **HR-MS:** calc. for [M+H]⁺ C₂₀H₂₂ON = 292.1695 found: 292.1697.

2-methoxy-7,8,13,13a-tetrahydro-5H-benzo[4,5]azepino[2,1-a]isoindol-5-one (68d)

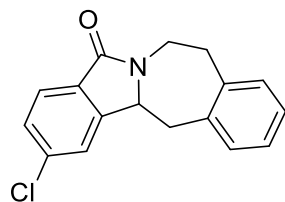
White solid, 40% yield. **¹H-NMR (500 MHz - CDCl₃):** 7.80 (d, *J* = 8.3 Hz, 1H), 7.31 (dd, *J* = 5.3, 3.5 Hz, 1H), 7.25 (dd, *J* = 5.6, 3.3 Hz, 2H), 7.24 – 7.20 (m, 1H), 7.03 (d, *J* = 2.1 Hz, 1H), 7.01 (dd, *J* = 8.3, 2.2 Hz, 1H), 4.83 – 4.75 (m, 1H), 4.38 (d, *J* = 10.9 Hz, 1H), 3.92 (s, 3H), 3.24 (dd, *J* = 14.7, 1.7 Hz, 1H), 3.06 – 2.97 (m, 2H), 2.96 – 2.89 (m, 2H); **¹³C-NMR (125 MHz - CDCl₃):** 165.92, 161.85, 146.08, 140.47, 136.80, 128.86 (2C), 126.43, 126.00, 124.14, 123.56, 113.61, 106.32, 59.88, 54.72, 41.77, 40.16, 35.42; **FT-IR:** $\tilde{\nu}$ = 2919, 2515, 2159, 2027, 1666, 1610, 1414 cm⁻¹; **HR-MS:** calc. for [M+H]⁺ C₁₈H₁₈O₂N = 280.1332 found: 280.1334.

8,9,14,14a-tetrahydro-6H-benzo[f]benzo[4,5]azepino[2,1-a]isoindol-6-one (68e)

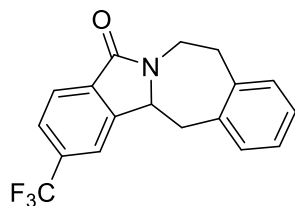
Yellow powder, 72% yield. **¹H-NMR (500 MHz - CDCl₃):** 8.40 (s, 1H), 8.03 (d, 1H), 7.99 (s, 1H), 7.96 (d, *J* = 8.2, 1.3 Hz, 1H), 7.64 – 7.52 (m, 2H), 7.38 – 7.32 (m, 1H), 7.31 – 7.27 (m, 1H), 7.26 – 7.21 (m, 2H), 4.95 – 4.79 (m, 1H), 4.60 (d, *J* = 11.1, 1.4 Hz, 1H), 3.40 (dd, *J* = 14.7, 1.8 Hz, 1H), 3.13 – 2.92 (m, 4H); **¹³C-NMR (125 MHz - CDCl₃):** 165.87, 140.34, 139.15, 136.86, 134.14, 132.16, 128.91, 128.81, 128.75, 128.53, 127.07, 126.64, 126.43, 126.05, 125.40, 122.96, 120.09, 60.01, 42.44, 40.44, 35.32; **FT-IR:** $\tilde{\nu}$ = 2923, 2519, 2031, 1976, 1686, 1418 cm⁻¹; **HR-MS:** calc. for [M+H]⁺ C₂₁H₁₈ON = 300.1382 found: 300.1386.

2-bromo-7,8,13,13a-tetrahydro-5H-benzo[4,5]azepino[2,1-a]isoindol-5-one (68f)

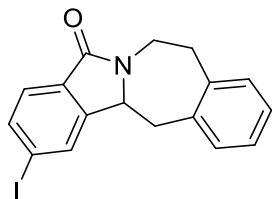
White solid, 55% yield. **¹H-NMR (700 MHz - CDCl₃):** δ 7.68 – 7.64 (m, 2H), 7.56 (dd, J = 8.0, 1.6 Hz, 1H), 7.22 (dd, J = 5.3, 3.5 Hz, 1H), 7.20 – 7.12 (m, 3H), 4.76 – 4.68 (m, 1H), 4.38 – 4.33 (m, 1H), 3.18 (dd, J = 14.7, 1.8 Hz, 1H), 2.98 – 2.91 (m, 2H), 2.91 – 2.82 (m, 2H); **¹³C-NMR (167 MHz - CDCl₃):** δ 166.21, 146.67, 141.25, 137.33, 131.92, 130.95, 129.92, 127.64, 127.21, 126.26, 125.65, 125.28, 60.76, 42.43, 41.31, 36.16, 29.71; **FT-IR:** $\tilde{\nu}$ = 3053, 2913, 2159, 1683, 1493, 1363, 1277, 1166, 1050, 994, 893, 828 cm⁻¹; **LC-MS:** calc. for [M+H]⁺ C₁₇H₁₄ONBr = 330.1 found: 331.1.

2-chloro-7,8,13,13a-tetrahydro-5H-benzo[4,5]azepino[2,1-a]isoindol-5-one (68g)

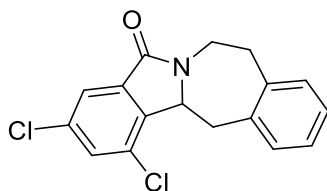
Yellow solid, 74% yield. **¹H-NMR (600 MHz - CDCl₃):** δ 7.74 (d, J = 8.1 Hz, 1H), 7.52 – 7.48 (m, 1H), 7.41 (dd, J = 8.1, 1.8 Hz, 1H), 7.27 – 7.10 (m, 4H), 4.73 (ddt, J = 11.1, 9.3, 4.6 Hz, 1H), 4.40 – 4.34 (m, 1H), 3.19 (dd, J = 14.6, 1.7 Hz, 1H), 3.00 – 2.80 (m, 4H); **¹³C-NMR (151 MHz - CDCl₃):** δ 166.13, 146.46, 141.25, 137.94, 137.34, 130.47, 129.93, 129.07, 127.64, 127.20, 125.07, 122.70, 60.80, 42.44, 41.33, 36.18, 29.72, 14.08; **FT-IR:** $\tilde{\nu}$ = 3054, 2918, 2160, 1683, 1452, 1306, 1166, 1027, 258, 894, 834 cm⁻¹; **LC-MS:** calc. for [M+H]⁺ C₁₇H₁₄ONCl = 284.3 found: 284.3.

2-(trifluoromethyl)-7,8,13,13a-tetrahydro-5H-benzo[4,5]azepino[2,1-a]isoindol-5-one (68h)

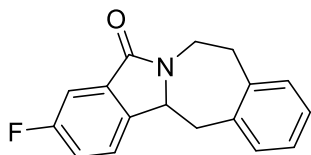
Yellow solid, 58% yield. **¹H-NMR (500 MHz - CDCl₃):** δ 7.93 (d, J = 7.8 Hz, 1H), 7.77 (s, 1H), 7.71 (dd, J = 7.9, 1.5 Hz, 1H), 7.44 (td, J = 7.0, 1.7 Hz, 1H), 7.26 (dd, J = 5.3, 3.6 Hz, 3H), 4.81 – 4.70 (m, 1H), 4.45 (dd, J = 11.0, 1.8 Hz, 1H), 3.26 (dd, J = 14.6, 1.8 Hz, 1H), 3.04 – 2.79 (m, 4H); **¹³C-NMR (125 MHz - CDCl₃):** δ 165.81, 145.22, 141.15, 137.15, 135.17, 133.97, 133.85, 133.71, 133.45, 129.99, 129.96, 128.11, 127.74, 127.68, 127.30, 125.88, 125.86, 124.93, 124.47, 122.76, 119.48, 119.45, 119.41, 116.99, 61.18, 42.30, 41.47, 37.29, 36.06; **¹⁹F-NMR (470 MHz - CDCl₃):** δ -62.20; **LC-MS:** calc. for [M+H]⁺ C₁₈H₁₄OF₃N = 318.1 found: 318.1.

2-iodo-7,8,13,13a-tetrahydro-5H-benzo[4,5]azepino[2,1-a]isoindol-5-one (68i)

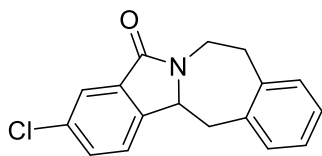
White solid, 68% yield. **¹H-NMR (600 MHz - CDCl₃):** δ 7.96 – 7.93 (m, 1H), 7.84 (dd, J = 8.0, 1.4 Hz, 1H), 7.61 (d, J = 7.9 Hz, 1H), 7.32 – 7.27 (m, 1H), 7.26 – 7.20 (m, 3H), 4.85 – 4.73 (m, 1H), 4.45 – 4.36 (m, 1H), 3.25 (dd, J = 14.7, 1.8 Hz, 1H), 3.06 – 2.97 (m, 2H), 2.97 – 2.88 (m, 2H); **¹³C-NMR (151 MHz - CDCl₃):** δ 166.38, 146.71, 141.26, 137.75, 137.36, 131.56, 131.53, 129.92 (2C), 127.63, 127.20, 125.32, 98.37, 60.61, 42.41, 41.25, 36.16; **FT-IR:** $\tilde{\nu}$ = 2896, 2352, 2115, 1997, 1674 cm⁻¹; **LC-MS:** calc. for [M+H]⁺ C₁₇H₁₄ONI = 376.1 found: 376.1.

1,3-dichloro-7,8,13,13a-tetrahydro-5H-benzo[4,5]azepino[2,1-a]isoindol-5-one (68j)

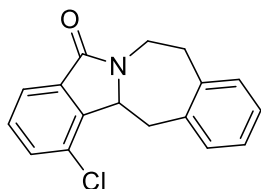
Yellow solid, 58% yield. **¹H-NMR (700 MHz - CDCl₃):** 7.69 (d, J = 1.7 Hz, 1H), 7.47 (d, J = 1.7 Hz, 1H), 7.26 – 7.21 (m, 1H), 7.20 – 7.12 (m, 3H), 4.76 – 4.68 (m, 1H), 4.41 (dd, J = 10.3, 1.7 Hz, 1H), 3.70 (dd, J = 14.5, 1.7 Hz, 1H), 3.01 – 2.94 (m, 2H), 2.91 – 2.83 (m, 1H), 2.66 (dd, J = 14.5, 10.3 Hz, 1H); **¹³C-NMR (176 MHz - CDCl₃):** 164.71, 141.02, 140.05, 137.31, 135.70, 135.61, 131.96, 130.07, 129.80, 129.77, 127.69, 127.25, 122.80, 60.89, 53.43, 41.65, 39.47, 35.94, 29.71; **FT-IR:** $\tilde{\nu}$ = 3042, 2917, 1688, 1450, 1319, 1230, 1102, 959, 890 cm⁻¹; **LC-MS:** calc. for [M+H]⁺ C₁₇H₁₃OCl₂N = 318.2 found: 318.2.

3-(fluoro)-7,8,13,13a-tetrahydro-5H-benzo[4,5]azepino[2,1-a]isoindol-5-one (68k)

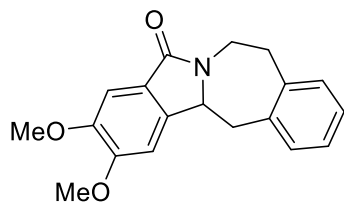
Off-white solid, 44% yield. **¹H-NMR (700 MHz - CDCl₃):** 7.69 (d, J = 7.4 Hz, 1H), 7.49 (td, J = 7.8, 4.5 Hz, 1H), 7.33 (dd, J = 5.3, 3.5 Hz, 1H), 7.26 – 7.23 (m, 3H), 7.24 – 7.20 (m, 1H), 4.82 (ddd, J = 9.9, 5.5, 1.5 Hz, 1H), 4.59 (dd, J = 10.9, 1.7 Hz, 1H), 3.55 (dd, J = 14.6, 1.7 Hz, 1H), 3.07 – 3.00 (m, 2H), 2.99 – 2.92 (m, 1H), 2.89 (dd, J = 14.6, 10.8 Hz, 1H); **¹³C-NMR (176 MHz - CDCl₃):** 164.96 (d, J = 2.3 Hz), 156.69 (d, J = 250.6 Hz), 140.21, 136.57, 134.13 (d, J = 4.2 Hz), 129.63 (d, J = 6.7 Hz), 129.46 (d, J = 16.0 Hz), 129.20, 128.76, 126.54, 126.14, 118.76 (d, J = 3.7 Hz), 117.51 (d, J = 20.1 Hz), 58.20 (d, J = 2.6 Hz), 40.43, 39.73, 35.14; **¹⁹F NMR (470 MHz, CDCl₃)** δ = -120.59 (dd, J = 9.3, 4.4 Hz); **HR-MS:** calc. for [M+H]⁺ C₁₈H₁₅OFN = 268.1132 found: 268.1134.

3-(chloro)-7,8,13,13a-tetrahydro-5H-benzo[4,5]azepino[2,1-a]isoindol-5-one (68l)

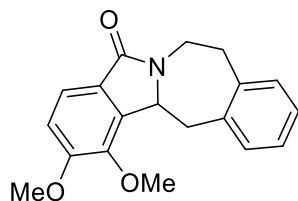
White solid, 36% yield. **¹H-NMR (500 MHz - CDCl₃):** 77.80 (dd, *J* = 7.4, 1.0 Hz, 1H), 7.54 (dd, *J* = 7.9, 1.0 Hz, 1H), 7.45 (dt, 1H), 7.34 (dd, *J* = 5.0, 3.7 Hz, 1H), 7.26 – 7.20 (m, 3H), 4.89 – 4.77 (m, 1H), 4.52 (dd, *J* = 10.3, 1.4 Hz, 1H), 3.84 (dd, *J* = 14.5, 1.5 Hz, 1H), 3.12 – 2.99 (m, 2H), 2.99 – 2.88 (m, 1H), 2.75 (dd, *J* = 14.4, 10.3 Hz, 1H); **¹³C-NMR (126 MHz - CDCl₃):** 165.80, 142.99, 141.21, 137.36, 134.74, 133.77, 131.70, 129.90, 129.87, 127.59, 127.14, 123.98, 123.36, 60.88, 42.41, 41.33, 36.11; **FT-IR:** $\tilde{\nu}$ = 2918, 2159, 2027, 1977, 1675 cm⁻¹; **HR-MS:** calc. for [M+H]⁺ C₁₇H₁₅ONCl = 284.0836 found: 284.0839.

1-(chloro)-7,8,13,13a-tetrahydro-5H-benzo[4,5]azepino[2,1-a]isoindol-5-one (68l')

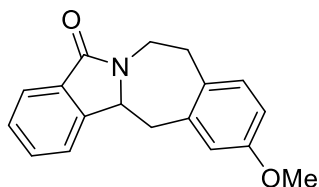
White solid, 36% yield. **¹H-NMR (500 MHz - CDCl₃):** 7.74 (dd, *J* = 7.4, 1.0 Hz, 1H), 7.48 (dd, *J* = 7.9, 1.0 Hz, 1H), 7.39 (t, *J* = 7.6 Hz, 1H), 7.28 (dd, *J* = 5.2, 3.6 Hz, 1H), 7.21 – 7.14 (m, 3H), 4.82 – 4.70 (m, 1H), 4.46 (dd, *J* = 10.4, 1.5 Hz, 1H), 3.77 (dd, *J* = 14.5, 1.6 Hz, 1H), 3.09 – 2.93 (m, 2H), 2.93 – 2.82 (m, 1H), 2.69 (dd, *J* = 14.4, 10.3 Hz, 1H); **¹³C-NMR (126 MHz - CDCl₃):** 165.88, 141.71, 141.16, 137.69, 134.44, 132.18, 130.11, 130.06, 129.73, 129.10, 127.53, 127.15, 122.39, 61.07, 41.47, 39.53, 36.06; **FT-IR:** $\tilde{\nu}$ = 2929, 2159, 2028, 1976, 1686 cm⁻¹; **HR-MS:** calc. for [M+H]⁺ C₁₇H₁₅ONCl = 284.0836 found: 284.0840.

2,3-(dimethoxy)-7,8,13,13a-tetrahydro-5H-benzo[4,5]azepino[2,1-a]isoindol-5-one (68m)

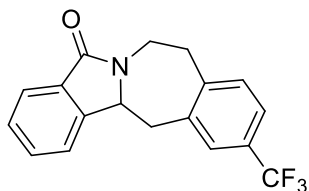
White solid, 27% yield. **¹H-NMR (700 MHz - CDCl₃):** 7.36 (s, 1H), 7.31 (m, 1H), 7.23 (m, 3H), 7.00 (s, 1H), 4.82 – 4.74 (m, 1H), 4.36 (dd, J = 11.0, 1.8 Hz, 1H), 4.02 (s, 3H), 3.96 (s, 3H), 3.25 (dd, J = 14.7, 1.8 Hz, 1H), 3.06 – 2.98 (m, 2H), 2.97 – 2.87 (m, 2H); **¹³C-NMR (176 MHz - CDCl₃):** 167.39, 152.68, 149.96, 141.50, 138.40, 137.77, 129.91, 129.86, 127.46, 127.05, 124.22, 105.47, 104.36, 60.88, 56.38, 56.33, 42.75, 41.31, 36.38; **FT-IR:** $\tilde{\nu}$ = 2924, 2159, 2029, 1977, 1663, 890 cm⁻¹; **HR-MS:** calc. for [M+H]⁺ C₁₉H₂₀O₃N = 310.1437 found: 310.1441.

1,2-(dimethoxy)-7,8,13,13a-tetrahydro-5H-benzo[4,5]azepino[2,1-a]isoindol-5-one (68m')

White solid, 39% yield. **¹H-NMR (700 MHz - CDCl₃):** 7.59 (d, J = 8.2 Hz, 1H), 7.33 – 7.30 (m, 1H), 7.25 – 7.19 (m, 3H), 7.05 (d, J = 8.2 Hz, 1H), 4.81 – 4.74 (m, 1H), 4.50 (dd, J = 10.6, 1.6 Hz, 1H), 4.01 (s, 3H), 3.96 (s, 3H), 3.64 (dd, J = 14.5, 1.7 Hz, 1H), 3.08 – 2.97 (m, 2H), 2.91 (dd, J = 13.3, 5.5 Hz, 1H), 2.80 (dd, J = 14.4, 10.6 Hz, 1H); **¹³C-NMR (176 MHz - CDCl₃):** 166.66, 155.36, 143.93, 141.48, 138.40, 136.91, 130.14, 129.73, 127.34, 127.01, 125.61, 119.65, 113.03, 60.68, 59.84, 56.25, 41.37, 40.75, 36.40; **FT-IR:** $\tilde{\nu}$ = 2925, 2159, 2029, 1977, 1689 cm⁻¹; **HR-MS:** calc. for [M+H]⁺ C₁₉H₂₀O₃N = 310.1437 found: 310.1439.

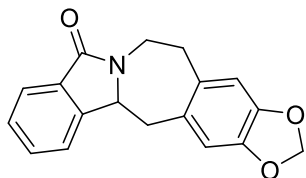
11-methoxy-7,8,13,13a-tetrahydro-5H-benzo[4,5]azepino[2,1-a]isoindol-5-one (68n)

White solid, 50% yield. **¹H-NMR (600 MHz - CDCl₃):** 7.88 (d, J = 7.6, 1.2 Hz, 1H), 7.60 (td, J = 7.3, 1.2 Hz, 1H), 7.56 (dtd, J = 7.6, 1.1 Hz, 1H), 7.49 (t, J = 7.3 Hz, 1H), 7.13 (d, J = 8.2 Hz, 1H), 6.87 (d, J = 2.7 Hz, 1H), 6.77 (dd, J = 8.2, 2.7 Hz, 1H), 4.83 – 4.74 (m, 1H), 4.44 (d, 1H), 3.84 (s, 3H), 3.23 (dd, J = 14.6, 1.7 Hz, 1H), 3.04 – 2.83 (m, 4H); **¹³C-NMR (151 MHz - CDCl₃):** 166.08, 157.44, 143.81, 137.98, 132.48, 130.94, 130.50, 129.82, 127.41, 122.77, 121.03, 115.14, 110.62, 60.14, 54.32, 41.75, 40.57, 34.32; **FT-IR:** $\tilde{\nu}$ = 2923, 2360, 2159, 2030, 1977, 1689 cm⁻¹; **HR-MS:** calc. for [M+H]⁺ C₁₈H₁₈O₂N = 280.1332 found: 280.1333.

11-(trifluoromethyl)-7,8,13,13a-tetrahydro-5H-benzo[4,5]azepino[2,1-a]isoindol-5-one (68o)

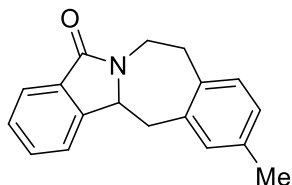
Yellow solid, 80% yield. **¹H-NMR (500 MHz - CDCl₃):** 7.83 (dt, J = 7.6, 1.0 Hz, 1H), 7.55 (td, J = 7.4, 1.2 Hz, 1H), 7.54 – 7.46 (m, 2H), 7.48 – 7.36 (m, 2H), 7.27 (d, J = 7.8 Hz, 1H), 4.83 – 4.73 (m, 1H), 4.39 (dd, J = 11.1, 1.7 Hz, 1H), 3.30 (dd, J = 14.8, 1.8 Hz, 1H), 3.04 – 2.85 (m, 4H); **¹³C-NMR (126 MHz - CDCl₃):** 167.15, 145.41, 144.46, 138.58, 131.85, 131.74, 130.32, 129.51, 129.25, 128.70, 126.69, 126.66, 125.17, 124.39, 124.36, 123.98, 122.10, 60.72, 42.48, 40.76, 36.25; **¹⁹F-NMR (470 MHz, CDCl₃):** δ = -62.34; **LC-MS:** calc. for [M+H]⁺ C₁₈H₁₄OF₃N = 318.1 found: 318.1.

5,6,12b,13-tetrahydro-8H-[1,3]dioxolo[4'',5'':4',5']benzo[1',2':4,5]azepino[2,1-a]isoindol-8-one (68p)

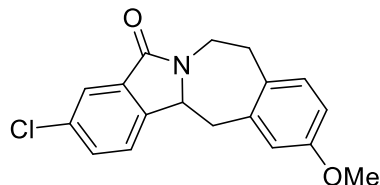


White solid, 31% yield. **¹H-NMR (500 MHz - CDCl₃):** 7.88 (d, J = 7.5, 1.0 Hz, 1H), 7.59 (td, J = 7.4, 1.2 Hz, 1H), 7.54 (dd, J = 7.5, 1.0 Hz, 1H), 7.49 (t, 1H), 6.80 (s, 1H), 6.72 (s, 1H), 5.96 (dd, 2H), 4.83 – 4.73 (m, 1H), 4.41 (d, 1H), 3.18 (dd, J = 14.8, 1.8 Hz, 1H), 3.04 – 2.90 (m, 2H), 2.89 – 2.80 (m, 2H); **¹³C-NMR (126 MHz - CDCl₃):** 167.10, 146.43, 146.16, 144.73, 134.82, 131.98, 131.56, 130.90, 128.46, 123.81, 122.06, 110.42, 110.40, 101.11, 61.19, 42.19, 41.31, 35.96; **FT-IR:** $\tilde{\nu}$ = 2930, 2522, 2363, 2159, 2028, 1977, 1698, 1038 cm⁻¹; **LC-MS:** calc. for [M+H]⁺ C₁₈H₁₅O₃N = 294.0 found: 294.0.

11-methyl-7,8,13,13a-tetrahydro-5H-benzo[4,5]azepino[2,1-a]isoindol-5-one (68q)



White solid, 39% yield. **¹H-NMR (600 MHz - CDCl₃):** 7.88 (d, J = 7.5, 1.0 Hz, 1H), 7.59 (td, J = 7.4, 1.1 Hz, 1H), 7.55 (d, J = 7.5, 1.1 Hz, 1H), 7.49 (t, J = 7.4, 0.8 Hz, 1H), 7.20 (d, J = 7.4 Hz, 1H), 7.05 (d, J = 7.9 Hz, 2H), 4.82 (d, J = 1.2 Hz, 1H), 4.42 (d, 1H), 3.27 (dd, J = 14.7, 1.8 Hz, 1H), 3.06 – 2.95 (m, 2H), 2.94 – 2.82 (m, 2H), 2.35 (s, 3H); **¹³C-NMR (151 MHz - CDCl₃):** 167.11, 144.94, 141.26, 137.11, 134.74, 132.01, 131.52, 130.74, 129.87, 128.40, 127.55, 123.79, 122.08, 61.39, 42.15, 41.28, 36.29, 20.98; **FT-IR:** $\tilde{\nu}$ = 2920, 2159, 2029, 1977, 1680 cm⁻¹; **HR-MS:** calc. for [M+H]⁺ C₁₈H₁₈ON = 264.1382 found: 264.1385.

3-chloro-11-methoxy-7,8,13,13a-tetrahydro-5H-benzo[4,5]azepino[2,1-a]isoindol-5-one (68r)

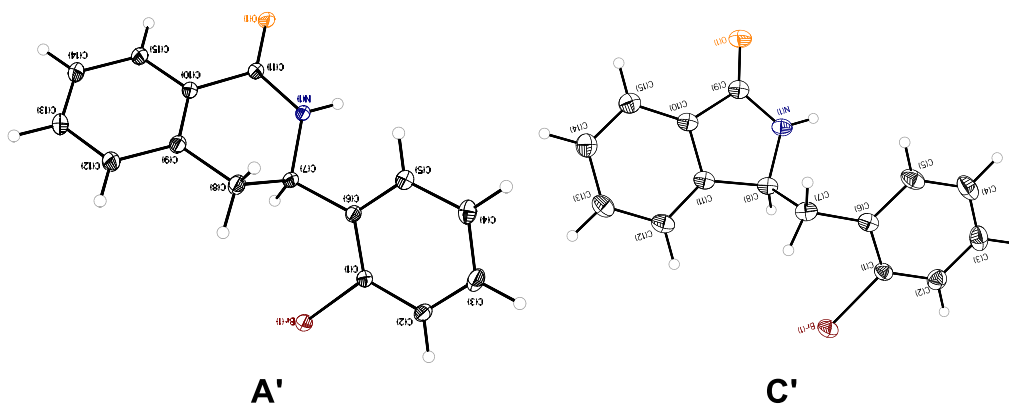
White solid (27%). **¹H NMR (700 MHz, CDCl₃)** δ = 7.36 (s, 1H), 7.31 (m, 1H), 7.23 (m, 3H), 7.00 (s, 1H), 4.82 – 4.74 (m, 1H), 4.36 (dd, J = 11.0, 1.8 Hz, 1H), 4.02 (s, 3H), 3.96 (s, 3H), 3.25 (dd, J = 14.7, 1.8 Hz, 1H), 3.06 – 2.98 (m, 2H), 2.97 – 2.87 (m, 2H). **¹³C NMR (176 MHz, CDCl₃)** δ = 167.39, 152.68, 149.96, 141.50, 138.40, 137.77, 129.91, 129.86, 127.46, 127.05, 124.22, 105.47, 104.36, 60.88, 56.38, 56.33, 42.75, 41.31, 36.38. **HRMS (ESI)** m/z [M+H]⁺ calculated for C₁₉H₂₀O₃N, 310.1437; found 310.1441.

3.3. X-ray Structure Analyses

Data collection was conducted on a Bruker D8 Venture four-circle diffractometer by Bruker AXS GmbH using a PHOTON II CPAD detector by Bruker AXS GmbH. X-ray radiation was generated by microfocus sources $I\mu S$ and $I\mu S$ 3.0 Cu or Mo by Incoatec GmbH with HELIOS mirror optics and a single-hole collimator by Bruker AXS GmbH.

For the data collection, the programs APEX 3 Suite (v.2018.7-2) with the integrated programs SAINT (integration) and SADABS (adsorption correction) by Bruker AXS GmbH were used. Using Olex2,^[193] the structures were solved with the ShelXT^[194] structure solution program using Intrinsic Phasing and refined with the XL^[195] refinement package using Least Squares minimization.

Crystal data and structure refinement for compound **A'** (CCDC 2033334) and **C'** (CCDC 2033335) with 50% ellipsoid probability level.



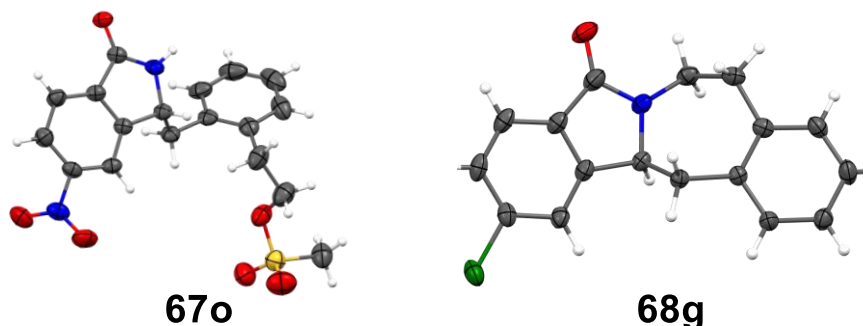
Compound	A'	C'
Empirical formula	$C_{15}H_{12}BrNO$	$C_{15}H_{12}BrNO$
Formula weight	302.17	302.17
Temperature/K	100.0	100.0
Crystal system	triclinic	monoclinic
Space group	P-1	C2/c
a/Å	6.9547(10)	21.0894(18)
b/Å	7.8252(6)	4.5726(4)

$c/\text{\AA}$	12.0854(12)	27.124(2)
$\alpha/^\circ$	71.231(3)	90
$\beta/^\circ$	77.870(4)	106.481(3)
$\gamma/^\circ$	88.052(4)	90
Volume/ \AA^3	608.43(12)	2508.2(4)
Z	2	8
$\rho_{\text{calc}}/\text{g/cm}^3$	1.649	1.600
μ/mm^{-1}	3.363	3.264
F(000)	304.0	1216.0
Crystal size/ mm^3	$0.278 \times 0.124 \times 0.111$	$1.942 \times 0.103 \times 0.084$
Radiation	MoK α ($\lambda = 0.71073$)	MoK α ($\lambda = 0.71073$)
2Θ range for data collection/ $^\circ$	5.502 to 63.082	4.344 to 66.324
Index ranges	$-9 \leq h \leq 10, -11 \leq k \leq 11, -17 \leq l \leq 17$	$-32 \leq h \leq 32, -7 \leq k \leq 7, -41 \leq l \leq 41$
Reflections collected	13350	50152
Independent reflections	3989 [$R_{\text{int}} = 0.0200, R_{\text{sigma}} = 0.0214$]	4716 [$R_{\text{int}} = 0.0535, R_{\text{sigma}} = 0.0275$]
Data/restraints/parameters	3989/0/167	4716/0/167
Goodness-of-fit on F^2	1.056	1.099
Final R indexes [$I \geq 2\sigma(I)$]	$R_1 = 0.0226, wR_2 = 0.0522$	$R_1 = 0.0367, wR_2 = 0.0863$
Final R indexes [all data]	$R_1 = 0.0262, wR_2 = 0.0536$	$R_1 = 0.0444, wR_2 = 0.0897$
Largest diff. peak/hole / $e \text{\AA}^{-3}$	0.52/-0.38	0.89/-1.02

Data collection was conducted on a Bruker D8 Venture four-circle diffractometer by Bruker AXS GmbH using a PHOTON II CPAD detector by Bruker AXS GmbH. X-ray radiation was generated by microfocus sources $I\mu S$ and $I\mu S$ 3.0 Cu or Mo by Incoatec GmbH with HELIOS mirror optics and a single-hole collimator by Bruker AXS GmbH.

For the data collection, the programs APEX 3 Suite (v.2018.7-2) with the integrated programs SAINT (integration) and SADABS (adsorption correction) by Bruker AXS GmbH were used. Using Olex2,^[7] the structures were solved with the ShelXT^[8] structure solution program using Intrinsic Phasing and refined with the XL^[9] refinement package using Least Squares minimization.

Crystal data and structure refinement for compound **67o** (CCDC 1990749) and **68g** (CCDC 1990750) with 50% ellipsoid probability level.



Compound	67o*	68g*
Empirical formula	C ₁₈ H ₁₈ N ₂ O ₆ S	C ₁₇ H ₁₄ ClNO
Formula weight	390.40	283.74
Temperature/K	100.0	100.0
Crystal system	monoclinic	monoclinic
Space group	P2 ₁ /n	P2 ₁ /c
a/Å	14.8594(8)	12.3505(13)
b/Å	5.4431(3)	9.3353(9)
c/Å	21.6605(12)	12.2839(11)
α/°	90	90
β/°	90.003(2)	105.592(4)
γ/°	90	90

Volume/Å ³	1751.93(17)	1364.2(2)
Z	4	4
$\rho_{\text{calc}}/\text{cm}^3$	1.480	1.382
μ/mm^{-1}	2.002	0.274
F(000)	816.0	592.0
Crystal size/mm ³	0.542 × 0.107 × 0.04	0.466 × 0.311 × 0.1
Radiation	CuK α ($\lambda = 1.54178$)	MoK α ($\lambda = 0.71073$)
2 Θ range for data collection/°	7.214 to 159.562	5.548 to 59.998
Index ranges	-18 ≤ h ≤ 18, -6 ≤ k ≤ 6, -27 ≤ l ≤ 26	-17 ≤ h ≤ 17, -13 ≤ k ≤ 13, -17 ≤ l ≤ 16
Reflections collected	28346	29747
Independent reflections	3739 [R _{int} = 0.0493, R _{sigma} = 0.0288]	3982 [R _{int} = 0.0313, R _{sigma} = 0.0210]
Data/restraints/parameters	3739/0/245	3982/0/245
Goodness-of-fit on F ²	1.064	1.062
Final R indexes [I ≥ 2 σ (I)]	R ₁ = 0.0714, wR ₂ = 0.2227	R ₁ = 0.0456, wR ₂ = 0.1121
Final R indexes [all data]	R ₁ = 0.0748, wR ₂ = 0.2263	R ₁ = 0.0531, wR ₂ = 0.1175
Largest diff. peak/hole / e Å ⁻³	0.67/-0.81	0.39/-0.41

*Disorder omitted for clarity.

3.4. DFT Calculations

Geometry optimizations and frequency analysis were carried out using Gaussian 16 Rev. B^[196] employing tight convergence criteria using the M06-2X functional.^[197] The 6-31G(2d,p) basis set was used for all elements except for Rh, for which LabL2DZ including pseudo potentials was used. The solvent environment was simulated by the IEFPCM of methanol as implemented in the software package.

Cartesian coordinates

Structure II'

C	-1.61797100	-1.77769800	2.33470600
C	-1.33605000	-0.39123300	2.55196900
C	-0.49547900	-2.34232600	1.69196800
C	0.53203400	-1.33640400	1.59338900
C	0.01267600	-0.14723700	2.12719300
H	-0.41510200	-3.36029900	1.33658600
H	1.50230200	-1.46399400	1.13421800
H	0.50249300	0.81405300	2.12528400
C	-3.64462100	0.98435200	-0.25669700
C	-3.34696400	-0.29535900	0.21621700
C	-4.39413900	-1.13835900	0.57906000
C	-5.71232600	-0.68575200	0.49058300
C	-5.99825400	0.60042500	0.03712400
C	-4.95642900	1.43835700	-0.34334300
C	-2.49605600	1.83031800	-0.68999300
H	-4.20226200	-2.15053900	0.92107000
H	-6.52199000	-1.34883800	0.77848900
H	-7.02594500	0.94038900	-0.02464500
H	-5.13622100	2.44303900	-0.71334600

O	-2.57247300	3.00050000	-1.04649600
N	-1.37657500	1.07300600	-0.65143700
O	-0.21779000	1.76518400	-0.99856800
C	0.17444700	2.71389400	-0.10539300
O	-0.27918400	2.80518600	1.00163800
Rh	-1.36417200	-0.71092300	0.36405300
C	-0.58185000	-1.58293900	-1.67729100
C	-1.94192400	-1.76268200	-1.56782100
C	0.44731000	-2.62271300	-1.45141900
C	1.81196900	-2.26863800	-1.40513600
C	0.07953000	-3.96386700	-1.30256300
C	2.75098900	-3.26855000	-1.15369800
C	1.02922700	-4.94838800	-1.06542800
H	-0.96521600	-4.24539000	-1.37702200
C	2.37050300	-4.59597800	-0.97982300
H	3.80312400	-3.02066000	-1.07792300
H	0.72202300	-5.98164100	-0.95076000
H	3.12477700	-5.35036500	-0.78610600
H	-2.54305800	-2.28438700	2.56364300
H	-1.99660700	0.33185400	3.00719900
C	1.15810800	3.68706000	-0.73669600
C	2.07944700	3.01257200	-1.75570500
H	2.70785700	2.27013000	-1.25966100
H	1.51389100	2.52656000	-2.55332200
H	2.73051400	3.76950700	-2.20356900
C	1.98084600	4.35557000	0.36404900
H	2.61190400	5.13344000	-0.07602800
H	1.32875900	4.81456000	1.11003100
H	2.62212200	3.62375100	0.86155900
C	0.27396100	4.73234300	-1.44429300
H	-0.37129800	4.25656600	-2.18587500

H	-0.36364700	5.24935200	-0.72188800
H	0.91359000	5.46946800	-1.93891300
C	2.22334500	-0.82585300	-1.62372200
H	1.59649400	-0.15378300	-1.02502600
H	2.04989000	-0.55091400	-2.67275800
C	3.67337700	-0.51493600	-1.31475500
H	4.37030000	-1.17261000	-1.83459000
H	3.92308400	0.51195300	-1.59219800
O	3.94659500	-0.70928200	0.09810500
S	3.84256300	0.61796100	0.97986200
O	4.87987700	1.52817900	0.58179500
O	2.48304600	1.09726800	0.94097300
C	4.19265100	-0.09990000	2.54760600
H	4.17441000	0.71993700	3.26591700
H	3.41384900	-0.82865100	2.76948500
H	5.17847400	-0.55936800	2.50202900
H	-0.24895600	-0.66563100	-2.15265000
H	-2.38254400	-2.70792500	-1.27024300
H	-2.60500500	-1.04920500	-2.03922600

Structure III

C	1.71934000	-0.54507800	2.85494600
C	0.37000800	-0.80278700	2.70086900
C	1.98740200	0.80936900	2.39018500
C	0.76037700	1.40246000	2.04009100
C	-0.23804100	0.37483500	2.09863600
H	2.95305300	1.29464400	2.38453600
H	0.62098600	2.40908700	1.67157700
H	-1.29030300	0.49220100	1.87289400
C	2.45335700	-2.12105900	-0.82902500

C	2.97773000	-0.84619900	-1.14325700
C	4.31316000	-0.58642000	-0.78441400
C	5.08947100	-1.52964500	-0.13233600
C	4.55862200	-2.78734800	0.16241500
C	3.25412500	-3.07935600	-0.19546800
C	1.02246500	-2.52832100	-1.10856600
H	4.75583500	0.36323700	-1.06908800
H	6.11681800	-1.29760100	0.12477300
H	5.16818900	-3.53480700	0.65753900
H	2.82334700	-4.05524200	0.00001300
O	0.71691000	-3.64051300	-1.52256400
N	0.21052000	-1.52210100	-0.75768100
O	-1.14481700	-1.84388200	-0.84823600
C	-1.57244500	-2.75435200	0.05963800
O	-0.90778400	-3.12953300	0.98689300
Rh	1.15650300	-0.18284500	0.56987300
C	1.17846500	0.99122100	-1.13178500
H	0.19116600	0.89244300	-1.57614400
C	2.20469400	0.19370000	-1.96097800
H	1.68159700	-0.32527500	-2.76724800
H	2.93310300	0.86932400	-2.41839500
C	1.52281500	2.42010100	-0.86298500
C	0.58519100	3.45932100	-1.03207700
C	2.80695500	2.75815100	-0.41112300
C	0.95300000	4.77222800	-0.72488100
C	3.16145800	4.06563500	-0.11364600
H	3.53383000	1.96574500	-0.26363900
C	2.22609500	5.08525500	-0.26704500
H	0.21997200	5.56298000	-0.85618900
H	4.16263600	4.28742500	0.23961800
H	2.48597000	6.11246900	-0.03755700

H	2.47315300	-1.25011800	3.17700800
H	-0.13156600	-1.74497000	2.85938600
C	-2.95868200	-3.27145800	-0.29422800
C	-3.86620700	-2.15307400	-0.81649700
H	-3.98739100	-1.36683800	-0.06653000
H	-3.45929400	-1.70676700	-1.72699200
H	-4.85130700	-2.57027000	-1.04700300
C	-3.57190600	-3.92066200	0.94581200
H	-4.54581900	-4.34768200	0.69034400
H	-2.92888500	-4.71619400	1.32744400
H	-3.71594000	-3.18479200	1.74225900
C	-2.74077300	-4.32699600	-1.39310500
H	-2.26553500	-3.88022200	-2.26934400
H	-2.10238300	-5.13774100	-1.03158900
H	-3.70695900	-4.74749200	-1.68750900
C	-0.83079000	3.20476400	-1.50003500
H	-0.85950400	2.51434200	-2.34787100
H	-1.28654100	4.14325600	-1.82577800
C	-1.65020200	2.62707900	-0.36053600
H	-1.22735400	1.68075500	-0.01340800
H	-1.70553200	3.33476900	0.47419500
O	-2.98290900	2.36951400	-0.85455500
S	-4.00673000	1.86644000	0.25900100
O	-3.41154000	0.75412000	0.95766900
O	-4.44881200	2.99036400	1.03565300
C	-5.28790900	1.31218600	-0.81203900
H	-6.08121700	0.92875500	-0.17007100
H	-5.63446500	2.16544100	-1.39311700
H	-4.88332200	0.52696300	-1.44892900

Structure A'

C	-2.84676300	2.79123800	1.00644200
C	-1.49340400	3.12972900	1.40579800
C	-3.36743800	1.88283700	1.93098100
C	-2.28503200	1.52260700	2.80939000
C	-1.17466500	2.40512300	2.54957000
H	-4.35569200	1.44646000	1.92789100
H	-2.35046600	0.82321200	3.63205600
H	-0.23163800	2.40810400	3.07823100
C	-1.95294900	-1.49558700	-2.26280000
C	-1.31357700	-2.59360600	-1.68216500
C	-1.95243600	-3.82956000	-1.70240600
C	-3.21032000	-3.95531600	-2.28456900
C	-3.83878500	-2.85385800	-2.86531900
C	-3.20220700	-1.62003200	-2.86676900
C	-1.23905700	-0.19723100	-2.30631200
H	-1.46690300	-4.69141800	-1.25647800
H	-3.70521700	-4.92024400	-2.28618200
H	-4.81764700	-2.96131600	-3.31762700
H	-3.65963200	-0.74902100	-3.32315800
O	-1.29095600	0.57093100	-3.23011800
N	-0.47140500	0.09761400	-1.13938800
O	0.56998900	0.99242700	-1.44729000
C	0.23189700	2.31092000	-1.52179100
O	-0.89188000	2.71363300	-1.48033300
Rh	-1.61271500	0.76428500	0.87788200
C	0.14147000	-1.03030800	-0.34991300
H	1.18988800	-0.74689000	-0.28183700
C	0.05274300	-2.36997300	-1.09232300
H	0.80261200	-2.38442100	-1.89290900

H	0.30632300	-3.17226300	-0.39367800
C	-0.48580100	-1.04078400	1.03624200
C	0.35435900	-1.07758800	2.21608600
C	-1.86921500	-1.39666900	1.16824300
C	-0.18239100	-1.45130700	3.41741300
C	-2.36565300	-1.80745400	2.44948700
H	-2.44654400	-1.70075000	0.30410700
C	-1.54800500	-1.83575100	3.53967900
H	0.45138400	-1.45317800	4.29962000
H	-3.39968800	-2.12855300	2.52672700
H	-1.92608400	-2.15714300	4.50419200
H	-3.36219400	3.20904500	0.15323500
H	-0.85270100	3.82291800	0.88016400
C	1.49841800	3.14614200	-1.61538900
C	2.25570300	2.97678900	-0.28647100
H	1.61281700	3.21409500	0.56833900
H	2.62251700	1.95273000	-0.17962100
H	3.11125500	3.65836100	-0.27103200
C	1.09696200	4.60461200	-1.82539800
H	1.99738200	5.22069700	-1.89558900
H	0.51962700	4.72428000	-2.74575900
H	0.49022900	4.97083900	-0.99319600
C	2.37136000	2.65125400	-2.77726700
H	2.69826800	1.62293000	-2.61024300
H	1.83033900	2.70125600	-3.72681400
H	3.25702200	3.28862300	-2.85380300
C	1.81070800	-0.68923500	2.12770800
H	2.16068700	-0.34456100	3.10449900
H	1.95198600	0.13497400	1.42031600
C	2.67487000	-1.86823400	1.69876400
H	2.69151400	-2.64292500	2.46674700

H	2.31693300	-2.31775400	0.76707600
O	4.05131500	-1.45709200	1.54164600
S	4.52815800	-1.03042500	0.08467500
O	3.42537900	-0.41501200	-0.60973300
O	5.74066000	-0.29955900	0.29218400
C	4.88596000	-2.58279500	-0.67403800
H	5.23655800	-2.36601500	-1.68313200
H	5.65967600	-3.07364300	-0.08600800
H	3.97229800	-3.17617800	-0.70796900

Structure IV

C	-0.20029300	0.81729700	2.81912600
C	0.99303300	0.65651500	2.02572900
C	-0.50910300	-0.44818700	3.40010100
C	0.40202800	-1.39749800	2.86950800
C	1.36005800	-0.69091300	2.05784700
H	-1.33168700	-0.65744000	4.06770900
H	0.41769900	-2.45477600	3.09041000
H	2.17434200	-1.13967900	1.50479900
C	-3.44017100	-0.60202400	-1.09059500
C	-3.06053200	-1.85444600	-0.56613800
C	-3.98462500	-2.90399800	-0.60032200
C	-5.24796300	-2.74934100	-1.15649900
C	-5.61231200	-1.52176600	-1.69462500
C	-4.70974300	-0.46724400	-1.65523600
C	-2.62919700	0.67982600	-1.09880900
H	-3.69521300	-3.86626300	-0.18952400
H	-5.93850000	-3.58525000	-1.16781800
H	-6.59325200	-1.38117800	-2.13418400
H	-4.97048500	0.50264600	-2.06040700

O	-2.96092700	1.61226700	-1.82977000
N	-1.58506200	0.72553200	-0.25831100
O	-0.88425500	1.93251900	-0.35955100
C	-1.44565000	2.97561500	0.29687000
O	-2.41466800	2.87730900	0.99667300
Rh	-0.84472700	-0.53979900	1.18062700
C	-0.52331600	-1.88203000	-0.61000300
C	-1.72883200	-2.20931900	0.00079500
C	0.75675200	-2.60679000	-0.46072700
C	1.88140400	-2.20066000	-1.20472400
C	0.88152700	-3.68441000	0.42634600
C	3.10033200	-2.84854900	-0.99217600
C	2.09820700	-4.31956800	0.62185000
H	0.01717300	-4.02416500	0.98686400
C	3.22050900	-3.89200500	-0.08295400
H	3.96800100	-2.51659600	-1.55457500
H	2.16964800	-5.14512100	1.32094200
H	4.17936200	-4.37562100	0.06572700
H	-0.73189100	1.74250200	2.98971900
H	1.47616800	1.43013200	1.44676800
C	-0.67244100	4.25439000	0.00921200
C	0.81612200	4.04588200	0.32274100
H	0.96795900	3.81798300	1.38304300
H	1.23677000	3.23364300	-0.27666100
H	1.36641100	4.96335900	0.09381900
C	-1.24496800	5.37642400	0.87258400
H	-0.70336500	6.30483700	0.67104400
H	-2.30362700	5.53464800	0.65450700
H	-1.14835300	5.14065600	1.93575000
C	-0.85148500	4.58028100	-1.48225600
H	-0.42822000	3.79039900	-2.10648300

H	-1.91051500	4.68741800	-1.73290300
H	-0.34338700	5.52174500	-1.71063200
H	-2.29976700	-0.71321700	1.54903400
H	-0.58231600	-1.19481900	-1.44644600
H	-1.76099800	-3.06909500	0.66310900
C	1.85268400	-1.06994300	-2.20959400
H	0.97226100	-1.12446700	-2.85792400
H	2.72709200	-1.16352800	-2.85478000
C	1.86254100	0.31947500	-1.57346300
H	0.90243000	0.57435500	-1.12069200
H	2.10678700	1.08380700	-2.31753100
O	2.78754800	0.39758600	-0.46660100
S	4.33652400	0.63206100	-0.75221000
C	4.43743100	2.39232100	-0.83356500
H	3.82489000	2.74007000	-1.66548900
H	4.08799300	2.79282200	0.11737200
H	5.48516800	2.64154800	-1.00245000
O	4.99413100	0.16665900	0.43193500
O	4.67481900	0.07764500	-2.03430500

Structure V

C	1.04187800	0.12986600	3.02642200
C	-0.15174400	-0.69640100	2.85191000
C	0.67049800	1.49340000	2.79380200
C	-0.63619800	1.47082700	2.27588200
C	-1.16593800	0.11633500	2.38313000
H	1.31717800	2.35525800	2.86400300
H	-1.17662000	2.32145100	1.87964800
H	-2.14808700	-0.18578600	2.04565100
C	3.37434900	-0.69896800	-1.00659000

C	3.39481700	0.58849300	-0.44241200
C	4.62899300	1.24719400	-0.36490900
C	5.80226700	0.66899600	-0.83178200
C	5.76683500	-0.59926600	-1.40347300
C	4.55602200	-1.27082300	-1.48458300
C	2.15871700	-1.57943300	-1.10299100
H	4.65835900	2.24352800	0.06759600
H	6.73971000	1.20880900	-0.75056900
H	6.67424800	-1.06233400	-1.77442900
H	4.49498500	-2.26345700	-1.91445200
O	2.18384500	-2.62563300	-1.74114300
N	1.07678900	-1.14452800	-0.41210700
O	0.01002000	-2.05355400	-0.50992100
C	0.05943800	-3.09121700	0.35083400
O	0.95972800	-3.27731700	1.12398100
Rh	0.69109200	0.30807600	0.95534900
C	1.49030800	2.07010300	-1.16730700
C	2.18339300	1.34831600	0.01868400
C	0.33517400	2.94256800	-0.71185500
C	-0.97932900	2.79760200	-1.18395700
C	0.60010200	3.92606500	0.24912600
C	-1.98975400	3.58936800	-0.62269700
C	-0.40584000	4.71921600	0.78357100
H	1.62397000	4.07127600	0.58285200
C	-1.71875300	4.53466000	0.35810400
H	-3.00526900	3.46042900	-0.98291700
H	-0.16728600	5.47291900	1.52609200
H	-2.52143400	5.13653500	0.76972200
H	1.99442400	-0.21851800	3.39890500
H	-0.16968000	-1.77161900	2.95724200
C	-1.21999700	-3.91013700	0.25800500

C	-2.29964600	-3.10115900	0.99866900
H	-2.06904100	-3.01661500	2.06564500
H	-2.38046600	-2.09268600	0.58071700
H	-3.26639500	-3.60649800	0.90473900
C	-1.00079400	-5.25650500	0.94429700
H	-1.93350500	-5.82737000	0.93601900
H	-0.23399700	-5.83903900	0.42615100
H	-0.68313900	-5.11771400	1.97979800
C	-1.62983900	-4.10714100	-1.20626000
H	-1.83801800	-3.15065100	-1.69140200
H	-0.83953600	-4.61042400	-1.77080400
H	-2.53135700	-4.72566200	-1.24933800
H	2.52482000	2.10894700	0.72512100
H	1.16788100	1.33167800	-1.90684900
H	2.24814400	2.69559500	-1.66139000
C	-1.36447500	1.89031100	-2.33625700
H	-0.60988800	1.93671400	-3.12917100
H	-2.29446800	2.26887500	-2.76345300
C	-1.54499100	0.40986300	-2.01015200
H	-0.59158300	-0.09332300	-1.84909800
H	-2.06144200	-0.09732200	-2.83085600
O	-2.25205900	0.17297000	-0.77087500
S	-3.83637900	0.27833500	-0.73512400
C	-4.37835000	-1.20149200	-1.53349300
H	-4.01889600	-1.20764400	-2.56194400
H	-4.00717600	-2.05686600	-0.97159200
H	-5.46814000	-1.16974000	-1.51776000
O	-4.15061700	0.20844800	0.66355800
O	-4.26913800	1.40162800	-1.51936900

3.5. Biological data

All assays and experiments were performed by Dr. Jana Flegel

Reagents

Purmorphamine was purchased from Cayman Chemical (#10009634) and DMSO from (Sigma Aldrich, #67685). The compound collection was synthesized as described in the paper. All other reagents used are mentioned in the respective protocols below, with the corresponding sources.

Cell lines

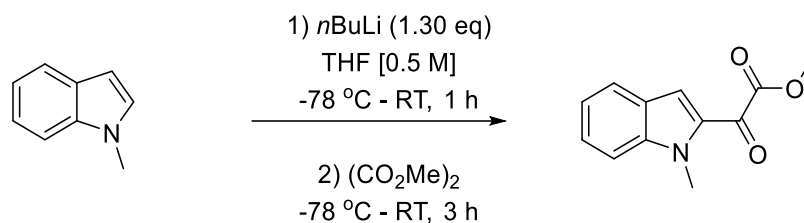
The murine mesenchymal stem cell line C3H10T1/2 (ATCC, CCL-226) was cultured in Dulbecco's Modified Eagle's medium (DMEM, high glucose, PAN, #P04-03550) supplemented with 10% of fetal calf serum (FCS, Fisher Scientific, #10136253, heat inactivated), 1 mM sodium pyruvate (PAN, #P04-43100) and 2 mM L-glutamine (PAN, #P0480100). The cells were cultured at 37°C and 5% CO₂ in a humidified atmosphere. Checks for mycoplasma contaminations were performed regularly and cells were always found to be free of any contaminations.

Osteoblast differentiation and viability assay

The osteoblast differentiation assay and the viability assay were performed using C3H10T1/2 cells.^[98] For the screening and IC₅₀ determinations 800 C3H10T1/2 cells per well were seeded in white 384-well plates. After incubation overnight, cells were treated with 1.5 µM purmorphamine and different concentrations of the compounds or DMSO as a control. After 96 h the cell culture medium was aspirated and the commercial luminogenic ALP substrate CDP-Star (Roche, #11685627001) was added. The cells were incubated for one hour at room temperature and in absence of light. Afterwards the luminescence signal was read. To identify and exclude toxic compounds, which would also lead to a reduced luminescent signal, cell viability measurements were conducted in parallel. For this purpose, C3H10T1/2 cells were seeded and treated as described above. The cellular ATP content was determined as a measure of cell viability using the Cell Titer Glo reagent (Promega). Compounds were considered as hit compounds if they caused at least 50% reduction in the luminescent signal in the osteoblast differentiation assay while retaining cell viability $\geq 80\%$ at a concentration of 10 µM. To determine IC₅₀ curves for hit compounds, three-fold dilution curves starting from 10 µM, were used. Calculations of the IC₅₀ values were conducted, using GraphPad Prism 7. (GraphPad Software, USA).

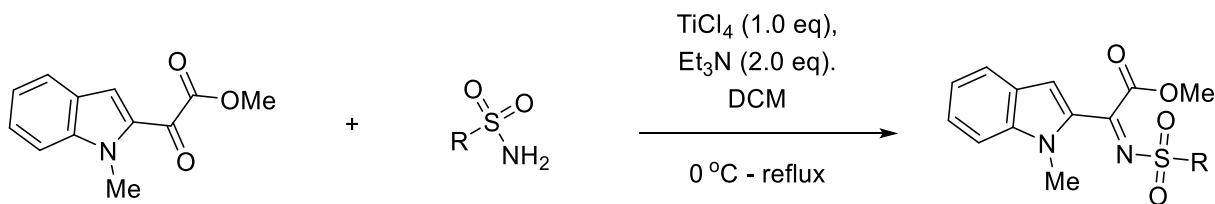
3.6 Chemical Synthesis for Chapter II

3.6.1 General Procedure for the Synthesis of α -Ketoester



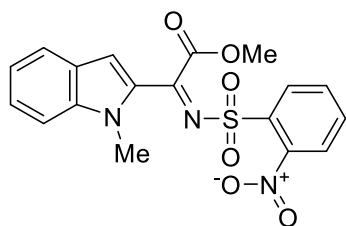
An oven-dried flask, under argon was charged with *N*-methyl indole (1.0 eq.) and THF (0.5M). The solution was then cooled to -78 °C and *n*BuLi (1.2 eq., 1.6 M solution in hexanes) was added dropwise. The reaction mixture was stirred for 10 min at -78°C and then 1 h at RT. The resulting solution was cooled to -78 °C then a solution of dimethyl oxalate (1.3 eq.) dissolved in THF was added. The reaction mixture was stirred for 1 h at -78°C and then for 3 h at room temperature. Then, H₂O was added and the mixture was extracted with Et₂O (5x 25 mL). The combined organic layers were then dried over MgSO₄, filtered and concentrated *in vacuo*. The crude material was purified by silica gel column chromatography (Pent/EtOAc (14:1 to 12:1) to afford a yellow oil. Colourless oil, 27% yield. **¹H-NMR (400 MHz - CDCl₃):** δ 7.72 (dq, *J* = 8.2, 0.9 Hz, 1H), 7.62 (d, *J* = 0.8 Hz, 1H), 7.45 (ddt, *J* = 8.5, 6.7, 0.9 Hz, 1H), 7.39 (dt, *J* = 8.5, 1.0 Hz, 1H), 7.17 (ddt, *J* = 8.6, 7.0, 0.9 Hz, 1H), 4.10 (d, *J* = 0.6 Hz, 3H), 3.99 (d, *J* = 0.7 Hz, 3H); **¹³C-NMR (101 MHz - CDCl₃):** δ 177.38, 163.40, 141.41, 131.14, 127.78, 126.06, 123.87, 121.31, 117.82, 110.45, 52.91, 32.20; **HR-MS:** calc. for [M+H]⁺, C₁₂H₁₂O₃N = 218.08117, found: 218.08081.

3.6.2 General procedure for the Synthesis of Ketimines

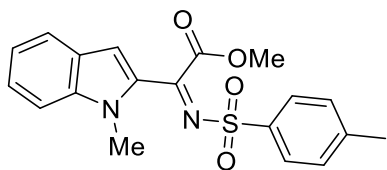


Following a modified procedure by Kwon *et al.*^[151] to a suspension of 1,2-diketone (1.0 eq.) and sulfonamide (1.0 eq.) in DCM was added Et₃N (2.0 eq.). The solution was cooled to 0 °C and TiCl₄ (1.0 eq) was added. The reaction mixture was heated at reflux overnight. Then, the solution was cooled to RT, quenched with H₂O the resulting mixture was filtered through celite and washed with DCM. The filtrate was extracted with DCM (3 x 25mL) and the combined organic extracts were dried over MgSO₄ and concentrated under reduced pressure. The crude material was purified by silica gel column chromatography (Pent/EtOAc (4:1 to 2:1)) to afford the corresponding imino-ester.

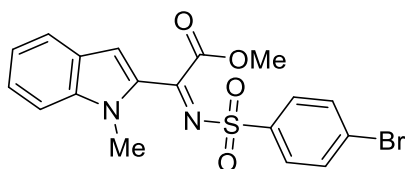
Methyl (Z)-2-(1-methyl-1H-indol-2-yl)-2-(((2-nitrophenyl)sulfonyl)imino)acetate (92)



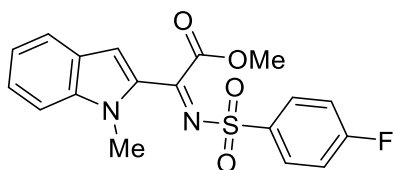
Yellow powder, 53%. **¹H-NMR (500 MHz – CDCl₃):** δ 8.28 – 8.23 (m, 1H), 7.83 – 7.73 (m, 3H), 7.65 (dt, *J* = 8.3, 1.0 Hz, 1H), 7.44 (m, *J* = 8.2, 6.9, 1.1 Hz, 1H), 7.35 (d, *J* = 8.8, 0.9 Hz, 1H), 7.31 (s, *J* = 0.8 Hz, 1H), 7.15 (ddd, *J* = 8.0, 6.9, 0.9 Hz, 1H), 4.09 (s, 3H), 4.05 (s, 3H).; **¹³C-NMR (126 MHz – CDCl₃):** δ 164.16, 160.94, 148.46, 143.30, 134.51, 133.11, 132.44, 130.87, 129.57, 129.06, 126.70, 124.79, 123.68, 121.86, 120.66, 110.83, 54.08, 33.25; **HR-MS:** calc. for [M+H]⁺, C₁₈H₁₆O₆N₃S = 402.07543, found: 402.07529.

Methyl (Z)-2-(1-methyl-1H-indol-2-yl)-2-(tosylimino)acetate (94a)

Dark yellow powder, 64%. **¹H-NMR (500 MHz – CDCl₃):** δ 7.95 – 7.89 (m, 2H), 7.64 (dt, *J* = 8.2, 1.0 Hz, 1H), 7.41 (ddd, *J* = 8.2, 6.8, 1.2 Hz, 1H), 7.38 – 7.30 (m, 3H), 7.19 (d, *J* = 0.9 Hz, 1H), 7.14 (ddd, *J* = 8.0, 6.9, 0.9 Hz, 1H), 4.11 (s, 3H), 3.99 (s, 3H), 2.44 (s, 3H); **¹³C-NMR (126 MHz – CDCl₃):** δ 164.91, 159.49, 144.63, 142.65, 136.61, 129.89 (2C), 128.27, 127.89 (2C), 126.57, 123.41, 121.60, 118.84, 110.60, 53.88, 33.23, 21.83; **HR-MS:** calc. for [M+H]⁺ C₁₉H₁₉O₄N₂S = 371.10600, found: 371.10628.

Methyl (Z)-2-(((4-bromophenyl)sulfonyl)imino)-2-(1-methyl-1H-indol-2-yl)acetate (94b)

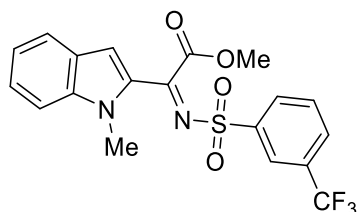
Dark yellow powder, 64%. **¹H-NMR (500 MHz – CDCl₃):** δ 7.93 – 7.87 (m, 2H), 7.70 – 7.67 (m, 2H), 7.66 – 7.63 (m, 1H), 7.44 – 7.40 (m, 1H), 7.33 (dd, *J* = 8.6, 1.0 Hz, 1H), 7.22 (d, *J* = 0.9 Hz, 1H), 7.15 (ddd, *J* = 8.0, 6.9, 0.9 Hz, 1H), 4.11 (s, 3H), 3.98 (s, 3H); **¹³C-NMR (126 MHz – CDCl₃):** δ 164.76, 160.14, 142.94, 138.71, 132.60 (2C), 129.62, 129.37 (2C), 128.85, 128.71, 126.63, 123.56, 121.81, 119.67, 110.70, 54.00, 33.29; **HR-MS:** calc. for [M+H]⁺, C₁₈H₁₆O₄N₂BrS = 435.0008, found: 435.00098 and C₁₈H₁₆O₄N₂⁸¹BrS = 436.99882, found: 436.99895.

Methyl (Z)-2-(((4-fluorophenyl)sulfonyl)imino)-2-(1-methyl-1H-indol-2-yl)acetate (94c)

Green powder, 50% **¹H-NMR (500 MHz – CDCl₃):** δ 8.10 – 8.02 (m, 2H), 7.64 (d, *J* = 8.2 Hz, 1H), 7.42 (ddd, *J* = 8.1, 6.9, 1.1 Hz, 1H), 7.36 – 7.31 (dd, 1H), 7.24 – 7.18 (m, 3H), 7.14 (ddd, *J* = 7.9, 6.9, 0.8 Hz, 1H), 4.11 (s, 3H), 3.99 (s, 3H); **¹³C-NMR (126 MHz – CDCl₃):** δ 166.67, 164.66, 159.79, 142.72, 135.56, 130.57 (d, *J* = 9.6 Hz, 2C), 129.49, 128.46, 126.47, 123.38, 121.63,

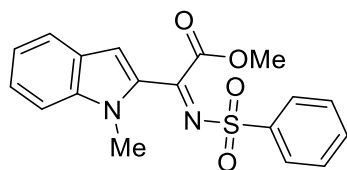
119.31, 116.46 (d, $J = 22.7$ Hz, 2C), 110.54, 53.85, 33.13; ^{19}F NMR (470 MHz, CDCl_3) δ -103.74; **HR-MS**: calc. for $[\text{M}+\text{H}]^+$, $\text{C}_{18}\text{H}_{16}\text{O}_4\text{N}_2\text{FS} = 375.08093$, found: 375.08132.

Methyl (Z)-2-(1-methyl-1H-indol-2-yl)-2-(((3-trifluoromethyl)phenyl)sulfonyl)imino)acetate (94d)



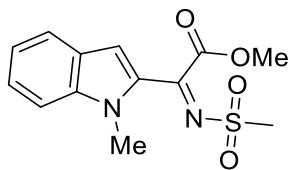
Dark yellow powder, 30%. ^1H -NMR (500 MHz – CDCl_3): δ 8.34 – 8.31 (m, 1H), 8.24 (dtt, $J = 7.5, 1.4, 0.7$ Hz, 1H), 7.91 – 7.86 (m, 1H), 7.71 (dtt, $J = 8.0, 7.1, 0.8$ Hz, 1H), 7.65 (dq, $J = 8.2, 1.2$ Hz, 1H), 7.47 – 7.41 (m, 1H), 7.34 (dq, $J = 8.6, 0.9$ Hz, 1H), 7.26 (d, $J = 1.0$ Hz, 1H), 7.15 (ddd, $J = 8.1, 6.9, 1.0$ Hz, 1H), 4.12 (d, $J = 1.4$ Hz, 3H), 4.00 (d, $J = 1.4$ Hz, 3H); ^{13}C -NMR (151 MHz – CDCl_3): δ 163.35, 159.45, 141.94, 139.83, 130.90, 130.67, 129.85, 128.97, 128.89, 128.40, 127.75, 123.81, 125.47, 122.45, 120.70, 118.96, 109.54, 52.87, 32.11; ^{19}F NMR (565 MHz, CDCl_3) δ -62.83.; **HR-MS**: calc. for $[\text{M}+\text{H}]^+$, $\text{C}_{19}\text{H}_{16}\text{O}_4\text{N}_2\text{F}_3\text{S} = 425.07774$, found: 425.07785.

Methyl (Z)-2-(1-methyl-1H-indol-2-yl)-2-((phenylsulfonyl)imino)acetate (94e)



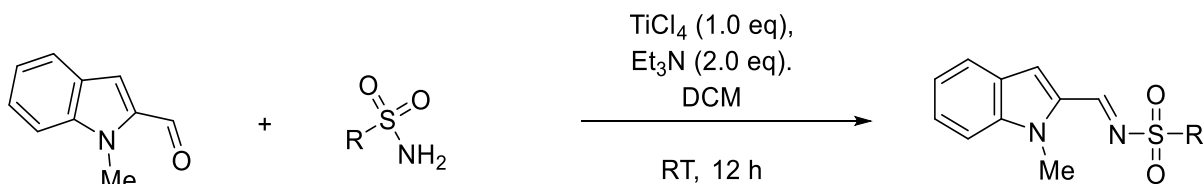
Dark yellow powder, 60%. ^1H -NMR (500 MHz – CDCl_3): δ 8.08 – 8.02 (m, 2H), 7.62 (tt, $J = 7.2, 1.2$ Hz, 2H), 7.58 – 7.52 (m, 2H), 7.42 – 7.36 (m, 1H), 7.31 (dt, $J = 8.6, 0.9$ Hz, 1H), 7.20 (d, $J = 0.9$ Hz, 1H), 7.13 (ddd, $J = 7.9, 6.8, 0.9$ Hz, 1H), 4.11 (d, $J = 0.8$ Hz, 3H), 3.97 (s, 3H); ^{13}C -NMR (126 MHz – CDCl_3): δ 165.02, 160.03, 142.95, 139.81, 133.80, 129.46 (2C), 128.62, 128.01 (2C), 127.92, 126.78, 123.66, 121.86, 119.34, 110.78, 54.10, 33.44; **HR-MS**: calc. for $[\text{M}+\text{H}]^+$, $\text{C}_{18}\text{H}_{17}\text{O}_4\text{N}_2\text{S} = 357.09035$, found: 357.09088.

Methyl (Z)-2-(1-methyl-1H-indol-2-yl)-2-((methylsulfonyl)imino)acetate (94f)



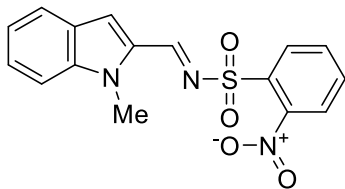
Dark yellow powder, 29%. **¹H-NMR (500 MHz – CDCl₃):** δ 7.67 (dt, *J* = 8.2, 1.0 Hz, 1H), 7.46 (ddd, *J* = 8.6, 6.8, 1.2 Hz, 1H), 7.39 (dq, *J* = 8.5, 0.9 Hz, 1H), 7.25 (d, *J* = 0.9 Hz, 1H), 7.17 (ddd, *J* = 7.9, 6.8, 1.0 Hz, 1H), 4.12 (s, 3H), 4.04 (s, 3H), 3.21 (s, 3H); **¹³C-NMR (126 MHz – CDCl₃):** δ 164.45, 161.42, 143.04, 129.64, 128.77, 126.79, 123.75, 121.95, 119.76, 110.89, 54.11, 42.10, 33.51; **HR-MS:** calc. for [M+H]⁺, C₁₃H₁₅O₄N₂S = 295.07470, found: 295.07461.

3.6.3 General Procedure for the Synthesis of Aldimines

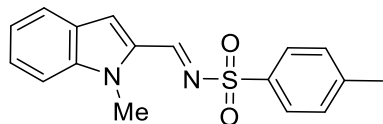


Following a modified procedure by Kwon *et al.*^[151], to a suspension of *N*-methyl indole-2-carboxaldehyde (1.0 eq), sulfonamide (1.0 eq.), and triethylamine (2.0 eq) in DCM at 0 °C was added TiCl₄ (1.0 eq). After 12 h at RT, the mixture was filtered through a pad of Celite and washed with DCM. The filtrate was concentrated under reduced pressure. The crude material was purified by silica gel column chromatography (Pent/EtOAc (6:1 to 4:1)) to afford the corresponding imine.

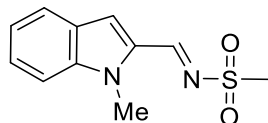
(E)-N-((1-methyl-1H-indol-2-yl)methylene)-2-nitrobenzenesulfonamide (94g)



Yellow powder, 51%. **¹H-NMR (500 MHz – CDCl₃):** δ 9.01 (s, 1H), 8.40 – 8.34 (m, 1H), 7.82 – 7.74 (m, 3H), 7.72 (dt, *J* = 8.2, 1.0 Hz, 1H), 7.49 – 7.42 (m, 2H), 7.38 (dd, *J* = 8.6, 1.0 Hz, 1H), 7.18 (ddd, *J* = 8.0, 6.8, 0.9 Hz, 1H), 4.10 (s, 3H); **¹³C-NMR (126 MHz – CDCl₃):** δ 163.00, 148.52, 143.01, 134.42, 132.61, 132.57, 131.66, 131.44, 128.51, 127.05, 124.79, 123.63, 121.94, 121.58, 110.70, 32.47; **HR-MS:** calc. for [M+H]⁺, C₁₆H₁₄O₄N₃S = 344.06995, found: 344.07004.

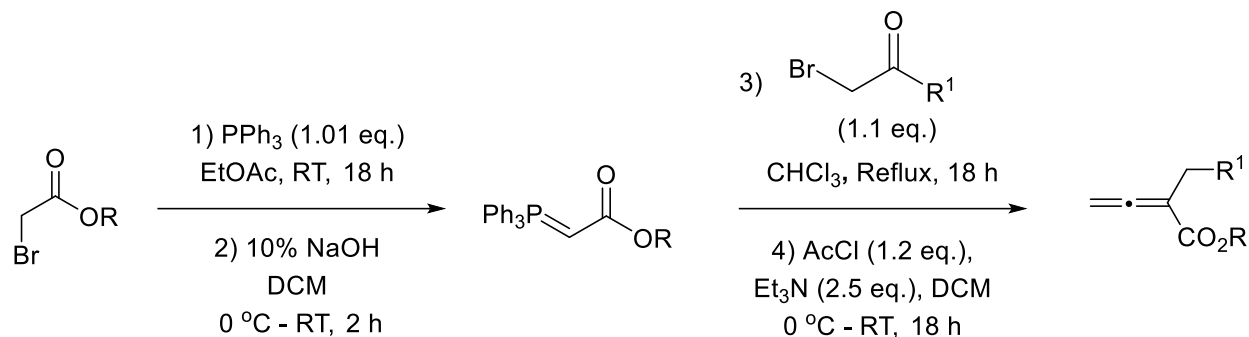
(E)-4-methyl-N-((1-methyl-1H-indol-2-yl)methylene)benzenesulfonamide (94h)

Dark yellow powder, 36%. **¹H-NMR (500 MHz – CDCl₃):** δ 8.99 (s, 1H), 7.91 – 7.86 (m, 2H), 7.69 (dt, *J* = 8.2, 1.0 Hz, 1H), 7.42 (ddd, *J* = 8.1, 6.8, 1.2 Hz, 1H), 7.37 – 7.33 (m, 3H), 7.30 (d, *J* = 0.9 Hz, 1H), 7.16 (ddd, *J* = 8.1, 6.8, 1.0 Hz, 1H), 4.08 (s, 3H), 2.44 (s, 3H); **¹³C-NMR (126 MHz – CDCl₃):** δ 160.29, 144.40, 142.46, 136.06, 131.69, 129.92 (2C), 127.89 (2C), 127.83, 126.92, 123.30, 121.34, 120.37, 110.55, 32.51, 21.80; **HR-MS:** calc. for [M+H]⁺, C₁₇H₁₇O₂N₂S = 313.10053, found: 313.10057.

(E)-N-((1-methyl-1H-indol-2-yl)methylene)methanesulfonamide (94i)

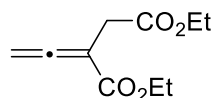
Dark yellow powder, 10%. **¹H-NMR (500 MHz – CDCl₃):** δ 8.98 (s, 1H), 7.72 (dt, *J* = 8.1 Hz, 1H), 7.45 (dd, *J* = 6.7, 1.2 Hz, 1H), 7.41 (dq, *J* = 8.6, 1.0 Hz, 1H), 7.34 (d, *J* = 1.0 Hz, 1H), 7.19 (ddd, *J* = 8.0, 6.8, 1.1 Hz, 1H), 4.15 (s, 4H), 3.14 (s, 3H).; **¹³C-NMR (126 MHz – CDCl₃):** δ 161.43, 142.45, 131.25, 127.92, 126.80, 123.31, 121.34, 120.64, 110.50, 40.68, 32.39; **HR-MS:** calc. for [M+H]⁺, C₁₁H₁₃O₂N₂S = 237.06922, found: 237.06888.

3.6.4 General Procedure for the Synthesis of Allenates

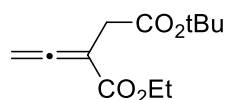


Following a modified procedure by Kwon *et al.*^[151], to a stirred solution of triphenylphosphine (1.01 eq.) in EtOAc at RT, was added the corresponding bromoacetate (1.0 eq), slowly. After stirring overnight, the resulting precipitate was collected by vacuum filtration, washed with EtOAc and dried on the vacuum to provide the phosphonium salt as a white solid. The crude material was dissolved in DCM and sodium hydroxide in water (10% solution) was added at $0\text{ }^\circ\text{C}$. After stirring for 2 h at room temperature the layers were allowed to separate and the aqueous phase was extracted with DCM (x3). The combined organic layers were dried over MgSO_4 and concentrated *in vacuo* to give the phosphorane as an off-white solid. To a solution of crude phosphorane (1.0 eq.) in CHCl_3 was added the corresponding bromoacetate (1.1 eq). After 18 h of reflux, the solvent was removed under reduced pressure. The crude product (1.0 eq) was dissolved in DCM and treated with Et_3N (2.5 eq). After stirring for 30 mins, the reaction was cooled $0\text{ }^\circ\text{C}$ and acetyl chloride (1.2 eq.) was added dropwise. The reaction mixture was allowed to warm to RT and stirred overnight.

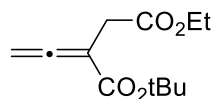
The solution was the concentrated to approximately 20% volume, and diluted with pentane. The triphenylphosphine oxide was removed by vacuum filtration, the filter cake was washed with 20% EtOAc/pentane. The filtrate was concentrated *in vacuo* and the resulting crude material was purified by silica gel column chromatography (Pent/EtOAc (20:1 to 15:1)) to afford the allenate as an oil.

diethyl 2-vinylidenesuccinate (86)

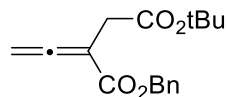
Yellow oil, 61%. **¹H-NMR (400 MHz – CDCl₃):** δ 5.16 (q, *J* = 2.1 Hz, 2H), 4.20 – 4.06 (m, 4H), 3.20 (q, *J* = 2.2 Hz, 2H), 1.21 (qd, *J* = 7.1, 2.1 Hz, 6H).; **¹³C-NMR (126 MHz – CDCl₃):** δ 214.45, 170.37, 166.20, 94.58, 79.39, 61.23, 60.84, 34.72, 14.09, 14.08; **HR-MS:** calc. for [M+H]⁺, C₁₀H₁₅O₄ [M+H]⁺ 199.0970, found: 199.0967.

4-(tert-butyl) 1-ethyl 2-vinylidenesuccinate (95a)

Yellow oil, 34%. **¹H-NMR (500 MHz – CDCl₃):** δ 5.20 (t, *J* = 2.2 Hz, 2H), 4.21 (q, *J* = 7.1 Hz, 2H), 3.17 (t, *J* = 2.2 Hz, 2H), 1.45 (s, 9H), 1.28 (t, *J* = 7.1 Hz, 3H); **¹³C-NMR (126 MHz – CDCl₃):** δ 214.81, 170.06, 166.75, 95.36, 81.45, 79.68, 61.64, 36.23, 28.37 (3C, tBu), 14.56; **HR-MS:** calc. for [M+H]⁺, C₁₂H₁₉O₄ = 227.1277, found: 227.12785.

1-(tert-butyl) 4-ethyl 2-vinylidenesuccinate (95b)

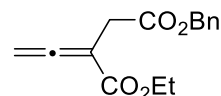
Colourless oil, 25%. **¹H-NMR (500 MHz – CDCl₃):** δ 5.16 (t, *J* = 2.2 Hz, 2H), 4.16 (q, *J* = 7.1 Hz, 2H), 3.21 (t, *J* = 2.2 Hz, 2H), 1.46 (s, 9H), 1.26 (t, *J* = 7.1 Hz, 3H); **¹³C-NMR (126 MHz – CDCl₃):** δ 214.44, 170.79, 165.53, 96.11, 81.56, 79.24, 61.03, 35.13, 28.12 (3C, tBu), 14.34; **HR-MS:** calc. for [M+H]⁺, C₁₂ H₁₉O₄ = 227.12779, found: 227.12791.

1-benzyl 4-(tert-butyl) 2-vinylidenesuccinate (95c)

Colourless oil, 37%. **¹H-NMR (500 MHz – CDCl₃):** δ 7.38 – 7.27 (m, 5H), 5.23 (t, *J* = 2.2 Hz, 2H), 5.20 (s, 2H), 3.20 (t, *J* = 2.2 Hz, 2H), 1.42 (s, 9H); **¹³C-NMR (126 MHz – CDCl₃):** δ 214.91,

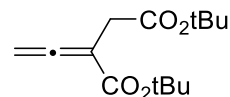
169.77, 166.42, 136.08, 128.61 (2C), 128.22, 128.03 (2C), 95.01, 81.33, 79.70, 66.93, 36.00, 28.14 (3C); **HR-MS**: calc. for $[M+H]^+$, $C_{17}H_{21}O_4 = 289.14344$, found: 289.14363.

4-benzyl 1-ethyl 2-vinylidenesuccinate (95e)



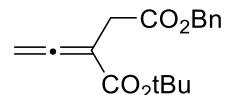
Yellow oil, 20%. **1H -NMR (500 MHz – $CDCl_3$)**: δ 7.39 – 7.26 (m, 5H), 5.21 (t, $J = 2.2$ Hz, 2H), 5.15 (s, 2H), 4.19 (q, $J = 7.2$ Hz, 2H), 3.33 (t, $J = 2.2$ Hz, 2H), 1.25 (t, $J = 7.1$ Hz, 3H); **^{13}C -NMR (126 MHz – $CDCl_3$)**: δ 214.67, 170.51, 166.42, 135.87, 128.67 (2C), 128.62, 128.40 (2C), 94.66, 79.81, 66.89, 61.57, 34.94, 14.31; **HR-MS**: calc. for $[M+H]^+$, $C_{15}H_{17}O_4 = 261.11214$, found: 261.11229.

Di-tert-butyl 2-vinylidenesuccinate (95f)

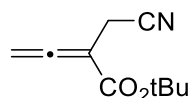


Orange oil, 30%. **1H -NMR (500 MHz – $CDCl_3$)**: δ 5.15 (t, $J = 2.3$ Hz, 2H), 3.12 (t, $J = 2.3$ Hz, 2H), 1.47 (s, 9H), 1.45 (s, 9H); **^{13}C -NMR (126 MHz – $CDCl_3$)**: δ 214.43, 169.96, 165.62, 96.51, 81.38, 81.07, 79.05, 36.20, 28.18 (3C, tBu), 28.14 (3C, tBu); **HR-MS**: calc. for $[M+H]^+$, $C_{14}H_{23}O_4 = 255.15909$, found: 255.15921.

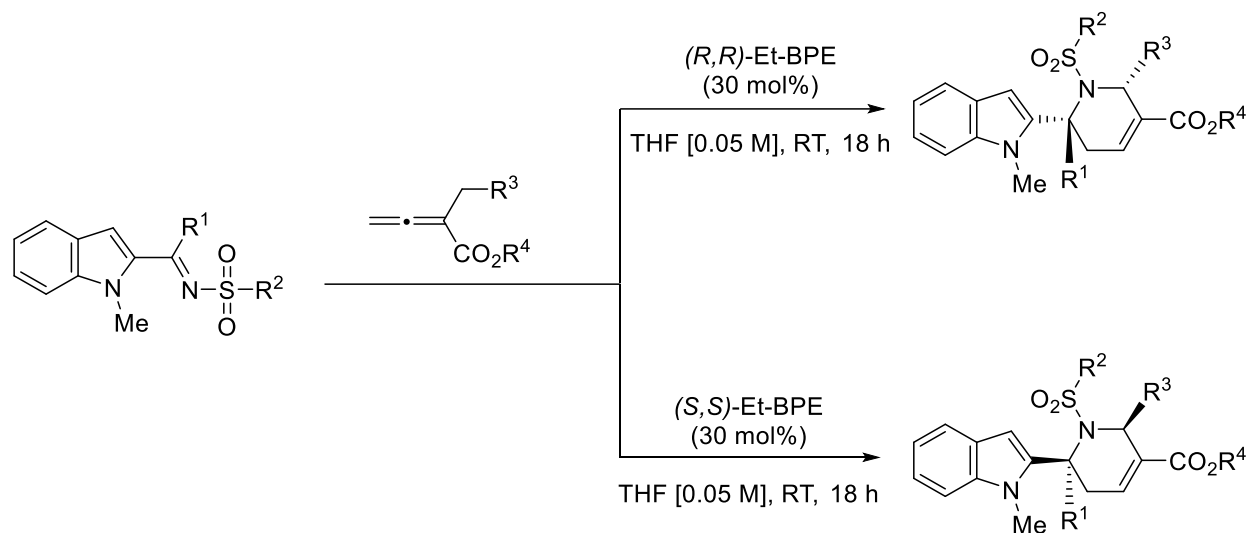
4-benzyl 1-(tert-butyl) 2-vinylidenesuccinate (95g)



Colourless oil, 37%. **1H -NMR (500 MHz – $CDCl_3$)**: δ 7.39 – 7.29 (m, 5H), 5.16 – 5.14 (m, 4H, overlapped triplet and singlet), 3.28 (t, $J = 2.2$ Hz, 2H), 1.44 (s, 9H); **^{13}C -NMR (126 MHz – $CDCl_3$)**: δ 214.48, 170.65, 165.47, 135.91, 128.66 (2C), 128.43 (2C), 128.37, 95.96, 81.62, 79.36, 66.82, 35.10, 28.10 (3C, tBu); **HR-MS**: calc. for $[M+H]^+$, $C_{17}H_{21}O_4 = 289.14344$, found: 289.14364.

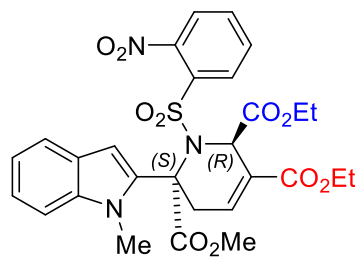
tert-butyl 2-(cyanomethyl)buta-2,3-dienoate (95h)

Orange oil, 15%. **¹H-NMR (500 MHz – CDCl₃):** δ 5.37 (t, *J* = 3.1 Hz, 2H), 3.29 (t, *J* = 3.1 Hz, 2H), 1.48 (s, 9H); **¹³C-NMR (126 MHz – CDCl₃):** δ 213.01, 163.95, 116.82, 93.73, 82.55, 82.01, 27.98 (3C, tBu), 18.25; **HR-MS:** calc. for [M+H]⁺, C₁₀H₁₄O₂N = 180.10191, found: 180.10183.

3.6.5. General Procedure for the Synthesis of Apoxidoles Pseudo-NPs

To a stirred solution of imino-ester (1.0 eq.) and allenoate (1.2 eq.) in THF [0.05M] was added the relevant chiral phosphine catalyst, Et-BPE (30 mol%). After 12 h, the reaction mixture was concentrated and purified by silica gel column chromatography (Pent/EtOAc) to afford the Apoxidole product.

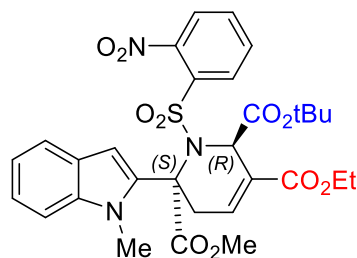
2,3-diethyl 6-methyl (2R,6S)-6-(1-methyl-1H-indol-2-yl)-1-((2-nitrophenyl)sulfonyl)-1,2,5,6-tetrahydropyridine-2,3,6-tricarboxylate (93)



(R,S)-93

White solid, 71% yield. Pent/EtOAc (7:1 to 4:1) $^1\text{H-NMR}$ (600 MHz - CDCl_3): δ 8.88 (bs, 1H), 7.79 (t, $J = 7.6$ Hz, 1H), 7.73 (td, $J = 7.8, 1.2$ Hz, 1H), 7.66 (dd, $J = 7.9, 1.2$ Hz, 1H), 7.52 (d, $J = 7.9$ Hz, 1H), 7.31 (t, $J = 4.0$ Hz, 1H), 7.25 – 7.16 (m, 2H), 7.09 – 7.04 (m, 1H), 6.48 (s, 1H), 6.04 (s, 1H), 4.24 – 4.13 (m, 2H), 3.62 (s, 3H), 3.60 - 3.51 (m, 4H), 3.39 (bs, 1H), 2.43 (bs, 2H), 1.26 (t, $J = 1.1$ Hz, 3H), 0.55 – 0.45 (m, 3H); $^{13}\text{C-NMR}$ (151 MHz - CDCl_3): δ 168.62, 167.85, 164.47, 148.10, 139.49, 136.95, 135.74, 133.62, 133.49, 131.61, 131.57, 130.68, 130.21, 126.14, 123.70, 123.59, 121.32, 121.01, 120.39, 109.78, 107.70, 61.98, 61.31, 57.57, 53.79, 34.29, 32.87, 13.20.; **HR-MS**: calc. for $[\text{M}+\text{H}]^+$ $\text{C}_{28}\text{H}_{29}\text{O}_{10}\text{N}_3\text{S} = 600.1574$, found: 600.1646. $[\alpha]_{\text{D}}^{\text{RT}} = +59.0^\circ$ (CH_2Cl_2 , $c = 1.00$); HPLC conditions: CHIRAPAK IC column, DCM:EtOH (100:2)/*iso*-hexane = 40/60, flow rate = 0.5 mL min^{-1} , minor enantiomer: $t_{\text{R}} = 15.85$ min; major enantiomer: $t_{\text{R}} = 24.42$ min, 88% *ee*.

2-(tert-butyl) 3-ethyl 6-methyl (2R,6S)-6-(1-methyl-1H-indol-2-yl)-1-((2-nitrophenyl)sulfonyl)-1,2,5,6-tetrahydropyridine-2,3,6-tricarboxylate (96a)

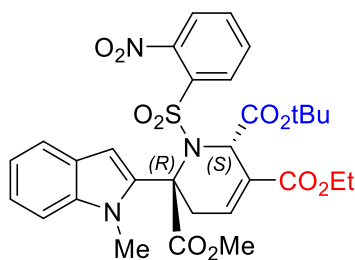


(R,S)-96a

Off-white solid, 85% yield. Pent/EtOAc (5:1 to 4:1) $^1\text{H-NMR}$ (500 MHz - CDCl_3): δ 8.88 (bs, 1H), 7.79 (t, $J = 7.8$ Hz, 1H), 7.71 (td, $J = 7.6, 1.3$ Hz, 1H), 7.64 (dd, $J = 7.9, 1.4$ Hz, 1H), 7.53 (dt, $J = 7.9, 1.0$ Hz, 1H), 7.24 – 7.15 (m, 3H), 7.09 – 7.04 (m, 1H), 6.50 (s, 1H), 6.05 (q, 1H), 4.32

– 4.22 (m, 1H), 4.21 – 4.11 (m, 1H), 3.59 (d, $J = 5.5$ Hz, 6H), 3.56 – 3.44 (m, 2H), 1.33 (t, $J = 7.2$ Hz, 3H), 0.72 (bs, 9H).; $^{13}\text{C-NMR}$ (126 MHz - CDCl_3): δ 168.58, 166.83, 164.78, 147.83, 139.62, 135.79, 135.27, 133.11, 131.44, 130.10, 126.06, 123.30, 123.25, 120.96, 120.12, 110.12, 107.15, 107.13, 83.02, 66.34, 61.13, 58.04, 53.52, 34.04, 32.86, 27.04 (3C, tBu), 23.84, 14.29; **HR-MS**: calc. for $[\text{M}+\text{H}]^+$ $\text{C}_{30}\text{H}_{34}\text{O}_{10}\text{N}_3\text{S} = 628.1959$, found: 628.1957. $[\alpha]_{\text{D}}^{\text{RT}} = +87.0^\circ$ (CH_2Cl_2 , $c = 1.00$); HPLC conditions: CHIRAPAK IC column, DCM:EtOH (100:2)/*iso*-hexane = 40/60, flow rate = 0.5 mL min^{-1} , minor enantiomer: $t_{\text{R}} = 24.24 \text{ min}$; major enantiomer: $t_{\text{R}} = 14.99 \text{ min}$, 78% *ee*.

2-(tert-butyl) 3-ethyl 6-methyl (2S,6R)-6-(1-methyl-1H-indol-2-yl)-1-((2-nitrophenyl)sulfonyl)-1,2,5,6-tetrahydropyridine-2,3,6-tricarboxylate (96a)

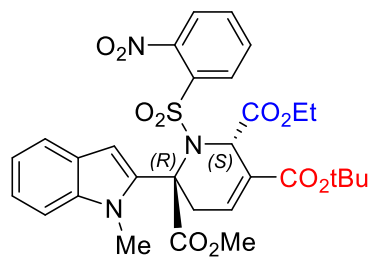


(S,R)-96a

Off-white solid, 67% yield. Pent/EtOAc (6:1 to 4:1). **HR-MS**: calc. for $[\text{M}+\text{H}]^+$ $\text{C}_{30}\text{H}_{34}\text{O}_{10}\text{N}_3\text{S} = 628.1959$, found: 628.1957. $[\alpha]_{\text{D}}^{\text{RT}} = -97.0^\circ$ (CH_2Cl_2 , $c = 1.00$); HPLC conditions: CHIRAPAK IC column, DCM:EtOH (100:2)/ *iso*-hexane = 40/60, flow rate = 0.5 mL min^{-1} , minor enantiomer: $t_{\text{R}} = 13.90 \text{ min}$; major enantiomer: $t_{\text{R}} = 22.14 \text{ min}$, 76% *ee*.

Single enantiomer purified using CHIRAPAK IC column, DCM:EtOH (100:2)/*iso*-hexane = 30/70, flow rate = 3 mL min^{-1} . White foam, 47%.

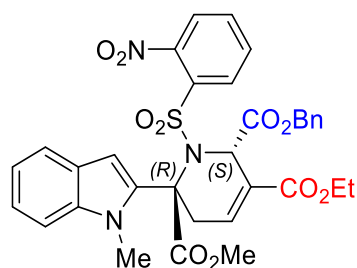
3-(tert-butyl) 2-ethyl 6-methyl (2S,6R)-6-(1-methyl-1H-indol-2-yl)-1-((2-nitrophenyl)sulfonyl)-1,2,5,6-tetrahydropyridine-2,3,6-tricarboxylate (96b)



(S,R)-96b

Off-white foam, 68% yield. Pent/EtOAc (5:1 to 4:1) ¹H-NMR (500 MHz - CDCl₃): δ 8.89 (bs, 1H), 7.79 (t, 1H), 7.72 (td, *J* = 7.7, 1.4 Hz, 1H), 7.65 (dd, *J* = 7.9, 1.4 Hz, 1H), 7.54 (dt, *J* = 7.9, 1.0 Hz, 1H), 7.25 – 7.15 (m, 3H), 7.07 (ddd, *J* = 8.0, 6.7, 1.2 Hz, 1H), 6.48 (s, 1H), 5.99 (q, *J* = 1.3 Hz, 1H), 3.62 (s, 3H), 3.59 – 3.51 (m, 5H), 3.39 (s, 1H), 2.52 (bs, 1H), 1.45 (s, 9H), 0.48 (bs, 3H).; ¹³C-NMR (126 MHz - CDCl₃): δ 168.54, 167.96, 163.25, 147.90, 139.28, 135.78, 135.47, 133.28, 131.42, 130.65, 130.09, 128.85, 125.97, 123.45, 123.35, 121.14, 120.15, 109.56, 107.43, 81.53, 66.08, 61.89, 57.43, 53.56, 34.05, 32.70, 28.01 (3C, tBu), 12.94; **HR-MS**: calc. for [M+H]⁺, C₃₀H₃₄O₁₀N₃S = 628.19594, found: 628.19574. [α]_D^{RT} = + 92.0° (CH₂Cl₂, c = 1.00); HPLC conditions: CHIRAPAK IC column, DCM:EtOH (100:2)/*iso*-hexane = 30/70, flow rate = 0.5 mL min⁻¹, minor enantiomer: t_R = 21.52 min; major enantiomer: t_R = 34.92 min, 86% *ee*.

2-benzyl 3-ethyl 6-methyl (2S,6R)-6-(1-methyl-1H-indol-2-yl)-1-((2-nitrophenyl)sulfonyl)-1,2,5,6-tetrahydropyridine-2,3,6-tricarboxylate (96c)

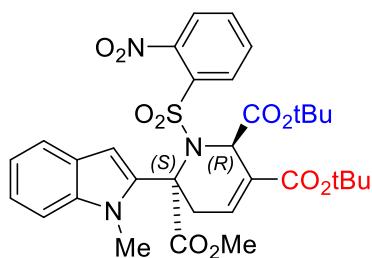


(S,R)-96c

Brown solid, 53 % yield. Pent/EtOAc (6:1 to 4:1) ¹H-NMR (500 MHz - CDCl₃): δ 8.86 (s, 1H), 7.78 – 7.71 (m, 2H), 7.66 (dd, 1H), 7.47 (d, 1H), 7.30 – 7.26 (m, 1H), 7.25 – 7.17 (m, 5H), 7.06 (ddd, *J* = 7.9, 5.0, 3.0 Hz, 1H), 6.78 (d, *J* = 6.8 Hz, 2H), 6.51 (s, 1H), 6.11 (q, *J* = 1.3 Hz, 1H), 4.47 (d, *J* = 12.1 Hz, 1H), 4.05 – 3.94 (m, 1H), 3.92 – 3.81 (m, 1H), 3.63 (s, 3H), 3.59 – 3.56 (m, 5H),

3.08 (s, 1H), 1.04 (t, $J = 7.1$ Hz, 3H); $^{13}\text{C-NMR}$ (126 MHz - CDCl_3): δ 168.41, 167.28, 164.12, 147.87, 139.34, 136.58, 135.55, 134.37, 133.31, 131.46, 130.46, 129.95, 128.21, 128.19 (2C), 128.08 (2C), 125.90, 127.17, 123.62, 123.43, 121.33, 120.28, 109.62, 107.62, 67.20, 66.12, 61.10, 57.36, 53.62, 34.03, 32.72, 13.89; **HR-MS**: calc. for $[\text{M}+\text{H}]^+$, $\text{C}_{33}\text{H}_{32}\text{O}_{10}\text{N}_3\text{S} = 662.18029$, found: 662.18000. $[\alpha]_{\text{D}}^{\text{RT}} = + 46.0^\circ$ (CH_2Cl_2 , $c = 1.00$); HPLC conditions: CHIRAPAK IC column, DCM:EtOH (100:2)/*iso*-hexane = 40/60, flow rate = 0.5 mL min^{-1} , minor enantiomer: $t_{\text{R}} = 17.28$ min; major enantiomer: $t_{\text{R}} = 25.65$ min, 76% *ee*.

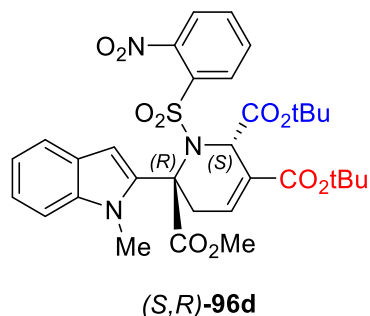
2,3-di-tert-butyl 6-methyl (2R,6S)-6-(1-methyl-1H-indol-2-yl)-1-((2-nitrophenyl)sulfonyl)-1,2,5,6-tetrahydropyridine-2,3,6-tricarboxylate (96d)



(*R,S*)-**96d**

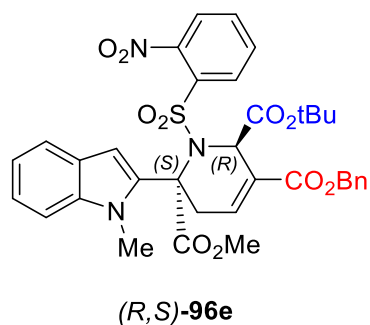
Off-white solid, 62% yield. Pent/EtOAc (5:1 to 4:1) $^1\text{H-NMR}$ (500 MHz - CDCl_3): δ 8.80 (bs, 1H), 7.79 – 7.72 (m, 1H), 7.69 (td, $J = 7.7, 1.4$ Hz, 1H), 7.62 (dd, $J = 7.9, 1.4$ Hz, 1H), 7.54 (dd, $J = 7.9, 1.0$ Hz, 1H), 7.23 – 7.16 (m, 2H), 7.12 (t, 1H), 7.08 (ddd, $J = 7.9, 5.3, 2.7$ Hz, 1H), 6.49 (s, 1H), 6.01 (d, $J = 1.4$ Hz, 1H), 3.60 (d, $J = 10.8$ Hz, 3H), 3.57 (s, 3H), 3.52 (d, $J = 5.0$ Hz, 1H), 3.45 (d, $J = 19.8$ Hz, 1H), 1.52 (s, 9H), 0.79 (bs, 9H); $^{13}\text{C-NMR}$ (126 MHz - CDCl_3): δ 169.20, 167.66, 164.04, 148.20, 140.00, 136.14, 135.25, 133.40, 131.76, 131.44, 130.62, 126.46, 123.61, 123.56, 121.31, 120.45, 110.50, 107.43, 83.28, 81.82, 66.57, 58.47, 53.82, 34.97, 33.22, 28.56 (3C, tBu), 27.51 (3C, tBu), 14.54; **HR-MS**: calc. for $[\text{M}+\text{H}]^+$, $\text{C}_{32}\text{H}_{38}\text{O}_{10}\text{N}_3\text{S} = 656.22724$, found: 656.22702. $[\alpha]_{\text{D}}^{\text{RT}} = - 88.0^\circ$ (CH_2Cl_2 , $c = 1.00$); HPLC conditions: CHIRAPAK IC column, DCM:EtOH (100:2)/*iso*-hexane = 40/60, flow rate = 0.5 mL min^{-1} , minor enantiomer: $t_{\text{R}} = 13.79$ min; major enantiomer: $t_{\text{R}} = 9.31$ min, 86% *ee*.

2,3-di-tert-butyl 6-methyl (2S,6R)-6-(1-methyl-1H-indol-2-yl)-1-((2-nitrophenyl)sulfonyl)-1,2,5,6-tetrahydropyridine-2,3,6-tricarboxylate (96d)



Off-white solid, 71% yield. Pent/EtOAc (5:1 to 4:1). **HR-MS:** calc. for $[M+H]^+$, $C_{32}H_{38}O_{10}N_3S = 656.22724$, found: 656.22706. $[\alpha]_D^{RT} = + 83.0^\circ$ (CH_2Cl_2 , $c = 1.00$); HPLC conditions: CHIRAPAK IC column, DCM:EtOH (100:2)/ *iso*-hexane = 40/60, flow rate = 0.5 mL min⁻¹, minor enantiomer: $t_R = 9.39$ min; major enantiomer: $t_R = 13.96$ min, 90% *ee*.

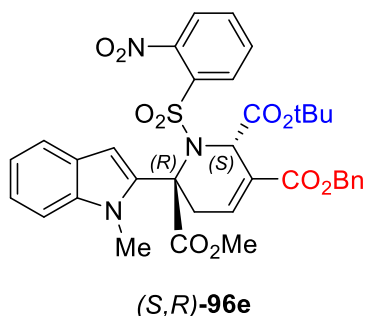
3-benzyl 2-(tert-butyl) 6-methyl (2R,6S)-6-(1-methyl-1H-indol-2-yl)-1-((2-nitrophenyl)sulfonyl)-1,2,5,6-tetrahydropyridine-2,3,6-tricarboxylate (96e)



Brown solid, 56% yield. Pent/EtOAc (6:1 to 4:1) **¹H-NMR (500 MHz - CDCl₃):** δ 8.87 (bs, 1H), 7.79 (t, $J = 7.5$ Hz, 1H), 7.71 (td, $J = 7.7, 1.3$ Hz, 1H), 7.64 (dd, $J = 7.9, 1.4$ Hz, 1H), 7.52 (dd, $J = 7.9, 1.0$ Hz, 1H), 7.42 – 7.30 (m, 5H), 7.25 (d, $J = 3.4$ Hz, 1H), 7.21 – 7.14 (m, 2H), 7.06 (ddd, $J = 7.9, 5.8, 2.0$ Hz, 1H), 6.49 (s, 1H), 6.09 (q, $J = 1.3$ Hz, 1H), 5.20 (dd, 2H), 3.58 (s, 6H), 3.56 – 3.46 (m, 2H), 0.64 (bs, 9H).; **¹³C-NMR (126 MHz - CDCl₃):** 168.55, 166.66, 164.59, 147.82, 139.62, 135.81, 135.48, 133.11, 131.47, 130.66, 130.09, 128.65, 128.59, 128.44, 128.42, 128.24, 126.05, 123.31, 123.26, 120.96, 120.12, 119.41, 110.12, 107.15, 83.12, 66.86, 66.09, 58.03, 53.53, 34.35, 32.85, 26.93 (3C, tBu), 14.17; **HR-MS:** calc. for $[M+H]^+$, $C_{35}H_{36}O_{10}N_3S = 690.21159$, found: 690.21137. $[\alpha]_D^{RT} = - 30.0^\circ$ (CH_2Cl_2 , $c = 1.00$); HPLC conditions: CHIRAPAK IC column,

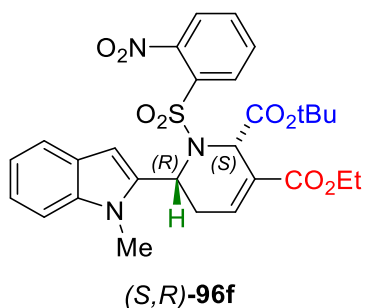
DCM:EtOH (100:2)/*iso*-hexane = 40/60, flow rate = 0.5 mL min⁻¹, minor enantiomer: t_R = 20.36 min; major enantiomer: t_R = 17.05 min, 84% *ee*.

3-benzyl 2-(tert-butyl) 6-methyl (2S,6R)-6-(1-methyl-1H-indol-2-yl)-1-((2-nitrophenyl)sulfonyl)-1,2,5,6-tetrahydropyridine-2,3,6-tricarboxylate (96e)



Brown solid, 70% yield. Pent/EtOAc (6:1 to 4:1). **HR-MS**: calc. for [M+H]⁺, C₃₅H₃₆O₁₀N₃S = 690.21159, found: 690.21131. $[\alpha]_D^{RT} = +36.0^\circ$ (CH₂Cl₂, c = 1.00); HPLC conditions: CHIRAPAK IC column, DCM:EtOH (100:2)/*iso*-hexane = 40/60, flow rate = 0.5 mL min⁻¹, minor enantiomer: t_R = 17.67 min; major enantiomer: t_R = 21.08 min, 82% *ee*.

2-(tert-butyl) 3-ethyl (2S,6R)-6-(1-methyl-1H-indol-2-yl)-1-((2-nitrophenyl)sulfonyl)-1,2,5,6-tetrahydropyridine-2,3-dicarboxylate (96f)

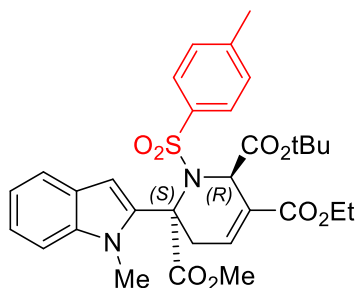


Off-white foam, 42% yield. Pent/DCM (1:5) **¹H-NMR (500 MHz - CDCl₃)**: δ 7.99 (dd, J = 8.0, 1.4 Hz, 1H), 7.73 (td, J = 7.8, 1.4 Hz, 1H), 7.66 (td, J = 7.7, 1.3 Hz, 1H), 7.56 (dd, J = 7.9, 1.3 Hz, 1H), 7.45 (dt, J = 7.8, 1.0 Hz, 1H), 7.29 (dd, J = 8.4, 0.9 Hz, 1H), 7.17 (ddd, J = 8.3, 7.0, 1.1 Hz, 1H), 7.01 (ddd, J = 7.9, 7.0, 1.0 Hz, 1H), 6.97 – 6.93 (m, 1H), 6.33 (d, J = 0.9 Hz, 1H), 5.65 (d, J = 7.2 Hz, 1H), 5.59 (dd, J = 2.4, 1.3 Hz, 1H), 4.32 – 4.16 (m, 2H), 3.87 (s, 3H), 2.84 (dd, J = 20.0, 5.4 Hz, 1H), 2.70 – 2.60 (m, 1H), 1.33 (t, J = 7.1 Hz, 3H), 0.77 (s, 9H); **¹³C-NMR (126 MHz - CDCl₃)**: δ 165.53, 165.28, 148.34, 138.09, 134.65, 134.19, 133.88, 132.79, 131.69, 130.47,

127.79, 126.64, 123.83, 122.40, 120.79, 119.51, 109.45, 103.40, 82.74, 61.11, 54.08, 46.77, 30.16, 27.46, 27.14 (3C, tBu), 14.29; **HR-MS**: calc. for $[M+H]^+$, $C_{28}H_{32}O_8N_3S = 570.19046$, found: 570.19016. $[\alpha]_D^{RT} = -82.0^\circ$ (CH_2Cl_2 , $c = 1.00$); HPLC conditions: CHIRAPAK IC column, DCM:EtOH (100:2)/ *iso*-hexane = 40/60, flow rate = 0.5 mL min⁻¹, minor enantiomer: $t_R = 15.19$ min; major enantiomer: $t_R = 17.46$ min, 81% *ee*

Single enantiomer purified using CHIRAPAK IC column, DCM:EtOH (100:3)/*iso*-hexane = 40/60, flow rate = 3 mL min⁻¹. Yellow foam.

2-(tert-butyl) 3-ethyl 6-methyl (2R,6S)-6-(1-methyl-1H-indol-2-yl)-1-tosyl-1,2,5,6-tetrahydropyridine-2,3,6-tricarboxylate (96g)

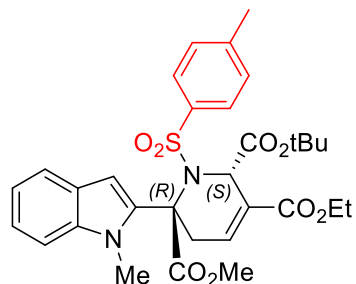


(R,S)-96g

Off-white foam, 91% yield. Pent/EtOAc (6:1 to 4:1) **¹H-NMR (500 MHz - CDCl₃)**: δ 7.88 (bs/d, 2H), 7.52 (dt, $J = 7.8, 1.0$ Hz, 1H), 7.29 (d, $J = 8.2$ Hz, 2H), 7.20 – 7.11 (m, 3H), 7.05 (ddd, $J = 7.9, 6.5, 1.4$ Hz, 1H), 6.46 (s, 1H), 5.92 (s, $J = 1.4$ Hz, 1H), 4.31 – 4.09 (m, 2H), 3.65 (s, 3H), 3.58 (s, 3H), 3.55 – 3.47 (m, 1H), 3.42 (d, $J = 19.9$ Hz, 1H), 2.44 (s, 3H), 1.32 (t, $J = 7.2$ Hz, 3H), 0.79 (bs, 9H); **¹³C-NMR (126 MHz - CDCl₃)**: δ 168.87, 166.74, 164.94, 143.35, 139.47, 138.96, 135.13, 131.66, 129.08 (2C), 128.68, 127.35, 126.17, 122.77, 120.83, 120.53, 119.85, 110.06, 106.16, 82.44, 65.07, 61.02, 58.39, 53.14, 33.88, 33.00, 27.16 (3C, tBu), 21.68, 14.32; **HR-MS**: calc. for $[M+H]^+$, $C_{31}H_{37}O_8N_2S = 597.22651$, found: 597.22631. $[\alpha]_D^{RT} = +88.0^\circ$ (CH_2Cl_2 , $c = 1.00$); HPLC conditions: CHIRAPAK IC column, DCM:MeOH (100:5)/ *iso*-hexane = 20/80, flow rate = 0.5 mL min⁻¹, minor enantiomer: $t_R = 33.58$ min; major enantiomer: $t_R = 27.00$ min, 84% *ee*.

Single enantiomer obtained using CHIRAPAK IC column, DCM:EtOH (100:2)/*iso*-hexane = 30/70, flow rate = 3 mL min⁻¹. White foam, 15%.

2-(tert-butyl) 3-ethyl 6-methyl (2S,6R)-6-(1-methyl-1H-indol-2-yl)-1-tosyl-1,2,5,6-tetrahydropyridine-2,3,6-tricarboxylate (96g)

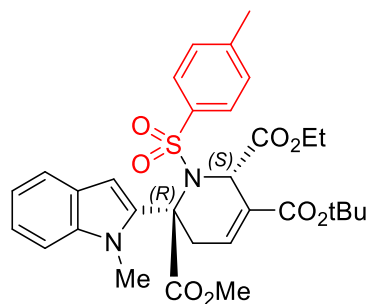


(S,R)-96g

Off-white foam, 93% yield. Pent/EtOAc (6:1 to 4:1). **HR-MS:** calc. for $[M+H]^+$, $C_{31}H_{37}O_8N_2S = 597.22651$, found: 597.22627. $[\alpha]_D^{RT} = -77.0^\circ$ (CH_2Cl_2 , $c = 1.00$); HPLC conditions: CHIRAPAK IC column, DCM:MeOH (100:5)/*iso*-hexane = 20/80, flow rate = 0.5 mL min^{-1} , minor enantiomer: $t_R = 29.64 \text{ min}$; major enantiomer: $t_R = 36.65 \text{ min}$, 84% *ee*.

Single enantiomer purified using CHIRAPAK IC column, DCM:EtOH (100:2)/*iso*-hexane = 30/70, flow rate = 3 mL min^{-1} . White foam, 40%.

3-(tert-butyl) 2-ethyl 6-methyl (2S,6R)-6-(1-methyl-1H-indol-2-yl)-1-tosyl-1,2,5,6-tetrahydropyridine-2,3,6-tricarboxylate (96h)

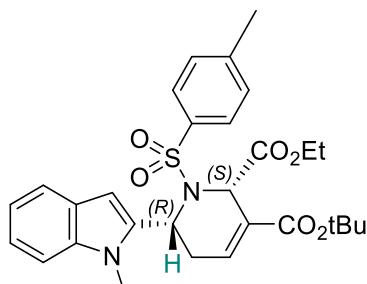


(S,R)-96h

Orange foam, 91% yield. Pent/EtOAc (6:1 to 5:1) **1H -NMR (500 MHz - $CDCl_3$):** δ 7.96 (d, $J = 7.9 \text{ Hz}$, 2H), 7.52 (dt, $J = 7.9, 1.0 \text{ Hz}$, 1H), 7.33 (d, $J = 8.0 \text{ Hz}$, 2H), 7.21 – 7.11 (m, 3H), 7.04 (ddd, $J = 7.9, 6.8, 1.1 \text{ Hz}$, 1H), 6.43 (s, 1H), 5.84 (s, 1H), 3.67 (s, 3H), 3.52 (s, 3H), 3.52 – 3.50 (m, 1H), 3.50 – 3.47 (m, 1H), 3.45 – 3.36 (m, 1H), 2.64 (bs, 1H), 2.45 (s, 3H), 1.43 (s, 9H), 0.43 (t, $J = 7.1 \text{ Hz}$, 3H); **^{13}C -NMR (126 MHz - $CDCl_3$):** δ 168.74, 167.78, 163.60, 143.69, 139.38, 138.94,

135.80, 131.84, 129.26 (2C), 128.69, 127.50 (2C), 126.29, 123.12, 121.14, 120.03, 109.60, 106.46, 81.42, 65.05, 61.86, 57.75, 53.29, 33.57, 33.02, 28.14 (3C, tBu), 21.83, 12.97; **HR-MS**: calc. for $[M+H]^+$, $C_{31}H_{37}O_8N_2S = 597.22651$, found: 597.22630. $[\alpha]_D^{RT} = -94.0^\circ$ (CH_2Cl_2 , $c = 1.00$); HPLC conditions: CHIRAPAK IC column, DCM:EtOH (100:2)/ *iso*-hexane = 30/70, flow rate = 0.5 mL min^{-1} , minor enantiomer: $t_R = 18.40$ min; major enantiomer: $t_R = 24.21$ min, 90% *ee*.

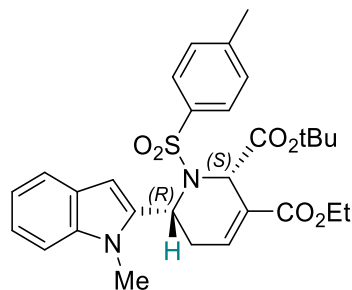
3-(tert-butyl) 2-ethyl (2S,6R)-6-(1-methyl-1H-indol-2-yl)-1-tosyl-1,2,5,6-tetrahydropyridine-2,3-dicarboxylate (96i)



(*S,R*)-**96i**

Off-white solid, 68% yield. Pent/EtOAc (5:1 to 3:1) **1H -NMR (700 MHz - $CDCl_3$)**: δ 7.80 – 7.77 (m, 2H), 7.44 (d, $J = 7.8$ Hz, 1H), 7.28 (m, $J = 8.6$ Hz, 3H), 7.18 (ddd, $J = 8.2, 7.0, 1.1$ Hz, 1H), 7.02 – 6.99 (m, 1H), 6.81 (m, $J = 4.4, 1.8$ Hz, 1H), 6.25 (s, 1H), 5.57 (d, $J = 7.5$ Hz, 1H), 5.35 (s, 1H), 3.87 (s, 3H), 3.06 – 2.89 (m, 2H), 2.70 (dd, $J = 19.9, 5.2$ Hz, 1H), 2.49 – 2.44 (ddt, 1H), 2.43 (s, 3H), 1.47 (s, 9H), 0.75 (t, $J = 7.2$ Hz, 3H).; **^{13}C -NMR (176 MHz - $CDCl_3$)**: δ 167.46, 164.20, 144.33, 138.13, 136.76, 134.70, 134.53, 129.82 (2C), 128.88, 127.68 (2C), 126.45, 122.49, 120.72, 119.58, 109.29, 103.30, 81.33, 61.61, 52.65, 46.41, 30.13, 28.18 (3C), 26.70, 21.75, 13.56; **HR-MS**: calc. for $[M+H]^+$, $C_{29}H_{35}O_6N_2S = 539.22103$, found: 539.22066. $[\alpha]_D^{RT} = -51.0^\circ$ (CH_2Cl_2 , $c = 1.00$); HPLC conditions: CHIRAPAK IC column, DCM:EtOH (100:2)/ *iso*-hexane = 30/70, flow rate = 0.5 mL min^{-1} , minor enantiomer: $t_R = 32.75$ min; major enantiomer: $t_R = 24.80$ min, 76% *ee*.

2-(tert-butyl) 3-ethyl (2S,6R)-6-(1-methyl-1H-indol-2-yl)-1-tosyl-1,2,5,6-tetrahydropyridine-2,3-dicarboxylate (96j)

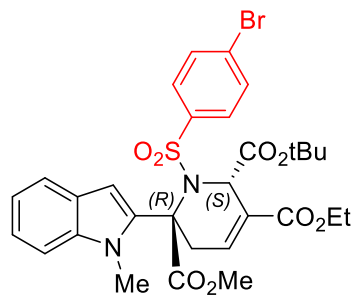


(S,R)-96j

Off-white foam, 52% yield. Pent/EtOAc (6:1 to 5:1) **¹H-NMR (700 MHz - CDCl₃)**: δ 7.81 – 7.77 (m, 2H), 7.43 (dt, *J* = 7.8, 1.0 Hz, 1H), 7.28 (d, *J* = 8.5, 1.0 Hz, 3H), 7.16 (ddd, *J* = 8.3, 7.0, 1.2 Hz, 1H), 7.00 (ddd, *J* = 7.9, 7.0, 0.9 Hz, 1H), 6.85 – 6.81 (m, 1H), 6.26 (s, 1H), 5.55 (d, *J* = 7.3 Hz, 1H), 5.40 (s, 1H), 4.28 – 4.16 (m, 2H), 3.90 (s, 3H), 2.70 (dd, *J* = 19.8, 5.4 Hz, 1H), 2.43 (s, 3H), 2.41 – 2.34 (m, 1H), 1.31 (t, *J* = 7.1 Hz, 3H), 0.74 (s, 9H); **¹³C-NMR (126 MHz - CDCl₃)**: δ 166.23, 165.75, 144.47, 138.39, 137.27, 135.00, 134.76, 130.14 (2C), 128.27, 127.77 (2C), 127.05, 122.51, 121.04, 119.72, 109.66, 103.11, 82.62, 61.23, 53.76, 46.58, 30.41, 27.47 (3C, tBu), 26.93, 21.96, 14.63; **HR-MS**: calc. for [M+H]⁺, C₂₉H₃₅O₆N₂S = 539.22103, found: 539.22061. [α]_D^{RT} = -136.0° (CH₂Cl₂, c = 1.00); HPLC conditions: CHIRAPAK IC column, DCM:EtOH (100:2)/*iso*-hexane = 30/70, flow rate = 0.5 mL min⁻¹, minor enantiomer: *t*_R = 27.18 min; major enantiomer: *t*_R = 24.49 min, 84% *ee*.

Single enantiomer purified using CHIRAPAK IC column, DCM:EtOH (100:2)/*iso*-hexane = 30/70, flow rate = 3 mL min⁻¹. White foam, 52%.

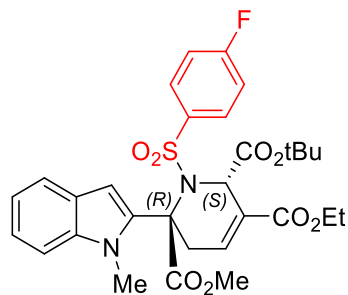
2-(tert-butyl) 3-ethyl 6-methyl (2S,6R)-1-((4-bromophenyl)sulfonyl)-6-(1-methyl-1H-indol-2-yl)-1,2,5,6-tetrahydropyridine-2,3,6-tricarboxylate (96k)



(S,R)-96k

Yellow oil, 75% yield. Pent/EtOAc (6:1 to 5:1) **¹H-NMR (500 MHz - CDCl₃)**: δ 7.97 – 7.72 (m, 2H), 7.60 (d, *J* = 8.1 Hz, 2H), 7.52 (dt, *J* = 7.9, 1.0 Hz, 1H), 7.21 – 7.11 (m, 3H), 7.06 (ddd, *J* = 8.0, 6.7, 1.2 Hz, 1H), 6.47 (s, 1H), 5.96 (s, 1H), 4.26 (dq, *J* = 10.8, 7.1 Hz, 1H), 4.17 (dq, *J* = 10.9, 7.2 Hz, 1H), 3.65 (s, 3H), 3.53 (m, 4H, overlapping of singlet and double doublet), 3.45 – 3.33 (m, 1H), 1.33 (t, *J* = 7.2 Hz, 3H), 0.82 (s, 9H); **¹³C-NMR (126 MHz - CDCl₃)**: δ 168.98, 166.95, 164.91, 139.49, 135.20, 131.74 (2C), 131.37, 129.06 (2C), 127.63, 126.25, 123.10, 121.00, 120.12, 110.18, 106.58, 82.82, 65.45, 61.24, 58.59, 53.36, 34.29, 32.93, 27.30 (3C, tBu), 14.44; **HR-MS**: calc. for [M+H]⁺, C₃₀H₃₄O₈N₂BrS = 661.12138, found: 661.12143 and C₃₀H₃₄O₈N₂⁸¹BrS = 663.11933, found: 663.11926. [α]_D^{RT} = - 53.0° (CH₂Cl₂, c = 1.00); HPLC conditions: CHIRAPAK IA column, DCM:EtOH (100:2)/ *iso*-hexane = 10/90, flow rate = 0.5 mL min⁻¹, minor enantiomer: t_R = 27.90 min; major enantiomer: t_R = 38.35 min, 83% *ee*.

2-(tert-butyl) 3-ethyl 6-methyl (2S,6R)-1-((4-fluorophenyl)sulfonyl)-6-(1-methyl-1H-indol-2-yl)-1,2,5,6-tetrahydropyridine-2,3,6-tricarboxylate (96I)

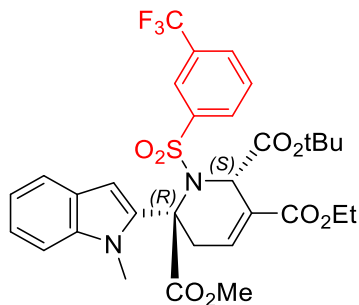


(S,R)-96I

Orange foam, 84% yield. Pent/EtOAc (7:1 to 6:1) **¹H-NMR (600 MHz - CDCl₃)**: δ 8.00 (bs, 2H), 7.52 (d, *J* = 7.9, 1.0 Hz, 1H), 7.20 – 7.10 (m, 5H), 7.06 (ddd, *J* = 7.9, 6.8, 1.1 Hz, 1H), 6.47 (d, *J* = 0.7 Hz, 1H), 5.95 (s, 1H), 4.22 (ddq, *J* = 56.7, 10.9, 7.2 Hz, 2H), 3.66 (s, 3H), 3.54 (dd, *J* = 5.2, 1.0 Hz, 1H), 3.54 (s, 3H), 3.44 – 3.36 (m, 1H), 1.33 (t, *J* = 7.1 Hz, 3H), 0.82 (s, 9H); **¹³C-NMR (126 MHz - CDCl₃)**: δ 167.90 (d, *J* = 303.8 Hz), 165.79, 164.80, 164.10, 139.40, 137.93, 135.07, 131.41, 130.25, 130.19, 128.82, 126.16, 122.93, 120.87, 119.97, 115.61, 115.46, 110.04, 106.39, 82.64, 65.31, 61.09, 58.50, 53.19, 34.14, 32.79, 27.18 (3C, tBu), 14.30; **¹⁹F NMR (565 MHz, CDCl₃)** δ -105.42; **HR-MS**: calc. for [M+H]⁺, C₃₀H₃₄O₈N₂FS = 601.20144, found: 601.20327. **[α]_D^{RT}** = - 70.0° (CH₂Cl₂, c = 1.00); HPLC conditions: CHIRAPAK IA column, DCM:EtOH (100:2)/ *iso*-hexane = 10/90, flow rate = 0.5 mL min⁻¹, minor enantiomer: *t_R* = 25.39 min; major enantiomer: *t_R* = 32.57 min, 84% *ee*.

Not submitted for biological testing.

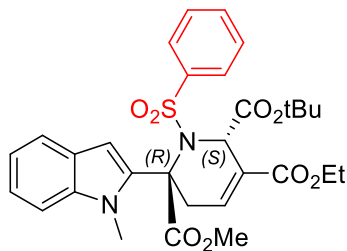
2-(tert-butyl) 3-ethyl 6-methyl (2*S*,6*R*)-6-(1-methyl-1*H*-indol-2-yl)-1-((3-(trifluoromethyl)phenyl)sulfonyl)-1,2,5,6-tetrahydropyridine-2,3,6-tricarboxylate (**96m**)



(*S,R*)-**96m**

Yellow solid, % yield. Pent/EtOAc (5:1 to 3:1) **¹H-NMR (500 MHz - CDCl₃)**: δ 8.35 (s, 1H), 8.22 – 8.01 (m, 1H), 7.81 (d, *J* = 7.8 Hz, 1H), 7.57 (bs, 1H), 7.52 (d, *J* = 7.9 Hz, 1H), 7.20 – 7.10 (m, 3H), 7.06 (ddd, *J* = 7.9, 6.7, 1.1 Hz, 1H), 6.47 (s, 1H), 6.00 (s, *J* = 1.7 Hz, 1H), 4.23 (ddq, *J* = 47.6, 10.9, 7.1 Hz, 2H), 3.64 (s, 3H), 3.55 (dd, *J* = 19.2, 5.0 Hz, 1H), 3.51 (s, 3H), 3.38 (m, *J* = 23.0, 6.7 Hz, 1H), 1.33 (t, *J* = 7.1 Hz, 4H), 0.85 (s, 9H); **¹³C-NMR (126 MHz - CDCl₃)**: δ 168.96, 167.01, 164.82, 139.46, 135.21, 131.30, 131.19, 130.93, 130.68, 129.20, 129.13 (d, *J* = 3.6 Hz), 126.22, 124.87, 124.59, 123.14, 122.42, 121.04, 120.15, 110.16, 106.72, 82.92, 65.59, 61.31, 58.61, 53.33, 34.51, 32.75, 27.30 (3C), 14.42; **¹⁹F NMR (470 MHz, CDCl₃)** δ -62.76; **HR-MS**: calc. for [M+H]⁺, C₃₁H₃₄O₈N₂F₃S = 651.19825, found: 651.19815. [α]_D^{RT} = - 61.0° (CH₂Cl₂, c = 1.00); HPLC conditions: CHIRAPAK IC column, IPA/ *iso*-hexane = 10/90, flow rate = 0.5 mL min⁻¹, minor enantiomer: t_R = 32.18 min; major enantiomer: t_R = 23.36 min, 84% *ee*.

2-(tert-butyl) 3-ethyl 6-methyl (2S,6R)-6-(1-methyl-1H-indol-2-yl)-1-(phenylsulfonyl)-1,2,5,6-tetrahydropyridine-2,3,6-tricarboxylate (96n)

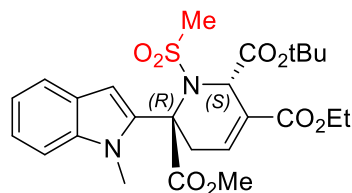


(*S,R*)-**96n**

Yellow foam, 70% yield. Pent/EtOAc (5:1 to 4:1) **¹H-NMR (500 MHz - CDCl₃)**: δ 8.01 (s, 2H), 7.57 (d, *J* = 7.4 Hz, 1H), 7.54 – 7.47 (m, 3H), 7.19 – 7.10 (m, 3H), 7.05 (ddd, *J* = 7.8, 6.7, 1.3 Hz, 1H), 6.47 (s, 1H), 5.96 (s, *J* = 1.4 Hz, 1H), 4.26 (dq, *J* = 11.0, 7.2 Hz, 1H), 4.22 – 4.11 (m, 1H), 3.64 (s, 3H), 3.55 (s, 3H), 3.53 – 3.49 (m, 1H), 3.43 (d, *J* = 21.1 Hz, 1H), 1.32 (t, *J* = 7.2 Hz, 3H), 0.80 (s, 9H); **¹³C-NMR (126 MHz - CDCl₃)**: δ 169.20, 167.13, 165.27, 142.25, 139.82, 135.50, 132.98, 131.93, 129.10, 128.81 (2C), 128.49, 127.68 (2C), 126.54, 123.20, 121.23, 120.26, 110.45, 106.65, 82.89, 65.55, 61.43, 58.79, 53.51, 33.25, 27.54 (3C, tBu), 14.69; **HR-MS**: calc. for [M+H]⁺, C₃₀H₃₅O₈N₂S = 583.21086, found: 583.21059. [α]_D^{RT} = - 68.0° (CH₂Cl₂, c = 1.00); HPLC conditions: CHIRAPAK IC column, DCM:MeOH (100:5)/*iso*-hexane = 20/80, flow rate = 0.5 mL min⁻¹, minor enantiomer: t_R = 23.61 min; major enantiomer: t_R = 28.12 min, 78% *ee*.

Single enantiomer purified using CHIRAPAK IC column, DCM:MeOH (100:5)/*iso*-hexane = 30/70, flow rate = 3 mL min⁻¹. White foam, 33%.

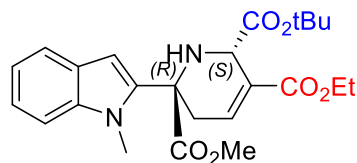
2-(tert-butyl) 3-ethyl 6-methyl (2S,6R)-6-(1-methyl-1H-indol-2-yl)-1-(methylsulfonyl)-1,2,5,6-tetrahydropyridine-2,3,6-tricarboxylate (96o)



(*S,R*)-**96o**

Off-white powder, 88% yield. Pent/EtOAc (5:1) **¹H-NMR (500 MHz - CDCl₃)**: δ 7.54 (dt, *J* = 8.0, 1.0 Hz, 1H), 7.24 (d, *J* = 1.1 Hz, 1H), 7.20 (ddd, *J* = 8.3, 6.8, 1.2 Hz, 1H), 7.16 (ddd, *J* = 5.5, 3.0, 1.5 Hz, 1H), 7.07 (ddd, *J* = 7.9, 6.8, 1.1 Hz, 1H), 6.47 (s, 1H), 5.71 (t, *J* = 1.7 Hz, 1H), 4.23 (dq, *J* = 10.9, 7.1 Hz, 1H), 4.13 (dq, *J* = 11.0, 7.2 Hz, 1H), 3.92 (s, 3H), 3.71 (s, 3H), 3.58 – 3.49 (m, 1H), 3.47 (s, 3H), 3.36 (dt, *J* = 19.6, 2.6 Hz, 1H), 1.30 (t, *J* = 7.1 Hz, 3H), 0.74 (s, 9H).; **¹³C-NMR (126 MHz - CDCl₃)**: δ 169.43, 166.90, 165.01, 139.70, 135.48, 131.53, 128.52, 126.27, 123.09, 121.01, 120.10, 110.28, 106.50, 82.65, 65.14, 61.13, 58.12, 53.46, 43.94, 33.95, 33.55, 27.24 (3C, tBu), 14.40; **HR-MS**: calc. for [M+H]⁺, C₂₅H₃₃O₈N₂S = 521.19521, found: 521.19471. [α]_D^{RT} = - 215.0° (CH₂Cl₂, c = 1.00); HPLC conditions: CHIRAPAK IC column, DCM:MeOH (100:5)/ *iso*-hexane = 20/80, flow rate = 0.5 mL min⁻¹, minor enantiomer: t_R = 28.76 min; major enantiomer: t_R = 36.13 min, 84% *ee*.

2-(tert-butyl) 3-ethyl 6-methyl (2S,6R)-6-(1-methyl-1H-indol-2-yl)-1,2,5,6-tetrahydropyridine-2,3,6-tricarboxylate (96p)



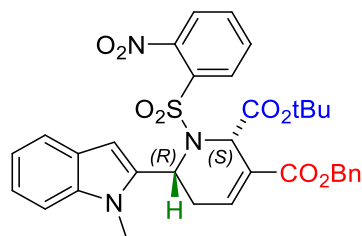
(*S,R*)-**96p**

To a solution of *N*-tosyl protected compound (1.0 equiv.) in dry DMF (0.2 ml) were added thiophenol (1.0 equiv) and K₂CO₃ (3.0 equiv). The reaction mixture was stirred at room temperature overnight, and then concentrated under reduced pressure. The residue was purified by preparative HPLC. Yellow foam, 20% yield. Pent/EtOAc (5:1 to 3:1) **¹H-NMR (600 MHz,**

CDCl₃-d₁): δ 7.52 (dt, $J = 7.9, 1.1, 0.7$ Hz, 1H), 7.27 – 7.26 (m, 1H), 7.22 – 7.17 (m, 1H), 7.14 (td, $J = 4.2, 1.6$ Hz, 1H), 7.06 (ddd, $J = 7.9, 7.0, 1.0$ Hz, 1H), 6.35 (d, $J = 0.8$ Hz, 1H), 4.54 (q, $J = 2.1$ Hz, 1H), 4.20 (m, 1H), 3.84 (s, 3H), 3.79 (s, 3H), 3.16 – 3.07 (m, 1H), 2.93 (m, 1H), 1.29 (t, $J = 7.1$ Hz, 3H), 1.06 (s, 9H); **¹³C-NMR (151 MHz, CDCl₃-d₁)**: δ 173.30, 169.70, 165.66, 138.89, 136.15, 135.23, 133.60, 130.32, 126.72, 122.54, 120.94, 119.93, 109.46, 103.05, 61.00, 59.61, 54.85, 53.43, 33.48, 31.23, 27.60 (3C), 14.40; **HR-MS**: calc. for [M+H]⁺, C₂₄H₃₁O₆N₂ = 442.5120, found: 442.8204. **[α]_D^{RT}** = + 26 ° (CH₂Cl₂, c = 1.00); HPLC conditions: CHIRAPAK IC column, DCM:EtOH (100:2)/ *iso*-hexane = 30/70, flow rate = 0.5 mL min⁻¹, minor enantiomer: t_R = 21.06 min; major enantiomer: t_R = 21.56 min, 82% *ee*.

3.6.5.1 Additional compounds for use in Bridged Bicyclic Synthesis

3-benzyl 2-(tert-butyl) (2*S*,6*R*)-6-(1-methyl-1*H*-indol-2-yl)-1-((2-nitrophenyl)sulfonyl)-1,2,5,6-tetrahydropyridine-2,3-dicarboxylate (**96q**)

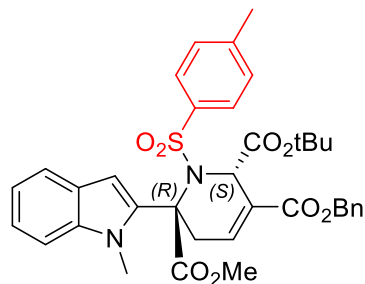


(*S,R*)-**96q**

Off-white foam, 54% yield. Pent/EtOAc (6:1 to 5:1) ¹H-NMR (500 MHz - CDCl₃): δ 7.90 (dd, *J* = 8.0, 1.3 Hz, 1H), 7.68 (td, *J* = 7.8, 1.3 Hz, 1H), 7.53 (dd, *J* = 8.0, 1.2 Hz, 1H), 7.49 – 7.43 (m, 2H), 7.42 – 7.34 (m, 5H), 7.29 (dd, *J* = 8.5, 0.9 Hz, 1H), 7.17 (ddd, *J* = 8.3, 7.0, 1.2 Hz, 1H), 7.01 (ddd, *J* = 8.1, 7.1, 1.0 Hz, 1H), 6.98 (m, 1H), 6.32 (s, 1H), 5.65 (d, *J* = 7.2 Hz, 1H), 5.60 (m, 1H), 5.26 – 5.18 (m, 2H), 3.87 (s, 3H), 2.87 – 2.79 (m, 1H), 2.67 (ddt, *J* = 20.1, 7.4, 2.5 Hz, 1H), 0.72 (s, 9H); ¹³C-NMR (126 MHz - CDCl₃): δ 165.41, 165.03, 148.26, 138.09, 135.65, 135.38, 134.15, 133.89, 132.64, 131.65, 130.45, 128.66 (2C), 128.50 (2C), 128.48, 127.53, 126.63, 123.79, 122.41, 120.79, 119.51, 109.45, 103.33, 82.85, 66.84, 54.03, 46.75, 30.15, 27.49, 27.09 (3C); HR-MS: calc. for [M+H]⁺, C₃₃H₃₄O₈N₃S = 632.20611, found: 632.20789. [α]_D^{RT} = - 41.0° (CH₂Cl₂, c = 1.00); HPLC conditions: CHIRAPAK IC column, DCM:EtOH (100:2)/ *iso*-hexane = 30/70, flow rate = 0.5 mL min⁻¹, minor enantiomer: t_R = 26.47 min; major enantiomer: t_R = 38.06 min, 76% *ee*.

Not submitted for biological testing.

3-benzyl 2-(tert-butyl) 6-methyl (2S,6R)-6-(1-methyl-1H-indol-2-yl)-1-tosyl-1,2,5,6-tetrahydropyridine-2,3,6-tricarboxylate (96r)

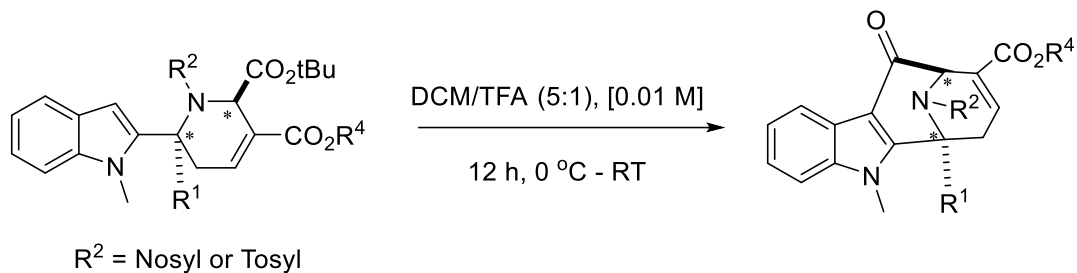


(S,R)-96r

Off-white foam, 58% yield. Pent/EtOAc (7:1) **¹H-NMR (600 MHz - CDCl₃)**: δ 7.87 (bs, 2H), 7.52 – 7.48 (m, 1H), 7.42 – 7.31 (m, 6H), 7.27 (m, 1H), 7.18 – 7.11 (m, 3H), 7.04 (ddd, *J* = 7.9, 6.5, 1.4 Hz, 1H), 6.44 (d, *J* = 0.7 Hz, 1H), 5.93 (q, *J* = 1.4 Hz, 1H), 5.25 – 5.10 (m, 2H), 3.64 (s, 3H), 3.59 (s, 3H), 3.50 (ddd, *J* = 19.5, 5.2, 1.0 Hz, 1H), 3.43 (d, 1H), 2.43 (s, 3H), 0.72 (s, 9H). **¹³C-NMR (151 MHz - CDCl₃)**: δ 168.86, 166.60, 164.69, 143.38, 139.49, 138.83, 135.66, 135.62, 131.68, 129.08 (2C), 128.62 (2C), 128.42 (2C), 128.38, 128.15, 127.39 (2C), 126.17, 122.77, 120.82, 119.84, 110.05, 106.11, 82.51, 66.72, 65.06, 58.38, 53.13, 33.03, 27.49, 27.08 (3C), 21.65; **HR-MS**: calc. for [M+H]⁺, C₃₆H₃₉O₈N₂S = 659.24216, found: 659.24406. [α]_D^{RT} = - 74.0° (CH₂Cl₂, c = 1.00); HPLC conditions: CHIRAPAK IA column, DCM:EtOH (100:5)/ *iso*-hexane = 15/85, flow rate = 0.5 mL min⁻¹, minor enantiomer: t_R = min; major enantiomer: t_R = min, 87% *ee*.

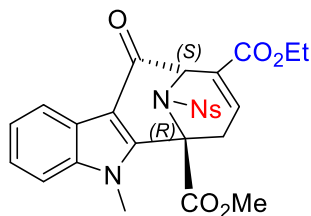
Not submitted for biological testing.

3.6.6. General Procedure for the Synthesis of Bridged-Bicyclic Compounds (98)



To a stirred solution of pseudo-NP **96** (1.0 eq.) in DCM was added TFA (DCM/TFA 5:1) dropwise at 0 °C. The reaction mixture was swarmed to room temperature. After 12 h, the reaction mixture was concentrated and purified by silica gel column chromatography (Pent/EtOAc) to afford the bridged-bicyclic product.

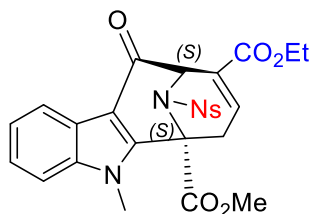
9-ethyl 6-methyl (6R,10S)-5-methyl-12-((4-nitrophenyl)sulfonyl)-11-oxo-5,7,10,11-tetrahydro-6H-6,10-epiminocycloocta[b]indole-6,9-dicarboxylate (98a)



(*R,S*)-**98a**

White powder, 63%. $^1\text{H-NMR}$ (700 MHz - CDCl_3): δ 8.28 – 8.21 (d, 1H), 8.00 (dd, $J = 8.1, 1.3$ Hz, 1H), 7.78 (dd, $J = 7.9, 1.3$ Hz, 1H), 7.68 (td, $J = 7.7, 1.4$ Hz, 1H), 7.62 (td, $J = 7.8, 1.3$ Hz, 1H), 7.41 – 7.38 (m, 1H), 7.38 – 7.34 (m, 2H), 7.02 (ddd, $J = 5.4, 2.7, 0.8$ Hz, 1H), 5.45 (d, $J = 1.2$ Hz, 1H), 4.31 – 4.19 (m, 2H), 3.84 (ddd, $J = 19.9, 2.7, 1.7$ Hz, 1H), 3.68 (s, 6H), 2.85 (dd, $J = 19.9, 5.3$ Hz, 1H), 1.30 (t, $J = 7.1$ Hz, 3H); $^{13}\text{C-NMR}$ (126 MHz - CDCl_3): δ 185.78, 168.21, 163.30, 148.38, 138.40, 135.59, 134.15, 133.91 (2C), 132.66 (2C), 129.87, 129.63, 124.99, 124.97, 123.84, 123.42, 122.30, 110.01, 109.87, 61.61, 60.73, 33.00, 30.76 (2C), 14.27; **HR-MS**: calc. for $[\text{M}+\text{H}]^+$ $\text{C}_{26}\text{H}_{24}\text{O}_9\text{N}_3\text{S} = 554.12278$, found: 554.12404. $[\alpha]_{\text{D}}^{25} = +33^\circ$ (CH_2Cl_2 , $c = 1.00$); HPLC conditions: CHIRAPAK IA column, DCM:EtOH (100:2)/ *iso*-hexane = 25/75, flow rate = 0.5 mL min^{-1} , minor enantiomer: $t_{\text{R}} = 37.48$ min; major enantiomer: $t_{\text{R}} = 41.45$ min, 80% *ee*.

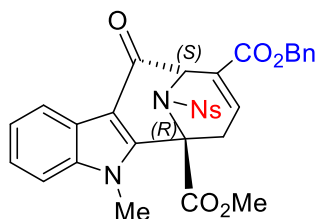
9-ethyl 6-methyl (6S,10S)-5-methyl-12-((4-nitrophenyl)sulfonyl)-11-oxo-5,7,10,11-tetrahydro-6H-6,10-epiminocycloocta[b]indole-6,9-dicarboxylate (98a)



(*S,R*)-**98a**

White powder, 38%. **HR-MS:** calc. for $[M+H]^+$ $C_{26}H_{24}O_9N_3S = 554.12278$, found: 554.12404. $[\alpha]^{RT}_D = -26^\circ$ (CH_2Cl_2 , $c = 1.00$); HPLC conditions: CHIRAPAK IA column, DCM:EtOH (100:2)/ *iso*-hexane = 25/75, flow rate = 0.5 mL min⁻¹, minor enantiomer: $t_R = 42.30$ min; major enantiomer: $t_R = 38.23$ min, 76% *ee*.

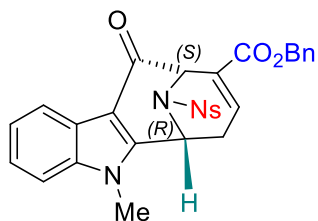
9-benzyl 6-methyl (6R,10S)-5-methyl-11-oxo-5,7,10,11-tetrahydro-6H-6,10-epiminocycloocta[b]indole-6,9-dicarboxylate (98b)



(*R,S*)-**98b**

Off-white powder, 54%. **¹H-NMR (500 MHz - CDCl₃):** δ 8.27 – 8.22 (m, 1H), 8.00 (dd, $J = 8.0$, 1.3 Hz, 1H), 7.77 (dd, $J = 8.0$, 1.3 Hz, 1H), 7.68 (td, $J = 7.7$, 1.4 Hz, 1H), 7.61 (td, $J = 7.8$, 1.3 Hz, 1H), 7.40 – 7.32 (m, 7H), 7.32 – 7.27 (m, 1H), 7.05 (ddd, $J = 5.4$, 2.7, 0.8 Hz, 1H), 5.51 – 5.46 (m, 1H), 5.27 – 5.18 (m, 2H), 3.83 (ddd, $J = 19.9$, 2.7, 1.7 Hz, 1H), 3.67 (s, 3H), 3.66 – 3.60 (bs, 3H), 2.84 (dd, $J = 20.0$, 5.3 Hz, 1H).; **¹³C-NMR (151 MHz - CDCl₃):** δ 185.73, 168.14, 163.13, 148.32, 145.32, 138.40, 136.31, 135.59, 134.10, 133.92, 132.66, 129.62, 129.54, 128.66 (2C), 128.35, 128.33 (2C), 125.01, 124.99, 123.87, 123.39, 122.28, 109.97, 109.89, 67.30, 63.12, 60.69, 53.89, 33.01, 30.76; **HR-MS:** calc. for $[M+H]^+$ $C_{31}H_{26}O_9N_3S = 616.13843$, found: 616.13985. $[\alpha]^{RT}_D = +40^\circ$ (CH_2Cl_2 , $c = 1.00$); HPLC conditions: CHIRAPAK IC column, DCM:EtOH (100:2)/ *iso*-hexane = 50/50, flow rate = 0.5 mL min⁻¹, minor enantiomer: $t_R = 47.73$ min; major enantiomer: $t_R = 41.88$ min, 82% *ee*.

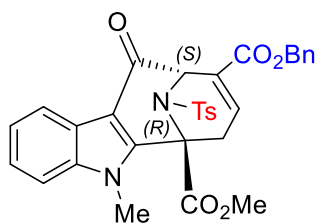
benzyl (10S)-5-methyl-12-((4-nitrophenyl)sulfonyl)-11-oxo-6,7,10,11-tetrahydro-5H-6,10-epiminocycloocta[b]indole-9-carboxylate (98c)



(*R,S*)-**98c**

Off-white powder. 68%. $^1\text{H-NMR}$ (500 MHz - CDCl_3): δ 8.10 (dd, $J = 8.0, 1.3$ Hz, 1H), 7.95 (dt, $J = 7.7, 1.0$ Hz, 1H), 7.64 (td, $J = 7.7, 1.2$ Hz, 1H), 7.52 (td, $J = 7.7, 1.3$ Hz, 1H), 7.42 – 7.26 (m, 8H), 7.21 (ddd, $J = 8.1, 6.9, 1.3$ Hz, 1H), 6.97 (dd, $J = 5.1, 2.7$ Hz, 1H), 5.77 (dd, $J = 6.8, 0.9$ Hz, 1H), 5.42 – 5.38 (m, 1H), 5.32 – 5.17 (m, 2H), 3.85 (s, 3H), 3.32 (dddd, $J = 19.4, 6.8, 2.6, 1.7$ Hz, 1H), 2.56 – 2.41 (dd, 1H); $^{13}\text{C-NMR}$ (126 MHz - CDCl_3): δ 186.46, 163.16, 147.85, 147.35, 137.31, 135.77, 135.56, 134.08, 132.40, 131.87, 131.39, 128.99, 128.58 (2C), 128.33 (2C), 128.30, 124.08, 124.05, 123.89, 123.14, 121.58, 109.61, 107.50, 67.15, 58.22, 46.51, 30.44, 30.41; **HR-MS**: calc. for $[\text{M}+\text{H}]^+$ $\text{C}_{30}\text{H}_{27}\text{N}_2\text{O}_5\text{S} = 558.12903$, found: 558.13256. $[\alpha]_{\text{D}}^{25} = -52^\circ$ (CH_2Cl_2 , $c = 1.00$); HPLC conditions: CHIRAPAK IA column, DCM:EtOH (100:2)/ *iso*-hexane = 25/75, flow rate = 0.5 mL min^{-1} , minor enantiomer: $t_{\text{R}} = 53.83$ min; major enantiomer: $t_{\text{R}} = 36.37$ min, 76% *ee*.

9-benzyl 6-methyl (6R,10S)-5-methyl-11-oxo-12-tosyl-5,7,10,11-tetrahydro-6H-6,10-epiminocycloocta[b]indole-6,9-dicarboxylate (98d)

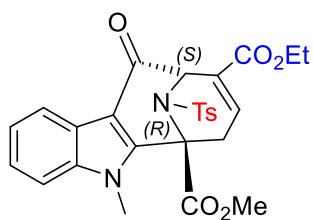


(*R,S*)-**98d**

Yellow foam, 52%. $^1\text{H-NMR}$ (700 MHz - CDCl_3): δ 8.17 (d, $J = 7.8$ Hz, 1H), 7.77 – 7.64 (bd, 2H), 7.41 – 7.35 (m, 4H), 7.35 – 7.29 (m, 3H), 7.14 (d, $J = 7.1$ Hz, 2H), 6.74 (bs, 1H), 5.33 (bs, 1H), 5.20 (d, $J = 2.1$ Hz, 2H), 3.95 – 3.84 (m, 2H), 3.65 (s, 3H), 3.60 (bs, 3H), 2.62 (d, $J = 19.9$ Hz, 1H), 2.36 (s, 3H); $^{13}\text{C-NMR}$ (176 MHz - CDCl_3): δ 185.82, 169.34, 163.23, 146.04, 144.70,

137.99, 135.83, 135.73, 135.66, 129.72 (2C), 128.57 (2C), 128.43 (2C), 128.29, 127.78 (2C), 124.53, 123.49, 123.32, 122.03, 109.65, 109.54, 66.97, 61.83, 59.92, 53.92, 31.35, 30.51 (2 x Me), 21.59; **HR-MS**: calc. for $[M+H]^+$ $C_{32}H_{29}O_7N_2S$ = 585.16900, found: 585.17032. $[\alpha]^{RT}_D = -17^\circ$ (CH_2Cl_2 , $c = 1.00$); HPLC conditions: CHIRAPAK IA column, DCM:EtOH (100:2)/ *iso*-hexane = 20/80, flow rate = 0.5 mL min^{-1} , minor enantiomer: $t_R = 40.04$ min; major enantiomer: $t_R = 48.02$ min, 84% *ee*.

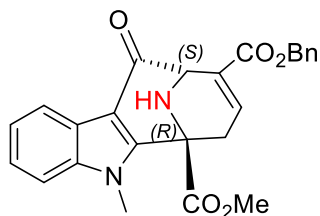
9-ethyl 6-methyl (6R,10S)-5-methyl-11-oxo-12-tosyl-5,7,10,11-tetrahydro-6H-6,10-epiminocycloocta[b]indole-6,9-dicarboxylate (98e)



(*R,S*)-**98e**

Yellow foam, 84%. **1H -NMR (700 MHz - $CDCl_3$)**: 8.15 (d, $J = 7.8$ Hz, 1H), 7.77 (d, $J = 7.9$ Hz, 2H), 7.37 – 7.32 (m, 2H), 7.32 – 7.28 (m, 1H), 7.27 (s, 1H), 7.26 (s, 1H), 6.76 (s, 1H), 5.27 (s, 1H), 4.27 – 4.18 (m, 2H), 3.89 (s, 3H), 3.66 (s, 3H), 2.67 (d, $J = 19.6$ Hz, 1H), 2.40 (s, 3H), 1.29 (t, $J = 7.1$ Hz, 3H); **^{13}C -NMR (126 MHz - $CDCl_3$)**: δ 185.86, 166.38, 163.43, 144.68, 138.00, 136.04, 135.14, 129.76 (2C), 129.31, 127.76 (2C), 127.71, 124.50, 123.45, 123.33, 122.03, 109.53, 107.92, 61.25, 59.97, 53.88, 31.46, 30.52, 29.69, 21.62, 14.19; **HR-MS**: calc. for $[M+H]^+$ $C_{27}H_{27}O_7N_2S$ = 523.15335, found: 523.15432. $[\alpha]^{RT}_D = -10^\circ$ (CH_2Cl_2 , $c = 1.00$); HPLC conditions: CHIRAPAK IA column, DCM:EtOH (100:2)/ *iso*-hexane = 20/80, flow rate = 0.5 mL min^{-1} , minor enantiomer: $t_R = 34.96$ min; major enantiomer: $t_R = 47.56$ min, 84% *ee*.

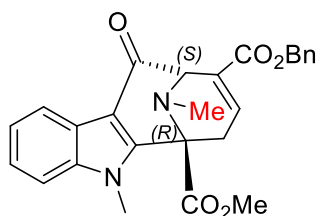
9-benzyl 6-methyl (6R,10S)-5-methyl-11-oxo-5,7,10,11-tetrahydro-6H-6,10-epiminocycloocta[b]indole-6,9-dicarboxylate (98f)



(R,S)-98f

White solid, 50%. **¹H-NMR (700 MHz - CDCl₃):** δ 8.22 (dt, *J* = 7.6, 1.1 Hz, 1H), 7.43 – 7.39 (m, 2H), 7.37 – 7.33 (m, 3H), 7.31 (ddt, *J* = 15.0, 7.6, 1.3 Hz, 4H), 6.98 (ddd, *J* = 5.2, 2.8, 0.8 Hz, 1H), 5.21 (q, *J* = 12.5 Hz, 2H), 4.73 (s, 1H), 3.89 (s, 3H), 3.63 (s, 3H), 3.62 – 3.56 (m, 1H), 2.65 (dd, *J* = 19.6, 5.1 Hz, 1H); **¹³C-NMR (176 MHz - CDCl₃):** δ 189.12, 169.06, 162.71, 145.62, 136.59, 134.70, 134.57, 127.55, 127.49 (2C), 127.26, 127.23 (2C), 127.15, 123.17, 123.06, 122.27, 121.09, 108.48, 108.28, 65.90, 56.34, 52.83, 30.75, 29.32; **FT-IR:** $\tilde{\nu}$ = ; **HR-MS:** calc. for [M+H]⁺ C₂₅H₂₃O₅N₂ = 431.16015, found: 431.16059. [α]_D^{RT} = -4° (CH₂Cl₂, c = 1.00); HPLC conditions: CHIRAPAK IA column, DCM:EtOH (100:2)/ *iso*-hexane = 30/70, flow rate = 0.5 mL min⁻¹, minor enantiomer: t_R = 41.48 min; major enantiomer: t_R = 20.11 min, 82% *ee*.

9-benzyl 6-methyl (6R,10S)-5,12-dimethyl-11-oxo-5,7,10,11-tetrahydro-6H-6,10-epiminocycloocta[b]indole-6,9-dicarboxylate (98g)

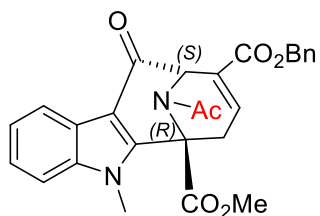


(R,S)-98g

White solid, 50%. **¹H-NMR (700 MHz - CDCl₃):** δ 8.22 (dt, *J* = 7.6, 1.1 Hz, 1H), 7.43 – 7.39 (m, 2H), 7.37 – 7.34 (m, 2H), 7.33 – 7.32 (m, 2H), 7.32 – 7.28 (m, 2H), 6.96 (ddd, *J* = 5.1, 2.8, 0.6 Hz, 1H), 5.27 – 5.15 (m, 2H), 4.41 (d, *J* = 1.7 Hz, 1H), 3.90 (s, 3H), 3.58 (s, 3H), 3.55 (ddd, *J* = 20.0, 2.8, 1.9 Hz, 1H), 2.43 (dd, *J* = 5.1 Hz, 1H) overlap with methyl signal, 2.43 (s, 3H); **¹³C-NMR (176 MHz - CDCl₃):** δ 189.34, 171.17, 164.39, 146.77, 137.86, 135.79, 135.00, 128.52 (2C),

128.25 (2C), 128.17, 127.63, 123.95, 123.87, 123.04, 122.12, 109.36, 109.33, 66.87, 65.96, 62.40, 53.77, 38.10, 30.57, 27.50; **HR-MS**: calc. for $[M+H]^+$ $C_{26}H_{25}O_5N_2 = 445.17580$, found: 445.17632. $[\alpha]^{RT}_D = + 35^\circ$ (CH_2Cl_2 , $c = 1.00$); HPLC conditions: CHIRAPAK IC column, DCM:EtOH (100:2)/ *iso*-hexane = 50/50, flow rate = 0.5 mL min^{-1} , minor enantiomer: $t_R = 31.45$ min; major enantiomer: $t_R = 37.47$ min, 79% *ee*.

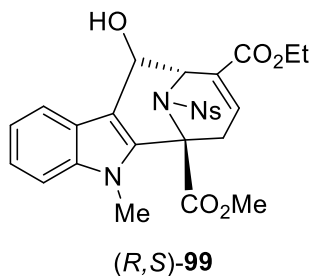
9-benzyl 6-methyl (6R,10S)-12-acetyl-5-methyl-11-oxo-5,7,10,11-tetrahydro-6H-6,10-epiminocycloocta[b]indole-6,9-dicarboxylate (98h)



(R,S)-98h

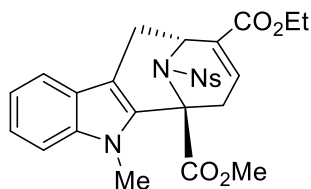
White solid, 32%. **1H -NMR (500 MHz - $CDCl_3$)**: δ 8.25 – 8.19 (m, 1H), 7.40 – 7.31 (m, 8H), 6.95 (ddd, $J = 5.3, 2.6, 0.8$ Hz, 1H), 5.44 – 5.41 (m, 1H), 5.21 (q, $J = 12.3$ Hz, 2H), 3.78 (s, 3H), 3.68 (m, 1H, overlaps with CH_3 singlet), 3.69 (s, 3H), 2.69 (dd, $J = 19.9, 5.3$ Hz, 1H), 2.21 (s, 3H); **^{13}C -NMR (126 MHz - $CDCl_3$)**: δ 181.55, 165.97, 164.77, 158.67, 140.86, 133.56, 132.66, 130.62, 125.26, 123.86 (2C), 123.66, 123.62 (2C), 119.75, 118.75, 118.63, 117.22, 104.93, 104.73, 62.49, 56.56, 54.39, 48.64, 26.03, 25.88, 17.48; **HR-MS**: calc. for $[M+H]^+$ $C_{27}H_{25}O_6N_2 = 473.17071$, found: 473.17140. $[\alpha]^{RT}_D = - 49^\circ$ (CH_2Cl_2 , $c = 1.00$); HPLC conditions: CHIRAPAK IA column, DCM:EtOH (100:2)/ *iso*-hexane = 30/70, flow rate = 0.5 mL min^{-1} , minor enantiomer: $t_R = 30.19$ min; major enantiomer: $t_R = 22.37$ min, 82% *ee*.

9-ethyl 6-methyl (6*R*,10*S*)-11-hydroxy-5-methyl-12-((2-nitrophenyl)sulfonyl)-5,7,10,11-tetrahydro-6*H*-6,10-epiminocycloocta[*b*]indole-6,9-dicarboxylate (99)



To a solution of (*R,S*)-**98f** (0.31 g, 0.56 mmol) in THF (3 mL), NaBH₄ (22 mg, 0.56 mmol, 1.0 eq) and MeOH (3 mL) were added at 0 °C. The mixture was warmed to rt and stirred for 1 h. The reaction mixture was quenched with aq. NH₄Cl and extracted with DCM. The combined organic phase was dried over MgSO₄, filtered, and concentrated under reduced pressure. The obtained residue was purified by flash silica gel column chromatography (DCM : EtOAc = 20:1) to afford the desired compound. Pale yellow amorphous 51% yield. **¹H-NMR (700 MHz - CDCl₃):** δ 8.18 (d, *J* = 8.0 Hz, 1H), 7.86 (dt, *J* = 7.9, 1.1 Hz, 1H), 7.78 (dd, *J* = 7.9, 1.4 Hz, 1H), 7.74 (td, *J* = 7.6, 1.4 Hz, 1H), 7.69 (td, *J* = 7.7, 1.4 Hz, 1H), 7.32 – 7.28 (m, 2H), 7.17 (ddd, *J* = 8.0, 6.1, 1.9 Hz, 1H), 7.14 (dd, *J* = 5.3, 2.6 Hz, 1H), 5.63 (d, *J* = 6.1 Hz, 1H), 5.38 (d, *J* = 6.1 Hz, 1H), 4.21 (ddq, *J* = 36.7, 10.9, 7.2 Hz, 2H), 3.72 (m, 1H), 3.69 (br s, 3H), 3.63 (s, 3H), 2.88 (dd, *J* = 19.8, 5.3 Hz, 1H), 1.28 (t, *J* = 7.1 Hz, 3H). **¹³C-NMR (176 MHz - CDCl₃):** δ 169.36, 166.68, 148.59, 138.19, 137.92, 133.93 (2C), 132.07, 131.75, 130.24, 128.84, 124.70, 124.39, 123.06, 121.10, 120.43, 111.31, 109.26, 67.35, 62.56, 61.58, 54.72, 53.34, 34.45, 30.11, 14.06; **HR-MS:** calc. for [M+H]⁺ C₂₆H₂₆O₉N₃S = 556.1384, found: 556.1378. **[α]_D^{RT}** = + 32 (CH₂Cl₂, *c* = 1.00); HPLC conditions: CHIRAPAK IC column, DCM:EtOH (100:2)/ *iso*-hexane = 50/50, flow rate = 0.5 mL min⁻¹, major enantiomer: *t*_R = 28.91 min; minor enantiomer: *t*_R = 32.77 min, 75% *ee*.

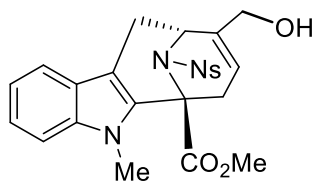
9-ethyl 6-methyl (6*R*,10*R*)-5-methyl-12-((2-nitrophenyl)sulfonyl)-5,7,10,11-tetrahydro-6*H*-6,10-epiminocycloocta[*b*]indole-6,9-dicarboxylate (100)



(*R,S*)-100

To a solution of (*R,S*)-**99** (0.14 g, 0.25 mmol) in DCM/TFA (80:1, 2.5 mL), Et₃SiH (0.20 ml, 1.3 mmol, 5 eq) was added at 0 °C. The mixture was warmed up to rt and stirred for 2 h, then concentrated under reduced pressure. The obtained residue was purified by flash silica gel column chromatography (DCM : EtOAc = 40:1). Pale yellow amorphous, 46% yield. **¹H-NMR (700 MHz - CDCl₃):** δ 8.18 (d, *J* = 8.0 Hz, 1H), 7.86 (dt, *J* = 7.9, 1.1 Hz, 1H), 7.78 (dd, *J* = 7.9, 1.4 Hz, 1H), 7.74 (td, *J* = 7.6, 1.4 Hz, 1H), 7.69 (td, *J* = 7.7, 1.4 Hz, 1H), 7.32 – 7.28 (m, 2H), 7.17 (ddd, *J* = 8.0, 6.1, 1.9 Hz, 1H), 7.14 (dd, *J* = 5.3, 2.6 Hz, 1H), 5.63 (d, *J* = 6.1 Hz, 1H), 5.38 (d, *J* = 6.1 Hz, 1H), 4.21 (ddq, *J* = 36.7, 10.9, 7.2 Hz, 2H), 3.72 (m, 1H), 3.69 (br s, 3H), 3.63 (s, 3H), 2.88 (dd, *J* = 19.8, 5.3 Hz, 1H), 1.28 (t, *J* = 7.1 Hz, 3H). **¹³C-NMR (176 MHz - CDCl₃):** δ 169.74, 164.23, 148.67, 137.93, 136.76, 134.39, 133.67, 132.03, 131.51, 130.93, 130.16, 125.42, 124.63, 122.95, 119.89, 118.78, 109.31, 107.93, 62.69, 60.96, 53.26, 51.74, 34.70, 30.23, 25.89, 14.15; **HR-MS:** calc. for [M+H]⁺ C₂₆H₂₆O₈N₃S = 540.1435, found: 540.1431. **[α]_D^{RT}** = + 44 (CH₂Cl₂, *c* = 1.00); HPLC conditions: CHIRAPAK IC column, DCM:EtOH (100:2)/ *iso*-hexane = 40/60, flow rate = 0.5 mL min⁻¹, minor enantiomer: *t_R* = 55.12 min; major enantiomer: *t_R* = 61.24 min, 78% *ee*.

methyl (6*R*,10*R*)-9-(hydroxymethyl)-5-methyl-12-((2-nitrophenyl)sulfonyl)-5,7,10,11-tetrahydro-6*H*-6,10-epiminocycloocta[*b*]indole-6-carboxylate (**101**)



(*R,S*)-**101**

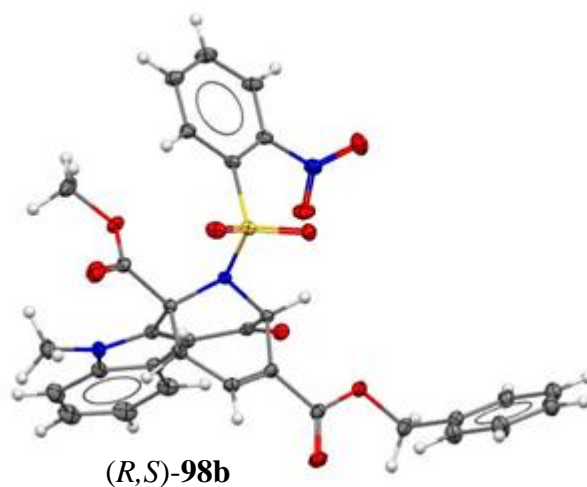
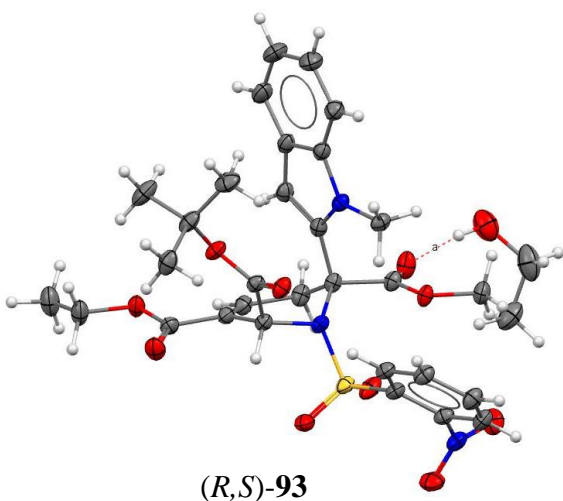
To a solution of (*R,S*)-**100** (42 mg, 0.077 mmol) in dry THF (1 mL) under Ar, 0.1 M DIBAL-H in *c*-Hex and dry THF (0.93 ml, 0.093 mmol, 1.2 eq) was added at -78 °C. The mixture was warmed up to rt and stirred for 1 h. The reaction mixture was quenched with H₂O and extracted with DCM. The combined organic phase was dried over MgSO₄, filtered, and concentrated under reduced pressure. The obtained residue was purified by flash silica gel column chromatography (*n*-Pent : EtOAc = 2:1) to obtain the desired. Yellow oil, 46% yield. **¹H-NMR (700 MHz - CDCl₃):** δ 8.23 (d, *J* = 7.4 Hz, 1H), 7.76 (dd, *J* = 7.8, 1.6 Hz, 1H), 7.72 (td, *J* = 7.6, 1.6 Hz, 1H), 7.68 (td, *J* = 7.6, 1.7 Hz, 1H), 7.53 (dt, *J* = 8.0, 0.9 Hz, 1H), 7.34 – 7.29 (m, 3H), 7.17 (ddd, *J* = 7.9, 6.4, 1.6 Hz, 1H), 5.78 (ddd, *J* = 5.1, 2.2, 1.1 Hz, 1H), 5.01 (d, *J* = 5.6 Hz, 1H), 4.10 (t, *J* = 1.7 Hz, 2H), 3.72 (s, 3H), 3.64 (s, 3H), 3.57 (d, *J* = 18.6 Hz, 1H), 3.24 (dd, *J* = 15.9, 5.8 Hz, 1H), 3.00 (dd, *J* = 16.0, 1.4 Hz, 1H), 2.64 (dd, *J* = 18.4, 5.3 Hz, 1H). **¹³C-NMR (176 MHz - CDCl₃):** δ 170.13, 148.72, 137.86, 137.84, 134.44, 133.60, 131.99 (2C), 130.27, 125.42, 124.50, 122.79, 122.27, 119.84, 118.56, 109.30, 107.68, 64.66, 63.29, 53.15, 52.22, 33.98, 30.21, 24.77; **HR-MS:** calc. for [M+H]⁺ C₂₄H₂₄O₇N₃S = 498.1329, found: 48.1323. [α]_D^{RT} = + 13 (CH₂Cl₂, *c* = 1.00); HPLC conditions: CHIRAPAK IA column, *iso*-propanol/ *iso*-hexane = 20/80, flow rate = 0.5 mL min⁻¹, major enantiomer: t_R = 29.84 min; minor enantiomer: t_R = 33.74 min, 80% *ee*.

3.7 X-Ray Structure Analyses

The crystal structure of compound (*R,S*)-**93** and (*R,S*)-**98b** was determined using the *Bruker D8 Venture* four-circle diffractometer equipped with a *PHOTON II* CPAD detector by *Bruker AXS GmbH*. The X-ray radiation was generated by the *I μ S/I μ S* microfocus source Cu ($\lambda = 1.54178 \text{ \AA}$) from *Incoatec GmbH* equipped with *HELIOS* mirror optics and a single-hole collimator by *Bruker AXS GmbH*. The selected single crystal of (*R,S*)-**93** and (*R,S*)-**98b** was covered with an inert oil (perfluoropolyalkyl ether) and mounted on the *MicroMount* from *MiTeGen*. The *APEX 3 Suite* (v.2018.7-2) software integrated with *SAINT* (integration) and *SADABS* (adsorption correction) programs by *Bruker AXS GmbH* were used for data collection. The processing and finalization of the crystal structure were performed using the *Olex2* program^[193]. The crystal structures were solved by the *ShelXT*^[194] structure solution program using the *Intrinsic Phasing* option, which were further refined by the *ShelXL*^[195] refinement package using *Least Squares* minimization. The non-hydrogen atoms were anisotropically refined. The C-bound H atoms were placed in geometrically calculated positions, and a fixed isotropic displacement parameter was assigned to each atom according to the riding-model: C–H = 0.95–1.00 \AA with $U_{\text{iso}}(\text{H}) = 1.5U_{\text{eq}}(\text{CH}_3)$ and $1.2U_{\text{eq}}(\text{CH}_2, \text{CH})$ for other hydrogen atoms. The O-bound H atom was placed free due to the hydrogen bonding.

The crystallographic data for the structures have been published as supplementary publication number 2144567 and 2171860 in the Cambridge Crystallographic Data Centre. A copy of these data can be obtained for free by applying to CCDC, 12 Union Road, Cambridge CB2 IEZ, UK, fax: 144-(0)1223-336033 or e-mail: deposit@ccdc.cam.ac.uk.

Crystal data and structure refinement for compound (*R,S*)-**93** (CCDC 2144567) and (*R,S*)-**98b** (CCDC 2171860) with 50% ellipsoid probability level.

Table S1: Crystallographic data of compound (*R,S*)-**93** and (*R,S*)-**98b**

Compound	(<i>R,S</i>)- 93	(<i>R,S</i>)- 98b
Empirical formula	C ₃₂ H ₃₉ N ₃ O ₁₁ S	C ₃₁ H ₂₅ N ₃ O ₉ S
Formula weight	673.72	615.60
Temperature/K	100.0	100.0
Crystal system	orthorhombic	monoclinic
Space group	<i>P</i> 2 ₁ 2 ₁ 2 ₁	<i>P</i> 2 ₁
a/Å	9.2130(3)	15.3235(5)
b/Å	15.3432(4)	10.2153(4)
c/Å	23.2044(4)	18.7998(7)
α/°	90	90
β/°	90	109.1030(10)
γ/°	90	90
Volume/Å ³	3280.10(15)	2780.75(18)
Z	4	4
ρ _{calc} /cm ³	1.364	1.470
μ/mm ⁻¹	1.431	0.181
F(000)	1424.0	1280.0

Crystal size/mm ³	0.267 × 0.109 × 0.056	0.63 × 0.362 × 0.328
Radiation	CuK α ($\lambda = 1.54178$)	MoK α ($\lambda = 0.71073$)
2 Θ range for data collection/ $^{\circ}$	6.906 to 159.432	4.17 to 66.402
Index ranges	-11 ≤ h ≤ 11, -19 ≤ k ≤ 19, -29 ≤ l ≤ 29	-23 ≤ h ≤ 23, -15 ≤ k ≤ 15, -28 ≤ l ≤ 28
Reflections collected	52330	275984
Independent reflections	7042 [$R_{\text{int}} = 0.0354$, $R_{\text{sigma}} = 0.0195$]	21282 [$R_{\text{int}} = 0.0361$, $R_{\text{sigma}} = 0.0154$]
Data/restraints/parameters	7042/0/446	21282/1/897
Goodness-of-fit on F ²	1.038	1.078
Final R indexes [$I \geq 2\sigma(I)$]	$R_1 = 0.0267$, $wR_2 = 0.0685$	$R_1 = 0.0282$, $wR_2 = 0.0766$
Final R indexes [all data]	$R_1 = 0.0275$, $wR_2 = 0.0691$	$R_1 = 0.0290$, $wR_2 = 0.0775$
Largest diff. peak/hole / e \AA^{-3}	0.2/-0.32	0.43/-0.24
Flack parameter	-0.012(5)	0.005(8)

4. References

- [1] Q. Li, C. Kang, *Int. J. Mol. Sci.* **2020**, *21*, 1–18.
- [2] A.-D. Gorse, *Curr. Top. Med. Chem.* **2005**, *6*, 3–18.
- [3] C. J. O’connor, L. Laraia, D. R. Spring, *Chem. Soc. Rev.* **2011**, *40*, 4332–4345.
- [4] M. Kawasumi, P. Nghiem, *J. Invest. Dermatol.* **2007**, *127*, 1577–1584.
- [5] D. R. Spring, *Chem. Soc. Rev.* **2005**, *34*, 472–482.
- [6] S. Ziegler, V. Pries, C. Hedberg, H. Waldmann, *Angew. Chemie - Int. Ed.* **2013**, *52*, 2744–2792.
- [7] R. S. Bohacek, C. McMartin, W. C. Guida, *Med. Res. Rev.* **1996**, *16*, 3–50.
- [8] A. H. Lipkus, Q. Yuan, K. A. Lucas, S. A. Funk, W. F. Bartelt, R. J. Schenck, A. J. Trippe, *J. Org. Chem.* **2008**, *73*, 4443–4451.
- [9] A. Nelson, G. Karageorgis, *RSC Med. Chem.* **2021**, *12*, 353–362.
- [10] A. H. Lipkus, S. P. Watkins, K. Gengras, M. J. McBride, T. J. Wills, *J. Org. Chem.* **2019**, *84*, 13948–13956.
- [11] T. Willis, “New findings reveal innovation in small molecule discovery is accelerating | CAS,” can be found under <https://www.cas.org/resource/blog/innovation-in-small-molecule-discovery-accelerating>, **n.d.**
- [12] A. M. Wassermann, E. Lounkine, D. Hoepfner, G. Le Goff, F. J. King, C. Studer, J. M. Peltier, M. L. Grippo, V. Prindle, J. Tao, A. Schuffenhauer, I. M. Wallace, S. Chen, P. Krastel, A. Cobos-Correa, C. N. Parker, J. W. Davies, M. Glick, *Nat. Chem. Biol.* **2015**, *11*, 958–966.
- [13] C. M. Dobson, *Nature* **2004**, *432*, 824–828.
- [14] R. MacArron, M. N. Banks, D. Bojanic, D. J. Burns, D. A. Cirovic, T. Garyantes, D. V. S. Green, R. P. Hertzberg, W. P. Janzen, J. W. Paslay, U. Schopfer, G. S. Sittampalam, *Nat. Rev. Drug Discov.* **2011**, *10*, 188–195.
- [15] P. Szymański, M. Markowicz, E. Mikiciuk-Olasik, *Int. J. Mol. Sci.* **2012**, *13*, 427–452.
- [16] M. Entzeroth, H. Flotow, P. Condrón, *Curr. Protoc. Pharmacol.* **2009**, *44*, 9.4.1-9.4.27.
- [17] J. L. Dahlin, M. A. Walters, *Future Med. Chem.* **2014**, *6*, 1265–1290.
- [18] I. Rothenaigner, K. Hadian, *SLAS Discov.* **2021**, *26*, 851–854.
- [19] A. C. Kasper, J. B. Baker, H. Kim, J. Hong, *Future Med. Chem.* **2009**, *1*, 727–736.
- [20] D. C. Swinney, J. Anthony, *Nat. Rev. Drug Discov.* **2011**, *10*, 507–519.

- [21] “BioRender,” can be found under <https://biorender.com/>, **n.d.**
- [22] J. G. Moffat, F. Vincent, J. A. Lee, J. Eder, M. Prunotto, *Nat. Rev. Drug Discov.* **2017**, *16*, 531–543.
- [23] M. A. Bray, S. Singh, H. Han, C. T. Davis, B. Borgeson, C. Hartland, M. Kost-Alimova, S. M. Gustafsdottir, C. C. Gibson, A. E. Carpenter, *Nat. Protoc.* **2016**, *11*, 1757–1774.
- [24] S. Ziegler, S. Sievers, H. Waldmann, *Cell Chem. Biol.* **2021**, *28*, 300–319.
- [25] C. States, S. M. Gustafsdottir, V. Ljosa, K. L. Sokolnicki, J. A. Wilson, D. Walpita, M. M. Kemp, K. P. Seiler, H. A. Carrel, T. R. Golu, S. L. Schreiber, P. A. Clemons, A. E. Carpenter, A. F. Shamji, *PLoS One* **2013**, *8*, DOI 10.1371/journal.pone.0080999.
- [26] A. Pahl, S. Sievers, in *Methods Mol. Biol.*, Humana Press Inc., **2019**, pp. 115–126.
- [27] C. K. Prier, D. A. Rankic, D. W. C. MacMillan, *Chem. Rev.* **2013**, *113*, 5322–5363.
- [28] S. H. Xiang, B. Tan, *Nat. Commun.* **2020**, *11*, 1–5.
- [29] H. M. L. Davies, D. Morton, *J. Org. Chem.* **2016**, *81*, 343–350.
- [30] R. H. Crabtree, A. Lei, *Chem. Rev.* **2017**, *117*, 8481–8482.
- [31] K. L. Stone, A. S. Borovik, *Curr. Opin. Chem. Biol.* **2009**, *13*, 114–118.
- [32] K. M. Altus, J. A. Love, *Commun. Chem.* **2021**, *4*, 1–11.
- [33] T. Rogge, N. Kaplaneris, N. Chatani, J. Kim, S. Chang, B. Punji, L. L. Schafer, D. G. Musaev, J. Wencel-Delord, C. A. Roberts, R. Sarpong, Z. E. Wilson, M. A. Brimble, M. J. Johansson, L. Ackermann, *C–H Activation*, **2021**.
- [34] T. Dalton, T. Faber, F. Glorius, *ACS Cent. Sci.* **2021**, *7*, 245–261.
- [35] L. Zhang, T. Ritter, *J. Am. Chem. Soc.* **2022**, *144*, 2399–2414.
- [36] G. Dyker, *Angew. Chemie - Int. Ed.* **1999**, *38*, 1698–1712.
- [37] J. Yamaguchi, A. D. Yamaguchi, K. Itami, *Angew. Chemie - Int. Ed.* **2012**, *51*, 8960–9009.
- [38] D. J. Abrams, P. A. Provencher, E. J. Sorensen, *Chem. Soc. Rev.* **2018**, *47*, 8925–8967.
- [39] F. Roudesly, J. Oble, G. Poli, *J. Mol. Catal. A Chem.* **2017**, *426*, 275–296.
- [40] C. Davies, S. Shaaban, H. Waldmann, *Trends Chem.* **2022**, *4*, 318–330.
- [41] S. Rej, A. Das, N. Chatani, *Coord. Chem. Rev.* **2021**, *431*, 213683.
- [42] Z. Chen, B. Wang, J. Zhang, W. Yu, Z. Liu, Y. Zhang, *Org. Chem. Front.* **2015**, *2*, 1107–1295.
- [43] C. Sambigiato, D. Schönbauer, R. Blicek, T. Dao-Huy, G. Pototschnig, P. Schaaf, T.

- Wiesinger, M. F. Zia, J. Wencel-Delord, T. Besset, B. U. W. Maes, M. Schnürch, *Chem. Soc. Rev.* **2018**, *47*, 6603–6743.
- [44] V. Snieckus, *Chem. Rev.* **1990**, *90*, 879–933.
- [45] G. Meng, N. Y. S. Lam, E. L. Lucas, T. G. Saint-Denis, P. Verma, N. Chekshin, J. Q. Yu, *J. Am. Chem. Soc.* **2020**, *142*, 10571–10591.
- [46] S. Murai, F. Kakiuchi, S. Sekine, Y. Tanaka, A. Kamatani, M. Sonoda, N. Chatani, *Nature* **1993**, *366*, 529–531.
- [47] T. Gensch, M. N. Hopkinson, F. Glorius, J. Wencel-Delord, *Chem. Soc. Rev.* **2016**, *45*, 2900–2936.
- [48] G. Song, F. Wang, X. Li, *Chem. Soc. Rev.* **2012**, *41*, 3651–3678.
- [49] R. Wang, X. Xie, H. Liu, Y. Zhou, *Catalysts* **2019**, *9*, 823.
- [50] K. Ueura, T. Satoh, M. Miura, *Org. Lett.* **2007**, *9*, 1407–1409.
- [51] D. R. Stuart, M. Bertrand-Laperle, K. M. N. Burgess, K. Fagnou, *J. Am. Chem. Soc.* **2008**, *130*, 16474–16475.
- [52] T. K. Hyster, T. Rovis, *J. Am. Chem. Soc.* **2010**, *132*, 10565–10569.
- [53] J. Wencel-Delord, T. Dröge, F. Liu, F. Glorius, *Chem. Soc. Rev.* **2011**, *40*, 4740–4761.
- [54] J. Mo, L. Wang, Y. Liu, X. Cui, *Synth.* **2015**, *47*, 439–459.
- [55] J. Wu, X. Cui, L. Chen, G. Jiang, Y. Wu, *J. Am. Chem. Soc.* **2009**, *131*, 13888–13889.
- [56] Y. Tan, J. F. Hartwig, *J. Am. Chem. Soc.* **2010**, *132*, 3676–3677.
- [57] M. Wasa, J. Q. Yu, *J. Am. Chem. Soc.* **2008**, *130*, 14058–14059.
- [58] N. Guimond, C. Gouliaras, K. Fagnou, *J. Am. Chem. Soc.* **2010**, *132*, 6908–6909.
- [59] S. Rakshit, C. Grohmann, T. Besset, F. Glorius, *J. Am. Chem. Soc.* **2011**, *133*, 2350–2353.
- [60] N. Guimond, S. I. Gorelsky, K. Fagnou, *J. Am. Chem. Soc.* **2011**, *133*, 6449–6457.
- [61] L. Ackermann, *Chem. Rev.* **2011**, *111*, 1315–1345.
- [62] R. Zeng, S. Wu, C. Fu, S. Ma, *J. Am. Chem. Soc.* **2013**, *135*, 18284–18287.
- [63] T. A. Davis, T. K. Hyster, T. Rovis, *Angew. Chemie Int. Ed.* **2013**, *52*, 14181–14185.
- [64] S. Cui, Y. Zhang, Q. Wu, *Chem. Sci.* **2013**, *4*, 3421–3426.
- [65] S. Cui, Y. Zhang, D. Wang, Q. Wu, *Chem. Sci.* **2013**, *4*, 3912–3916.
- [66] S. P. Upadhyay, P. Thapa, R. Sharma, M. Sharma, *Fitoterapia* **2020**, *146*, 104722.
- [67] G. Zhang, S. Sun, T. Zhu, Z. Lin, J. Gu, D. Li, Q. Gu, *Phytochemistry* **2011**, *72*, 1436–1442.

- [68] A. Buttinoni, M. Ferrari, M. Colombo, R. Ceserani, *J. Pharm. Pharmacol.* **2011**, *35*, 603–604.
- [69] P. A. Horton, R. E. Longley, O. J. McConnell, L. M. Ballas, *Experientia* **1994**, *50*, 843–845.
- [70] E. Li, L. Jiang, L. Guo, H. Zhang, Y. Che, *Bioorganic Med. Chem.* **2008**, *16*, 7894–7899.
- [71] V. Kumar, Poonam, A. K. Prasad, V. S. Parmar, *Nat. Prod. Rep.* **2003**, *20*, 565–583.
- [72] S. M. Evans, R. W. Foltin, F. R. Levin, M. W. Fischman, *Behav. Pharmacol.* **1995**, *6*, 176–186.
- [73] E. Deniau, D. Enders, *Tetrahedron Lett.* **2000**, *41*, 2347–2350.
- [74] R. Savela, C. Méndez-Gálvez, *Chem. - A Eur. J.* **2021**, *27*, 5344–5378.
- [75] G. Stajer, F. Csende, *Curr. Org. Chem.* **2005**, *9*, 1277–1286.
- [76] Y. S. Song, C. H. Lee, K. J. Lee, *J. Heterocycl. Chem.* **2003**, *40*, 939–941.
- [77] L. Liu, S. H. Bai, Y. Li, L. X. Wang, Y. Hu, H. L. Sung, J. Li, *J. Org. Chem.* **2017**, *82*, 11084–11090.
- [78] E. M. De Marigorta, J. M. De Los Santos, A. M. O. De Retana, J. Vicario, F. Palacios, *Beilstein J. Org. Chem.* **2019**, *15*, 1065–1085.
- [79] L. Y. Fu, J. Ying, X. Qi, J. B. Peng, X. F. Wu, *J. Org. Chem.* **2019**, *84*, 1421–1429.
- [80] K. H. Son, J. Y. Min, G. Kim, *Bull. Korean Chem. Soc.* **2014**, *35*, 985–986.
- [81] T. K. Hyster, K. E. Ruhl, T. Rovis, *J. Am. Chem. Soc.* **2013**, *135*, 5364–5367.
- [82] S. Wu, X. Wu, C. Fu, S. Ma, *Org. Lett.* **2018**, *20*, 2831–2834.
- [83] F. Wang, G. Song, X. Li, *Org. Lett.* **2010**, *12*, 5430–5433.
- [84] S. Shaaban, C. Davies, C. Merten, J. Flegel, F. Otte, C. Strohmam, H. Waldmann, *Chem. - A Eur. J.* **2020**, *26*, 10729–10734.
- [85] E. A. Trifonova, N. M. Ankudinov, M. V Kozlov, M. Y. Sharipov, Y. V Nelyubina, D. Perekalin, *Chem. - A Eur. J.* **2018**, 16570–16575.
- [86] T. J. Potter, D. N. Kamber, B. Q. Mercado, J. A. Ellman, *ACS Catal.* **2017**, *7*, 150–153.
- [87] M. D. Wodrich, B. Ye, J. F. Gonthier, C. Corminboeuf, N. Cramer, *Chem. - A Eur. J.* **2014**, *20*, 15409–15418.
- [88] K. Speck, T. Magauer, *Beilstein J. Org. Chem.* **2013**, *9*, 2048–2078.
- [89] K. D. Hesp, M. Stradiotto, *ChemCatChem* **2010**, *2*, 1192–1207.
- [90] L. Xu, Q. Zhu, G. Huang, B. Cheng, Y. Xia, *J. Org. Chem.* **2012**, *77*, 3017–3024.

- [91] T. Piou, F. Romanov-Michailidis, M. Romanova-Michaelides, K. E. Jackson, N. Semakul, T. D. Taggart, B. S. Newell, C. D. Rithner, R. S. Paton, T. Rovis, *J. Am. Chem. Soc.* **2017**, *139*, 1296–1310.
- [92] M. Beckerman, *Cellular Signaling in Health and Disease*, Springer US, New York, NY, **2009**.
- [93] J. Briscoe, P. P. Thérond, *Nat. Rev. Mol. Cell Biol.* **2013**, *14*, 418–431.
- [94] G. B. Carballo, J. R. Honorato, G. P. F. De Lopes, T. C. L. D. S. E. Spohr, *Cell Commun. Signal.* **2018**, *16*, 1–15.
- [95] L. Kremer, E. Hennes, A. Brause, A. Ursu, L. Robke, H. T. Matsubayashi, Y. Nihongaki, J. Flegel, I. Mejdrová, J. Eickhoff, M. Baumann, R. Nencka, P. Janning, S. Kordes, H. R. Schöler, J. Sternecker, T. Inoue, S. Ziegler, H. Waldmann, *Angew. Chemie* **2019**, *131*, 16770–16781.
- [96] A. Rutkovskiy, K.-O. Stensløkken, I. J. Vaage, *Med. Sci. Monit. Basic Res.* **2016**, *22*, 95–106.
- [97] S. Peukert, K. Miller-Moslin, *ChemMedChem* **2010**, *5*, 500–512.
- [98] X. Wu, S. Ding, Q. Ding, N. S. Gray, P. G. Schultz, *J. Am. Chem. Soc.* **2002**, *124*, 14520–14521.
- [99] O. O. Grygorenko, D. M. Volochnyuk, S. V. Ryabukhin, D. B. Judd, *Chem. – A Eur. J.* **2020**, *26*, 1196–1237.
- [100] D. J. Newman, G. M. Cragg, *J. Nat. Prod.* **2020**, *83*, 770–803.
- [101] H. Van Hattum, H. Waldmann, *J. Am. Chem. Soc.* **2014**, *136*, 11853–11859.
- [102] P. Ertl, A. Schuffenhauer, in *Nat. Compd. as Drugs Vol. II* (Eds.: F. Petersen, R. Amstutz), Birkhäuser Basel, Basel, **2008**, pp. 217–235.
- [103] S. L. Schreiber, *Nature* **2009**, *457*, 153–154.
- [104] W. R. J. D. Galloway, A. Isidro-Llobet, D. R. Spring, *Nat. Commun.* **2010**, *1*, 1–13.
- [105] R. J. Spandl, M. Díaz-Gavilán, K. M. G. O’Connell, G. L. Thomas, D. R. Spring, *Chem. Rec.* **2008**, *8*, 129–142.
- [106] K. M. G. O’Connell, W. R. J. D. Galloway, B. M. Ibbeson, A. Isidro-Llobet, C. J. O’Connor, D. R. Spring, in *Solid-Phase Org. Synth.*, John Wiley & Sons, Inc., Hoboken, NJ, USA, **2011**, pp. 131–150.
- [107] T. E. Nielsen, S. L. Schreiber, *Angew. Chemie Int. Ed.* **2008**, *47*, 48–56.

- [108] E. Comer, E. Rohan, L. Deng, J. A. Porco, *Org. Lett.* **2007**, *9*, 2123–2126.
- [109] R. W. Huigens, K. C. Morrison, R. W. Hicklin, T. A. Timothy, M. F. Richter, P. J. Hergenrother, *Nat. Chem.* **2013**, *5*, 195–202.
- [110] K. C. Morrison, P. J. Hergenrother, *Nat. Prod. Rep.* **2014**, *31*, 6–14.
- [111] A. Garcia, B. S. Drown, P. J. Hergenrother, *Org. Lett.* **2016**, *18*, 4852–4855.
- [112] L. Furiassi, E. J. Tonogai, P. J. Hergenrother, *Angew. Chemie Int. Ed.* **2021**, *60*, 16119–16128.
- [113] E. Llabani, R. W. Hicklin, H. Y. Lee, S. E. Motika, L. A. Crawford, E. Weerapana, P. J. Hergenrother, *Nat. Chem.* **2019**, *11*, 521–532.
- [114] S. Wetzel, R. S. Bon, K. Kumar, H. Waldmann, *Angew. Chemie - Int. Ed.* **2011**, *50*, 10800–10826.
- [115] G. Karageorgis, H. Waldmann, *Synth.* **2019**, *51*, 55–66.
- [116] B. Over, S. Wetzel, C. Grütter, Y. Nakai, S. Renner, D. Rauh, H. Waldmann, *Nat. Chem.* **2013**, *5*, 21–28.
- [117] M. A. Koch, A. Schuffenhauer, M. Scheck, S. Wetzel, M. Casaulta, A. Odermatt, P. Ertl, H. Waldmann, *Proc. Natl. Acad. Sci. U. S. A.* **2005**, *102*, 17272–17277.
- [118] P.-Y. Dakas, J. A. Parga, S. Höing, H. R. Schöler, J. Sternecker, K. Kumar, H. Waldmann, *Angew. Chemie Int. Ed.* **2013**, *52*, 9576–9581.
- [119] C. W. Murray, D. C. Rees, *Nat. Chem.* **2009**, *1*, 187–192.
- [120] P. Kirsch, A. M. Hartman, A. K. H. Hirsch, M. Empting, *Molecules* **2019**, *24*, DOI 10.3390/molecules24234309.
- [121] L. R. de Souza Neto, J. T. Moreira-Filho, B. J. Neves, R. L. B. R. Maidana, A. C. R. Guimarães, N. Furnham, C. H. Andrade, F. P. Silva, *Front. Chem.* **2020**, *8*, 93.
- [122] Z. Konteatis, *Expert Opin. Drug Discov.* **2021**, *16*, 723–726.
- [123] Q. Li, *Front. Mol. Biosci.* **2020**, *7*, 180.
- [124] H. Jhoti, G. Williams, D. C. Rees, C. W. Murray, *Nat. Rev. Drug Discov.* **2013**, *12*, 644.
- [125] H. Chen, X. Zhou, A. Wang, Y. Zheng, Y. Gao, J. Zhou, *Drug Discov. Today* **2015**, *20*, 105–113.
- [126] “Fragment-based design of isoquinoline derivatives as anti-inflammatory drugs - Research Outreach,” can be found under <https://researchoutreach.org/articles/fragment-based-design-isoquinoline-derivatives-anti-inflammatory-drugs/>, **n.d.**

- [127] M. Congreve, R. Carr, C. Murray, H. Jhoti, *Drug Discov. Today* **2003**, *8*, 876–877.
- [128] H. Prescher, G. Koch, T. Schuhmann, P. Ertl, A. Bussenault, M. Glick, I. Dix, F. Petersen, D. E. Lizos, *Bioorganic Med. Chem.* **2017**, *25*, 921–925.
- [129] J. Hert, J. J. Irwin, C. Laggner, M. J. Keiser, B. K. Shoichet, *Nat. Chem. Biol.* **2009**, *5*, 479–483.
- [130] G. Karageorgis, D. J. Foley, L. Laraia, S. Brakmann, H. Waldmann, *Angew. Chemie - Int. Ed.* **2021**, *60*, 15705–15723.
- [131] D. J. Foley, S. Zinken, D. Corkery, L. Laraia, A. Pahl, Y. W. Wu, H. Waldmann, *Angew. Chemie - Int. Ed.* **2020**, *59*, 12470–12476.
- [132] M. Grigalunas, S. Brakmann, H. Waldmann, *J. Am. Chem. Soc.* **2022**, *144*, 3314–3329.
- [133] M. Grigalunas, A. Burhop, S. Zinken, A. Pahl, J. M. Gally, N. Wild, Y. Mantel, S. Sievers, D. J. Foley, R. Scheel, C. Strohmam, A. P. Antonchick, H. Waldmann, *Nat. Commun.* **2021**, *12*, 1–11.
- [134] G. Karageorgis, D. J. Foley, L. Laraia, H. Waldmann, *Nat. Chem.* **2020**, *12*, 227–235.
- [135] J. Liu, G. S. Cremonnik, F. Otte, A. Pahl, S. Sievers, C. Strohmam, H. Waldmann, *Angew. Chemie Int. Ed.* **2021**, *60*, 4648–4656.
- [136] A. Burhop, S. Bag, M. Grigalunas, S. Woitalla, P. Bodenbinder, L. Brieger, C. Strohmam, A. Pahl, S. Sievers, H. Waldmann, *Adv. Sci.* **2021**, *8*, 1–10.
- [137] A. Christoforow, J. Wilke, A. Binici, A. Pahl, C. Ostermann, S. Sievers, H. Waldmann, *Angew. Chemie - Int. Ed.* **2019**, *58*, 14715–14723.
- [138] J. Ceballos, M. Schwalfenberg, G. Karageorgis, E. S. Reckzeh, S. Sievers, C. Ostermann, A. Pahl, M. Sellstedt, J. Nowacki, M. A. Carnero Corrales, J. Wilke, L. Laraia, K. Tschapalda, M. Metz, D. A. Sehr, S. Brand, K. Winklhofer, P. Janning, S. Ziegler, H. Waldmann, *Angew. Chemie - Int. Ed.* **2019**, *58*, 17016–17025.
- [139] G. Karageorgis, E. S. Reckzeh, J. Ceballos, M. Schwalfenberg, S. Sievers, C. Ostermann, A. Pahl, S. Ziegler, H. Waldmann, *Nat. Chem.* **2018**, DOI 10.1038/s41557-018-0132-6.
- [140] T. Schneidewind, S. Kapoor, G. Garivet, G. Karageorgis, R. Narayan, G. Vendrell-Navarro, A. P. Antonchick, S. Ziegler, H. Waldmann, *Cell Chem. Biol.* **2019**, *26*, 512–523.e5.
- [141] J. M. Gally, A. Pahl, P. Czodrowski, H. Waldmann, *J. Chem. Inf. Model.* **2021**, *61*, 5458–5468.

- [142] N. N. Mateeva, L. L. Winfield, K. K. Redda, *Curr. Med. Chem.* **2005**, *12*, 551–571.
- [143] N. K. Kaushik, N. Kaushik, P. Attri, N. Kumar, C. H. Kim, A. K. Verma, E. H. Choi, *Molecules* **2013**, *18*, 6620–6662.
- [144] I. Hardardottir, E. S. Olafsdottir, J. Freysdottir, *Phytomedicine* **2015**, *22*, 277–282.
- [145] C. Willson, in *XPharm Compr. Pharmacol. Ref.*, Elsevier Inc., **2009**, pp. 1–9.
- [146] CRC Press, “Dictionary of Natural Products,” can be found under <https://dnp.chemnetbase.com/faces/chemical/ChemicalSearch.xhtml>, **n.d.**
- [147] M. Sorokina, P. Merseburger, K. Rajan, M. A. Yirik, C. Steinbeck, *J. Cheminform.* **2021**, *13*, 2.
- [148] S. Khong, T. Venkatesh, O. Kwon, *Asian J. Org. Chem.* **2021**, *10*, 2699–2708.
- [149] Y. Xiao, Z. Sun, H. Guo, O. Kwon, *Beilstein J. Org. Chem.* **2014**, *10*, 2089–2121.
- [150] X. F. Zhu, J. Lan, O. Kwon, *J. Am. Chem. Soc.* **2003**, *125*, 4716–4717.
- [151] Y. S. Tran, O. Kwon, *Org. Lett.* **2005**, *7*, 4289–4291.
- [152] B. Mao, W. Shi, J. Liao, H. Liu, C. Zhang, H. Guo, *Org. Lett.* **2017**, *19*, 6340–6343.
- [153] K. Lu, O. Kwon, K. M. Brummond, M. M. Davis, *Org. Synth.* **2009**, *86*, 212–224.
- [154] R. P. Wurz, G. C. Fu, *J. Am. Chem. Soc.* **2005**, *127*, 12234–12235.
- [155] X. Han, Y. Wang, F. Zhong, Y. Lu, *J. Am. Chem. Soc.* **2011**, *133*, 1726–1729.
- [156] Y. Qiao, K. L. Han, *Org. Biomol. Chem.* **2012**, *10*, 7689–7706.
- [157] Y. Ogata, T. Harada, T. Sugimoto, *Can. J. Chem.* **1977**, *55*, 1268–1272.
- [158] R. Kaul, Y. Brouillette, Z. Sajjadi, K. A. Hansford, W. D. Lubell, *J. Org. Chem.* **2004**, *69*, 6131–6133.
- [159] N. N. Pavlova, C. B. Thompson, *Cell Metab.* **2016**, *23*, 27–47.
- [160] J. Hematol, K. Tang, Y. H. Wu, Y. Song, B. Yu, *J. Hematol. Oncol.* **2021**, 1–21.
- [161] E. Hennes, P. Lampe, L. Dötsch, N. Bruning, L. M. Pulvermacher, S. Sievers, S. Ziegler, H. Waldmann, *Angew. Chemie - Int. Ed.* **2021**, *60*, 9869–9874.
- [162] H. J. Ball, F. F. Fedelis, S. M. Bakmiwewa, N. H. Hunt, H. J. Yuasa, *Front. Immunol.* **2014**, *5*, 485.
- [163] I. Theate, N. Van Baren, L. Pilotte, P. Moulin, P. Larrieu, J. C. Renaud, C. Herve, I. Gutierrez-Roelens, E. Marbaix, C. Sempoux, B. J. Van Den Eynde, *Cancer Immunol. Res.* **2015**, *3*, 161–172.
- [164] Y. Ozaki, M. P. Edelstein, D. S. Duch, *Proc. Natl. Acad. Sci. U. S. A.* **1988**, *85*, 1242–

- 1246.
- [165] J. L. Adams, J. Smothers, R. Srinivasan, A. Hoos, *Nat. Publ. Gr.* **2015**, *14*, 603–622.
- [166] L. Hornyák, N. Dobos, G. Koncz, Z. Karányi, D. Páll, Z. Szabó, G. Halmos, L. Székvölgyi, *Front. Immunol.* **2018**, *9*, DOI 10.3389/fimmu.2018.00151.
- [167] G. C. Prendergast, W. P. Malachowski, J. B. Duhadaway, A. J. Muller, **2017**, 6795–6812.
- [168] M. Liu, X. Wang, L. Wang, X. Ma, Z. Gong, S. Zhang, Y. Li, *J. Hematol. Oncol.* **2018**, *11*, 100.
- [169] G. C. Prendergast, R. Metz, A. J. Muller, L. M. F. Merlo, L. Mandik-Nayak, *Front. Immunol.* **2014**, *5*, 585.
- [170] J. Croitoru-Lamoury, F. M. J. Lamoury, M. Caristo, K. Suzuki, D. Walker, O. Takikawa, R. Taylor, B. J. Brew, *PLoS One* **2011**, *6*, e14698.
- [171] C. E. Blunt, C. Torcuk, Y. Liu, W. Lewis, D. Siegel, D. Ross, C. J. Moody, *Angew. Chemie - Int. Ed.* **2015**, *54*, 8740–8745.
- [172] U. F. Röhrig, A. Reynaud, S. R. Majjigapu, P. Vogel, F. Pojer, V. Zoete, *J. Med. Chem.* **2019**, *62*, 8784–8795.
- [173] K. Tang, Y. H. Wu, Y. Song, B. Yu, *J. Hematol. Oncol.* **2021**, *14*, 68.
- [174] E. Fox, T. Oliver, M. Rowe, S. Thomas, Y. Zakharia, P. B. Gilman, A. J. Muller, G. C. Prendergast, *Front. Oncol.* **2018**, *8*, 370.
- [175] U. F. Röhrig, S. R. Majjigapu, A. Reynaud, F. Pojer, N. Dilek, P. Reichenbach, K. Ascencao, M. Irving, G. Coukos, P. Vogel, O. Michielin, V. Zoete, *J. Med. Chem.* **2021**, *64*, 2205–2227.
- [176] S. W. Smith, *Toxicol. Sci.* **2009**, *110*, 4–30.
- [177] P. Häfliger, R. P. Charles, *Int. J. Mol. Sci.* **2019**, *20*, DOI 10.3390/ijms20102428.
- [178] Y. D. Bhutia, E. Babu, V. Ganapathy, *Biochim. Biophys. Acta - Biomembr.* **2015**, *1848*, 453–462.
- [179] E. Timosenko, H. Ghadbane, J. D. Silk, D. Shepherd, U. Gileadi, L. J. Howson, R. Laynes, Q. Zhao, R. L. Strausberg, L. R. Olsen, S. Taylor, F. M. Buffa, R. Boyd, V. Cerundolo, *Cancer Res.* **2016**, *76*, 6193–6204.
- [180] Y. Kudo, C. A. R. Boyd, *J. Physiol.* **2001**, *531*, 405–416.
- [181] M. T. Nelp, P. A. Kates, J. T. Hunt, J. A. Newitt, A. Balog, D. Maley, X. Zhu, L. Abell, A. Allentoff, R. Borzilleri, H. A. Lewis, Z. Lin, S. P. Seitz, C. Yan, J. T. Groves, *Proc.*

- Natl. Acad. Sci. U. S. A.* **2018**, *115*, 3249–3254.
- [182] S. Panda, A. Roy, S. J. Deka, V. Trivedi, D. Manna, *ACS Med. Chem. Lett.* **2016**, *7*, 1167–1172.
- [183] R. Jafari, H. Almqvist, H. Axelsson, M. Ignatushchenko, T. Lundbäck, P. Nordlund, D. M. Molina, *Nat. Protoc.* **2014**, *9*, 2100–2122.
- [184] Y. Zhang, S. A. Kang, T. Mukherjee, S. Bale, B. R. Crane, T. P. Begley, S. E. Ealick, *Biochemistry* **2007**, *46*, 145–155.
- [185] Y. K. Lee, H. B. Lee, D. M. Shin, M. J. Kang, E. C. Yi, S. Noh, J. Lee, C. Lee, C. K. Min, E. Y. Choi, *Exp. Mol. Med.* **2014**, *46*, e121.
- [186] S. Samanta, T. L. Lim, Y. Lam, *ChemMedChem* **2013**, *8*, 994–1001.
- [187] Y. Hu, Y. Xie, Z. Shen, H. Huang, *Angew. Chemie Int. Ed.* **2017**, *56*, 2473–2477.
- [188] B. Ye, N. Cramer, *Science (80-.)*. **2012**, *338*, 504.
- [189] E. A. Trifonova, N. M. Ankinov, A. A. Mikhaylov, D. A. Chusov, Y. V. Nelyubina, D. S. Perekalin, *Angew. Chemie - Int. Ed.* **2018**, *57*, 7714–7718.
- [190] Y. Kita, T. Yata, Y. Nishimoto, M. Yasuda, *J. Org. Chem.* **2018**, *83*, 740–753.
- [191] A. Saxena, F. Perez, M. J. Krische, *J. Am. Chem. Soc.* **2015**, *137*, 5883–5886.
- [192] E. S. Sherman, P. H. Fuller, D. Kasi, S. R. Chemler, *J. Org. Chem.* **2007**, *72*, 3896–3905.
- [193] O. V. Dolomanov, L. J. Bourhis, R. J. Gildea, J. A. K. Howard, H. Puschmann, *J. Appl. Crystallogr.* **2009**, *42*, 339–341.
- [194] G. M. Sheldrick, *Acta Crystallogr. Sect. A Found. Crystallogr.* **2015**, *71*, 3–8.
- [195] G. M. Sheldrick, *Acta Crystallogr. Sect. A Found. Crystallogr.* **2008**, *64*, 112–122.
- [196] D. J. F. M. J. Frisch, G. W. Trucks, H. B. Schlegel, G. E. Scuseria, M. A. Robb, J. R. Cheeseman, G. Scalmani, V. Barone, G. A. Petersson, H. Nakatsuji, X. Li, M. Caricato, A. V. Marenich, J. Bloino, B. G. Janesko, R. Gomperts, B. Mennucci, H. P. Hratchian, J. V., **2016**.
- [197] Y. Zhao, D. G. Truhlar, *Theor. Chem. Acc.* **2008**, *120*, 215–241.

5. Abbreviations

Ac	Acetyl
AhR	Ary hydrocarbon receptor
aq.	Aqueous
BIOS	Biology oriented synthesis
BMS	Bristol Myers Squibb
Bn	Benzyl
Boc	tert-butyloxycarbonyl
Bu	Butyl
Bz	Benzoyl
n-Buli	n-Butyllithium
cat.	Catalyst/catalytic
CtD	Complexity-to-diversity
COCONUT	COLleCtion of Open Natural ProdUCtS
d	Doublet
Da	Daltons
DCM	Dichloromethane
DCE	Dichloroethane
DFT	Density functional theory
DHQ	Dihydroisoquinolone
DMF	Dimethylformamide
DMSO	Dimethylsulfoxide
DNA	Deoxyribonucleic acid
DNP	Dictionary of natural products
DOS	Diversity oriented synthesis
ee	Enantiomeric excess
ESI	Electrospray ionisation
Et	Ethyl
EtOAc	Ethyl acetate
equiv	Equivalent(s)

EWG	Electron-withdrawing group
FBDD	Fragment-based drug discovery
FDA	Food and drug administration
h	Hour(s)
Hh	Hedgehog
HRMS	High resolution mass spectrometry
HTS	High-throughput screen/screening
IC ₅₀	Half-maximal inhibitory concentration
IDO	Indoleamine 2,3-Dioxygenase
IFN- γ	Interferon- γ
K ₂ CO ₃	Potassium carbonate
KOtBu	Potassium tert-butoxide
Kyn	Kynurenine
LDA	Lithium Diisopopyl Amine
m	multiplet
<i>m</i>	Meta
Me	Methyl
MeCN	Acetonitrile
MeOH	Methanol
[M]	Molar (concentration)
MSC	Mesenchymal stem cells
NaH	Sodium Hydride
NEt ₃	Triethylamine
NK	Natural killer
NMR	Nuclear magnetic resonance
NP	Natural product
Ns	Nosyl
<i>o</i>	Ortho
<i>p</i>	Para
Pd	Palladium
PG	Protecting group

Ph	Phenyl
PhSH	Thiophenol
Piv	Pivalate
ppm	Parts per million
q	quartet
rac	Racemic
Rh	Rhodium
RNA	Ribonucleic acid
Ro3	Rule of 3
Ru	Ruthenium
RT	Room temperature
SAR	Structure-activity-relationship
SCONP	Structural classification of natural products
(<i>S,S</i>)-Et-BPE	(-)-1,2-Bis((2 <i>S</i> ,5 <i>S</i>)-2,5-diethylphospholano)ethane,
t	Triplet
T	Temperature
TDO	Tryptophan 2,3-dioxygenase
TFA	Trifluoroacetic acid
TLC	Thin layer chromatography
THF	Tetrahydrofuran
THP	Tetrahydropyridine
Trp	Tryptophan
Ts	Tosyl

6. Appendix

6.1 Curriculum Vitae (Lebenslauf)

Personal Information

Name Caitlin Davies

Date of Birth 09.01.1995

Place of Birth Kettering, Northamptonshire, UK

Nationality British

Education and Work Experience

04/2019 - 07/2022 **Max Planck Institute for Molecular Physiology, Dortmund**

PhD in Chemistry and Chemical Biology

Thesis: “Development of Methods toward the Synthesis of Novel Bioactive Natural Product-like Scaffolds”

Supervisor: Prof. Dr. Dr. h.c. Herbert Waldmann

09/2013 - 07/2017 **University of Leeds**

MChem Chemistry –1st

Master’s Thesis:

Supervisor: Prof. Dr. John Blacker

08/2015 - 08/2016 *Year in Industry: Roche Internship in Medicinal Chemistry (RiCH)*

Bachelor’s Thesis:

Supervisor: Dr. Uwe Grether

Publications

1. **C. Davies***, L. Doetsch*, M. G. Ciulla, E. Hennes, R. Scheel, S. Sievers, C. Strohmann, K. Kumar, S. Ziegler, H. Waldmann. *Angew. Chem. Int. Ed.* **2022** manuscript submitted
2. **C. Davies**, S. Shaaban, H. Waldmann. *Trends in Chemistry*, **2022**, <https://doi.org/10.1016/j.trechm.2022.01.005>
3. S. Shaaban, **C. Davies**, H. Waldmann, *Eur. J. Org. Chem.* **2020**, 6512.
4. S. Shaaban*, **C. Davies***, C. Merten, J. Flegel, F. Otte, C. Strohmann, H. Waldmann, *Chem. Eur. J.* **2020**, 26, 10729

6.2 Eidesstattliche Versicherung (Affidavit)

Davies, Caitlin

Name, Vorname
(Surname, first name)

Matrikel-Nr.
(Enrolment number)

Belehrung:

Wer vorsätzlich gegen eine die Täuschung über Prüfungsleistungen betreffende Regelung einer Hochschulprüfungsordnung verstößt, handelt ordnungswidrig. Die Ordnungswidrigkeit kann mit einer Geldbuße von bis zu 50.000,00 € geahndet werden. Zuständige Verwaltungsbehörde für die Verfolgung und Ahndung von Ordnungswidrigkeiten ist der Kanzler/die Kanzlerin der Technischen Universität Dortmund. Im Falle eines mehrfachen oder sonstigen schwerwiegenden Täuschungsversuches kann der Prüfling zudem exmatrikuliert werden, § 63 Abs. 5 Hochschulgesetz NRW.

Die Abgabe einer falschen Versicherung an Eides statt ist strafbar.

Wer vorsätzlich eine falsche Versicherung an Eides statt abgibt, kann mit einer Freiheitsstrafe bis zu drei Jahren oder mit Geldstrafe bestraft werden, § 156 StGB. Die fahrlässige Abgabe einer falschen Versicherung an Eides statt kann mit einer Freiheitsstrafe bis zu einem Jahr oder Geldstrafe bestraft werden, § 161 StGB. Die oben stehende Belehrung habe ich zur Kenntnis genommen:

Official notification:

Any person who intentionally breaches any regulation of university examination regulations relating to deception in examination performance is acting improperly. This offence can be punished with a fine of up to EUR 50,000.00. The competent administrative authority for the pursuit and prosecution of offences of this type is the chancellor of the TU Dortmund University. In the case of multiple or other serious attempts at deception, the candidate can also be unenrolled, Section 63, paragraph 5 of the Universities Act of North Rhine-Westphalia.

The submission of a false affidavit is punishable.

Any person who intentionally submits a false affidavit can be punished with a prison sentence of up to three years or a fine, Section 156 of the Criminal Code. The negligent submission of a false affidavit can be punished with a prison sentence of up to one year or a fine, Section 161 of the Criminal Code.

I have taken note of the above official notification.

Dortmund,

Ort, Datum
(Place, date)

Unterschrift
(Signature)

Titel der Dissertation:
(Title of the thesis)

Development of Methods toward the Synthesis of Novel Bioactive Natural Product-like Scaffolds

Ich versichere hiermit an Eides statt, dass ich die vorliegende Dissertation mit dem Titel selbstständig und ohne unzulässige fremde Hilfe angefertigt habe. Ich habe keine anderen als die angegebenen Quellen und Hilfsmittel benutzt sowie wörtliche und sinngemäße Zitate kenntlich gemacht.

Die Arbeit hat in gegenwärtiger oder in einer anderen Fassung weder der TU Dortmund noch einer anderen Hochschule im Zusammenhang mit einer staatlichen oder akademischen Prüfung vorgelegen.

I hereby swear that I have completed the present dissertation independently and without inadmissible external support. I have not used any sources or tools other than those indicated and have identified literal and analogous quotations.

The thesis in its current version or another version has not been presented to the TU Dortmund University or another university in connection with a state or academic examination.*

***Please be aware that solely the German version of the affidavit ("Eidesstattliche Versicherung") for the PhD thesis is the official and legally binding version.**

Dortmund,

Ort, Datum
(Place, date)

Unterschrift
(Signature)